Proceedings of the Fourth International Workshop

on

Laser ranging instrumentation

held at the
University of Texas in Austin, Texas, U.S.A.
October 12 – 16, 1981

Volume I

compiled and edited
by
Peter Wilson
President, Special Study Group 2.33, I.A.G.
Earth-satellite laser ranging

published by the
Geodetic Institute, University of Bonn, 1982

PREFACE

The Fourth International Workshop on Laser Ranging Instrumentation was held at the Thomson Center on the campus of the University of Texas in Austin during the week of 12-16 October, 1981. It was sponsored under the auspices of the Special Study Group 2.33 (Earth-satellite laser ranging) of the International Association of Geodesy and the University of Texas.

The Workshop, which for three of the five days comprised parallel sessions on hardware and software aspects of laser ranging, was attended by participants from 15 nations and information was exchanged on the status of 44 of the 51 ranging systems for which hardware is known to exist. The meeting was opened by Prof. Dr. Harland Smith, Chairman of the Astronomy Dept. at the University of Texas. In his remarks Prof. Smith spoke of the intimate association his department and the University of Texas have had with the course of laser ranging to both the moon and to Lageos, laying stress on the progress which has been made over the years since first the technique was applied.

Indeed, with this, the third set of published proceedings, it can be seen that considerable consolidation has gone on in the four years since the previous Workshop in Lagonissi. Laser ranging is at last moving from experimental to application oriented research. The contents of these proceedings high-light the changes which have taken place in system design over this time and represent the state of the art in 1981.

In the interests of expediting publication there has been no extensive editing of individual papers, which are generally presented in the form submitted by the authors. Several papers have been included which were submitted

for publication, although the authors were unable to attend the Workshop. Only two or three of the papers presented at the sessions have not been submitted for inclusion in the proceedings.

Particular thanks are due to:

- the Programme-Committee (Prof. Dr. L. Aardoom - Netherlands, Prof. Dr. K. Hamal - Czechoslovakia, Dr. E. Silverberg - U.S.A. and Dr. P. Wilson - Fed. Rep. of Germany) and the session chairman, for preparing the programme;
- the hosts and hostesses of the University of Texas, for making the Workshop a valuable scientific and social experience;
- the authors, for their valuable contributions;
- the publisher, for making it possible to produce extensive Proceedings within the limitations of the available budget.

P. Wilson
President, S.S.G.-2.33

AUSTIN, TEXAS USA OCTOBER 12-16, 1981

FOURTH INTERNATIONAL WORKSHOP ON LASER RANGING INSTRUMENTATION

OCT. 12
MONDAY

8:00
Registration

9:00
Opening Remarks

9:30
Purpose of the Measurements

P. Bender

11:00
Laser Ranging Progress Since 1978

S. Tatevjan

15:00
Current Priorities in Software

E. Silverberg and J. Latimer

Reception

OCT. 13
TUESDAY

8:30
General Status of the Networks

P. Wilson

10:00
Latest Trends in Optics and Mount Development

Y. Kozai and J. Wohn

14:00
Lasers

K. Hamal and D. Hall

Meeting of SSG 2:32

OCT. 14
WEDNESDAY

8:30
Critical Look at Current Data Quality

B. Tapley

10:00
Problems Specific to Lunar Ranging

B. Greene and P. Shelus

14:00
Timing, Time Keeping and Calibration

J. Gaignebet and M. Pearlman

OCT. 15
THURSDAY

8:30
Current Results

D. Smith

10:00
Electro-optics and Detection Hardware

F. Zeeman and R. Neubert

14:00
MERIT Meetings (Communications & Standards)

19:30
Banquet - San Miguel Restaurant

OCT. 16
FRIDAY

9:00
Developmental Priorities

M. Pearlman

10:30
The Status of Advanced Ranging Developments

C. Alley and P. Morgan

14:00
Remaining Problems (panel discussion)
Concluding Summary
G. Veis and Y. Kokurin

HARDWARE WORKSHOP

SOFTWARE WORKSHOP - ROOM 2-110

10:00
Organizational Session

11:00
Realtime Operating Systems

10:00
Predictions and Pointing

10:00
Data Handling Communications and Other

FOURTH INTERNATIONAL WORKSHOP ON LASER RANGING INSTRUMENTATION PARTICIPANTS

Alley, C.
Dept. of Physics & Astronomy
University of Maryland
College Park, MD 20742

Beard, Charles
Hughes Aircraft Co.
P. O. Box 90515
Bldg. 130/20
Los Angeles, CA 90009

Bender, P. L.
JILA/NBS
Univ. of Colorado
Boulder, CO 80309

Borman, Kurt L.
EG&G
6801 Kenilworth Ave.
Riverdale, MD 20840

Bourdet, M.
INAG
77 Av. Denfert Rochereau
75014 Paris
FRANCE

Bowman, Steve
Physics & Astronomy
Univ. of Maryland
College Park, MD 20742

Bryant, R.
Division of National Mapping
P. O. Box 31
Belconnen 2616
AUSTRALIA

Buisson, J.
Naval Research Lab (NRL)
Code 7966
4555 Overlook Ave. S.W.
Washington, D.C. 20375

Byrns, David A.
10500 Sun Hills Dr.
Los Altos, Calif. 94022

Calame, Odile
Centre d'Etudes et de Recherches
Geodynamiques et Astronomiques
Avenue Nicholai Copernic
06130 Grasse
FRANCE

Cao, Wei-Lou
Physics & Astronomy
Univ. of Maryland
College Park, MD 20742

Degnan, John J.
NASA/Goddard Space Flight Center
Code 723
Greenbelt, MD 20771
USA

Duncombe, Raynor
Aerospace Engineering
University of Texas
Austin, TX 78712

Dunn, P.
EG&G/WASC
6801 Kenilworth Ave.
Riverdale, MD 20840

Economou, George A.
Contraves Goerz
610 Epsilon Dr.
Pittsburgh, PA 15215

Edge, D.
Code BFEC/TDO
NASA/Goddard Space Flight Center
Greenbelt, MD 20771

Feissel, Ms. M.
Bureau International de l'Heure
61 Av. de L'Observatoire
75014 Paris
FRANCE

Futaully, R.
CERGA
Avenue Nicholai Copernic
06130 Grasse
FRANCE

Gaignebet, J.
CERGA/CRGS
Av. Copernic
06130 Grasse
FRANCE

Greene, B. A.
Division of National Mapping
P. O. Box 31
Belconnen ACT 2616
AUSTRALIA

Guan, Zhen-Hua
P. O. Box 8511
North China Research Institute
of Electro-Optics
Beijing
Peoples' Republic of China

Hall, D. R.
Dept. of Applied Physics
Hull University
Hull, HU6 7RX
U.K.

Hamal, Karel
Faculty of Nuclear Science
& Physical Engineering
Brehova 7
Prague 1
CZECHOSLOVAKIA

Hatat, J. L.
CERGA
Av. Copernic
06130 Grasse
FRANCE

Hirayama, T.
Tokyo Astronomical Observatory
Univ. of Tokyo
Mitaka, Tokyo 181
JAPAN

Hyde, R. L.
Dept. of Applied Physics
Hull University
Hull, HU6 7RX
U.K.

Jelinkova, Ms. Helena
Faculty of Nuclear Science &
Physical Engineering
Brehova 7
115 19 Prague 1
CZECHOSLOVAKIA

Johnson, Craig
EG&G/WASC
6801 Kenilworth Ave.
Riverdale, MD 20840

Johnson, Thomas
Code 723.2
NASA/Goddard Space Flight Center
Greenbelt, MD 20771

Jones, George
Contraves Goerz
610 Epsilon Drive
Pittsburgh, PA 15215

Kiebuzinski, George
DBA Systems Inc.
9301 Annapolis Rd.
Lanham, MD 20801

Kielek, W.
Radiotechnical Institute
Technical University
Novowiejska 15/19
Warsaw
POLAND

King, Robert
Dept. of Earth & Planetary Sciences
Massachusetts Institute of Technology
Cambridge, MASS 02139

Kirchner, George
Observatory Graz Lustbuhel
Institute for Space Research
Austrian Academy of Sciences
Lustbuhelstrasse 45, A-8042
Graz
AUSTRIA

Kloeckler, Paul
Astronomisches Inst.
Sidlerstrasse 5
CH-3012 Bern
SWITZERLAND

Kolenkiewicz, Ronald
NASA/Goddard Space Flight Center
Code
Greenbelt, MD 20771

Kovalevsky, J.
CERGA
Avenue Copernic
Grasse 06130
FRANCE

Kozai, Y.
Tokyo Astronomical Observatory
Osawa
Mitaka - Tokyo 181
JAPAN

Larden, Douglas
Joint Institute for Laboratory
Astrophysics
University of Colorado
Boulder, CO 80309

Latimer, J.
Smithsonian Astrophysical
Observatory
60 Garden St.
Cambridge, MASS 02138

Mangin, J.
CERGA
Avenue Copernic
Grasse 06130
FRANCE

Morgan, Peter
Dept. of Earth & Planetary Science
Code 54-620
MIT
Cambridge, MASS 20139

Morrison, David
Drews Systems, Inc.
599 N. Mathilda Ave.
Suite 245
Sunnyvale, CA 94086

Mueller, I. I.
Dept. of Geodetic Science
Ohio State University
1958 Neil Ave.
Columbus, OHIO 43210

McCarthy, D.
USNO/Time Service Division
34th & Mass. Ave. N.W.
Washington, D.C. 20390

McCarthy, John F.
S41/B322
Hughes Aircraft Space and
Communications Group
P. O. Box 92919
Los Angeles, CA 90009

Nottarp, Klemens
Institut fur Angewandte Geodasie
Satellitenbeobachtungsstation Wettzell
D-8493 Kotzting
FEDERAL REPUBLIC OF GERMANY

Novotny, A.
Faculty of Nuclear Science
& Physical Engineering
Brehova 7
115 19 Prague
CZECHOSLOVAKIA

Oaks, J.
Naval Research Lab (NRL)
Code 7966
4555 Overlook Ave. S.W.
Washington, D.C. 20375

Otten, K.
Delft University of Technology
P. O. Box 581
7300 AN Apeldoorn
NETHERLANDS

Palutan, Franco
Telespazio SPA
Corso D'Italia 43
00198 Rome
ITALY

Paunonen, Matti
Finnish Geodetic Institute
Ilmalankatu 1A
SF-00240 Helsinki 24
FINLAND

Pearlman, M.
Smithsonian Astrophysical Obs.
60 Garden St.
Cambridge, MASS 02138

Pesec, Peter
Observatory Graz Lustbuhel
Institute for Space Research
Austrian Academy of Sciences
Lustbuhelstrasse 46, A-8042
AUSTRIA

Pierron, F.
CERGA
Avenue Copernic
Grasse 06130
FRANCE

Pilkington, J.
Royal Greenwich Observatory
Herstmonceux Castle, Hailsham
East Sussex BN27 1RP
ENGLAND

Prochazka, Ms. Irena
Faculty of Nuclear Science
& Physical Engineering
Brehova 7
115 19 Prague 1
CZECHOSLOVAKIA

Puell, Heinz
Kristalloptik Laserbau GMBH
AM Sulzbogen 62
8080 Fuerstenfeldbruck
West Germany

Rayner, John
Physics & Astronomy
University of Maryland
College Park, MD 20742

Ricklefs, Randall
Dept. of Astronomy
University of Texas
Austin, Texas 78712

Rueger, Lauren J.
The Johns Hopkins University
Applied Physics Laboratory
Johns Hopkins Road
Laurel, MD 20810

Serene, B. E. H.
E.S.A., Centre Spatial de Toulouse
18, Avenue Edouard Belin
31055 Toulouse Cedex
FRANCE

Sharman, P.
Royal Greenwich Observatory
Herstmonceux Castle, Hailsham
East Sussex BN27 1RP
ENGLAND

Shelus, Peter J.
Dept. of Astronomy
University of Texas
Austin, Texas 78712

Silverberg, Eric C.
Department of Astronomy
University of Texas
Austin, Texas 78712

Smith, David
Lageos Project Scientist
Code 921
NASA/Goddard Space Flight Center
Greenbelt, MD 20771

Smith, Floyd
Hughes Aircraft Co.
P. O. Box 90515
Bldg. 130, MS:20
Los Angeles, CA 90009

Snyder, Stanley
610 Epsilon Dr.
Pittsburgh, PA 15238

Steggerda, C.
Physics & Astronomy
University of Maryland
College Park, MD 20742

Tapley, B.
Aerospace Engineering
University of Texas
Austin, TX 78712

Torre, J.
CERGA
Avenue Copernic
Grasse 06130
FRANCE

FOURTH INTERNATIONAL WORKSHOP AND LASER RANGING INSTRUMENTATION

SESSION 1

PROGRESS SINCE 1978; A REPRESENTATIVE OVERVIEW

CHAIRMAN

ERIC C. SILVERBERG

Within the limits of a short proceedings it is impossible to go into great detail on all of the changes which have occurred in the last few years. There are now well over forty active laser ranging efforts in the world, many of which were not in existence in 1978 at the time of the last workshop. Some of these systems have undergone major overhauls, involving from first and second generation laser ranging to systems of third generation capability, while others have had only minimal improvements. The intent of this first session is to give a representative, but by no means complete, sample of the various programs and to outline these changes which have resulted in improvements to this area of technology since 1978. The following papers, some of which were not read at the meeting, serve that purpose admirably and place in context the more specific discussions which follow in the later sessions.

UPGRADE AND INTEGRATION OF THE NASA LASER TRACKING NETWORK

CONTACT: JOHN J. DEGNAN
ANDREW ADELMAN
NASA/GODDARD SPACE FLIGHT CENTER
GREENBELT, MARYLAND 20771 USA

1.0 Overview of the NASA Laser Tracking Network

The Goddard Laser Tracking Network (GLTN) consists of both fixed and mobile laser tracking systems used for precision satellite tracking to provide precise geodetic measurements. The mobile systems are deployed and operated at various locations around the world in response to program requirements. The composition of the GLTN will vary throughout the decade. Initially, the network will consist of seven mobile laser systems (Moblas-2, 3, 4, 5, 6, 7, and 8); three transportable laser ranging systems (TLRS-2, 3 and 4); and two fixed laser ranging stations (SAO-2 and 4) located at Arequipa, Peru and Orroral Valley, Australia, respectively.

The SAO-4 at Orroral will be deactivated at the end of FY84, and will be replaced by the Australian National Mapping Laser (NATMAP). This laser will be operated and maintained by the Government of Australia.

In 1983 a single mission contractor will manage the GLTN to provide specified tracking data in a timely and cost-effective manner. He will be responsible for generation of the necessary orbit predictions, scheduling of GLTN activities, data management and preprocessing, and data quality assessment. He will also be responsible for planning, analysis, and design of new systems; evaluation and analysis of operational systems; and co-equal responsibility with the government for technology development and maintenance, preparation of operations and technical documentation, property management, hardware and software configuration management, implementation of GSFC directed improvements, training, telephone communications, site design and construction at GSFC direction, and maintenance and operation of the laser systems. Additionally, the contractor will have property accountability for these systems and will be responsible for associated facilities and utilities.

Figure 1 depicts the entire network of existing and planned observatories locations including the foreign cooperating observatories we hope will support the program.

From an observatory standpoint, figure 2 clearly shows the extent of measurements possible across most of the important global tectonic plates.

2.0 Upgrade of the Mobile Laser Stations

2.1 Subnanosecond Transmitter

The first set of Mobile Laser stations (MOBLAS 1-3) were equipped with high energy, cavity dumped ruby laser transmitters built by Korad. Upgrading of the latter stations, which currently achieve 2 to 3 cms precision, has been deferred for fiscal reasons. The second set of stations (MOBLAS 4-8) were equipped with Q-switched Nd:YAG laser transmitters built by General Photonics having a FWHM pulsewidth of about 7 nanoseconds. Current MOBLAS receivers are designed to detect and process laser pulses of about 5 nsec duration. In the field, these stations typically achieve ranging accuracy on the order of 8 to 12 centimeters and a serious effort is currently underway to upgrade the performance of these stations, using the best available commercial components, in order to meet the scientific requirements of the next decade.

In order to minimize the interruption of data from the stations during the upgrade period, all engineering modifications (hardware and software) will be implemented and verified on MOBLAS 4 prior to its adoption by the entire MOBLAS network. Modification and upgrade of MOBLAS 4 is being carried out in stages at the Goddard Space Flight Center and began with the installation of a passively-modelocked Nd:YAG laser transmitter in late July 1981. As of September 1981 the system has successfully tracked three satellites - LAGEOS, BEC and Starlette. The transmitter, built by Quantel International, currently provides a single 150 picosecond pulse at a repetition rate of 5 pps. The single pulse output energy is between 60 and 80 mJ and, after two stages of collimation, is confined within a 25 to 30 arcsecond transmitter field of view. In a recent LAGEOS night time pass, a total of 4700 range observations resulted in a single shot RMS scatter about the orbit of only 2.5 cms and a

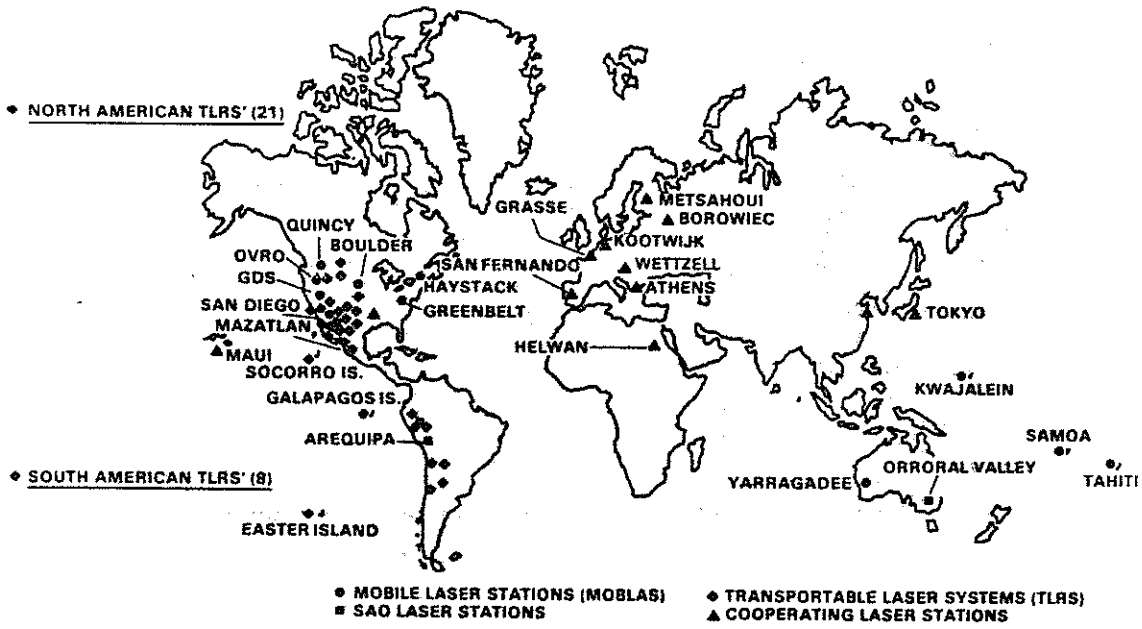

FIGURE 1: LASER TRACKING NETWORK

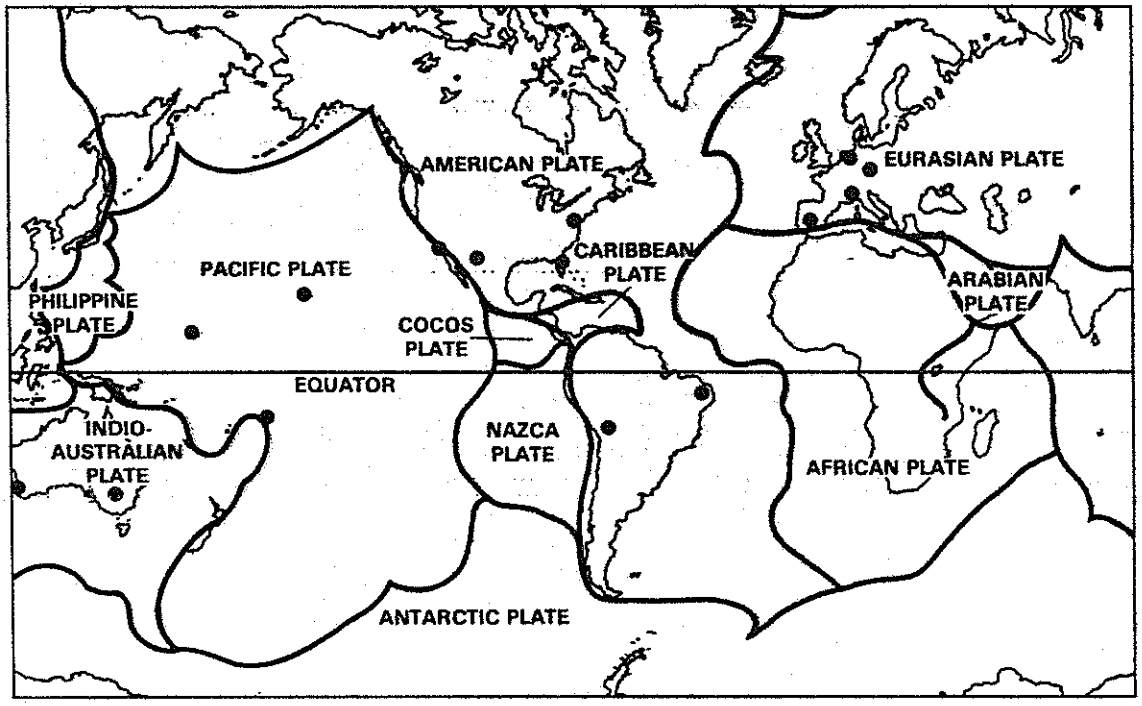

FIGURE 2: GLOBAL LASER RANGING STATIONS

normal point scatter of 1 to 2 cms as determined by the LASPREP processor. MOBLAS 4 has routinely tracked LAGEOS down to the 20° minimum elevation angle and has had a few successful daylight passes as well with no modifications to the receiver. The passive transmitter, which is considerably less expensive than a comparable actively modelocked laser due to its relative simplicity, has proved reliable in the field, and it is anticipated that similar lasers will be installed in Moblas 5 through 8 by Spring 1983.

2.2 MOBLAS Receiver

One difficulty that remains is an occasional but, sizeable discrepancy between the pre and post-calibration measurements of the mean range to the target board. In an effort to eliminate, or at least reduce, systematic biases and to further improve the overall ranging performance, several modifications to the MOBLAS 4 receiver will be implemented and tested during October 1981. These include the replacement of the 2233B photomultiplier, which has a 2 nanosecond risetime and a transit time jitter on the order of 200 picoseconds, with a new low jitter, 300 picosecond risetime, high gain photomultiplier. Laboratory tests are currently underway to evaluate new internal microchannel plate photomultipliers available from ITT and Hamamatsu. The performance of these devices will be compared to that of signficantly more expensive electrostatic and static cross field dynode chain photomultipliers built by Varian. The latter devices are no longer available as an off-the-shelf component but quantity buys may still be possible.

In a second modification, the current dual channel range receiver will be replaced by a single channel receiver which will accept both the start and the stop pulse. Single channel receivers have the advantage that timing delays caused by temperature, voltage, or radiative background changes are automatically compensated for.

Third, an additional pre-calibration procedure will be added in order to determine the time walk of the receiver as a function of the signal amplitude. This information will then be used to correct, via software in the preprocessor, for timing errors introduced by fluctuations in the signal amplitude from either the satellite or calibration retroreflector.

Finally, the HP5360 Time Interval Unit, which has a 100 picosecond bin resolution, will be replaced by the newer HP5370 having a 35 picosecond timing resolution. A similar wideband receiver operated from our Advanced Laser Ranging Laboratory to a fixed retroflector located 0.5 Km away, has provided range data with a single shot RMS scatter of only 4 to 6 mm. Typical pre-and-post calibration runs (100 point averages) typically agree to better than 50 picoseconds which is very near the limiting timing resolution of the receiver. It is hoped that comparable results can be obtained in the field.

Consistent and reliable daylight operation is also an important goal. Recent improvements in our transmitter-receiver boresight techniques have allowed us to narrow the receiver field of view for successful daylight operation - even with the 10 Angstrom bandpass filter. Star calibrations and boresighting have been greatly simplified by the recent addition of a TV monitor which displays the receiver field-of-view on a CRT screen for the computer console operator. Daylight ranging experiments will continue in which two narrow-band spectral filters ($1A^{o}$ and $3A^{o}$) will be evaluated.

In November 1981, the MOBLAS 4 configuration will be frozen. The system will then undergo collocation testing with MOBLAS 7. A spare actively-modelocked Sylvania laser has been installed in the latter station, and MOBLAS 7 is replacing STALAS as the operational GSFC system. Due to the advanced age and poor reliability of several key subsystems, the STALAS operation was terminated following collocation tests with MOBLAS 7.

Following completion of collocation tests with MOBLAS 7 in mid-December, the MOBLAS 4 ranging subsystem will be installed in MOBLAS 8 and will participate in the 1982 measurement campaign in Southern California. Since the MOBLAS 4 ranging system detects multiple photoelectrons, it will provide a valuable comparison to other subnanosecond pulse systems, such as TLRS-1 and TLRS-2, which use single photoelectron detection schemes.

2.3 Safety Radar

New safety radars will only be required for MOBLAS 2, 3, 5, and 7. One spare will be procured to be used in Mexico or any other location. Installation will be completed by June 1983.

3.0 Smithsonian Astrophysical Observatory Laser (SAO)

The four SAO stations are currently operating day and night on low satellites and nighttime only for LAGEOS, with a normal point accuracy of about 10 cm. During the 1981 period, modifications will be made to improve data yield and quality on LAGEOS. These will include (1) increasing the pulse repetition rate on LAGEOS to 30 ppm, (2) upgrading the photoreceiver with a narrower band interference filter and a faster risetime photodetection system, and (3) replacing the waveform digitizer with a less complex and more accurate analog waveform detector. It is anticipated that these modifications will lead to 5 cm normal point accuracy for nighttime ranging to LAGEOS. Engineering analysis indicates that the changes needed to improve the point-to-point accuracy to 4 cm would be feasible but extensive.

4.0 Transportable Laser Ranging Station (TLRS)

Significant increases in station mobility are now possible because of technology improvements and the years of experience accumulated in satellite and lunar laser ranging.

The Transportable Laser Ranging Stations-1 and -2 developed by the University of Texas and GSFC, respectively, are expected to achieve the 1 cm normal point goal of the Project.

TLRS-1 is presently operational and has become an integral part of the crustal dynamics measurement program.

The TLRS-2 is based on a modular concept, which differs from TLRS-1 in that the station is transported by truck and aircraft and assembled at the site. It has been designed for high mobility and low cost and represents the limit on size reduction achievable with current technology. TLRS-2 is currently in the integration and testing phase scheduled for September-December 1981. Tests are scheduled for completion by December 1981, with deployment and field use starting in January-December 1982.

Two additional TLRS systems are planned for procurement beginning in FY82. These stations are required to meet Crustal Dynamics Project needs for regional deformation studies in South America, New Zealand, and the Caribbean.

The combination of operational data accumulated by TLRS-1 and engineering/packaging data and test data accumulated by TLRS-2 will be used to determine the design of the follow on TLRS. At that time, a decision will be made as to whether TLRS-3 and -4 should be fabricated by GSFC or procured through a competitively selected contractor. Primary considerations in arriving at this decision will be the Crustal Dynamics Project schedules as dictated by project objectives and international agreements, costs, and availability of in-house manpower.

5.0 Haleakala Laser Facility

It is expected that the Haleakala Laser Facility will have two separable ranging functions in the Crustal Dynamics Project. The first function is ranging to LAGEOS and the second is ranging to the lunar retroreflector arrays.

According to data submitted to the University of Texas, there were about 100 returns from the lunar arrays in 1977 using the combination of the multi-element Lurescope receiver telescope and the Lunastat transmit optics. There have been no attempts to range to the moon since 1978 due to problems with staffing, the multi-element telescope and and priorities for satellite ranging.

At the present time the station has ranged recently only to satellites. However, there are some serious limitations to the amount and quality of the data being collected. For example, the station does not have daylight LAGEOS capability, due primarily to the unique arrangement of the transmit/receive optics.

In July 1980, operation of the facility was interrupted to incorporate satellite laser ranging upgrade and improvements. The following changes are completed. These changes are expected to improve the accuracy (4 cms or less) by reducing systemmatic errors and to increase the quantity of satellite ranging data.

1. Establish system delay calibration
2. Optimize receiver
3. Install new time interval unit

4. Optimize electronics/optics

5. Install new computer and develop additional software

Following the satellite ranging upgrades, it is planned to devote effort to achieving lunar laser ranging on a regular basis. At present, it is not evident whether this will require minor or major system modification. Tests of the Lurescope will be conducted in early 1982 and will provide the basis for a definitive plan.

6.0 McDonald Laser Ranging Station (MLRS)

In December 1979 a contract was issued to the University of Texas for design and fabrication of the MLRS. This system, which is a result of earlier work leading to TLRS-1, will be capable of ranging to the moon and to LAGEOS.

The MLRS will be permanently located at the site of the McDonald Observatory. After completion of the MLRS testing program in late 1981, the MLRS will assume the lunar ranging function performed by the Observatory since 1969.

7.0 Australian National Mapping (NATMAP) Laser Facility

The Australian National Mapping Laser Facility at Orroral Valley was provided by the U.S. to Australia on a loan basis in 1974. This system currently has only a lunar ranging capability. Initial ranging with this system has achieved lunar ranging at the 30 cm level. Improvements being carried out by NATMAP should result in ranging at the 15-18 cm level. However, this accuracy is not adequate to support the global program of lunar ranging. In addition, it would be desirable (from the U.S. viewpoint particularly) for this facility to also range to LAGEOS.

Through a series of discussions during the past year, it has become evident that both Australia and the U.S. would benefit from a cooperative program to modify and upgrade the NATMAP facility for both lunar and satellite ranging.

This modification would include:

1. Replacement of the current telescope mount with a new X-Y system.

2. Installation of a Coude system.

3. Replacement of the laser and laser electronics.

It is planned to accomplish the modification through agreement with NATMAP. The U.S. would provide funds for system hardware and NATMAP would provide personnel to manage the development, assist in the installation and checkout, and to operate the facility.

PERFORMANCE AND RESULTS OF SATELLITE RANGING LASER STATION AT KAVALUR, INDIA IN 1980 - 81

by

P.S.DIXIT, P.K.RAO, R.RANGA RAO, K.GOPALAKRISHNAN and K.L.RAO

Indian Space Research Organisation, India

S.SCHILLAK

Space Research Centre, Poland

W.KIELEK

Technical University of Warsaw, Poland

and

M.ABELE

University of Riga, USSR

ABSTRACT

In this paper, the environmental data during 1980-81, Laser ranging system, system calibration and its accuracy under various conditions, system stability, quality of the data obtained during 1980-81, methods of range reduction, system limitations and the proposed method for upgrading the system accuracy and its capability with reference to Interkosmos laser ranging station at Kavalur (India) are discussed.

1 INTRODUCTION

A Satellite Tracking and Ranging Station (STARS) is established in the campus of Indian Institute of Astrophysics, Kavalur ($12^{o}34'$N, $78^{o}51'$E and 700 M above MSL), India for a joint scientific and technical collaboration between the Indian Space Research Organisation (ISRO) and the Academy of the Sciences of the USSR (AS-USSR) for the investigations

in the field of Geodesy, Geodynamics and upper atmospheric research. The Station is equipped with Interkosmos satellite ranging laser radar, AFU-75 satellite tracking camera, timing equipments and data processing systems. The basic characteristics of the Interkosmos laser ranging radar has been described in the references cited (A.G.Massevitch et al. 1973, K. Hamal, 1978).

In Fig.1 is shown the monthly statistics of cloud-free nights for satellite observations at Kavalur during 1980-81. In Fig.2 is shown the monthly statistics of the trend in refraction constant during 1980-81 at Kavalur, showing the quality of environment for the satellite and astronomical observations.

II DESCRIPTION OF LASER EQUIPMENTS

The detailed description of the first and second generation Interkosmos laser radars are described in the referenc es cited (A. Asaad et. al, 1978, K.Hamal et. al, 1978). At Kavalur laser ranging station, the first generation Interkosmos laser radar is equipped with HP 5061A Cesium beam frequency standard, HP 105B crystal controlled oscillator with time code generator, Datum 9880A VLF receiver and Volana-K all-wave HF receiver to maintain epoch for laser and camera in UTC and UT_1 (BIH time scales) respectively.

Epoch at the station is maintained primarily by means of portable clock trips from National Physical Laboratory (NPL), New Delhi, custodian of time and frequency in India. VLF tracking receiver provides an accurate method of monitoring record of time position relative to the setting obtain ed from the portable clock comparision. The HF time signals offeres the station a convenient epoch of the order of ± 0.5 ms as well as regular DUT_1 correction to UTC time scale. The current accuracy of the Station's clock in UTC is of the order of ± 5 micro seconds.

III SYSTEM CALIBRATION

Fig.3 shows the target calibration in micro seconds for

the return signal strength measured in photo-electrons for a fixed target located at a distance of 519.18 ± 0.01 meter from the laser radar and using a median detector (W.Kielek, 1977). The performance of three photomultipliers i.e. RCA 8852, FEU 84 (0560) and FEU 84 (9143) of USSR origin are shown in the Fig.3. Except for detector internal delay for a given pulse detection system (adaptive threshold) all the three photomultipliers, show similar performances. The detailed target calibration shows the overall laser ranging system accuracy of the order of 30 cm. In Fig.4 is shown the performance of the above said three detectors using a constant fraction (0.125) detection system with an integrating amplifier. For the Kavalur laser radar both the adaptive threshold as well as constant fraction detection technique gives almost the same accuracy in the range measurements. This may be due to the fact that the resolution of the time interval counter which is of the order of 2 nano seconds and the detectable errors between adaptive threshold and constant fraction detection technique are less than 2 nano seconds.

Data taken from day to day pre and post pass calibration difference over 60 days are plotted in Fig.5 and gives a standard deviation of the order of 0.65 ns. The long term stability of the laser radar therefore could be assessed from the long term pre and post pass target calibrations. The short term stability of the system is shown in Fig.4 and Fig.5 by plotting the rms error of each observation at a pre-selected input signal strength.

IV QUALITY OF DATA EVALUATION AND RANGE REDUCTION

The laser range data obtained are processed on IBM 370/155 computer using least square polynomials, Tsechebycheff's polynomials (short arc fitting technique) and long arc orbit fitting technique (P.S.DIXIT et. al, 1978). For laser ranging radar at Kavalur the above;three methods give equivalent results if number of observations are suffciently greater than the degree of the polynomial used. In Fig.6 is shown the predicted epoch against range (ms) for Geos C (7502701) satellite The true laser returns obtained after computer processing are also shown in this figure. Least squares filtering programme

is used to eliminate the spurious laser returns (P.Lala, 1976). In Fig.7 is shown the distribution of range residuals for Geos C (7502701) satellite computed from several passes for 1980-81.

In Table 1 are shown the number of laser shots fired, estimated probable returns and actual laser returns obtained from computer processing of Geos A (6508901) and Geos C (7502701) satellites between September - October 1980 and January - May 1981. The overall laser ranging accuracy of the laser radar is of the order of 60 cm (RMS). In Table 2 is shown the comparision between the orbital elements of Geos C as derived from the observations (Kavalur) and that obtained from SAO for the same mean epoch in order to access the quality of tracking data. Since 1st September 1980, Kavalur laser station is involved in the tracking of Geos A (6508901) and Geos C (7502701) satellites for MERIT programme i.e. determination of polar motion and variations in the rotation of the earth in cooperation with other Interkosmos, CNES and SAO Laser network stations.

Table 1 : Statistics of laser return signals for Kavalur station during September - October 1980 and January - May 1981

Satellites	Number of laser shots fired	Number of probable returns	Number of good returns within RMS accuracy of one meter
6508901	125	95	80
7502701	1530	1170	920

Table 2 : Orbital elements of 7502701 satellite derived from laser observations at Kavalur using indigenous differential orbit improvement programme (IDOIP)

MJD : 44610.0

PARAMETER	STARS	STANDARD DEVIATION	SAO
a (km)	7219.5942	0.157705D-02	7219.593107
e (--)	0.0006005316	0.7868577D-05	0.001212951
i (deg)	114.9932	0.2634692D-02	114.9887
w (deg)	29.26217	0.1162906D+01	64.87311
Ω (deg)	197.8669	0.1379284D-02	198.2673
m (deg)	373.3692	0.1160242D+01	337.7824
n (deg/day)	5095.665	0.1669645D-05	5095.668
$\dot{n}/2$(deg/day^2)	0.001750845	0.1394849D-02	0.001350
MJD : 44694.0			
a (km)	7219.374746	0.00054676	7219.3905456
e (--)	0.001282280	0.2455407D-03	0.001250845
i (deg)	114.9930	0.14654230-02	114.9891
w (deg)	305.8063	0.1264736D+02	35.82264
Ω (deg)	67.02369	0.1836457D-02	67.41879
m (deg)	70.58636	0.1269409D+02	340.4544
n(deg/day)	5095.897	0.5789041D-03	5095.881
$\dot{n}/2$(deg/day^2)	0.002681672	0.5540522D-04	0.00167652

V CONCLUSIONS

The capability of laser range radar at Kavalur to range fainter than 9^m satellites and to improve the visibility of Geos A and similar satellites is under consideration. A three-stage image intensifier coupled with a low light level camera and a television system (Sofreterc, CF 123 NV camera with Nocticon TH 9659) will be incorporated in the laser radar guiding mechanism by June 1982. The TV guidance control is expected to improve the pointing accuracy of the laser to the satellite and thereby eliminating personal errors due to eye-sight fatigue during the observation and inturn increase the number of laser returns (P.S.Dixit et.al, 1979). The

possibility of Kavalur laser station for the participation in LASSO-SIRIO time synchronisation experiment is under consideration (B.Serene et.al, 1980).

VI ACKNOWLEDGEMENT

Authors would like to express their thanks to Prof.A.G. Massevitch, Vice President of the Astronomical Council of the USSR, Dr. S.Tatevian of AC-AS USSR, Dr. K.Hamal Karel, Co-ordinator of the Interkosmos Laser Radar Working Group, Technical University of Prague, Czechoslovakia and Col.N.Pant, Director, SHAR Centre (ISRO), India for the continued suggestions and keen interest taken in our work.

VII REFERENCES

Massevitch, A.G., Abele,M., Almar.I., Daricek.T., Hamal.K., Kellek.W., Navara.P., Novotny.A.,and Stecher.R., " Interkosmos Mobile Satellite Laser Ranging Observatory", Proceedings of the International Symposium on the Uses of Artificial Satellites for Geodesy and Geodynamics, Atens, Greece, 1973.

Lala.P., " Accuracy of Laser Ranging to Satellites from Ondrejov Observatory ", Paper presented at working session Poland CSSR, GDR on 'Problems of Satellite Geodesy' Zgorzelec, Poland, April, 1976.

Hamal,K., " Interkosmos Laser Radar Network", Third workshop on Laser Ranging Instrumentation, National Technical University, Athens, Greece, 1978.

Asaad.A., Baghous.B., Fahim.M.,Jelinkova.H., Novotny.A., Hamal.K., Tatevian.S., Rubans.A., Massevitch,A.G., Latimer.J., Gaposchkin.E.M., and Pearlman.M.R. " Up - grading of Interkosmos Laser Ranging Station at Helwan (Egypt)", The proceedings of the T hird Workshop on Laser Ranging Instrumentation.,Lagonissi, Greece, 1978.

Kielek.W., Patent No.102469, Poland, 1975

Dixit.P.S., " Upgrading the Tracking Capabilities of Satellite Ranging Laser Radar by incorporating the Image Intensifier and Television Guidance Control," M.S. (Electrical Engineering) Research project proposal Report, Indian Institute of Technology, Madras,India 1979.

Dixit.P.S., Lala.P., and Sen.A.K., " Comparisons of Ordinary Least Squares Polynomials, Tschebycheff's Polynomials and an Orbital Method for Fitting Laser Range Data to a Satellite Orbit", Nablyudenia, IS², Nr.18, Warszawa, 1979.

Serene, B., and Albertinoli.P., " The LASSO Experiment on the SERIO 2 Spacecraft", ESA Journal, Vol.4, PP 59-72, 1980.

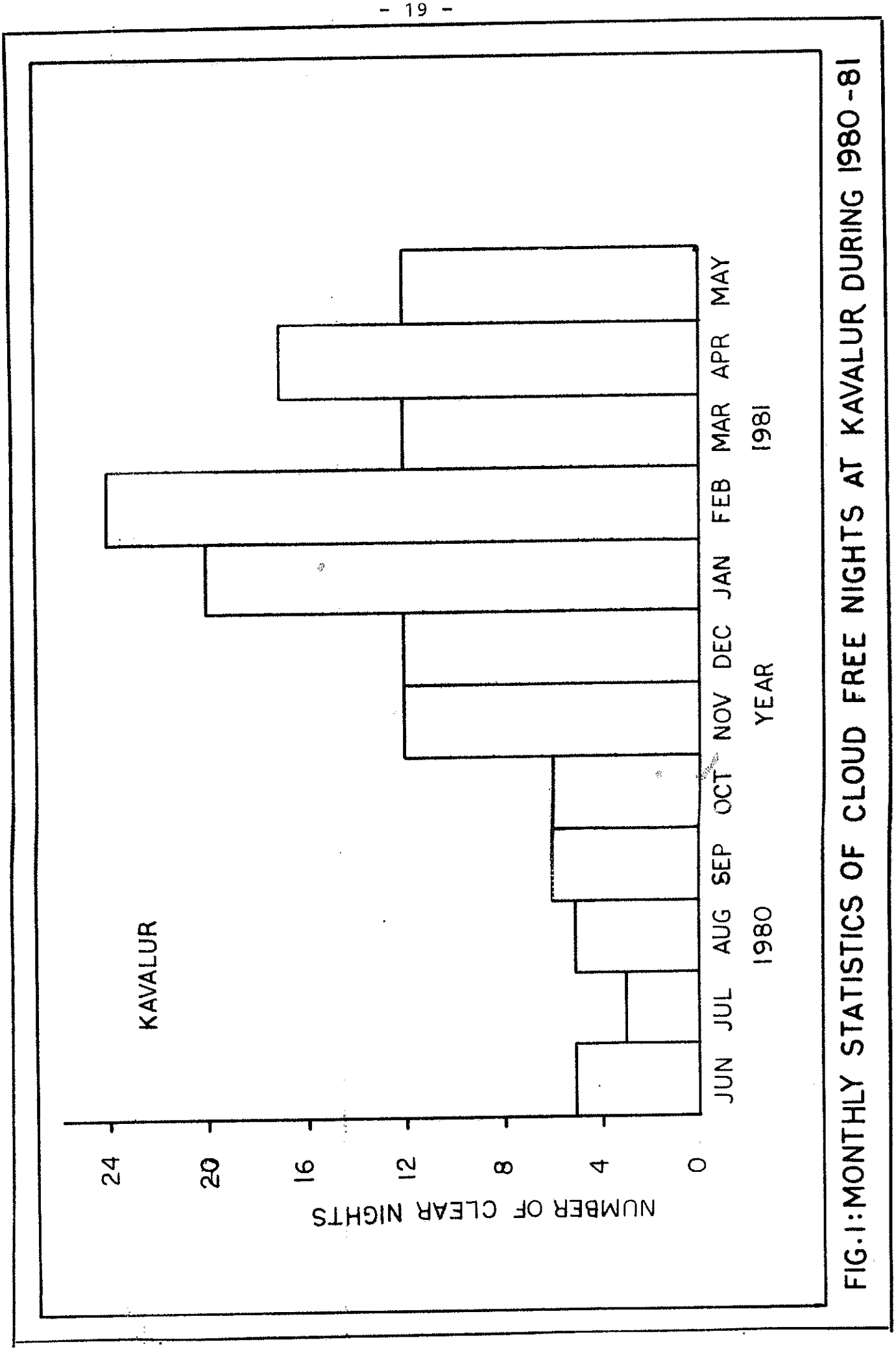

FIG.1: MONTHLY STATISTICS OF CLOUD FREE NIGHTS AT KAVALUR DURING 1980-81

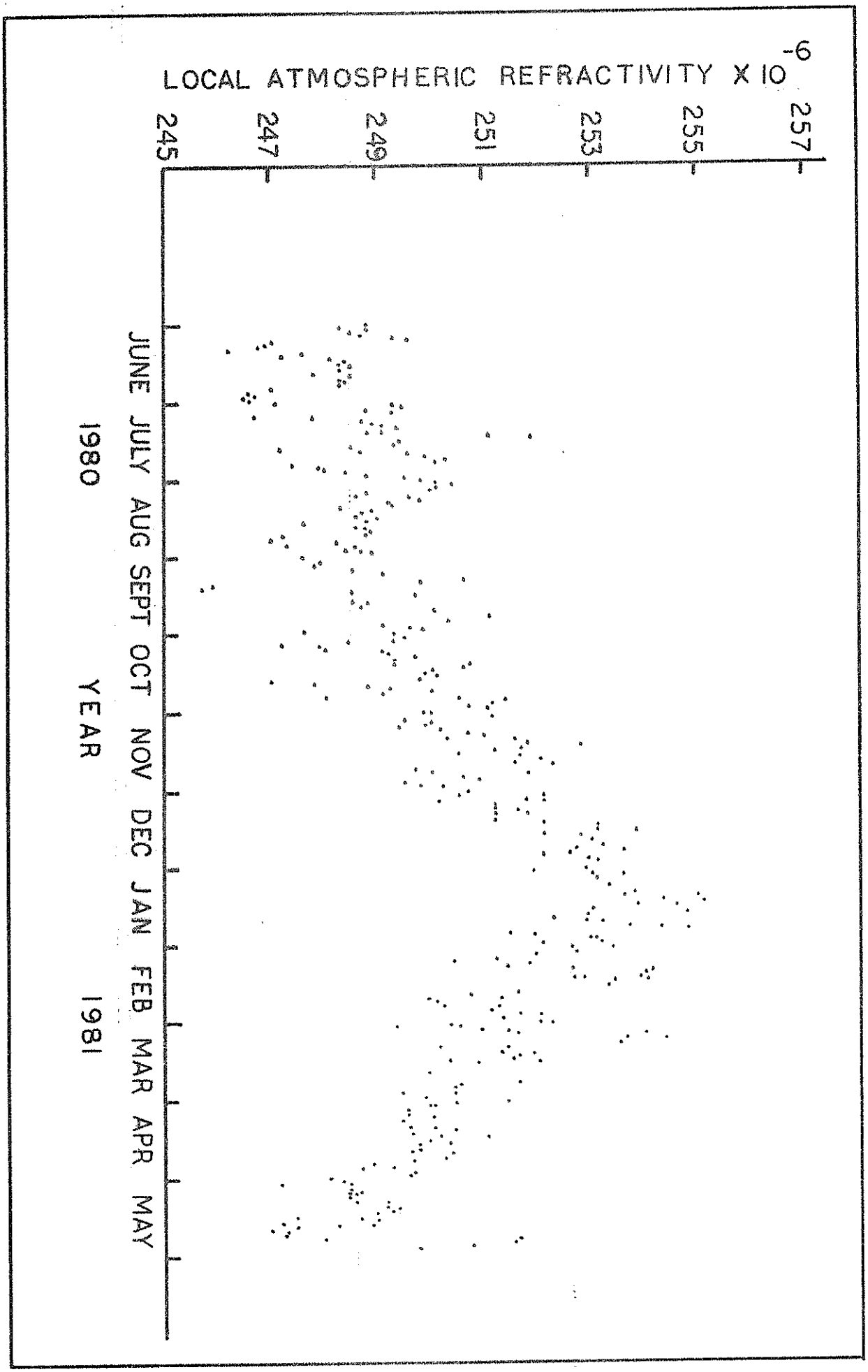

FIG.2: DAY Vs REFRACTIVITY PLOT FOR KAVALUR (1980 - 1981)

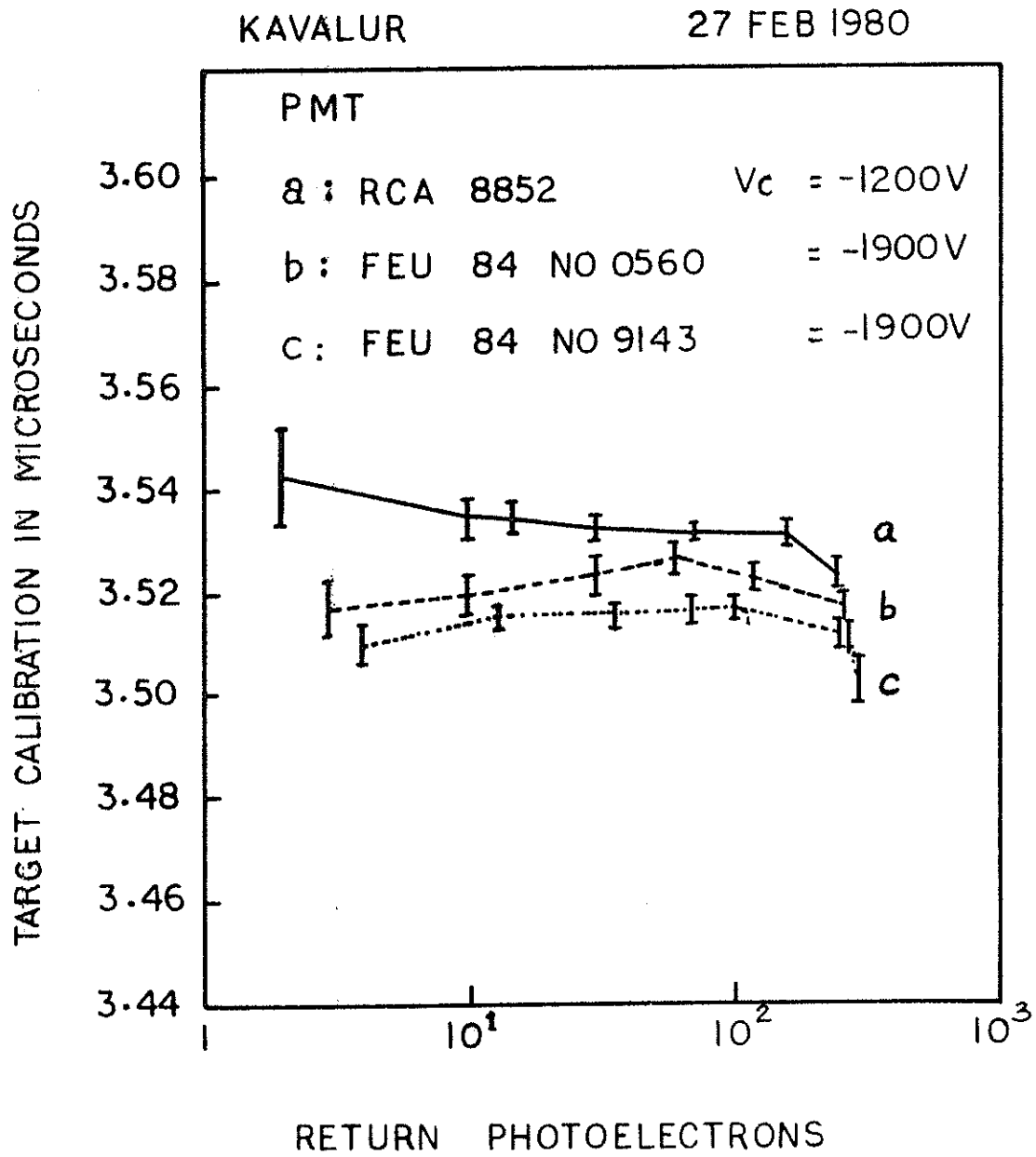

FIG.3: RETURN SIGNAL STRENGTH Vs CALIBRATION DISTANCE FOR A FIXED TARGET FOR KAVALUR STATION

(MEDIAN DETECTION TECHNIQUE)

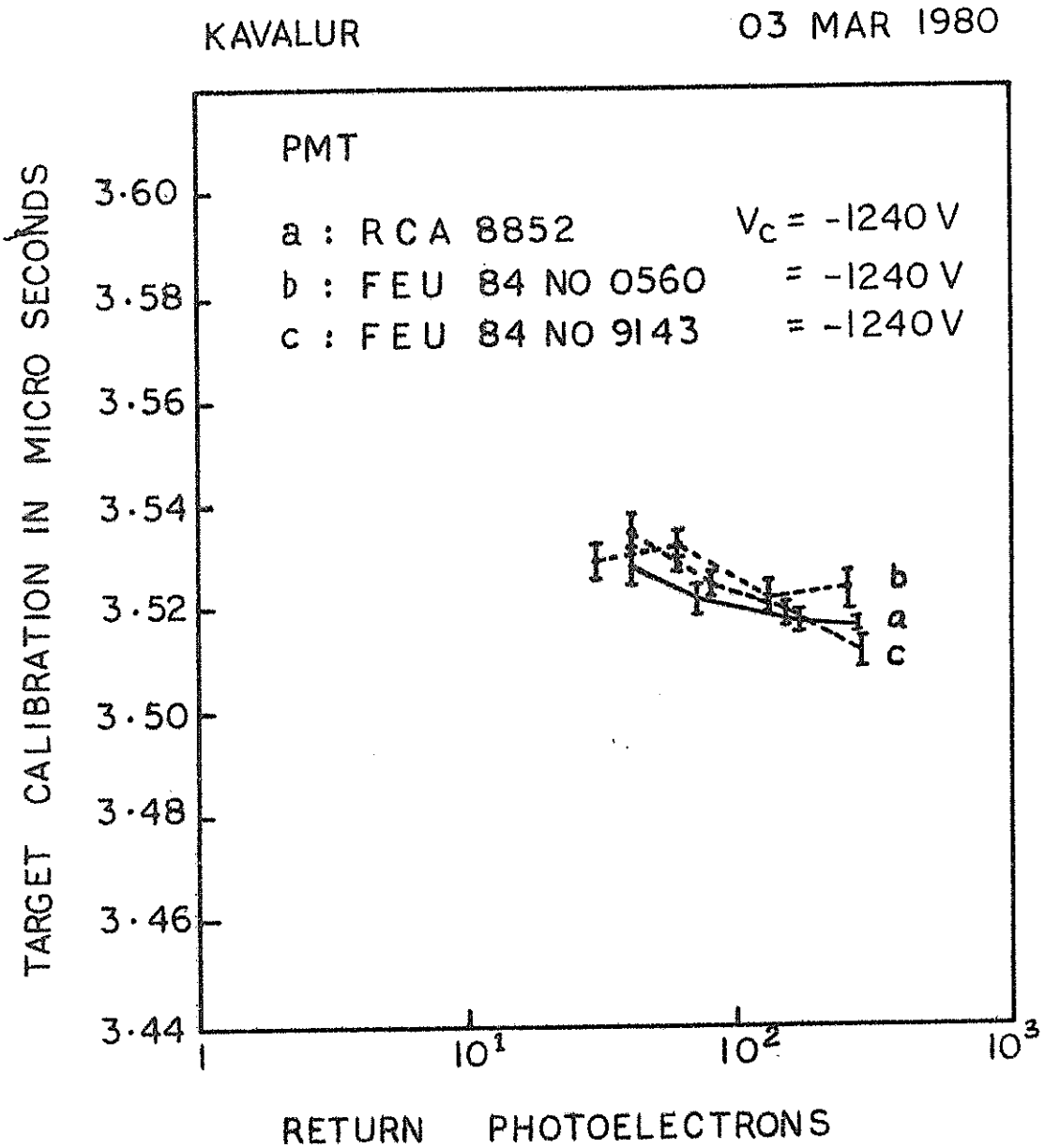

FIG. 4: RETURN SIGNAL STRENGTH Vs CALIBRATION DISTANCE FOR A FIXED TARGET FOR KAVALUR STATION

(CONSTANT FRACTION DETECTION)

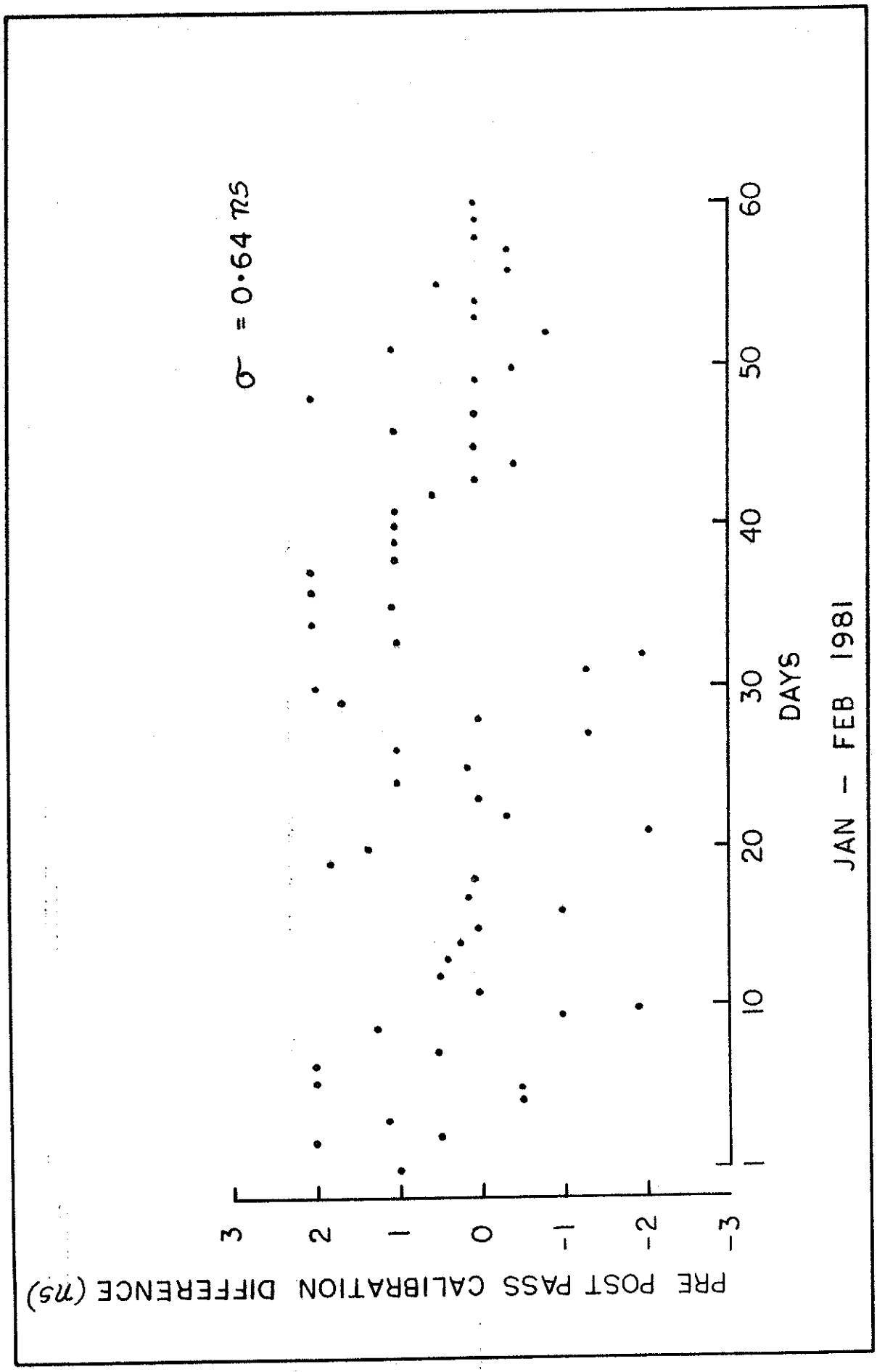

FIG. 5 : PRE POST PASS CALIBRATION STABILITY FOR KAVALUR LASER 1980-81

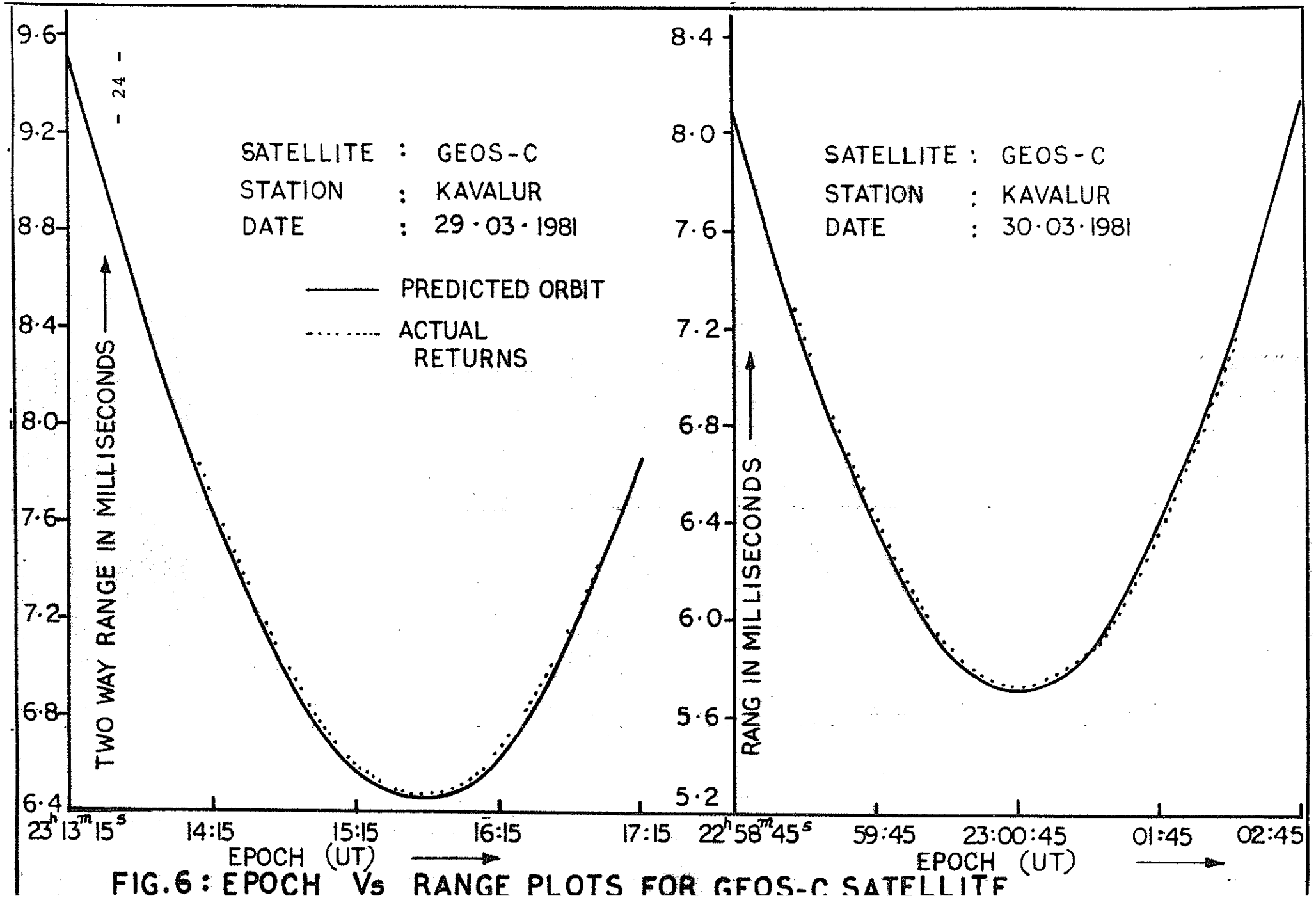

FIG.6 : EPOCH Vs RANGE PLOTS FOR GEOS-C SATELLITE

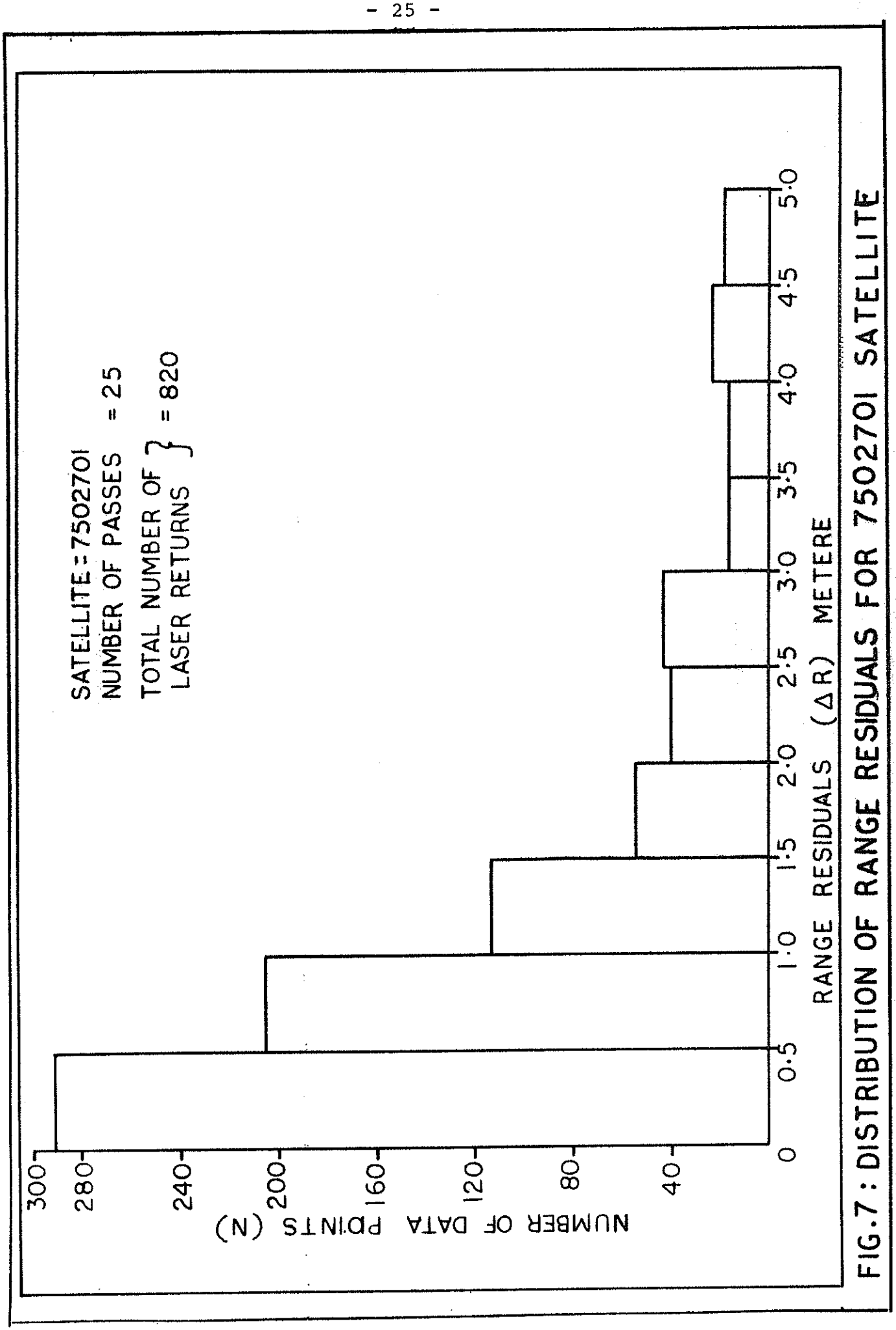

FIG.7 : DISTRIBUTION OF RANGE RESIDUALS FOR 7502701 SATELLITE

INTERKOSMOS SECOND GENERATION SATELLITE LASER RADAR

K.Hamal, H.Jelínková, A.Novotný, I.Procházka, M.Čech
INTERKOSMOS

Faculty of Nuclear Science and Physical Engineering
Czech Technical University
Brehova 7, 115 19 Praguel
Czechoslovakia

To range the satellites, the Interkosmos Laser Radar Network of the first generation has been built since 1971 /1/ /2/.The network consists of 14 stations located in Africa, Asia,Europe,South America and Cuba/3/. The visual tracking, inherent for most of these stations, allowes a broad field of view; however, the operational efficiency is limited because of sun ilumination requirements, daylight observations are excluded. To avoid these limitations, the prototype of the second generation laser station /hardware+software package/ had been built during 1978-80 and since December 1980 it has been operating in Helwan, Egypt /4/.

Content :

INTERKOSMOS LASER RADAR NETWORK

TABLE 1

2. GENERATION LASER RADAR (HELWAN 7831)

MOUNT	CONFIGURATION	AZIMUTH - ELEVATION
	TRACKING	CONTINUAL
	TRACKING RATE	UP TO 1 DEG/SEC
	RESOLUTION	4.5 ARCSEC
LASER	TYPE	OSCILLATOR - AMPLIFIER
	OPERATIONAL	Q-SWITCH/PTM/PFM
	ENERGY	0.1-0.2 JOULE/NSEC
	PULSE LENGTH	20/6/5/4/3/2 NSEC
	PULSE REPRATE	15/MIN
RECEIVER	OPTICAL ARRANGEMENT	REFRACTOR,ASPHERICAL
	DIAMETER	0.4 METER,F=0.8 METER
	RANGE GATE	COMPUTER CONTROL,100 NS
		MANUAL VERNIER
	THRESHOLD DETECTOR	CONSTANT FRACTION
	DETECTOR	PMT RCA 8852/RCA C31034
TIMING	TIME INTERVAL RES	100 PICOSEC
	FREQUENCY STANDARD	CESIUM CLOCK
	EPOCH REFERENCE	LORAN C,FLYING CLOCK
COMPUTER	CPU FLOATING POINT	32 KWORDS OF 16 BITS
	STORAGE MEDIUM	5 MBYTE DISC
	I/O FACILITIES	CONSOLE,PAPER TAPE,PRINT
SOFTWARE	PREDICTION	MODIFIED SAO WETTZELL
	CALIBRATION	POINTING,RANGING,ETC
	SAT TRACKING	MANUAL TIME VERNIER
		ON-SITE PREDICTION
	POST DATA HANDLING	NOISE REJECTION
		INTERNAL ACCURACY CHECK
		TELEX TRANSMITTION

Fig.1.

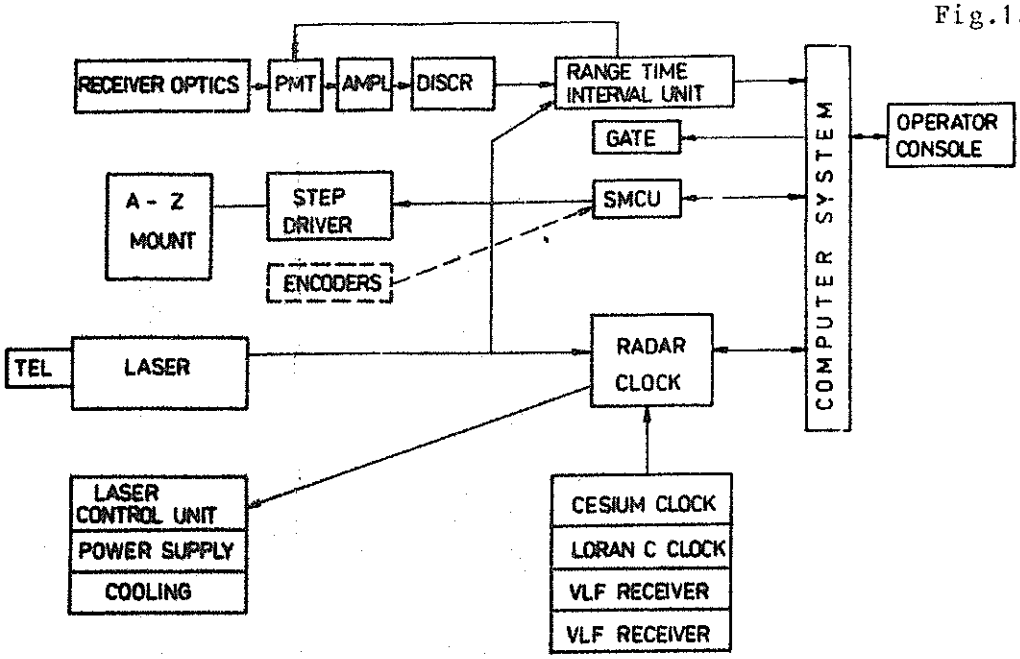

Laser ranging system.

Fig.2.

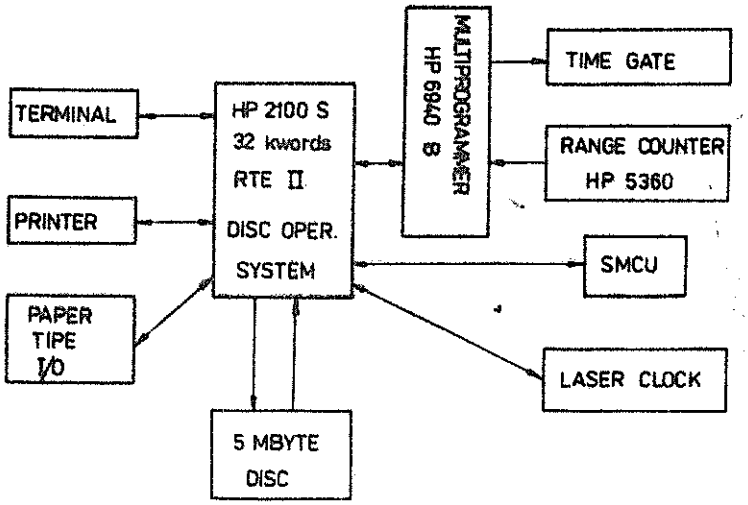

Hardware computer system.

FIG. 3.

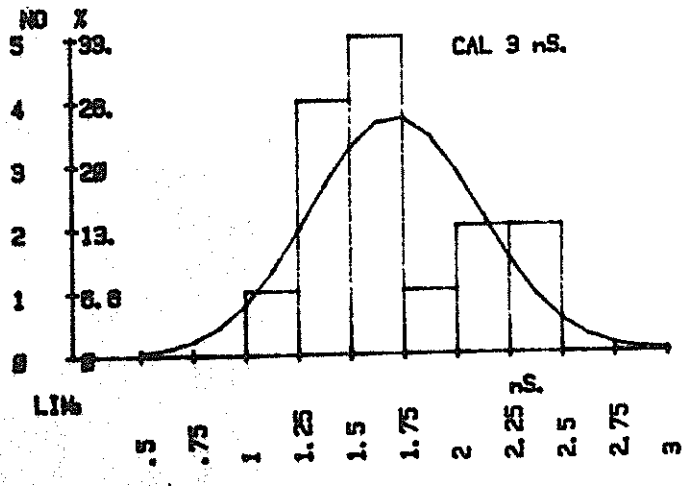

TIME INTERVAL MEASUREMENT	+/-2.2 CM
GEODIMETER	+/-0.5 CM
ATMOSPHERIC CORRECTION	+/-1.0 CM
TOTAL	+/-2.5 CM

CALIBRATION ACCURACY

M O N T H L Y R E P O R T TABLE II.

PERIOD AUGUST 1981
STATION HELWAN 2, 7831

	BE-C	GE-A	STARL	GE-C	LAG	TOTAL
TRACKED	31	33	39	25	27	155
MEASURED	26	29	33	21	24	133
NO RETURN	2	4	0	2	2	10
HARW.FAILURE	3	0	1	2	0	6
SOFT.FAILURE	0	0	1	0	1	2
CLOUDY SKY	0	0	4	0	0	4
NO.OF ECHOES	1459	2860	1412	889	1710	8321

TOTAL NO.OF OBSERVING NIGHTS : 29
TOTAL NO.OF LASER SHOTS : 36 000

SYSTEM CAPABILITY,OPERATIONAL SUMMARY

FIG. 4

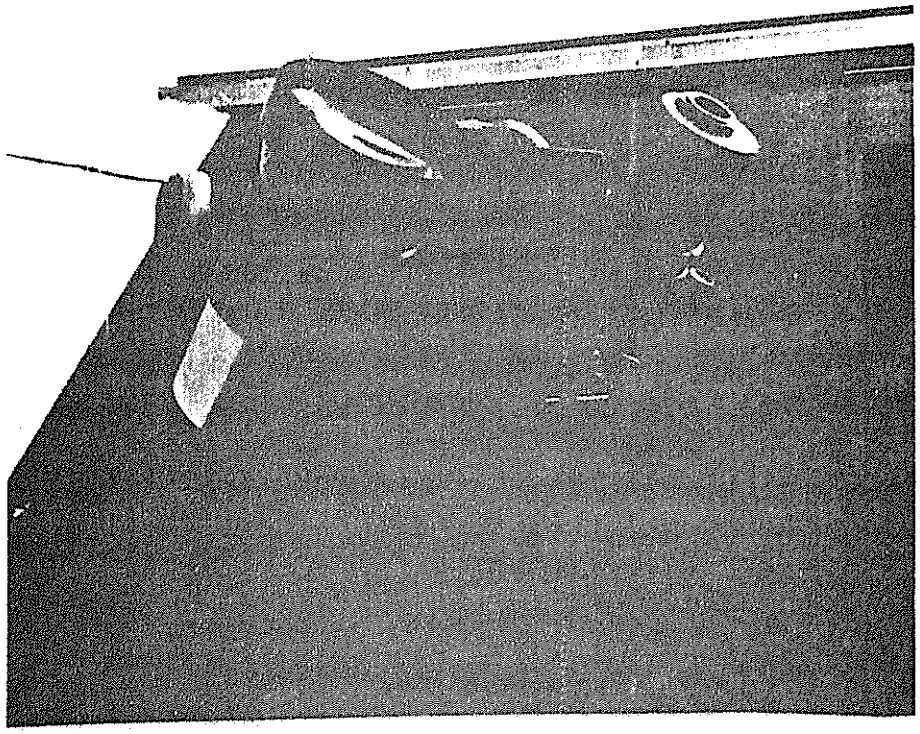

Photograph of the mount/laser/receiver subsystem

L I T E R A T U R E

/1/ A.G.Massevitch,M.Abele,I.Almar,T.Daricek,K.Hamal,W.Kielok P.Navara,A.Novotny,R.Stoecher,in:First International Symposium of the Use of Artificial Satellites for Geodesy and Geophysics,Athens, May 1973

/2/ A.G.Masevitch,K.Hamal,In Cospar, Philadelphia, 1976

/3/ K.Hamal,in:Third Workshop on Laser Ranging Instrumentation, Lagonissi, May, 1978

/4/ K.Hamal,H.Jelinkova,A.Novotny,I.Prochazka,A.Asaad,M.Fahim A.G.Masevitch,S.Tatevan,M.R.Pearlman,Interkosmsos Second Generation Laser Radar,Rep.80/121,FJFI-CVUT,Prague 1980

LASER RANGING SYSTEMS IN THE FAR EAST AREA (CHINA AND JAPAN)

YOSHIHIDE KOZAI

TOKYO ASTRONOMICAL OBSERVATORY

MITAKA, TOKYO, JAPAN 181

There are not so many satellite tracking facilities, particularly, satellite and/or lunar laser ranging instruments in the Far East Area. As far as I know there is one laser ranging system at Tokyo Astronomical Observatory in Japan and there are four systems in China, namely, at Peking(Beijing), Shanghai(Zo-se), Yunnan and Shensi observatories. Also in Japan the Hydrographic Department intends to install a modern satellite laser ranging system by this December(1981).

At the Tokyo Astronomical Observatory the project to install a satellite laser ranging instrument was started around 1967 with cooperation of technical staff of the Hitachi Ltd.(T. Takenouchi et al., Satellite Ranging with a Laser, Hitachi Review, 19, 153, 1969). It was installed at the Dodaira Station of the Tokyo Astronomical Observatory where a Baker-Nunn camera was. We could range geodetic satellites by this instrument with 60cm accuracy, however, since the instrument was driven manually any daytime observations as well as those when satellites were invisible were not possible(Y. Kozai et al., Satellite Laser Ranging Instruments Operated at Tokyo Astronomical Observatory, Tokyo Astron. Bull., No. 223, 1973).

Then by use of 188cm reflector at Okayama Astrophysical Station we made some experiments for lunar laser ranging in 1970-1971(Y.Kozai, Lunar Laser Ranging Experiments in Japan, Space Research XII, 211, 1972; A.Tachibana et al., Lunar Laser Ranging System in Japan, Space Research XII, 187, 1972).

After that we intended to install a new laser ranging instrument for both satellites and the moon at the Dodaira Station and a reflect-

ing telescope of 50cm aperture and 380cm metal-mirror telescope were installed there. The 50cm telescope is on X-Y mount and for the tansmitting for the moon and the receiving for satellites and the 38cm telescope is on alt-azimuth mount and for the receiving for the moon. All the axes are driven by torque motors which are connected with a minicomputor. We bought also a ruby laser oscillator with three amplifiers for the moon and an electric chopper for satellites.

Unfortunately the progress after that is very slow. We could range some of geodetic satellites even in daytime and when satellites are invisible, however, the percentage of the number of the returned signals over that of the transmitting ones is not so high because alignments of the three axes, the optical axes of the transmitting and receiving telescopes and the laser beam axis are not good and changing as the telescopes move because of flexure of the transmitting telescopes. We are now trying to range Lageos satellites by introducing new techniques to keep good alignments and by using the laser oscillator for the moon.

For the moon we have been struggled with the torque motors to drive the telescopes. Our problem is that once the telescope points the predicted direction the computor, of course, does not want to move the telescope and, therefore, no torque acts on the motors. However, once wind comes the telescope moves. Such a standing torque is our serious problem, however, by introducing new device I hope that we can solve the problem in near future.

The instrument which the Hydrographic Department wants to have is one of the same type Wettzel station has. It will be Wakayama, south of Osaka, and will be in operation as soon as it will arrive there.

There are reports on the laser ranging instruments at Shanghai and Yunnan observatories. It is very glad to hear that a new system will be installed at Shanghai and it will range Lageos satellite even in daytime.

METSÄHOVI SATELLITE LASER RANGING STATION

Matti V. Paunonen*

Finnish Geodetic Institute
Ilmalankatu 1 A
SF- 00240 Helsinki 24, Finland

1. INTRODUCTION

This report gives a brief description of the status of the Metsähovi satellite laser ranging station (7805) of the Finnish Geodetic Institute. System planning was initiated in 1972 in cooperation with the Helsinki University of Technology with financial support from the Academy of Finland. The system has been in operation since September 1978 and has so far produced about 6000 range observations to various satellites.

2. EQUIPMENT

The equipment is in essence similar to that reported at the previous Laser Workshop in Lagonissi /1/. The main technical data are given in Table 1.

The laser transmitter uses an electro-optically Q-switched multimode ruby laser oscillator with an output energy of 1 J, a pulse length of 25 ns, a collimated beam divergence of 1.2 mrad and a repetition rate of 1/15 Hz.

A 630 mm diameter parabolic mirror is used in the receiver. The field of view is also 1.2 mrad. An RCA C 31034

---

*Also with the Communications Laboratory, Helsinki University of Technology, SF- 02150 Espoo 15, Finland

photomultiplier is used in night work and an RCA 8852 in daylight. The pass band of the interference filter is 3 nm. An electromechanical shutter is used to protect the photomultiplier from laser light backscattering from the near atmosphere. Approximated matched filtering with an impulse response of $t \cdot \exp(-t/\tau)$ /2,3/ is used in detection. The half widths of the laser pulse and the impulse response of the filter are equal. Presently the integration time of the photomultiplier preamplifier has been increased to 40 ns to test the performance of median detection /4/. The start pulse is filtered in the same way. The travel time of the laser pulse is measured with a Nanofast 536B counter and a M/2 half-max plug-in (detection fraction 0.5 of the true peak), providing about 0.15 ns instrumental resolution.

A new equatorial, sidereally driven, telescope mount was installed in 1979. The telescope system uses open loop, computer operated, stepper motor actuated point-to-point tracking with a step size of 6 arcsec. The pointing accuracy is about 0.3 mrad. The laser is mounted on top of the telescope. The laser and telescope systems are operable down to at least $-22^{\circ}C$. The ranging system can be operated by one person. Aircraft detection is done visually.

Satellite positions are calculated in advance using SAO elements and a new quick orbit program /5/ and stored on magnetic tape. The range gate, which is computer controlled, has a resolution of 1 µs. The gate widths used are in the range 10 - 40 µs. The difference between the observed and predicted (O-C) satellite distance is calculated on line and fed to a printer to allow monitoring of the return rate and gate position. The resulting data (epoch with 1 µs resolution, time interval with 0.1 ns resolution, the direction angles used, air pressure, temperature and humidity and O-C differences) are logged on magnetic tape. Corrections to the firing time of the laser can be made via the keyboard. Visual detection of the satellite, when possible, is used to check any time offsets.

Station time keeping is achieved using a quartz oscillator (HP 105 B), which is phase locked to LORAN C transmission (Sylt). The accuracy is better than 10 µs. The operating frequency of the counter (1 MHz) is derived from this source.

Several problems have been encountered in the course of operations. A major problem has been inadequate fastening of the flashlamp electrode. Also, the original Pockels cell was replaced by a liquid filled cell when it was found to be producing multiple pulses. The counter is somewhat

Table 1. Technical data of the Metsähovi laser rangefinder

Laser	ruby, helical flashlamp, water cooling, Pockels cell Q-switched
Energy	1 J, stability 10%
Pulse width	25 ns
Repetition rate	1/15 Hz
Beam divergence (laser)	3 mrad
Transmitting optics	Inverted Galilean telescope, aspherical objective Ø 115 mm, power 7 X, adjustable collimation, 1.2 mrad used
Receiver optics	Ø 630 mm parabolic mirror, f=1730 mm
Field of view	1.2 mrad
Interference filter	3 nm pass band, 0.7 transmission
Overall transmission	0.5
Photomultiplier	RCA 8852, quantum eff. 4 %, for day and night operation RCA C 31034, quantum eff. 10%, for night operation
Electronic amplifier	8 MHz bandwidth (3dB), two cascaded RC- stages, impulse response 25 ns (FWHM), also preintegration possible
Time interval counter	Nanofast 536B
Timing processor	" M/2, half-maximum plug-in, 50 % of the true peak detected 0.15 ns r.m.s. resolution
Telescope mount	Equatorial, sidereally driven, offsetted by stepper motors and worm gears, computer controlled, computer 16 bit, 32kwords
Tracking	Automatic, point-to-point, speed 1.5 degrees/s max.
Guiding telescope	Celestron 8, Ø 200 mm, field of view 1 degree.
Timing	Quartz clock HP 105B, phase-locked to LORAN C (Sylt), accuracy better than 10 μs
Calibration	Flat target, 333.48 m distance

temperature sensitive and can produce quite stable false sublevels in readings. Also, the timing discriminator creates variable positive biases, even over 10 ns, for small pulses that are just sufficiently over the treshold. Because no return pulse monitoring is in use, the effects of small and saturating pulses may be found in the observations.

3. RESULTS

The number of observed passes and ranges are shown in Table 2. Passes with less than five ranges are not included. The best ranging season is expected during the months March-May and August-December. There are 50-80 clear nights during these months in one year. June and July nights are luminous.

Table 2. Satellite passes and observations

Period	LAGEOS		STARLETTE		GEOS-3		GEOS-1	
	Passes	Obs	Passes	Obs	Passes	Obs	Passes	Obs
1978 Sept-Oct	-	-	-	-	16	140	-	-
1979 Sept-Oct	8	85	1	5	2	25	16	380
1980 March-May	14	420	1	13	8	130	13	360
1980 Aug-Dec	25	1180	13	200	16	250	15	270
1981 March-May	34	1160	11	195	-	-	11	370
1981 Aug-Sept	8	330	2	30	6	110	-	-
	89	3175	28	443	48	655	55	1380

3.1. Range capability

The measured range capability of the Metsähovi laser ranger is shown in Table 3. Ranges to LAGEOS are currently limited by the capacity of the storage system for predictions (150 points, minimum elevation 34°). Daylight operation to GEOS-3 has been found feasible (ranges to 1700 km).

3.2. Precision

Several common methods of data preprocessing have been used: polynomial fitting to the O-C differences, Kepler orbit fitting with J_2 term (called Sterne solution /6/) and direct polynomial fitting to ranges. Also a new method called Quick-orbit has been tested. A reference orbit is constructed using the first and last observation of the pass (accurate ranges, directions taken from the predictions, accurate to

Table 3. Range capability

Satellite	Measured range (km)	Min. elevation (degrees)	Data yield (%, max.)
LAGEOS	7550	34	60
STARLETTE	2490	17	80
GEOS-3	1850	20	100
GEOS-1	3600	25	95

±0.6 mrad as in /6/. The range differences of the observations are then formed. The quality of the range observations can be determined by fitting a polynomial of suitable degree to the range differences(generally under 1000 m).

No iterations nor precisely computed predictions are needed. Fig. 1 shows an example of the residuals obtained with different methods. For this and the previous pass the SAO QUICK LOOK processed data was also available. It is easy to see that the QUICK LOOK and the double pass Sterne solutions show trend-like residual behaviour. The single pass Sterne, QUICK LOOK with a third degree polynomial and the Quick-orbit with a fourth degree polynomial produce very similar residuals, but with somewhat different standard deviations. It is obvious that this phenomenon is connected with the quality of the reference orbit used and the degree of the polynomial required to remove the trends.

In ranging to LAGEOS photon counting or single photoelectron detection /7,8/has been used from the very beginning. The voltage of the photomultiplier is increased until the single photoelectron impulses are able to trigger the counter. Both photomultiplier have been used. Fig. 2 shows an example of range residuals obtained with the Quick-orbit (sixth degree polynomial). There were 74 signal counts from 116 possible, and no noise counts. The air pressure was 1014 mb, temperature 2.8°C, humidity 80% and the gate width 12 μs. The histogram of the distribution of the residuals is shown in Fig. 3. The standard deviation is 0.68 m. Generally, the precision to LAGEOS has been about 1 m. In one monitored pass (signal counts amounting to 20, RCA 8852 tube), where only a couple of two photoelectron pulses was seen, the precision was 0.84 m. This is somewhat better than could be expected theoretically by noting the duration of the transmitted pulse ($\sigma_R = 0.5c \cdot 0.425T$). The precision to GEOS-3 has generally been in the range 0.3-0.8 m, and to STARLETTE and GEOS-1 0.4-1 m.

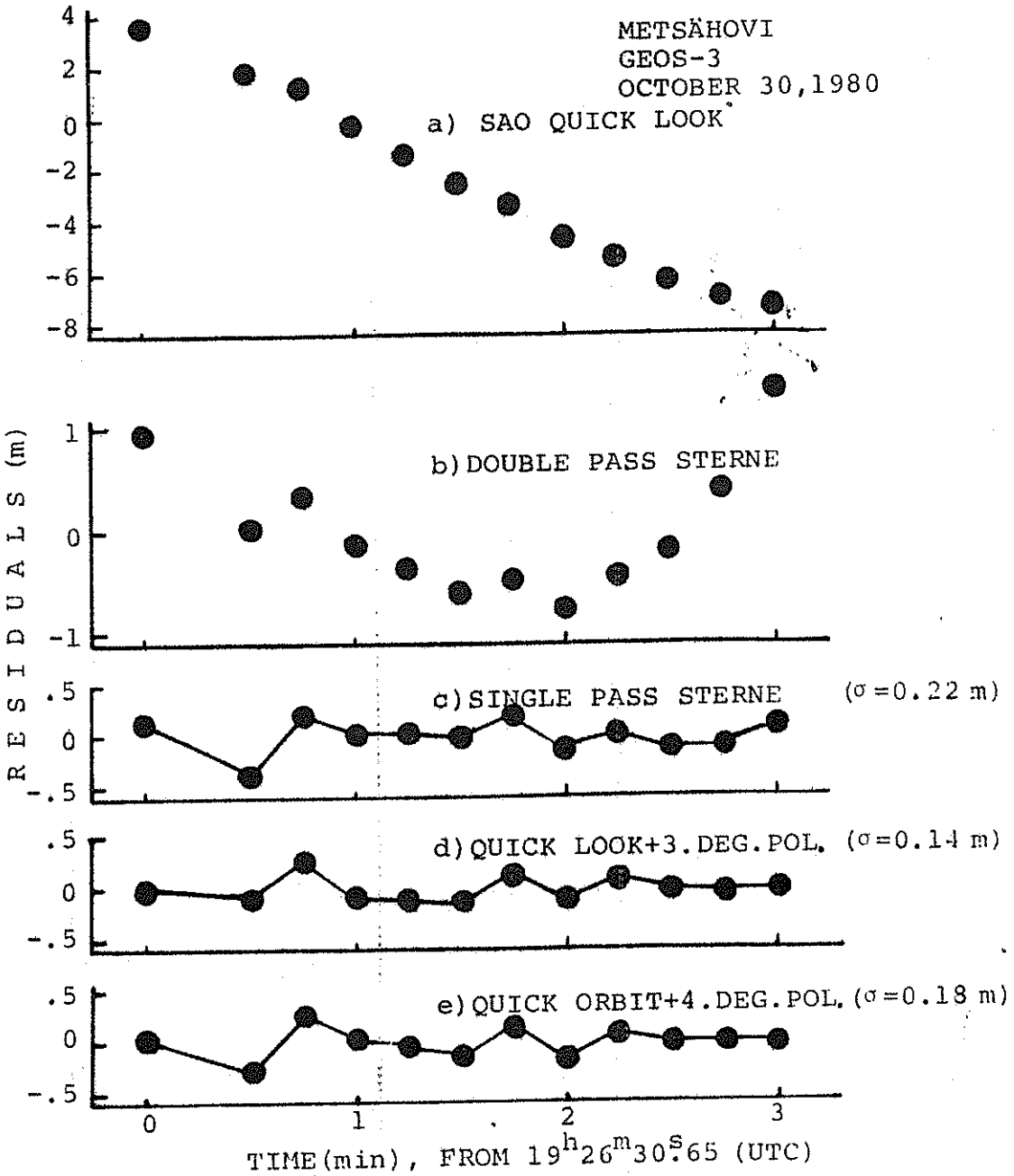

Fig. 1. Range residuals of a GEOS-3 pass from different processing methods

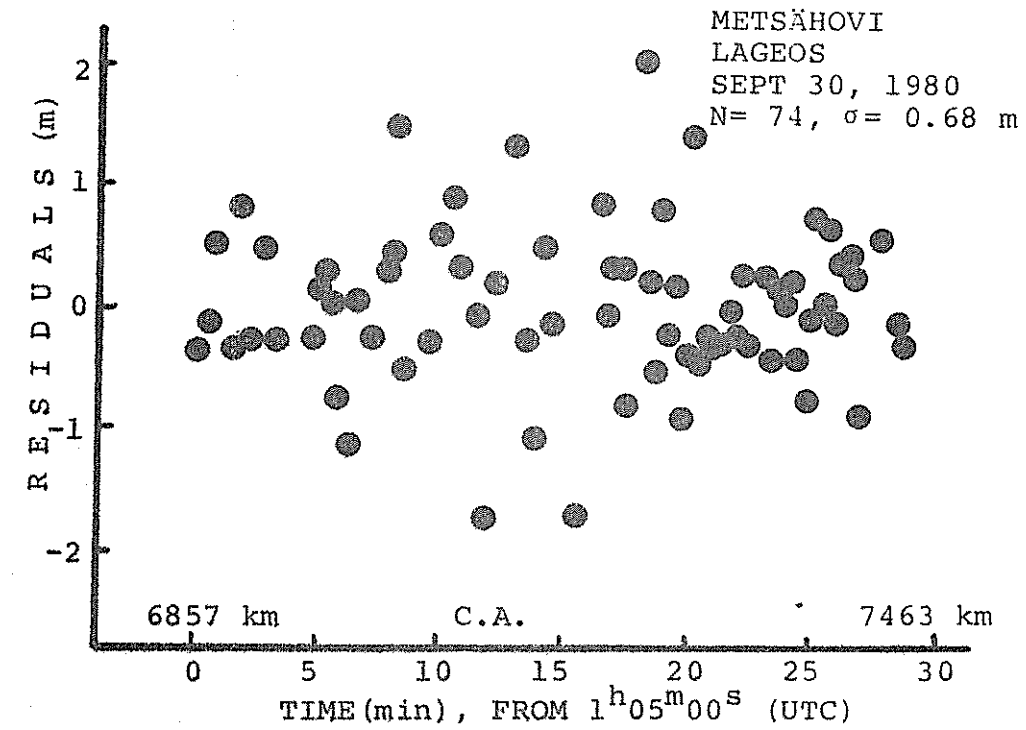

Fig. 2. Range residuals of a LAGEOS pass processed by the Quick orbit (6th degree polynomial).

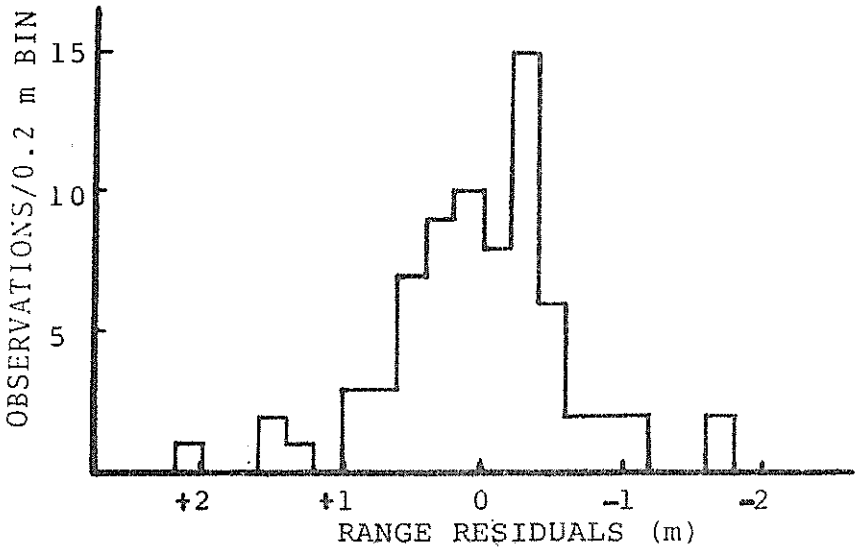

Fig. 3. Histogram of the residuals of the LAGEOS pass Sept 30, 1980, Fig. 2.

3.3. Accuracy

The coordinates of the Metsähovi laser have recently been determined from the LAGEOS data obtained during the short MERIT Campaign /9/. These coordinates and the Doppler coordinates (NSWC 9Z-2) of the laser from the EROS-DOC determination /10/ are compared in Table 4. A small correction (Δx= 0.05 m, Δy= 0.00 m, Δz= -0.20 m) to the Doppler coordinates is applied because of the new mount. Because different coordinate systems are used, a coordinate transformation is necessary before the results can be compared. Applying recently reported corrections to Laser and Doppler coordinates with respect to VLBI /11/ (to Laser: rotation angles ε= -0".09, ψ = 0".01, ω = -0".23, scale $-0.01 \cdot 10^{-6}$, translations Δx= 0.44 m, Δy= -0.84 m, Δz= -3.64 m and to Doppler: rotation angles ε= 0".07, ψ= -0".01, ω= -0".84, scale $-0.51 \cdot 10^{-6}$, translations = 0 m) gives the transformed coordinates shown in Table 4. The resulting difference in distance is 0.54 m. If a recently published combined Doppler solution is used (corrections Δx= -0.66 m, Δy= 0.18 m, Δz= 0.13 m) the difference in Laser and Doppler determinations becomes $(\Delta x, \Delta y, \Delta z)_{L'-D'}$ = (0.13 m, -0.04 m, -0.09 m) or in range 0.16 m. The comparison with the Kootwijk and Wettzell stations also shows consistency of the ellipsoidal height to within 0.5 m, longitude to within 0".22 and latitude to within 0".04.

Table 4. Coordinates of the optical center of the Metsähovi laser ranger

Determination	x (m)	y (m)	z (m)
LAGEOS, MERIT data /9/	2892598.21	1311806.00	5512609.93
DOPPLER, EROS-DOC /10/	2892603.97	1311796.61	5512609.42
LASER, TRANSFORMED	2892596.89	1311805.97	5512606.95
DOPPLER, TRANSFORMED	2892597.42	1311805.83	5512606.91

4. PLANS FOR FUTURE WORK

To improve the performance of the Metsähovi laser station, construction of a short pulse Nd:YAG laser has been started. The pulse length should be around 1 ns and the repetition rate 1 Hz. So far, only the power supplies and discharge circuits have been designed. The telescope will use 50 cm diameter Cassegrain optics. The mount will be azimuthal.

There may still be some interest in uppgrading the old ruby laser. A technique for shuttering a pulse of a few nanoseconds duration has been developed using KN 22 (EG&G) krytron switch tubes.

5. CONCLUSION

The Metsähovi laser ranger still belongs to the first generation. The performance has met, and in some respects surpassed, the initial expectations. However, more work is required to stabilize operation. The precision obtained is about 0.5 m. The first results concerning station coordinate determination indicate an accuracy of about 1 m or better.

6. ACKNOWLEDGMENT

The author is indebted to the Academy of Finland for support during different phases of this project.

7. REFERENCES

/1/ S.J.Halme, M.V.Paunonen, A.B.R.Sharma, J.Kakkuri, K.Kalliomäki, The Metsähovi laser ranging system. Proc. Third International Workshop on Laser Ranging Insrumentation. National Technical University of Athens, 1978, pp. 119-124.

/2/ M.Paunonen, Estimation of the arrival time of light pulse using approximated matched filtering. Paper presented at the Third International Workshop on Laser Ranging Instrumentation, Lagonissi, Greece, May 23-27, 1978.

/3/ M.Paunonen, Use of approximated matched filtering and photon counting in satellite laser ranging. Paper at this conference.

/4/ A.B.Sharma and S.J.Halme, Receiver design for laser ranging to satellites. IEEE Trans. Instrum. Meas.

IM-30,1(1981)3-7.(Presented also in Lagonissi in 1978).

/5/ M.Vermeer, QIKAIM, a fast semi-numerical algoritm for the generation of minute-of-arc accuracy satellite predictions. Reports of the Finnish Geodetic Institute, 81:1, Helsinki 1981, 17 pp.

/6/ J.Kakkuri, O.Ojanen,and M.Paunonen, Ranging precision of the Finnish satellite laser range finder. Reports of the Finnish Geodetic Institute, 78:8, Helsinki 1978, 11 pp.

/7/ S.K.Poultney, Single photon detection and timing: Experiments and Techniques. Advances in Electronics and Electron Physics (Ed. L.Marton) 31(1972)39-117.

/8/ C.O.Alley, J.D.Rayner, R.F.Chang, R.A.Reisse, J.Degnan, C.L.Steggerda, L.Small, and J.Mullendore, Experimental range measurements at the single photo-electron level to the Geos-A and BE-C satellites. Paper presented at the Third International Workshop on Laser Ranging Instrumentation, Lagonissi, Greece, May 23-27, 1978.

/9/ B.E.Schutz, The University of Texas at Austin, Dept of Aerospace Engineering and Engineering Mechanics, private communication.

/10/ W.Schlüter, P.Wilson, and H.Seeger, Final results of the EROS- Doppler observation campaign. Paper presented at the XVII General Assembly of the IUGG, Canberra, Australia, Dec. 2-15, 1979.

/11/ J.G.Gergen, Modern observation techniques for terrestrial networks. Paper presented at the IUGG/IAG Symposium on Geodetic Networks and Computations. Munich, FRG, Aug. 31 - Sept. 5, 1981.

/12/ W.Schlüter and P.Wilson, Combining the results of European Doppler observation campaigns computed at the IfAG/SFB 78. Ibid.

CURRENT STATUS AND UPGRADING OF THE SAO LASER RANGING SYSTEMS

M. R. PEARLMAN, N. LANHAM,
J. WOHN and J. THORP

SMITHSONIAN ASTROPHYSICAL OBSERVATORY
CAMBRIDGE, MASSACHUSETTS 02138

The SAO lasers, which have been in routine operation since 1971, have been upgraded several times with resulting improved accuracy, data yield and reliability. At the last Laser Workshop in 1978 we reported on the installation of the pulse processing system centered around a waveform digitizer and some fast pulse modules to determine pulse centroid and signal strength. The work reported was based on our experience with the 25 nsec wide ruby laser pulse. See Pearlman, et al., 1978.

CURRENT STATUS

Since the last Laser Workshop, SAO has introduced pulse choppers into the laser systems to reduce laser pulse width to 6 nsec. This, coupled with the previously installed signal processing system centered around a waveform digitizer, gave us a very dramatic improvement in system ranging accuracy now estimated at about 10cm (1 sigma).

The chopper is, basically, a Krytron-activated Pockels cell with entrance and exit dielectric polarizers for necessary transmission and isolation. (See Figure 1). A Blumlein circuit provides the proper high-voltage pulse to operate the Pockels cell and a PIN diode and avalanche transistor circuit to trigger the system. The Blumlein is

essentially a delay-line structure, in which delays and reflections are used to produce a high voltage rectangular pulse of desired width from a voltage step provided by the Krytron. The configuration, installed in 1978, used a ceramic Blumlein with a length of 15 cm, a width of 1.75 cm, and a dielectric constant E = 30. This reduced the laser pulse width from 25 nsec to a 6 nsec output pulse with a 2-3 nsec risetime.

The optical assembly of the chopper was designed to fit between the original laser oscillator and amplifier sections, thus minimizing installation impact in the field. The assembly consists of a thin-film dielectric polarizer sharpener and analyzer, a KDP 50Ω Pockels cell. The Pockels cell is operated in pulse-on for transmission mode. The pulse chopper timing is controlled in a gross sense by an optical attenuation in front of the PIN diode. Fine tuning is made by bias adjustments to the pin diode.

The chopper was designed by SAO and Lasermetrics Inc. of Teaneck, New Jersey. It was built by and is available from Lasermetrics.

The return pulse shape, is recorded with the LeCroy Waveform Digitizer (WD2000) with sampling channels set 1 nsec apart. Pulse centroid is determined in real time on the station minicomputer using a cross-correlation technique based on a sample output pulse recorded at the beginning of each pass. Experience has shown that the pulse shape is well constrained by the pulse chopper and does not vary appreciably during a pass (or even day to day).

The current characteristics of the system are summarized in Figure 2. Further details on the hardware and software are given in Pearlman et. al., 1978.

ASSESSMENT OF PERFORMANCE

The ranging performance capability of the lasers with the pulse chopper has been assessed by examination of both systematic errors and range noise. These refer to performance of the ranging machine itself, leaving aside issues such as atmospheric correction, spacecraft center of mass correction, and epoch timing for discussion elsewhere.

The systematic errors of the laser system have been divided into three categories: spatial, temporal, and signal-strength variations. Spatial variations refer to differences in time of flight depending on the position of

the target within the laser beam. Temporal variations relate to system drift between prepass calibration and postpass calibration. Variations in range due to changes in signal strength from pulse to pulse are a function of receiver characteristics and digitizer sampling interval.

Spatial variations, or the wavefront error, which arise from the multimode operation of the ruby lasers, have been measured at Mt. Hopkins using a distant target retroreflector to probe the beam. Figures 3A and 3B shows the results before and after installation of the pulse chopper. The wavefront measurements performed with the chopper show a maximum deviation within the beam of +/-0.3 nsec (4.5 cm) from the mean value across the wavefront. The standard deviation of the excursions is about 0.2 nsec (3 cm).

The temporal variations on system drift are estimated by the difference between prepass and postpass calibrations measurements. These differences represent an upper bound, since other statistical errors are also included. A typical example of a month's calibration data is shown in Figure 4; monthly means for all of the SAO stations average 4-6 cm.

Variations in apparent range with signal strength have been examined with extended target calibrations over the dynamic range of the laser instrument. Figure 5 shows an example of one such calibration. The mean calibration over the operating range of 1-300 photoelectrons is typically flat to better than +/-0.4 nsec (+/-6 cm).

Using systematic error values of 4.5, 6, and 6 cm for the spatial, temporal, and signal-strength variations respectively; and assuming that these errors are independent, the root-sum squares (rss) error due to systematic sources is about 10 cm. We use this value to characterize the systematic errors that can be expected for data averaged over a pass.

In the SAO laser point-to-point range noise varies from 7-15 cm on passes of low orbiting satellites with high effective cross-section (such as Geos 1 and 3) to 25-50cm on Lageos (See Figure 6). At intermediate signal strengths the noise is dominated by the quantization statistics for the 6 nsec output pulse.

In the low signal strength Lageos operating regime of 1-3 photoelectrons we anticipate a noise level of 25-35 cm due to the 6 nsec wide pulse. In reality, we have additional corruption due to the poor response of the

photomultiplier and the inadequate sampling of the digitizer at the single photoelectron level. The 5 nsec wide pulse (at the single photoelectron level) is sampled only at 1 nsec intervals. At high signal strengths, inherent PMT and detection system jitter which amounts to .2-.3 nsec (3-5 cm) plus additional contributions from propagation effects, satellite characteristics and wavefront distortions begin to play a significant role in the range noise value. See Pearlman et. al., 1981.

CURRENT LASER UPGRADING PROGRAM

An upgrading program is now underway to improve laser performance in the areas of pulse repetition rate, accuracy, and signal-to-noise (daylight) response. The current operational characteristics for the SAO lasers and those anticipated after upgrading are shown in Figure 2.

The laser power supply control unit is being modified to enable the system to fire at rates up to 30 ppm. The fundamental limitation in the past has been the tracking regime of the mount which must stop at each point to fire and is thereby limited by rates of speed and acceleration. By adding the capability to vary the firing rate by satellite and geometry, the "slower moving" LAGEOS satellite can be tracked at much higher firing rates (15-30 ppm). There will also be an advantage with some of the lower satellites that can be tracked at rates above the current 8ppm.

To improve range accuracy, the pulse width is being reduced to 2-3 nsec by changing the Blumlein structure and some of electronics in the pulse chopper. The limitation here will probably be the response of the Krytrons and the tradeoff with output energy (depth of chop). Based on our experience to date, we anticipate that the wavefront distortion effect will be reduced in proportion to pulse width with the chopper. The 2-3 nsec pulse should reduce the effect to about +/-2 cm (peak to peak). The current RCA 7265 PMT is being changed for an Amperex 2233A with an EMI Gencom base which has been tuned for low signal level response. This combination gives a considerably improved waveform stability at low signals (See Figure 7). In addition, the front of the PMT is being apertured down to 1.5 cm to reduce jitter. We were able to reduce the jitter (peak to peak) from about 0.5 nsec to 0.25 nsec (peak to peak) with this method.

To avoid accuracy limitations due to waveform sampling (at 1 nanoseconds) and to accommodate the faster pulse repetition rate, the waveform digitizer is being replaced by an analog pulse detection system. This detector consists of a matched filter tuned for the laser pulse. The filter is followed by a differentiator and slope-triggered low threshold discriminator, which functions essentially as a cross-over detector. Results of an initial field test of the analog detector with a 6 nsec lase pulse using the Amperex 2233 PMT and EMI Gencom base are shown in Figure 8. The results are similar to those found using the digitizer. The importance of this system will increase when the laser pulse width in the field is narrowed. An additional advantage of the analog detector is the simplification of system hardware and software.

Several modifications are being made to improve the signal to background noise ratio. The photoreceiver is being modified to accommodate a fast shutter and a 3 Angstrom Day Star filter, which replaces the current 8 Angstrom interference filter. The range gate system is being upgraded to accept range gate windows down to +/- 0.1 microsecond (30 meters) from the currently used +/-5 microsecond window. See Latimer et al., 1981, for a discussion on the capability of the SAO prediction software. These improvements will increase signal to noise by about 16-20 db which should permit the laser to operate on Lageos further into daylight conditions.

The prototype of the upgraded hardware and software are being installed and tested now at Mt. Hopkins. The production units are in different stages of completion depending upon the questions yet to be answered in testing. We expect to field the production units in the Arequipa, Orroral Valley and Mt. Hopkins lasers in early 1982. The modifications are also to be built for the Natal laser for installation when and if the laser is relocated.

With these modifications in place we anticipate a factor of 2-3 improvement in each of the systematic error components which should give the systems a range accuracy of 3-5 cm. Similarly, range noise should be reduced by about a factor of 3, giving a sigma of 10-15 cm on Lageos and 3-5 cm on low orbiting satellites.

REFERENCES

Pearlman, M. R., N. W. Lanham, J. Wohn, J. M. Thorp, E. Imbier, F. D. Young, J. Latimer and I. G. Campbell, 1978. A report on The Smithsonian Astrophysical Observatory Laser Ranging Systems, presented at the Third International Workshop on Laser Ranging Instrumentation, Lagonissi, Greece, in May.

Latimer, J., D. Hills, S. Vrtilek, A. Chaiken, and M. R. Pearlman, 1981. An Evaluation and Upgrading of SAO Prediction Software, to be Presented at the 4th Workshop on Laser Ranging Instrumentation at Austin, Texas in October.

Pearlman, M. R., N. W. Lanham, J. Wohn and J. M. Thorp, 1981. The Smithsonian Astrophysical Observatory Calibration Techniques, to be Presented at the 4th Workshop on Laser Ranging Instrumentation at Austin, Texas in October.

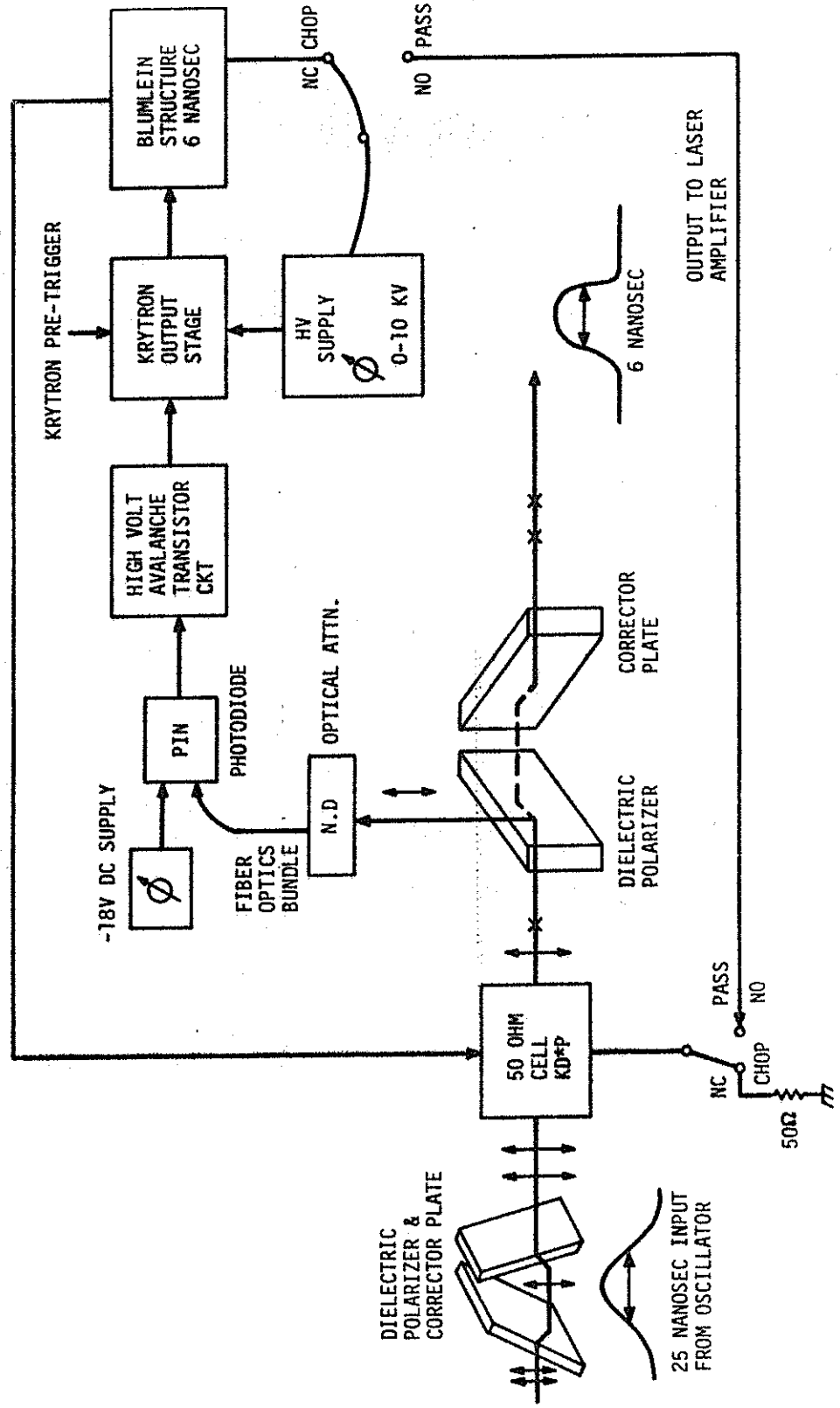

Figure 1.
Krytron activated pulse-chopping system.

SAO LASER SYSTEM

PARAMETER	CURRENT	UPGRADED
WAVELENGTH (Å)	6943	6943
ENERGY/PULSE (J)	1.0	0.3
PULSE WIDTH (NSEC)	6	2
REP. RATE (PER MIN)	8	30
DIVERGENCY (MR)	0.6	0.6
QUANTUM EFFICIENCY (%)	4	4
SYSTEM EFFICIENCY (%)	25	25
RECEIVER DIAMETER (M)	.50	.50

Figure 2

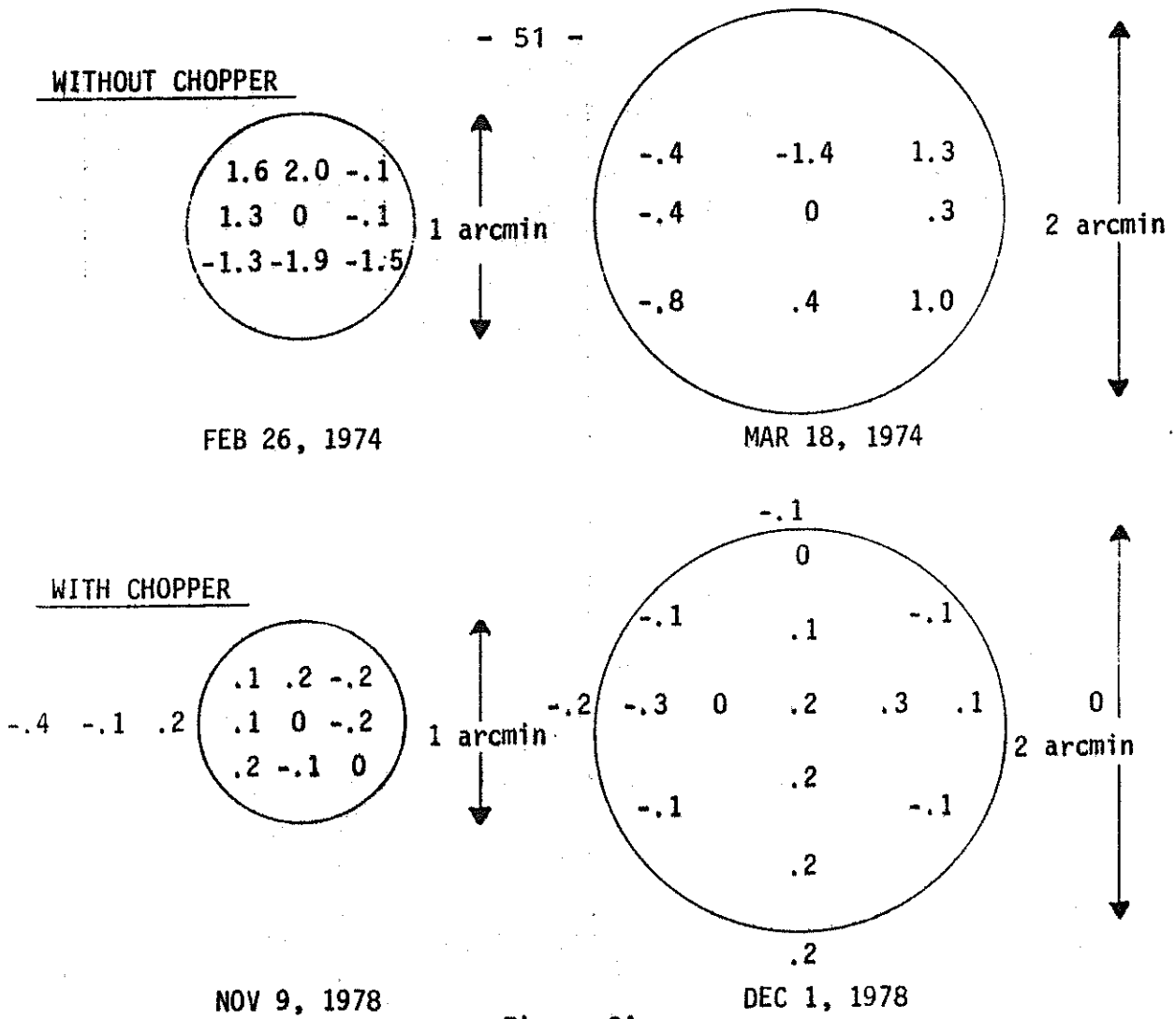

Figure 3A
Wavefront distortion in nsec. determined from
20 shot means within the laser beam (0.1 nsec = 1.5 cm)

DATE	SPACING BETWEEN POINTS (ARC MIN)	AVERAGE NUMBER OF PHOTOELECTRONS RECEIVED	RMS WAVEFRONT DISTORTION (CM)	MAXIMUM EXCURSION (CM)
FEB 26, 1974	.3	88	22.5	58.5
MAR 18, 1974	.6	56	12.0	40.5
NOV 9, 1978	.3	56	2.9	9.0
DEC 1, 1978	.42	87	2.6	9.0

Figure 3B.

Summary of Wavefront Distortion Data

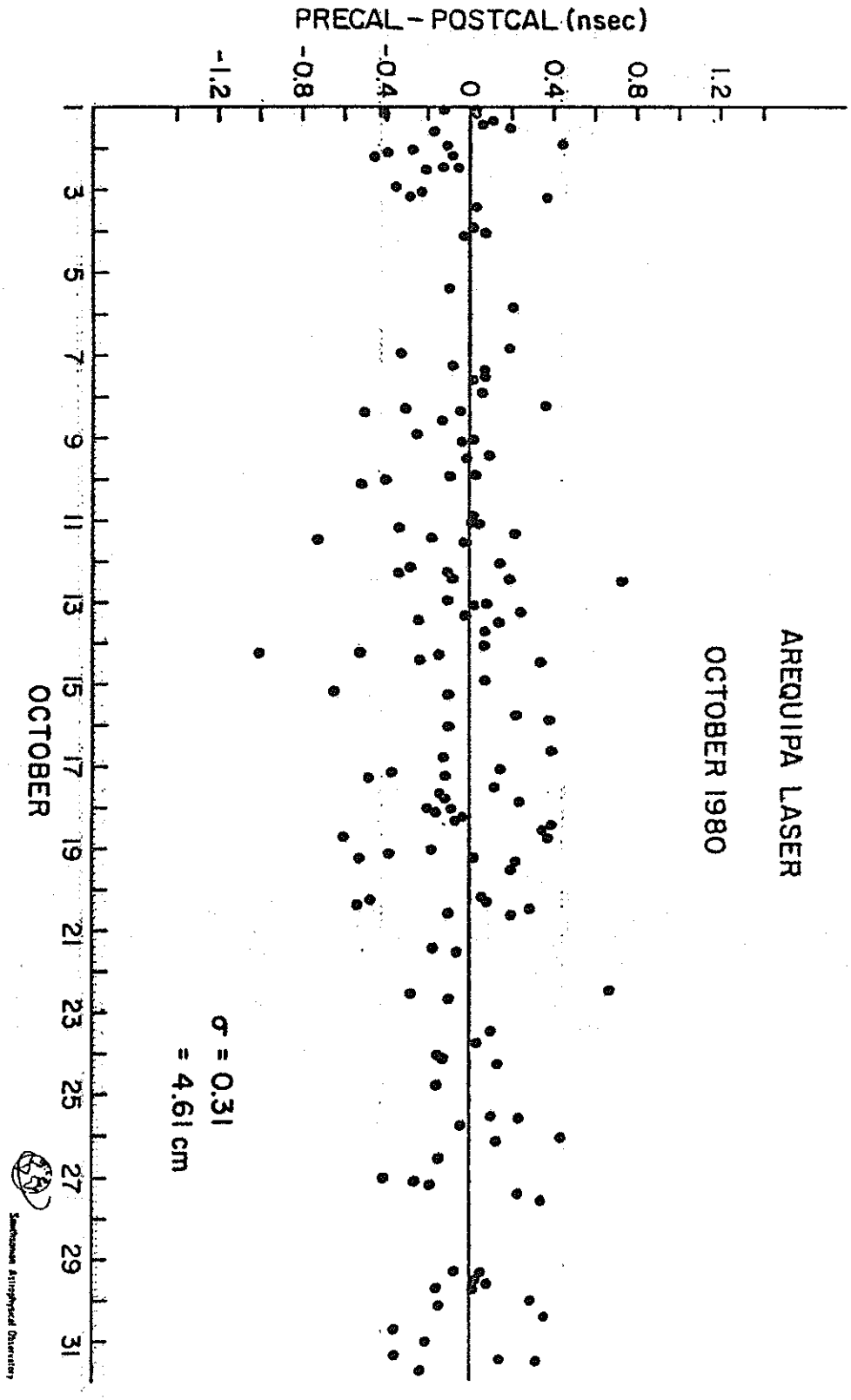

Figure 4.

Precalibration minus Postcalibration differences based on 20 shots each.

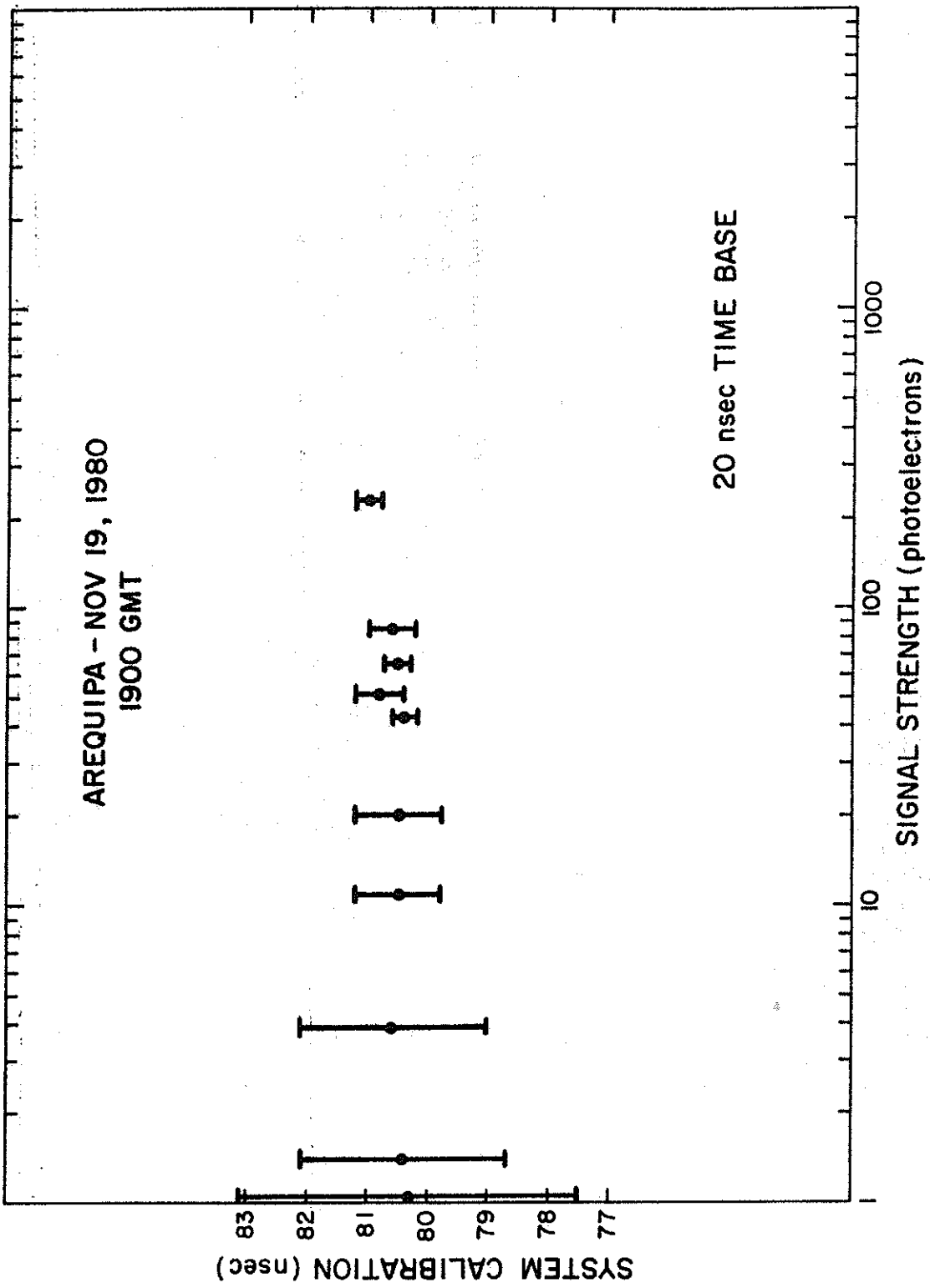

Figure 5.

Extended target calibrations based on at least 100 photoelectrons in each signal strength interval.

Figure 6
Starlette
Final Data
July 1 - 7
(1981)

Station	Date	RMS (cm)	Number of Points
Peru	7/1	33.2	65
Peru	7/1	30.3	27
Peru	7/1	17.7	32
Brazil	7/1	29.1	26
Peru	7/2	14.9	72
Peru	7/2	21.7	61
Peru	7/3	28.3	17
Peru	7/3	15.6	75
Brazil	7/4	22.3	26
Peru	7/4	9.0	78
Peru	7/4	21.0	53
Australia	7/4	14.5	39
Australia	7/4	23.2	60
Peru	7/5	8.8	78
Brazil	7/5	16.0	43
Brazil	7/6	12.5	41
Peru	7/6	22.4	63
Peru	7/6	16.8	70
Australia	7/6	9.4	14
Australia	7/6	21.1	13
Australia	7/6	21.7	32
Peru	7/7	15.4	68
Peru	7/7	23.1	46
Australia	7/7	18.9	33
Peru	7/7	22.6	49
Australia	7/7	39.8	13

Figure 6
(cont.)
LAGEOS
Final Data
July 1 - 7
(1981)

Station	Date	RMS (cm)	Number of Points
Brazil	7/1	40.4	21
Peru	7/2	31.4	118
Peru	7/2	45.8	39
Peru	7/3	26.2	98
Peru	7/3	39.8	119
Brazil	7/4	32.8	98
Peru	7/4	27.2	102
Australia	7/4	39.4	113
Australia	7/5	50.0	24
Peru	7/5	30.9	147
Peru	7/5	31.9	90
Peru	7/6	35.5	39
Peru	7/6	32.9	107
Australia	7/6	41.6	117
Australia	7/6	51.9	98
Peru	7/7	37.0	101
Australia	7/7	34.9	77

Figure 6
(cont.)
GEOS-C
Final Data
July 1 - 7
(1981)

Station	Date	RMS (cm)	Number of Points
Peru	7/1	6.8	66
Brazil	7/2	27.5	55
Peru	7/2	7.0	79
Peru	7/2	10.5	47
Peru	7/2	9.8	65
Peru	7/2	31.4	118
Peru	7/2	45.8	39
Peru	7/3	26.2	98
Peru	7/3	4.8	69
Brazil	7/3	8.0	43
Peru	7/4	10.1	32
Peru	7/4	7.5	75
Brazil	7/4	9.6	62
Australia	7/5	45.4	21
Brazil	7/5	18.9	50
Peru	7/5	9.4	74
Australia	7/6	10.6	45
Peru	7/7	8.2	35
Peru	7/7	10.1	57
Peru	7/7	9.8	74
Australia	7/7	54.3	7

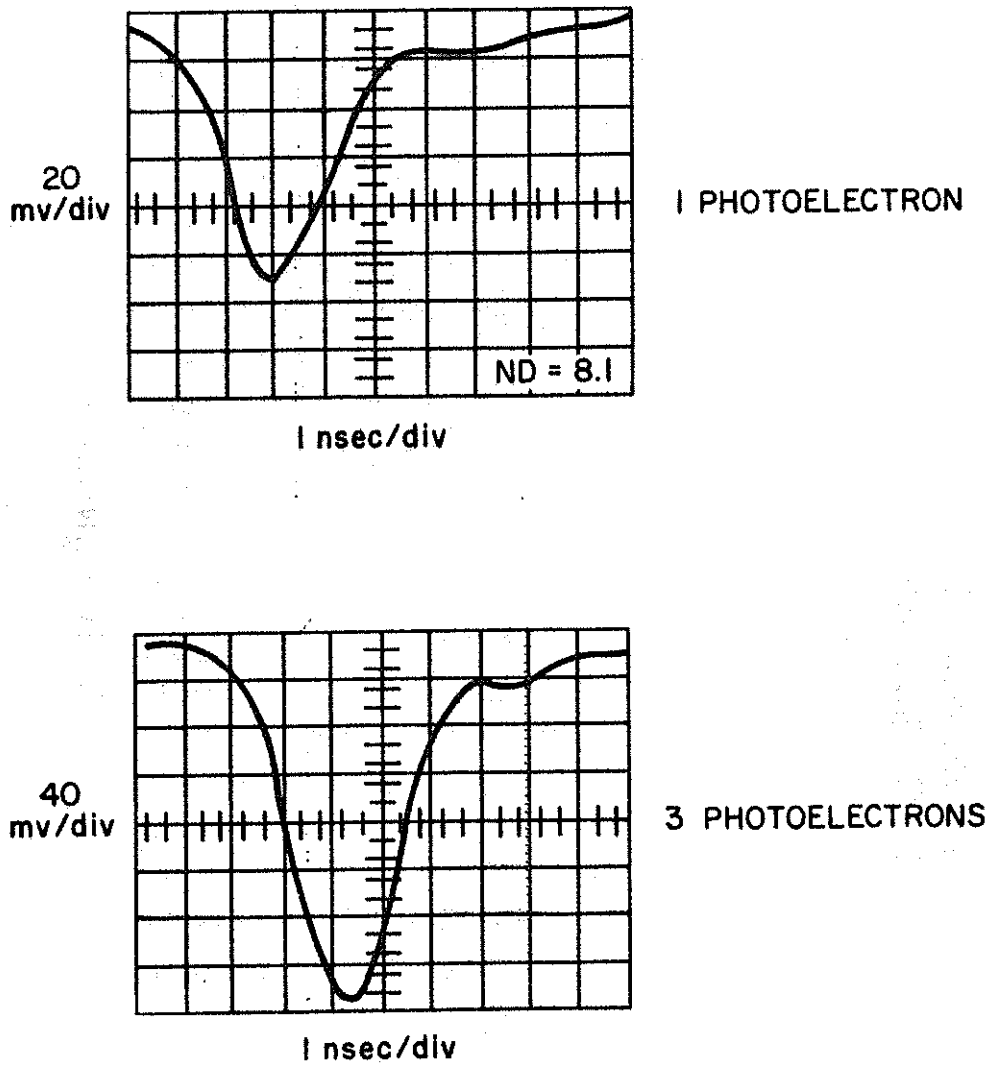

Figure 7.

Pulse response of the Amperex 2233 PMT with EMI Gencom base using 130 picosec. light pulse input.

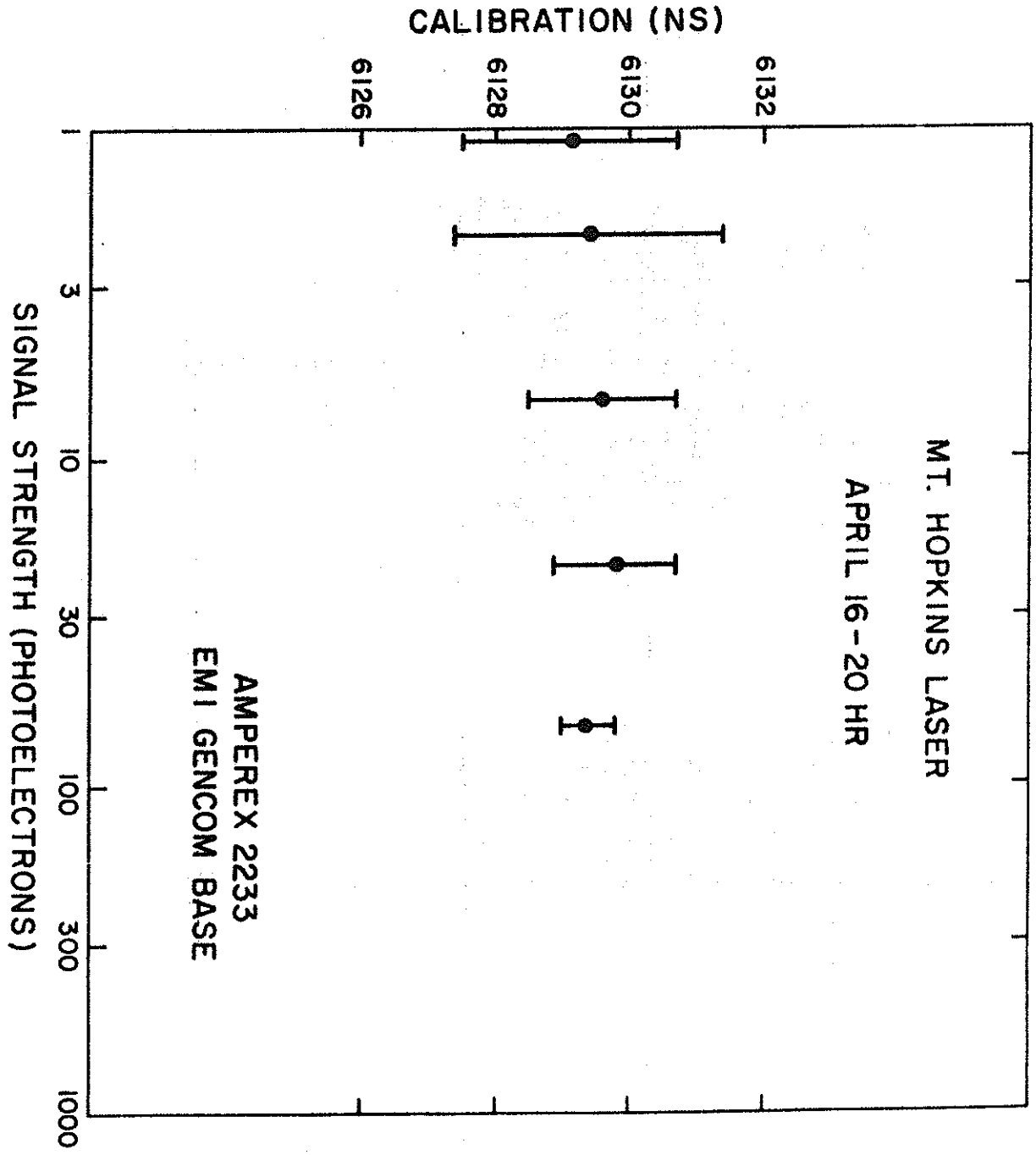

Figure 8.

Extended target calibration using the Analog Pulse Processor.

THE TLRS AND THE CHANGE IN MOBILE STATION DESIGN SINCE 1978

BY

ERIC C. SILVERBERG
UNIVERSITY OF TEXAS McDONALD OBSERVATORY
AUSTIN, TEXAS 78712

We have witnessed a tremendous revolution since 1978 concerning the characteristics of transportable laser stations fueled by the necessity to develop cost-effective systems for geodesy. At the last workshop we had a number of movable stations in field operation, but none which were truly mobile. The situation has now changed. One highly mobile system is fully operational, a second even more compact station is close to operational status, and at least two others are currently under construction. The development of these systems has resulted not so much from a technological breakthrough, but through the application of single photoelectron techniques heretofore reserved for lunar ranging. We have had the recognition that the tracking problems presented by LAGEOS are more similar to those which have been solved with the moon than those previously used on lower satellites.

The use of the term single photoelectron ranging should be looked upon not necessarily as an indication that the signal is less than one photoelectron per shot, but as the ability to co-add a number of shots and locate your ranging target by a statistical inspection of the residuals. Earlier satellite ranging required that the satellite be located principally by means of a signal strength greater than the noise in the range gate. Single photoelectron techniques, on the other hand,

do not depend on any greater signal but on the fact that the returns from the target will be highly correlated with the prediction ephemerous as opposed to noise returns which are not. The practical necessity of maintaining this approach is due to the fact that any aperture ranging system which can be easily transported (less than 0.5 meters) will not produce a reliable multi-photoelectron return on the LAGEOS satellite with less than about 100 millijoules output energy. Single photoelectron techniques on the other hand can detect LAGEOS even in the presence of high background noise with energies fifty times less. The regulatory environment alone regarding aviation eye safety is reason enough to consider the low power techniques. The added advantages in calibration ease, cost and reliability of the laser system weigh heavily in the direction of these lower-power high-repetition rates systems for applications which concentrate on the LAGEOS target.

The first system to fully realize operational single photoelectron ranging for satellites was constructed by The University of Texas between 1978 and 1980. A special attempt was made to make the station reliable and mobile using a number of special features. The system, dubbed the TLRS, has operating parameters such as shown in the station report forms. One of the unusual aspects is that the TLRS uses a mode-locked laser limited to 3.5 millijoules per burst of pulses and transmits the entire pulse comb rather than pulse selecting as has been the case in the past. High accuracy pointing is critical. In order to be able to work at unprepared sites, the system has a on-site mount orientation routine which is practical to run prior to each satellite pass. The system also employs a feedback calibration system to calibrate the single stop timing electronics. These and other hardware are more fully described another paper in these proceedings. Figure 1 gives a schematic diagram of the system as it is configured at this time.

The operating characteristics of the TLRS can best be shown by describing the first few hours of activity after arriving at any given site. The TLRS van is driven to the site as would any small truck. Most of the auxiliary equipment is contained in a 32-foot office trailer which is pulled by a second vehicle. All of the clocks run off the truck generator during the moves. The van is first driven along side the chosen geodetic marker and positioned within about five centimeters of the ideal location. The van is then manually jacked on 3 cones, leveled and stabilized. If the surface on which the system is being parked is relatively soft, plywood sheets are used under the cones to stabilize the foundation. Power is then hooked to the van (approximately 20 kW, single phase, 220 volt) at which time the clocks automatically switch to the mains. The beam director is then raised through the roof and the entire coude assembly jacked on three more cones so that the optical system is supported independent of the truck chassis. The coude system is levelled by means of an electronic level on the base of the beam director. After the computer is started, the

software quizes the crew on the approximate geodetic position of the truck, the azimuth at which it is parked and other initialization parameters. The time in the van is checked by comparing it with a cesium standard which rides in the auxiliary office trailer. Loran C communication is established to monitor the frequency of the clocks during that occupation. At this point the elapsed time is approximately two hours.

If all features are functional to this point, the laser is aligned and tested. The finder telescope of the beam director is used to locate a bright star which is centered in the field so as to determine the basic azimuth offsets of the instrument. A second star is then located at which time it is possible to solve for the tilt and azimuth of the tower. This process continues until about ten to fifteen stars are acquired and an exact 8-10 parameter mount model is determined. (Further information on this mount model is given in these proceedings.) If the geodetic position which was entered by the operator is in error, the mount solution will show a significant tilt in the tower relative to the electronic level. This allows the operators to determine whether or not their location guess is sufficiently accurate for a satellite acquisition. The efficiency of the optical system is usually checked at this point by monitoring the count rate on a bright star. The exact offsets to the geodetic marker are then read from a small vertical-looking telescope which is poised near the driver's door.

The ephemeris for LAGEOS, with the position and velocity of the satellite at three-hour intervals, is mailed to the TLRS several months in advance. On command the computer will predict the azimuth and altitude of subsequent passes from the nearest prediction point. After the pass is integrated the system is ready to range. Normally the crews tailor their mount models to each pass by selecting a few stars along the expected arc prior to the event; however, each team may use a slight variation on this technique depending on their previous experience. The elapsed time at this point can be as little as four hours, but is frequently longer if it is necessary to wait for darkness in order to develop a proper mount model. The TLRS will continue to range at a site with two men crews, sending the data to the data reduction center in one-week segments, until approximately 600 minutes of tracking have been derived. If practical, phone communications are installed in the TLRS for their month-long occupations.

Based on early observations the TLRS has proven to be a reliable and quite accurate device for ranging the LAGEOS satellite. The quality of the data which is possible with this system is indicated in Figure 2, where we have plotted the residual deviations from a low order of polynomial versus the number of range observations which were averaged to achieve these normal points. The best passes of the TLRS have over three thousand single photoelectron hits with an RMS from the

best fit orbit of about 7-8 centimeters. One hundred point return normal places fit to these data show a scatter from the best arc approaching one centimeter. Since the system is highly mobile, the occupation time at any given location is limited only by the number of tracks which are necessary on the target and not in general the logistics of moving the station between the sites. Clearly this one station alone represents a drastic change in the compliment of laser ranging equipment since 1978. In the next few years the extent of crustal dynamics studies should fuel this evolution to the point where several truly mobile stations are in the field gathering data from orbiting satellites.

This work is supported by NASA Contracts NASW-2974 and NAS5-25948.

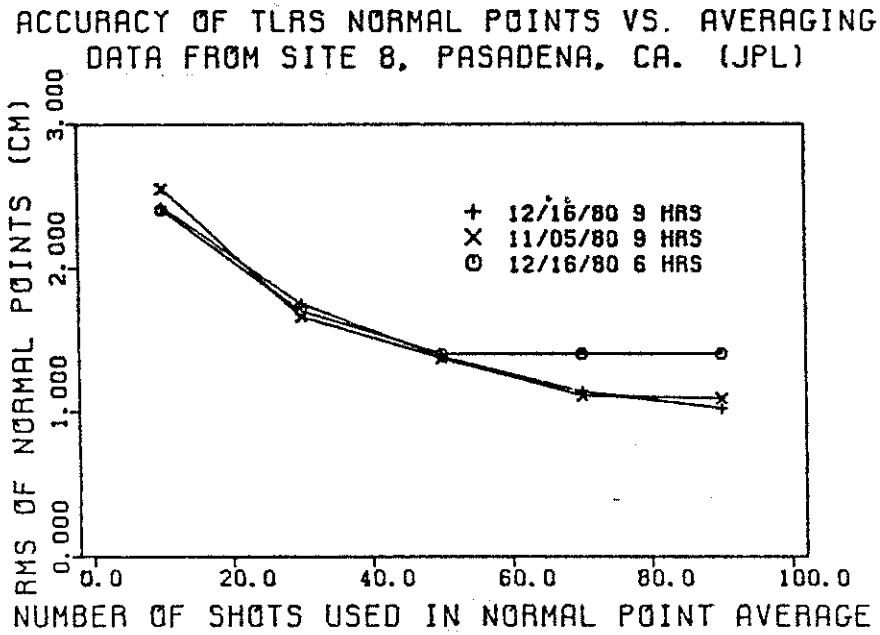

Figure 2: Normal points were formed from several strong passes to determine the precision limits of the current TLRS. Starting with a single point RMS scatter of 8cm, the data improved nearly as predicted for a gaussian distribution of residuals.

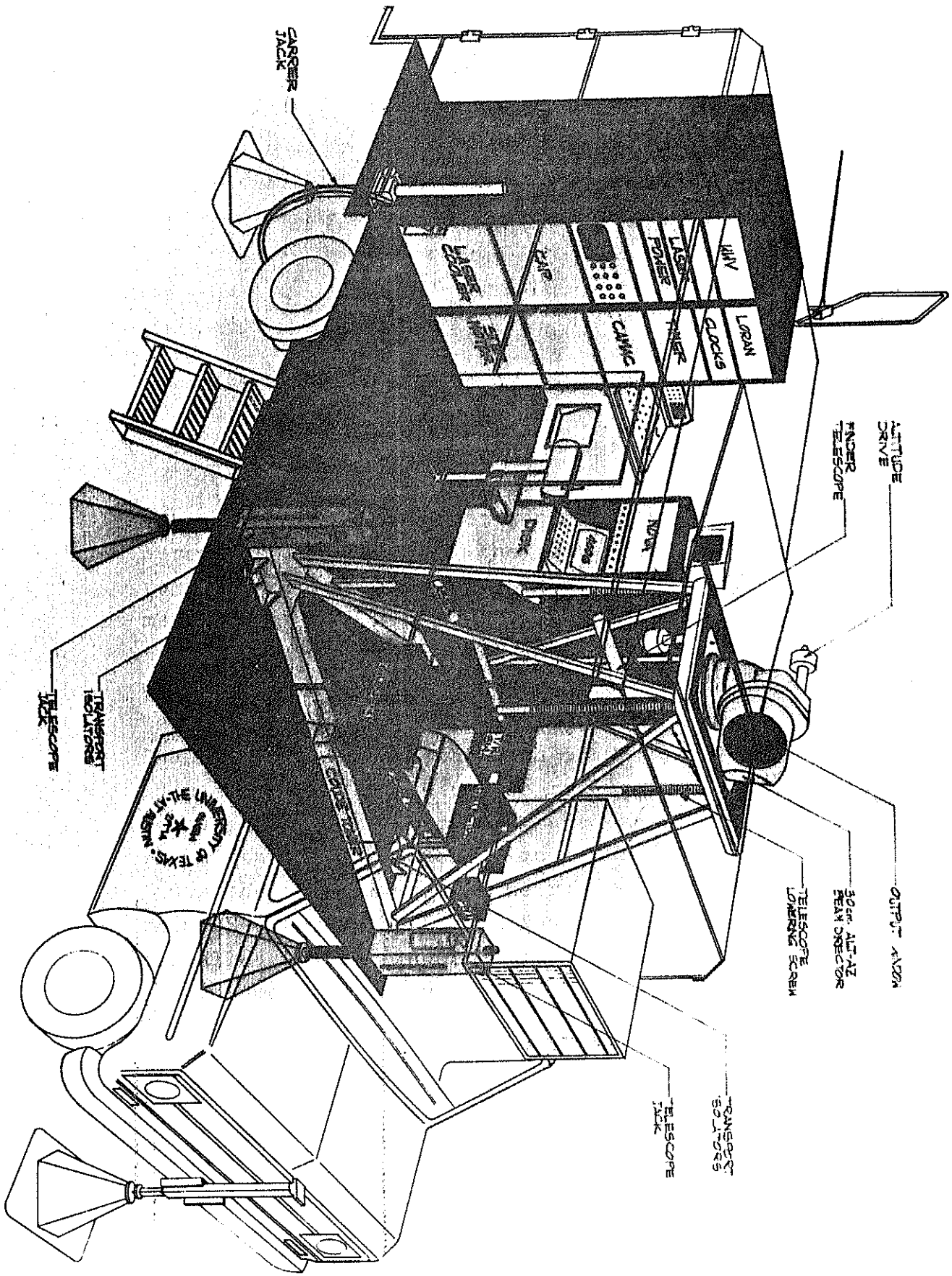

Figure 1: The TLRS is housed in a small single chassis van which is leveled at the site on three jacks. The beam director retracts to below the roof line for transport.

SATELLITE LASER RANGING WORK AT SHANGHAI OBSERVATORY

Satellite Laser Ranging Group

Shanghai Observatory, Academia Sinica

Shanghai, China

1. The First-generation Ruby Laser System

The satellite laser ranging work at the Shanghai Observatory(SO) is one of the topics of the astro-geodynamics research program of the Observatory. We began the development of the first-generation satellite laser ranging system in 1972 in collaboration with the Shanghai Institute of Optics and Fine Mechanics(SIOM). A dye-cell Q-switch ruby laser which produced 2.5 joules in 25-nsec duration time (half-power, full width) with 30 ppm repetition rate was adopted. The aperture of the receiving telescope was 30cm. Because of the poor pointing accuracy of the old alt-az mount, the visual tracking mode only could be used. Table 1 lists the performance of the ruby system. The first echoes from BE-C were received in November 1973. The system was installed at Zô-Sè section of the Shanghai Observatory in the autumn of 1975, which is in the southwest suburb of Shanghai and the coordinates of the laser system are as follows: $\lambda=121^{\circ}\,11'\,19''.63E$ $\varphi=31^{\circ}\,05'\,46''.86$ h=118.3 m.

The system has been in operation since December of the same year, four satellites, BE-C, GEOS-1, GEOS-2 and GEOS-3, have been tracked. The maximum ranges were over 2700km and the accuracy of ranges was about 1-2 meters[1].

2. Prediction of Satellite and Work for the Chinese Ranging Network

The prediction of the satellites(BE-C and GEOS-1) were provided by Purple Mountain Observatory in Nanjing during the early years. Since 1975, we have done the predictions independently. Because we did not participate in any international cooperation at that time and had no new orbital elements of the laser satellites, a method for acquiring the tracks of satellite was developed. By the method, we can in a short time, acquire the tracks of some laser satellites such as GEOS-2, GEOS-3 and LAGEOS at a single station, based only on the previous orbital elements or the observation data collected from references about 1-2 years ago[2].

Five more first-generation ruby ranging systems have been gradually set up in China since 1977. Three of them are at the Beijing Observatory(operation in 1977), the Yunnan Observatory(operation in 1978) and the Guangzhou Satellite Observation Station(operation in 1981). The above three stations and ours all belong to the Academia Sinica. The other two systems, just the same as Guangzhou's, which are in operation in 1980-1981, belong to the geodesy departments. The five systems all use a Pockels cell for a Q-switch and operate at 30 pulses per minute. The lasers generate an output of 1.5 joules in 20-nsec pulse. The resolution of the counters is 6.7-nsec. The apertures of the receiving telescopes are 40-50cm. The visual tracking mode is still adopted, but because of better mounts the percentage of hits typically is 40-60 %.

Now a laser ranging network which consists of the

above-mentioned six stations has been run for a common project organized by the Shanghai Observatory. The first goal of the project is to determine the chord lengthes between the laser stations. The satellites tracked by the network are: GEOS-3, GEOS-1 and BE-C, and no station has the ability to track LAGEOS yet. The predictions of these satellites for the network have been provided routinely by our observatory, the preprocessings of all laser range data obtained by the six stations and reductions of the chord lengthes are being done by our observatory also. For lack of enough range data, no result of the chord lengthes has been got yet.

3. Experimental Nd:YAG Ranging System

In order to participate in the MERIT short campaign (August 1st to October 31st,1980), a great deal of improvements have been made to our ruby system since April 1980 in collaboration with SIOM again, and a decimeter accuracy Nd:YAG experimental laser ranging system was set up.[3] Fig.1 is the block diagram of the Nd:YAG system, the instruments in the figure marked SO were made by our observatory, and the laser and its power supply were made by SIOM. Table 1 lists the main charateristics of the system. The instruments and devices in the laser ranging system were all made in China except a discriminator(Ortec 473A). The Nd:YAG laser consists of an oscillator, an amplifier and a frequency doubler. The oscilator has a transmission coupling unstable plano-convex cavity with an electro-optic Q-switch, the structure being quite simple and compact. The width of the output pulse is about 4-5 nsec, the divergence is about 0.5 mrad and the center of the near field pattern is solid. The energy of output is 80-100 mj in 5320Å. The laser was installed on the top of the telescope tube, and rotated with it. Experiments showed that the output energy did not decrease when the laser had been operated for a month, no ad-

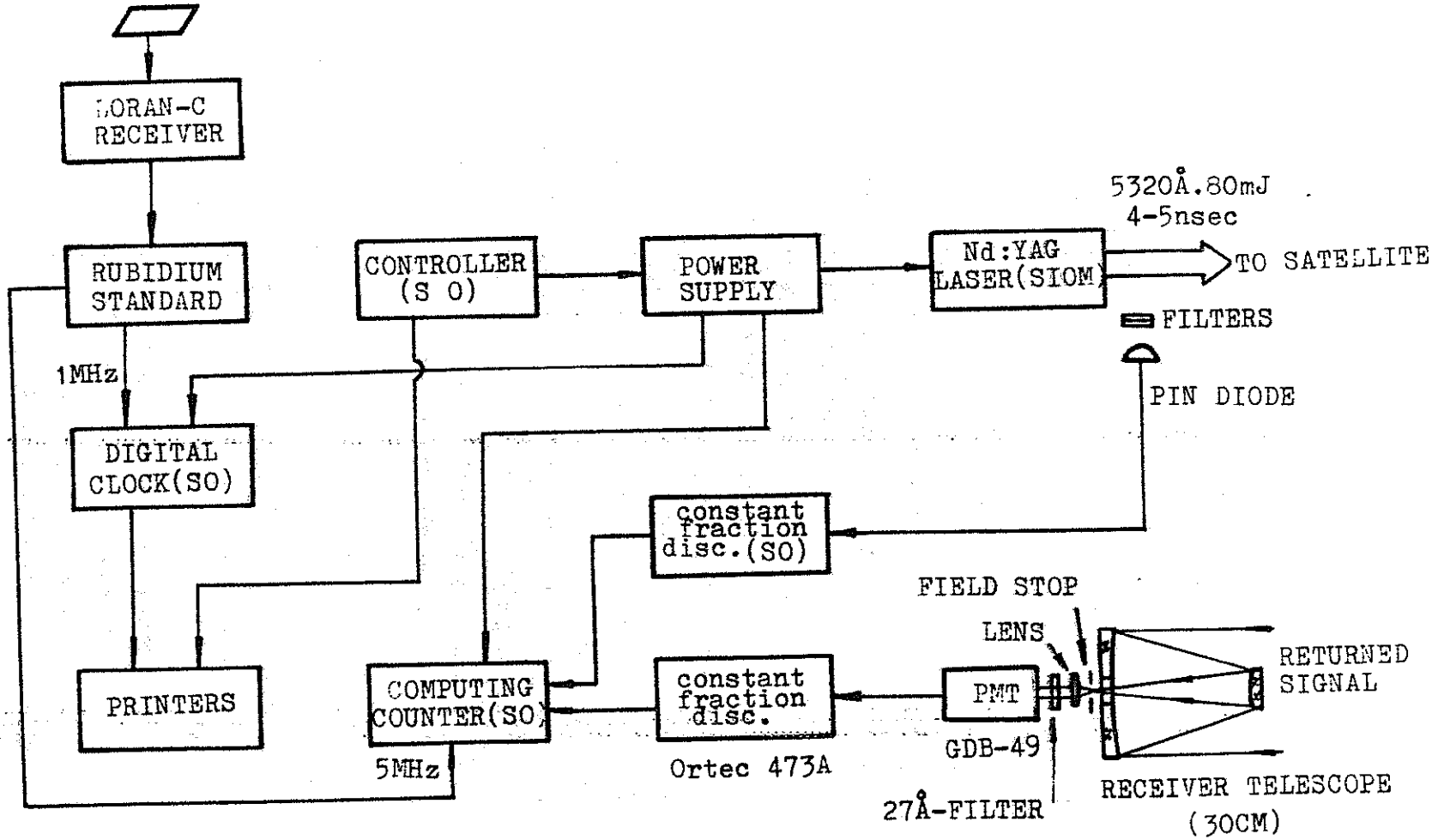

FIG.1 BLOCK DIAGRAM OF Nd:YAG EXPERIMENTAL RANGING SYSTEM

justment was needed.

The photoreceiver and data recording parts consist of a fast photomultiplier, two constant fraction discriminators, a computing counter, a controller, a digital clock and two printers, etc. A Si-pin photodiode which risetime is less than 1-nsec is used for sampling the transmitting pulse attenuated by the filters. A photomultiplier(Type GDB-49) which has a K-Cs-Sb cathode and twelve dynodes is chosen for detecting the returned signals. The PMT has a gain of 3×10^7 and a risetime of 1.9-nsec. In order to improve the accuracy of the measurement of the flight time, a new time interval counter or so-called computing counter was made by ourselves in collaboration with the Shanghai Electronic Instrument Factory, which was designed according to the analogue interpolation method, so that the main frequency is 10 MHz and the resolution is 0.1-nsec. It is shown in the experiment that the performance of the counter is good. Considering the returned signals fluctuating over a wide range in amplitude, we use the constant fraction discriminators to replace the fixed threshold discriminators adopted in the old ruby system for reducing the errors of pulse position measurement. The Model 473A(Ortec) constant fraction discriminator with 100:1 dynamic range is chosen for the receiving channel, and another one made by ourselves is for the transmitting channel which is simpler than commercial products. A lower-level discrimination circuit is designed to estimate and to prevent the noise of the ranging system. The time jitter of the discriminator is less than 0.5-nsec for 4-5 nsec pulse with 40:1 dynamic range. A digital clock which is externally provided with 1MHz frequency from one of the rubidiums is made for recording the epoch of the fired pulse with a resolution of 1μs. We use Loran-C for epoch reference. It has been proved that the synchronization between the UTC of the Shanghai Observatory and UTC of USNO is better than 1μs by com-

parison of portable cesium clock of USNO in August 1981. We believe the time synchronization of our system with UTC of USNO is better than 3μs.

The tracking mount is still the old one, but has been slightly reformed, two new guiding telescopes with apertures of 150mm are installed.

The ranging experiments, mainly to GEOS-3, were made with the above-mentioned Nd:YAG ranging system from September 1980 to January 1981. But only a few range data were obtained because of the abnormal weather and the wobbles of the old mount which was simple and crude. Most of the data have been sent to SAO and the University of Texas at Austin for reductions. The orbit elements of GEOS-3 and GEOS-1 have been weekly provided to us from SAO by telegram since July 1980.

The method of ranging to an extended-target, a retro-reflector on the top of a water power seperated by 5.6km away from the laser, is used for calibration of the ranging system. Experiments show that the error of the pulse position measurement for single shot would be 1-1.2nsec arose from the variations of the shape of the returned signals and other factors such as the timing jitter in photomultiplier. But the variation of averages of the system calibration is quite small for different returned signals in the range of 5 to 500 photoelectrons because of adopting two constant fraction discriminators(see Fig.2, each point is an average of 20 measurements). The variation of calibration averages during a time-interval may be used to verify system stability and the experiments showed that the short-term stability of our system was about 4cm(see Figure 3). Taking all errors in account, the total range accuracy for single shot is about 20-30cm. The budget of errors of our ranging system is given in table 2. The estimation is basically supported by the preliminary analysis for GEOS-3 laser ranging data[4], and

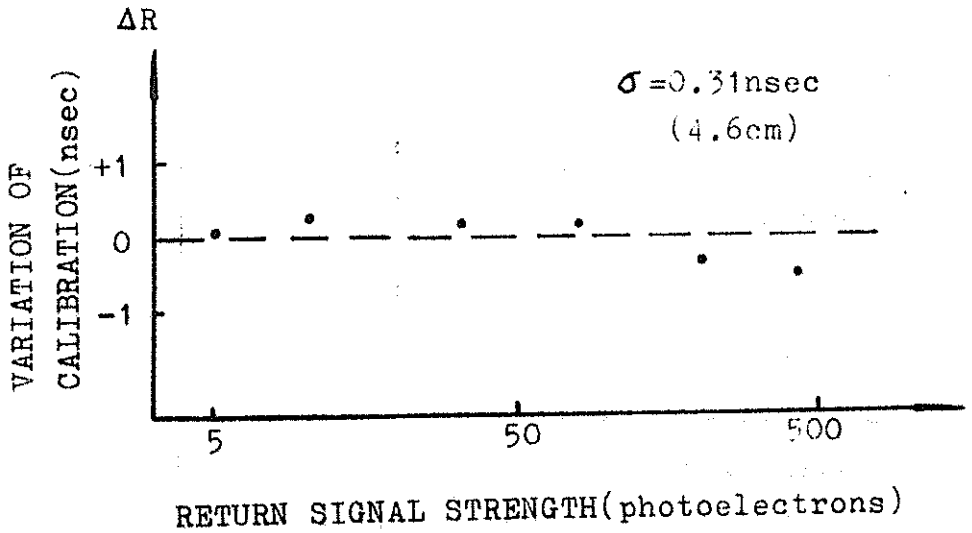

FIG.2

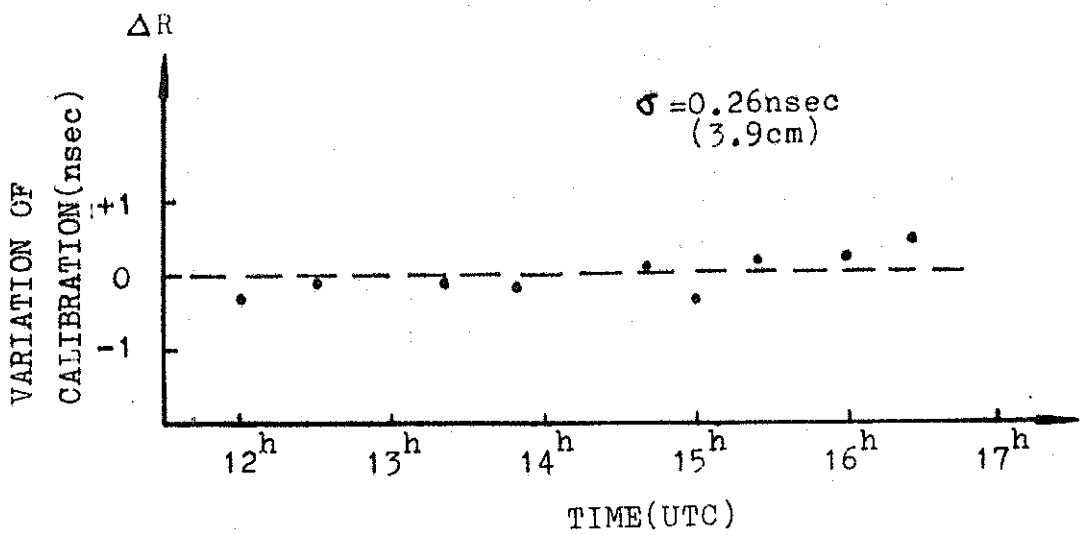

FIG.3 SHORT-TERM STABILITY OF Nd:YAG RANGING SYSTEM

Table 2 Error Budget of Nd:YAG Experimental Ranging System (4-5 nsec)

	(cm)
measuring error of counter	4.5
pulse position measurement	15-18
system stability(drift)	4
corner cube array	9
atmospheric correction	5
clock synchronization	2
total range accuracy(r.m.s.)	20-22

figure 4 shows the range residuals obtained from one pass orbit for GEOS-3 in 3 January 1981. The analysis has also shown that there is no obvious systematic error in our laser range data.

4. A Brief Description of the Second-generation Ranging System

The second-generation satellite laser ranging system has been being developed since 1978 by our observatory in collaboration with several institutes of the Academia Sinica which has long been supporting the work. The main goals of the new system are:

1. ability to track Lageos and other low orbit satellites (including Space Shuttle);
2. 10-20cm range accuracy;
3. automatic tracking with a microcomputer system.

Table 1 also lists the characteristics of the new system. Table 3 lists the main performance of the mount and servo subsystem. Fig.5 shows the optical scheme of the mount. The 600mm aperture receiver telescope is of R-C configuration, and a dichroic beamsplitter reflects almost all laser wave-

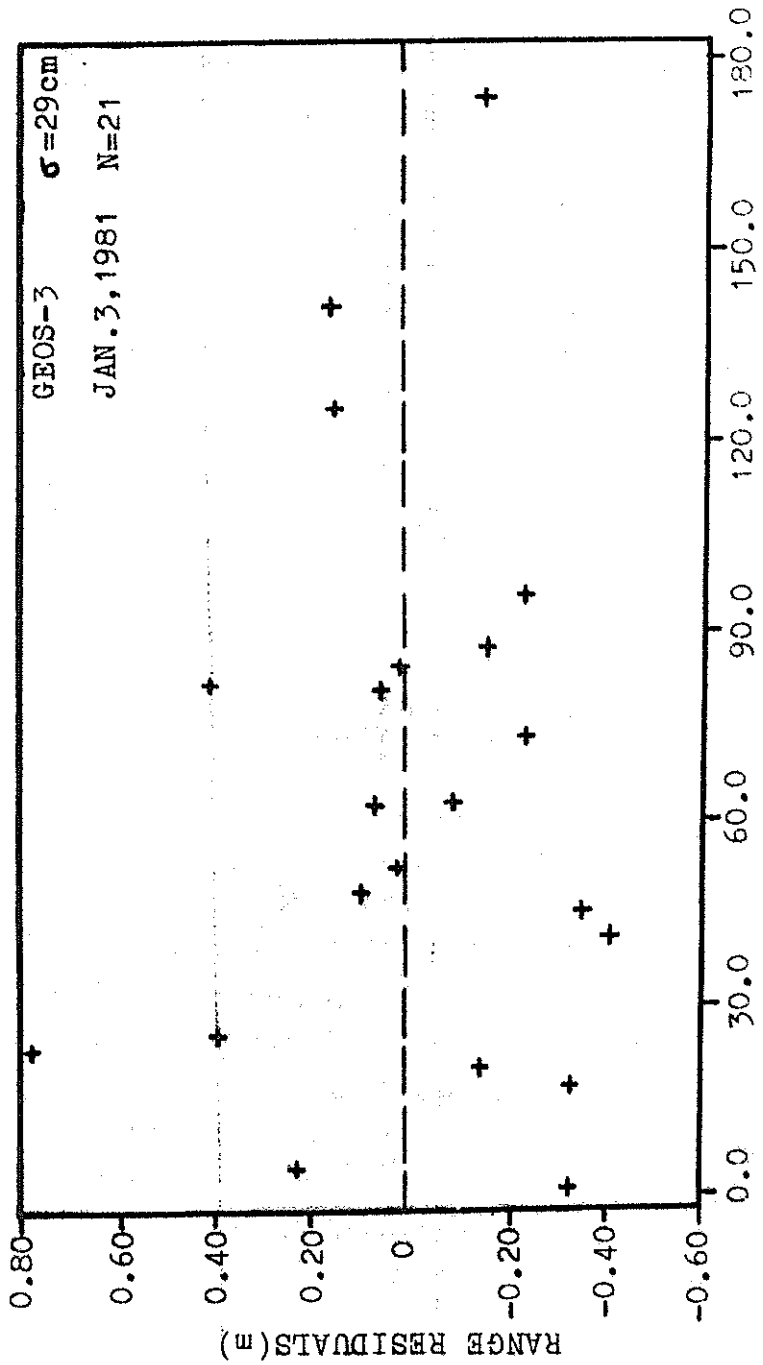

FIG.4 LASER RANGE RESIDUALS FOR GEOS-3, JAN.3, 1981

Table 3 Main Characteristics of Mount and Servo-System

Type of Mount	Altitude-azimuth and Coude optics
Range of travel	-5°—$+185^{\circ}$ in altitude
	$\pm 270^{\circ}$ in azimuth
Orthogonality	$\leqslant \pm 2$ arc second
Wobble	$\leqslant \pm 1$ arc second
Optical Encoders	20 bit, $< \pm 1.5$ arc second
Static Pointing Accuracy	+10 arc second(designed goal)
Servo System	Two axes are directly coupled torque motors, torque: 8kg-m in altitude 40kg-m in azimuth
Computer	Z-80 microcomputer system
	8 bit, 64k
	disk, printer

lenǵth(5320Å) onto photoreceiver and allows the rest wavelengthes pass to the 45° bending mirror, and then to an eyepiece for guiding faint satellites(such as Lageos), it will be effective when the automatic tracking part is out of order or when the predictions of some fast and weak satellites are occasionally inaccurate. A joystick is prepared for the visual track mode, and a 150mm aperture quiding telescope is used for tracking the low orbit satellites. Another 150mm aperture telescope is the transmitter of laser, but the 600mm primary mirror could be used for a transmitter after some modifications, if it is neccesary in future.

Now, the frequency doubled Nd:YAG laser has been completed, the receiving telescope and the mount have been being assembled and adjusted. We expect that the new system will be installed at Zô-Sè section by the fall of 1982, and will participate in the MERIT main campaign in 1983. We also intend to do the intercontinental time synchronization experiment with laser ranging technique.

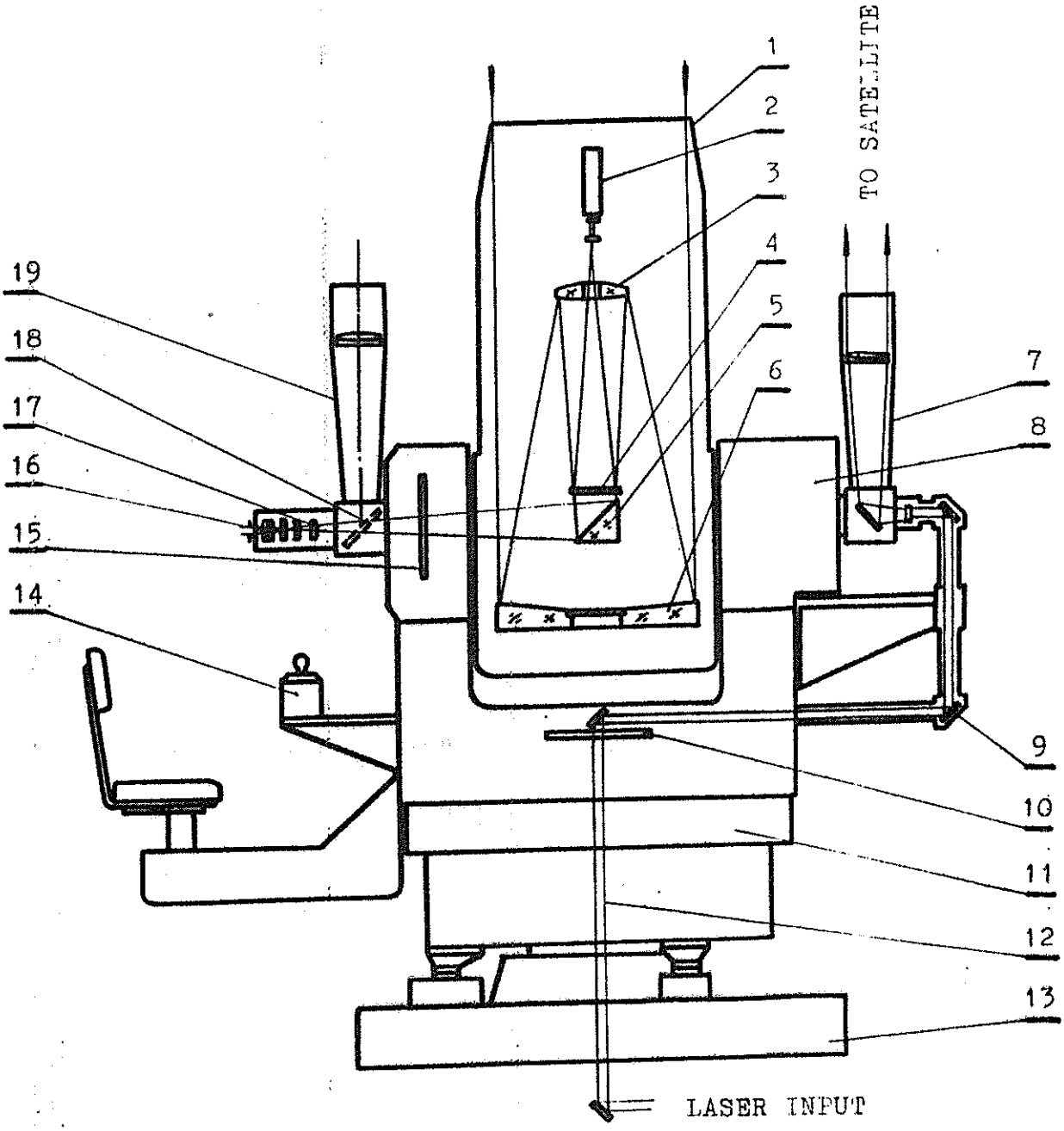

FIG.5 SCHEMATIC OF MOUNT AND OPTICS OF SECOND-GENERATION RANGING SYSTEM AT SHANGHAI OBSERVATORY(IN CONSTRUCTION)

FIG.5(continued)

1.RECEIVER TELESCOPE
2.PHOTOMULTIPLIER
3.SECONDARY MIRROR
4.DICHROIC BEAMSPLITTER
5.45° BENDING MIRROR
6.PRIMARY MIRROR(600mm)
7.TRANSMITTER TELESCOPE(150mm)
8.ALTITUDE TORQUE MOTOR AND D.C.TACHOMETER
9.45° DIELECTRIC COATED MIRROR
10.OPTICAL ENCODER(AZIMUTH)
11.TORQUE MOTOR AND D.C. TACHOMETER(AZIMUTH)
12.COUDE OPTICAL PATH
13.PIER
14.JOYSTICK
15.OPTICAL ENCODER(ALTITUDE)
16.QUIDING EYEPIECE
17.CORRECTING LENS
18.45° FLIP MIRROR
19. QUIDING TELESCOPE(150mm)

We are gratefully indebted to Prof.Ye Shuhua and Prof. Wan Lai for their supports and encouragements in this work.

This laser ranging group consists of Yang Fumin, Zhu Youming, Shi Xiaoliang, Tan Detong, Lin Qinchang, Zhang Yanlin, Su Jinyuan, Liu Jiaqian and other colleaques. This paper is presented by Mr.Cheng Hao, one of the members of our group, who has stayed at the University of Texas at Austin for a short-term work.

References

1. Yang Fumin, et al., The Satellite Laser Ranging System at Shanghai Observatory, Annals of Shanghai Observatory, No.1, 83, (1979).
2. Lin Qinchang, Niu Xiulan, A Method for Acquiring the Tracks of Artificial Satellites, Ibid,, 92, (1979).
3. Yang Fumin, et al., A Satellite Laser Ranging System with Decimeter Precision, Science Bulletin, (1981), (in English, in press).
4. He Miaofu, et al., A Preliminary Estimation of Accuracy for GEOS-3 Laser Range Data from Shanghai Observatory, (1981), to be published.

Table 1 Performances of the Satellite Ranging Systems at Shanghai Observatory

	first generation system	Nd:YAG experiment. system	second generation system
Laser subsystem			
material	ruby	Nd:YAG	Nd:YAG
output wavelength	6943Å	5320Å	5320Å
type	single oscillator	oscillator, amplifier, freq. doubl.	oscillator, two amplifiers freq. doubler
output energy	2.5j	80-100mj	250mj
width of pulse (FWHM)	25ns	4-5ns	4-5ns
repetition	0.5pps	0.5pps	1pps
Q-switch mode	dye-cell	$LiNbO_3$ crystal	$LiNbO_3$ crystal
Transmitting Optics			
type	galilean	galilean	galilean and coudé optics
aperture	120mm	42mm	150mm
beam divergence	1 mrad	0.3-0.8mr	0.2-2 mrad
Receiver			
aperture	300mm	300mm	600mm
field stop	3 mrad	2 mrad	0.2-2 mrad
filter bandwidth	60 Å	27 Å	5-7 Å
type of PMT	EMI9558	GDB-49	GDB-49, RCA C31034A
quantum effeciency	3%	10%	10-24%
risetime	10ns	2ns	2ns
gain	5×10^6	3×10^7	10^6-3×10^7
resolution of timer	10ns	0.1ns	0.1ns
Quiding Optics			
type	sighting scope	sighting scope	receiver telescope with a dichroic beam-splitter, sighting scope
aperture	90mm	150mm	600mm; 150mm

(Table continues)

Table 1 (Continued)

field of view	4°	3°	30'; 3°
Type of Mount	alt-az	alt-az	alt-az and coudé optics
Time System			
freqency standard	quartz oscillator	rubidium (2 sets)	rubidium (2 sets)
stability	1×10^{-8}/day	3×10^{-12}/day	3×10^{-12}/day
synchronization	microwave	Loran-C	Loran-C
accuracy of synchr.	50 μs	3 μs	3 μs
General			
range accuracy	1-2 m	20-30cm	10-20cm
maximum range	2700km	2000km	over 7000km
tracking mode	visual	visual	microcomputer control, and joystick
Time in Operation	1975	1980	in construction (1982)

Satellite laser tracking. Construction of normal points

D. GAMBIS

GRGS/BIH

Abstract

Many stations, in particular in the NASA network, have an observational rate of about one measurement per second. For a 45 mn pass of Lageos, this gives more than 2000 measurements. Processing the whole data set is a heavy task, so a sampling of data is performed to reduce the number of points to 100 or 200 over a satellite pass. This solution, currently used is not satisfactory for it leads to a loss of information. Data compression, taking into account the full rate measurements has been carried out to give about 10 to 15 normal points over a pass. The method uses the approximation by the Tchebycheff polynomial expansion. The devised software can be easily implemented with mini-computers, so that every tracking station taking part in a worldwide network would be able to calculate from its own data, normal points to be forwarded to a computing center for the global processing. Data compression permits also to reduce the local random noise of an order of magnitude. The method has been applied to a limited data interval of Merit campaign.

I Introduction

Let D(t) be the discrete function representing the distance station-satellite during a pass. This distance varies approximatively

from 6000 to 10 000 km for a Lageos arc and the duration of the tracking is about 45 mn. Depending on the capability of the station, observation densities are around 1 per second for NASA stations, some units per mn for other ones. Of course, laser observations require clear weather and all passes don't offer good data distribution.

The idea of making normal points consists in compressing the information contained in a certain number of measurements into one data. To make this compression, one has to find a good representation of the function D(t). Two main philosophies are possible ;

a) Using a model of forces, a good reference orbit is computed for several revolutions of the satellite. Pseudo-measurements are calculated from the difference between the arc of the reference orbit and the corrected arc (Lago and Mainguy 1971). The main drawback of this method is its heavyness ; it requires elaborate orbit computation with several data files for the models of forces introduced.

b) The function D(t) may be approximated by analytical expressions, for instance polynomial expansion. It is what we have chosen in this study.

II Simulation.

In order to investigate the faisability of the method, simulations have been made. A 45 mn orbit was computed using a complete model of forces and at the same time, the distances station-satellite, representing the measurements, have been generated at 1 second intervals. The simulated pass is considered as perfect without uncertainties on the data. The normal points must be restituted with an inaccuracy, say, an order of magnitude inferior to the nominal accuracy of the laser tracking station (i.e. about 1 cm). We have tried to approximate the function D(t) over a pass, through different representations ;

1) Low-order polynomial representation.

We did not intend to restitute directly D(t) with the 1 cm precision but, in a first step, to remove of it most of the variations. A fourth order polynomial $P_4(t)$ was found to best fit the observations. $[E_4(t) = D(t) - P_4(t)]$. Residuals $E_4(t)$ are between - 6 km and + 3 km.

A Vondrak smoothing (Vondrak 1977) is then performed onto

$E_4(t)$. The optimal smoothing will be the strongest one restituting the 1 cm precision.

We have $E'_4(t) = E_4(t) - V(t,\varepsilon)$

represents the smoothing strength

$$\varepsilon = 10^{-n} \quad n \in N$$

For $\varepsilon = 1$ the smoothing fits all the points, for $\varepsilon = 0$ it is a parabole. The analysis of the perturbations of the satellite-trajectory due to the earth gravity field shows no effect of wavelength inferior to 45 mn.

We can see from figure 1 than values of $\varepsilon = 10^{-n}$ may be tested for $n \geq 6$.

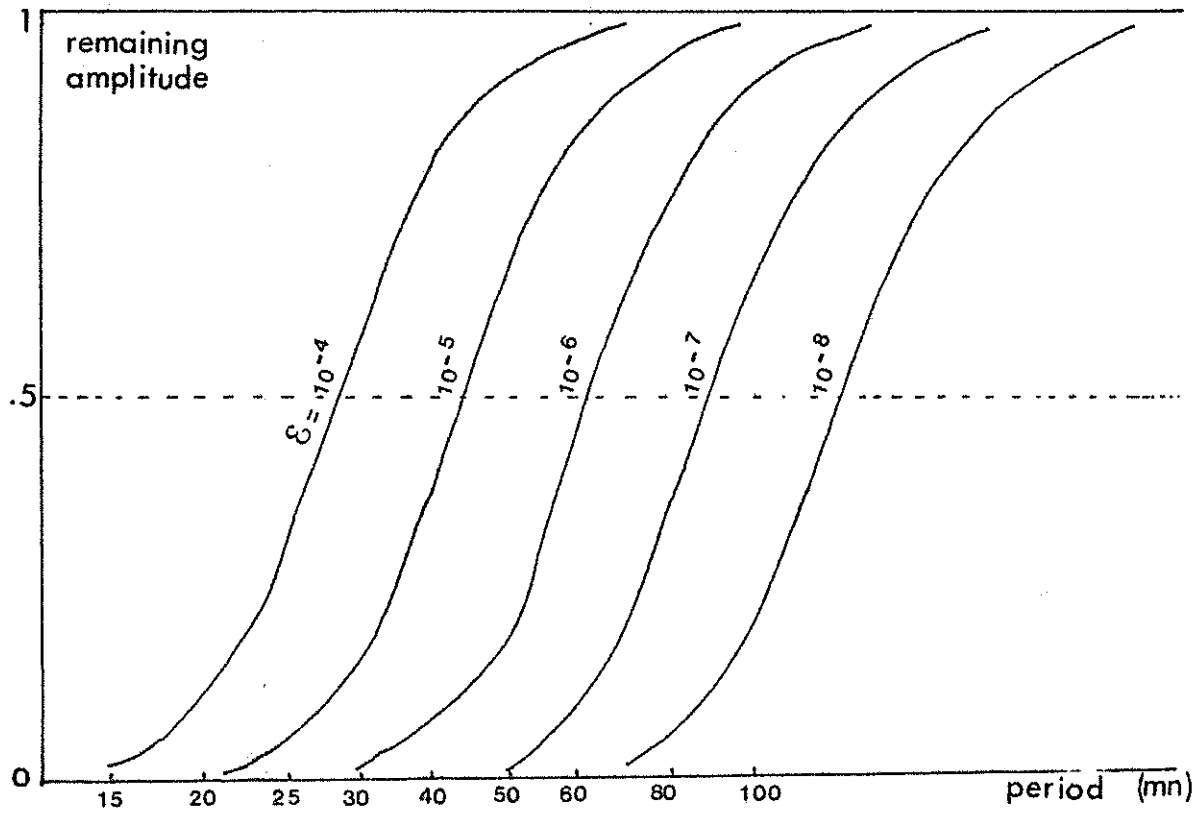

Figure 1. Filter corresponding to different degrees of smoothing (characterized by ε)by Vondrak's algorithm.

Table 1 shows the values of the root-mean square of the residuals $E'_4(t)$ with respect to the smoothing.

Smoothing coefficient	root-mean square of $E'_4(t)$ with respect to the smoothing (in cm)
10^{-6}	12.4
10^{-7}	47.0
10^{-8}	172.3

Table 1. Simulated pass-smoothing of the residuals to a 4th order polynomial fit.

The inadequacy of the polynomial fit, particularly at the extremities of the interval (Gibbs phenomenon), is in fact responsible of the impossibility of reaching the 1 cm precision. This leads to the idea to use a more sophisticated parametrized representation using polynomial expansions.

2) Tchebycheff polynomial expansions have been used for several years by the Bureau des Longitudes for ephemeris calculations (Connaissance des Temps). Among other polynomial expansions (Hermite, Laguerre, Lagrange, Legendre) Tchebycheff's ones have simple expressions.

Their form is

$$P_n(t) = \sum_{k=1}^{n} C_k \; T_k(t)$$

n order of the expansion

$T_k(t)$ Tchebycheff polynomial of k^{ieth} order

$T_k(t) = \cos(k \arccos t)$

C_k are defined as

$$C_o = \frac{1}{n} \sum_{i=0}^{n-1} P_n(t_i)$$

$$C_k = \frac{2}{n} \sum_{i=0}^{n-1} P_n(t_i) \cos \frac{k\Pi}{2n} (2i + 1)$$

$$\text{with } t_i = \cos \frac{\Pi}{2n} (2i + 1)$$

Further details can be found in mathematical handbooks (as J. Legras 1963). We have used the software of interpolation and approximation by Tchebycheff polynomial expansions implemented by J. F. Lestrade (1976) for a study about the representation of the attitude of the astrometric satellite Hipparcos.

Over the pass interval I

$$E_n(t) = D(t) - P_n(t)$$

is the error of the representation of D(t) by $P_n(t)$. The size of this error can be characterized by a norm

$$M_n = \sup_{t \in I} |E_n(t)| \qquad \text{maximum error}$$

$$\text{or} \quad s = \sum_{t \in I} E_n(t)^2 \qquad \text{quadratic error}$$

The "best approximation" of D(t) on I can be defined as the polynomial expansion yielding either M_n or s minimal.

Application to a simulated pass.

The table 2 gives, function of the expansion order, the values of the two norms

expansion order	$M_n = \sup_I \lvert E_n(t) \rvert$ (in cm)	$s = \sum_I E_n(t)$ (in cm)
12	270.0	148.0
14	29.0	15.0
16	4.3	1.7
18	2.1	.6
20	1.3	.5
22	.8	.5
24	.6	.4
26	.6	.4

Table 2. Simulated pass. Convergence of the residuals to a Tchebycheff representation.

The requirement of the 1 cm precision is fulfilled ; the method can be applied to real data.

III Case of real data.

1) Example of application to dense passes.

A first approximation is performed with an expansion order n = 8 ; the procedure is iterated (n = n + 2) until the determination of the "best approximation" (with respect to the quadratic norm s).

When the root-mean square between two consecutive values is stable (i. e. the difference is inferior to a preset quantity) the convergence is declared. During this procedure, identification and deletion of spurious data is done on the basis of the comparison of their residuals to the global root-mean square.

For construction of normal points the pass is cut into 3 mn intervals I_P. The datation of the normal point t_p is chosen to be the closest possible to the center of the interval (at a real data datation), in order to avoid new interpolation and for use of the calculated refraction correction usually transmitted with the observational data.

The value of the normal point is

$$N(t_P) = P_n(t_P) + \frac{1}{n_P} \sum_{j=1}^{n_P} E_n(t_j)$$

this for dense passes when the residuals $E_n(t_j)$ are gaussian. A typical histogram of the number of the residuals with respect to their values is shown figure 2, the mean of the residuals is different of zero.

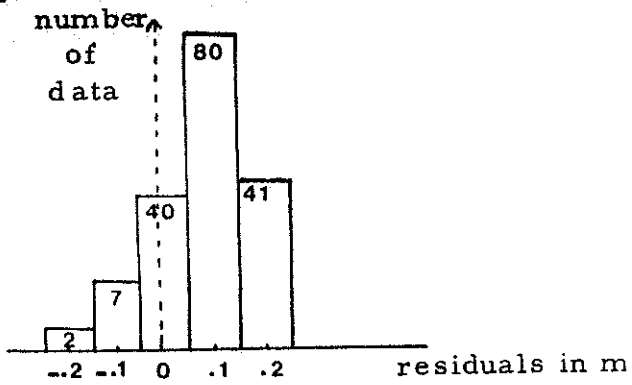

Figure 2. Dense pass histogram number of data per residual interval for station Yarragadee (7090).

Figure 3 represents the residuals (raw data -Tchebycheff representation) over a pass of station Grasse (7835). For most of the 3 mn normal intervals, the residual function is gaussian.

For other passes with small density of observations (some per mn) the residual function is usually not gaussian over the 3 mn intervals (fig. 4). The averaging should be made by another way.

In case where $E_n(t)$ is gaussian over the 3 mn interval I_P, the root mean square of a single residual with respect to the mean $\frac{1}{n_P}\sum E_n(t)$ is :

$$\sigma_{o,\,P} = \sqrt{\frac{n_P \sum E_n(t)^2 - \left(\sum_{I_P} E_n(t)\right)^2}{n_P\,(n_P - 1)}}$$

To take into account the number of data n_P in I_P the root-mean square of the normal point will be

$$\sigma_P = \sigma_{o,P} \sqrt{\frac{1}{n_P}}$$

When the number of data is small ($\lesssim 5$) over I_P the expression herebefore of σ_P has few signification. In this case, a conventional expression has to be chosen for σ_P, for example

$$\sigma_P = \sigma_o \sqrt{\frac{1}{n_P}}$$

σ_o being the root-mean square of the whole pass with respect to the fitted representation.

To avoid an overweight of the normal points of some stations compared to the others it will be necessary to give an inferior limit to their σ_P.

Tables 3 to 5 show the observational normal points of typical passes of different laser tracking stations : Yarragadee (7090), Haystrack (7091), Grasse (7835), Orroral (7943) and Arequipa (7907).

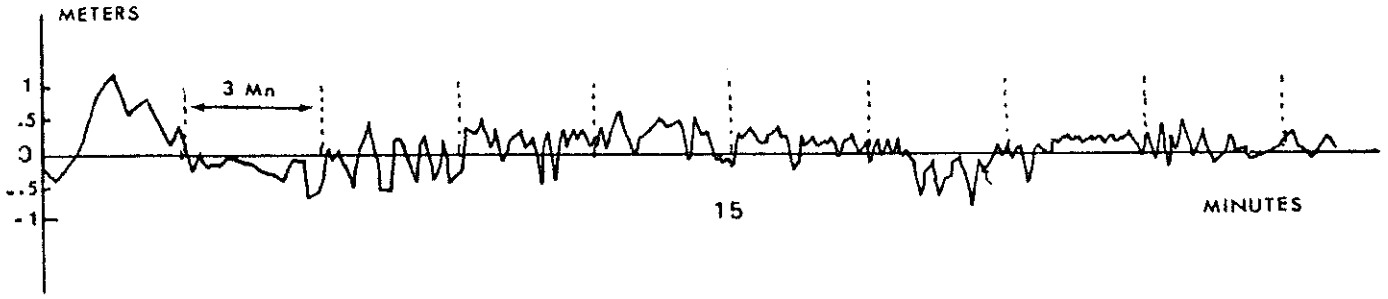

FIGURE 3 GRASSE (7835). Residuals over a dense pass

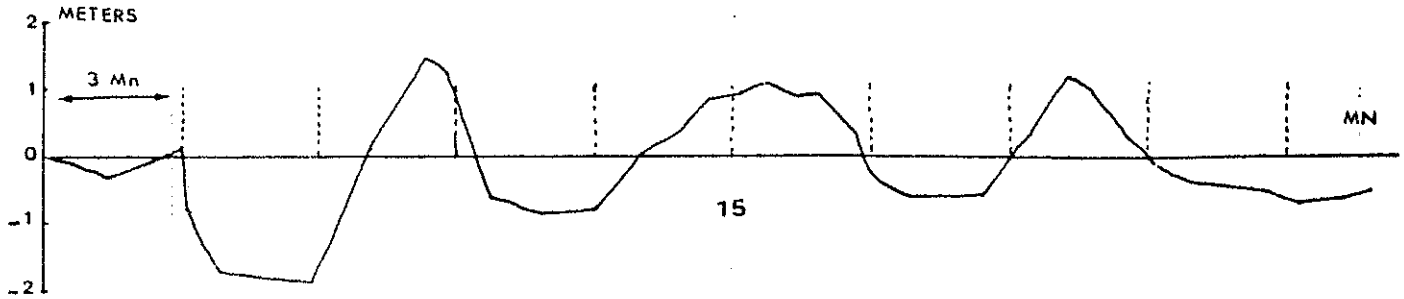

FIGURE 4 GRASSE. Case of a pass with a poor data distribution

NORMAL POINTS EVERY 180. S STATION 7090 DAY = 219 PASS 18 H 2 MN

LENGTH OF THE PASS = 31. MN NUMBER OF DATA = 1514 DENSITY =48.7 MES. PER MN

DATE IN SECONDS	NORMAL POINT(M)	SIGMA(M)	NUMBER OF DATA
65055.024823	7291576.196	.008	135
65235.023828	6993460.851	.008	140
65414.023085	6770529.905	.008	151
65594.022617	6630111.008	.007	154
65773.022451	6580632.286	.010	127
65954.022599	6624847.583	.009	151
66134.023063	6760928.643	.008	170
66314.023793	6982690.143	.009	132
66494.024787	7280812.034	.006	170
66673.025992	7642081.960	.009	120
66827.027173	7995987.556	.017	39

NORMAL POINTS EVERY 180. S STATION 7091 DAY = 214 PASS 9 H 13 MN

LENGTH OF THE PASS = 46. MN NUMBER OF DATA = 2096 DENSITY =45.4 MES. PER MN

DATE IN SECONDS	NORMAL POINT(M)	SIGMA(M)	NUMBER OF DATA
33329.033575	8102650.880	.110	31
33509.032098	7659847.325	.025	74
33689.030749	7255330.624	.016	124
33868.029569	6901499.131	.012	155
34048.028582	6605700.550	.011	169
34228.027834	6381398.543	.010	176
34408.027358	6238692.904	.008	176
34588.027179	6184952.424	.006	173
34768.027307	6223487.879	.008	168
34948.027739	6352903.572	.011	172
35128.028455	6567416.254	.010	175
35308.029424	6857988.652	.009	171
35488.030611	7213804.507	.012	143
35655.031873	7592435.559	.027	25
35849.033497	8079238.527	.025	73
35998.034834	8480065.516	.042	17

Table 3. Observational normal points for YARRAGADEE (7090) and HAYSTACK (7091).

NORMAL POINTS EVERY 180. S STATION 7835 DAY = 268 PASS 20 H 33 MN

LENGTH OF THE PASS = 34. MN NUMBER OF DATA = 213 DENSITY = 6.2 MES. PER MN

DATE IN SECONDS	NORMAL POINT(M)	SIGMA(M)	NUMBER OF DATA
74178.419422	7667431.525	.187	8
74308.418851	7385276.923	.073	15
74493.419633	7038015.392	.081	20
74658.405520	6791393.727	.065	22
74843.384960	6596337.070	.051	26
75028.382256	6496275.659	.034	28
75203.374117	6493737.522	.064	21
75388.371423	6588390.756	.041	28
75568.433195	6771716.180	.053	15
75743.465609	7027917.738	.041	18
75923.343449	7360653.731	.040	9
76078.416694	7695067.734	.219	2

NORMAL POINTS EVERY 180. S STATION 7835 DAY = 323 PASS 19 H 31 MN

LENGTH OF THE PASS = 40. MN NUMBER OF DATA = 215 DENSITY = 5.4 MES. PER MN

DATE IN SECONDS	NORMAL POINT(M)	SIGMA(M)	NUMBER OF DATA
70379.151165	8433620.657	.143	14
70574.139353	8001245.100	.093	15
70754.116162	7656231.990	.103	20
70934.167699	7373625.228	.060	16
71114.188048	7163397.833	.072	18
71299.150107	7031309.871	.083	9
71474.162679	6989902.833	.075	23
71659.155714	7036306.990	.108	21
71834.132708	7163365.241	.091	18
72014.179387	7372834.768	.108	18
72184.195106	7636452.918	.112	11
72374.200836	7996267.958	.108	13
72554.191649	8389932.663	.185	15
72699.178368	8737395.459	.353	2

Table 4. Observational normal points for GRASSE (7835).

NORMAL POINTS EVERY 180. S STATION 7943 DAY = 218 PASS 19 H 17 MN

LENGTH OF THE PASS = 12. MN NUMBER OF DATA = 79 DENSITY = 6.3 MES. PER MN

DATE IN SECONDS	NORMAL POINT(M)	SIGMA(M)	NUMBER OF DATA
69547.550798	7756274.611	.079	10
69727.480796	7460786.461	.071	20
69907.450796	7225638.910	.089	22
70087.450797	7058088.086	.046	23
70199.930796	6990246.336	.191	3

NORMAL POINTS EVERY 180. S STATION 7907 DAY = 217 PASS 9 H 17 MN

LENGTH OF THE PASS = 38. MN NUMBER OF DATA = 135 DENSITY = 3.5 MES. PER MN

DATE IN SECONDS	NORMAL POINT(M)	SIGMA(M)	NUMBER OF DATA
33570.030776	7193551.064	.215	7
33750.040777	6817125.741	.215	7
33930.160777	6506930.794	.129	10
34102.660777	6283498.590	.166	15
34267.560777	6146025.484	.145	12
34462.560777	6087256.934	.175	15
34650.080777	6139556.805	.163	16
34837.580777	6294986.591	.204	8
35010.080777	6521321.762	.181	11
35175.080777	6803254.297	.150	8
35355.080777	7172289.317	.215	7
35542.580768	7611795.641	.179	8
35707.580775	8034772.430	.254	5

Table 5. Observational normal points for ORRORAL (7943) and AREQUIPA (7907).

2) Example of a complete processing

The procedure for the construction of normal points has been applied to a 5 day data span of august 1980 (Merit Campaign) for NASA and SAO tracking stations.

For dense passes (several tens per minute) with good data distribution, the "best approximation" is easily reached with about 20 Tchebycheff coefficients. In some cases, however, the identification of bad data is not correctly done ; the procedure has to be refined.

For passes with weak number of data or with low observational rate (some measurements per minute) the procedure, because of the interpolation method, does not seem to be adapted.

A preliminary orbit computation with the pole components determination, has been performed over a 5 day interval. Although many passes have been deleted in the normal points constructions, the results obtained are equivalent to these obtained during the same period using a sampling of the data. The values of the computed pole components are given table 6.

	Pole computation with sampling of data	Pole computation with normal points	BIH Circ. D
Number of data	2308	195	
x	- .009	- .057	- .024
σ_x	.008	.020	
y	.317	.306	.304
σ_y	.004	.009	

Table 6. Pole components determinations using the sampling of data and the normal points.

IV Conclusion. Advantages, limitations and possibilities of the method.

Tchebycheff polynomial expansions seem well adapted for the construction of normal points when measurements are dense enough during a pass.

The software may be easily implemented on mini-computers. The algorithms have to be refined to take into account the multiplicity of the data distributions ; yet for passes with low density data, another treatment has to be used.

The root-mean square associated with normal points is optimistic. The normal points values, depending on the polynomial representation are correlated. To minimize the dependence, good methods for averaging the residuals (raw data - representation) are required.

Within the framework of the organization of an earth rotation service, each laser tracking station using this procedure or a similar one, could reduce its own data in order to send normal points to this service. The volume of data may be highly reduced (see the annex). The task of the processing to calculate the earth rotation parameters would be lightened and the delay of availability of the results shortened.

References.

B. Lago and A. M. Mainguy. Condensation des données d'observation en vue d'une utilisation géodésique. Space Research XI. Akademie Verlag, Berlin 1971, p. 515.

J. Legras. Précis d'Analyse Numérique. Ed. Dunod 1963.

J. F. Lestrade. Communication personnelle.

J. Vondrak. Problem of smoothing observational data. Bull. Astron. Inst. Czech. 28 (1977), p. 84-89.

A N N E X

	Number of characters
Satellite	6
Station	4
Meteorological data	10
Date (year, day)	6
Center of mass correction	4
Various indexes	4
Total	34

General informations over the pass

	Number of characters
Datation (μs)	11
Measurement normal point(mm)	11
Sigma (mm)	5
Tropospheric correction (mm)	5
Total per normal point	32

Information per normal point

for the whole pass (14 normal points) 34 + 32 x 14 = 482 characters

So about 3/1000 of the global volume transmitted in format SEASAT

Number of characters sufficient for representing a pass. Example of a 40 mn pass with 2000 data.

AN EVALUATION AND UPGRADING OF THE SAO PREDICTION TECHNIQUE

J. H. LATIMER, D. M. HILLS, S. D. VRTILEK,
A. CHAIKEN, D. A. ARNOLD and M. R. PEARLMAN

ABSTRACT

We review the current SAO prediction system capability and discuss recent improvements that show results for 60-day test prediction periods for Lageos. The improvement package is machine-accessible.

OVERVIEW OF THE CURRENT SYSTEM

The current prediction system at SAO is based upon two key programs: an orbit determination program (GRIPE) used at the central computation facility in Cambridge, and a look-angle and predicted range generator program used at field sites (FLPPS). Observations obtained at field sites are fed to the GRIPE program, and Keplerian elements derived from GRIPE are supplied to the FLPPS program. This data flow is the basis of the tracking cycle.

GRIPE is a general purpose orbit analysis program for artificial earth satellites which has been developed as a research tool. It is based primarily on analytical perturbation theory and can take as observations a variety of data types including optical or electronic direction observations, ranging data, range rate or velocity data, and altimetric ranging data. In addition to computing orbital elements, GRIPE can solve for corrections to the gravity field coefficients, station coordinates, frequency offsets and drift rates for range rate observations, the earth's

pole position, the gravitational constant GM, and an earth radius scale factor.

GRIPE is a differential improvement program requiring that initial estimates for modelling parameters be reasonable in order that convergence of iterated solutions can occur. The observation model computes the vector between the observing site and the satellite and must consider perturbations to both positions. Perturbation theory applied to the satellite position includes the following:

1. Kinoshita's Short Periodic Oblateness (to first and second orders in J2, and optionally to third order),
2. Gaposchkin's Tesseral Harmonics development,
3. Kozai's Direct Lunar and Solar effects (both long and short periodic),
4. Kozai's Body Tide treatment (due to both Lunar and Solar effects),
5. Kinoshita's Long Periodic Zonal Harmonics to first and second orders. Other perturbations not used in acquisition ephemeris work are:
6. Doodson's Ocean Tide effects (lunar and solar),
7. Kinoshita's reference system adjustment,
8. Aksnes' Direct Effect Radiation Pressure,
9. Lautman's Albedo and Infra-red effects.

Station positions are adjusted for the effects of UT1 (when known), for pole position, and for the effect of solid earth body tides due to the sun and moon.

The observed quantity relating the station and the satellite is reduced for the tropospheric or parallactic refraction, and if ranging data, for the offset between the center of mass and the reflector array and a small general relativity effect.

GRIPE has the capability of displaying the observation residuals and then halting execution before improving any modelling parameters. This mode of operation is known as a "residual run", and is a basic tool used in the analysis of prediction orbit quality described below.

UPDATING

The motivation for upgrading prediction accuracy at SAO is to be able to tighten the range gate for better discrimination against noise pulses in the return pulse detection process. The improvement sought involves a mixture of software changes and procedural changes. Changes to the GRIPE orbit determination are purely procedural in that no coding changes are necessary. Our testing shows that we would benefit by lengthening the data span for orbit determination and by holding constant some orbital parameters more accurately determined over long term studies. These parameters include the rate of perigee, and the quadratic term in mean anomaly. Our tests have no rate of eccentricity or inclination in the model, which differs from our current operational technique. The final change in the GRIPE procedure is the inclusion of solar perturbations, both long and short periodic. The current technique absorbs to a certain extent these effects in the mean elements.

For the field program, FLPPS, the changes are algorithmic, in that the older analytic lunar perturbation package, which only computed the principal lunar term, has been replaced with a lunar perturbation package identical to that in GRIPE. This package is a numerical integration package and facilitates now the computation of the solar perturbations as well, so that the FLPPS has this additional capability.

Users of the SAO orbital element service would do well to consider including this a)improved lunar and b)solar perturbation capabilities for the following reasons:

1. Obtaining improved prediction accuracies as demonstrated below.
2. Avoiding the problem of incompatibility between field software expecting solar perturbations to be absorbed into the determination of mean elements (the present situation) and orbit computation expecting solar perturbations to be separately and explicitly applied.
3. The key routines are available separately in machine-accessible form in order to ease the task of updating code.

RESULTS

As it is impractical to try prediction experiments with an operational network, our measurement of prediction quality decomposes into two stages. The first stage is to demonstrate that the central facility and the field site software are in agreement in terms of orbit theory as manifested by the computation of angles and ranges between stations and satellites. This stage does not address the issue of inherent quality of representation of a trajectory, but only that of consistent algorithmic treatment of an orbit model. This may be done with simulations or other analytic methods. Our tests (see figure 1.) indicate that this agreement is within the noise of the method of testing for about 30 days and within 0.25 microsec of range gate for about 60 days using the LAGEOS orbit. This is the software implementation, or "ZEROSET" test.

The other aspect is that of the quality of an orbit as a description of a satellite trajectory, and this can only be measured with real observational data, and thus we are obliged to use data archives to draw conclusions. However, having done the ZEROSET test, we are here unconcerned with software compatibility and can test the orbit extrapolation qualities with the orbit determination program run in residual mode. Figure 2 shows the extrapolation over time of an orbit of LAGEOS obtained with the current operational procedure. Next, we see a factor of two improvement when the solar perturbation is added. Some additional improvement is noticeable when the test orbit is generated with data from seven stations instead of only one station. Further improvement is noticed when the test orbit is generated from 18 instead of 9 days of data. When the rate of perigee and the quadratic term in mean motion are fixed still further improvement is noticed although there is no significant difference in the orbits obtained from 18 and 9 days of data. These last orbits, as the figure shows, are within 0.50 microsec of range gate for about 30 days.

These tests were performed with data from the summer of 1981, and to confirm these results the final test (18 days, fixed rate of perigee and quadratic term in mean motion) was performed with data from the fall of 1980. The results of this test are shown in figure 3. These results are similar to the above, which suggest that even better results could be obtained by using rates obtained from long-term analysis. Further study ought to also consider any effects from degradation of elements other than mean anomaly, which is emphasized in this analysis.

ACKNOWLEDGMENT

This work was supported by Grand NGR 09-015-002 from the National Aeronautical and Space Administration.

REFERENCES

Brown, E. W., 1908, "Theory of the motion of the Moon; containing a new calculation of the expression for the coordinates of the moon in terms of the time." Mem. Royal Astr. Society 53.

Cartwright, D. E., and A. C. Edden, 1973, Corrected table of Tidal Harmonics" Geophys. J. 33:253-264.

Doodson, A. E., 1921, The harmonic development of the tide-generating potential. Proc. Roy. soc. A. 100: 305-329.

Gaposchkin, E. M., 1970, "Improved values for the tesseral harmonics of the Geopotential and Station Coordinates." Dynamics of Satellites 1969, ed. by B. Morando, Springer-Verlag, Berlin, 109-118.

Gaposchkin, E. M., 1973, Standard Earth iii, Smithsonian Astrophysical Observatory Special Report 315.

Gaposchkin, E. M. and E. Lambeck, 1969 Standard Earth III, Smithsonian Astrophysical Observatory Special Report 315.

Gaposchkin, E. M. and E. Lambeck, 1971, "The Earth's gravity field to sixteenth degree and station coordinates from satellite and terrestrial data." Journ. Geophys. res., vol. 76, 4855-4883.

Hori, G., 1973, "Theory of General Perturbations" In Recent Advances in Dynamical Astronomy, ed. by B. D. Tapley and V. Szebehely, D. Reidel Publ. Co., Dordrecht-Holland, 231-249.

Izsak, I. G., 1964, "Tesseral Harmonics of the Geopotential and Corrections to Station Coordinates." Journ. Geophys. Res., vol. 69, 2621-2630.

Kaula, W. M., 1967, "Theory of Statistical Analysis of Data Distributed over a Sphere" Rev. Geophys., vol. 5, 38-107.

Kinoshita, H., 1977, "Third-order Solution of an Artificial Satellite Theory" Smithsonian Astrophysical observatory Special Report 379.

Kozai, Y., 1973, "A New Method to Compute Perturbations in Satellite Motions" Smithsonian Astrophysical Observatory special Report 349. Modifications by Kozai were made in 1979 and 1980.

Love, A. E. H., 1908, "Note of the Representation of the Earth's Surface by Means of Spherical Harmonics of the First Three Degrees." Proc. Roy. Soc. A. 80: 553-556.

Veis, G., 1963, "Precise Aspects of Terrestrial and Celestial Reference Frames" Smithsonian Astrophysical Observatory Special Report 123.

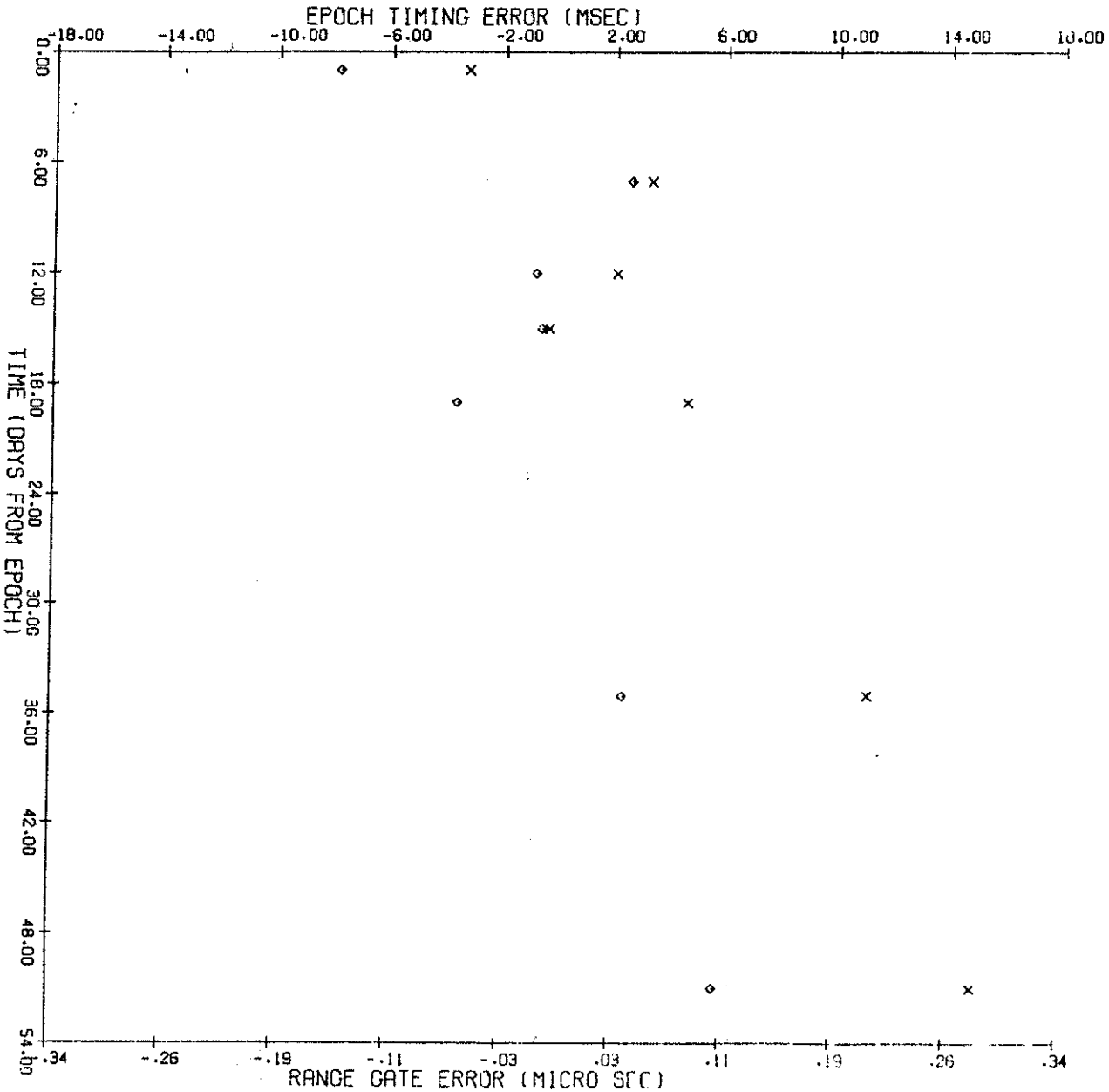

Figure 1.
"Zeroset"
Consistency between field and central software implementations (Zeroset).
New FLPPS pseudo-obs. vs. new GRIPE in FLPPS mode
X = beg.; ◊ = end obs. in each pass (≳ 30° elevation angle)

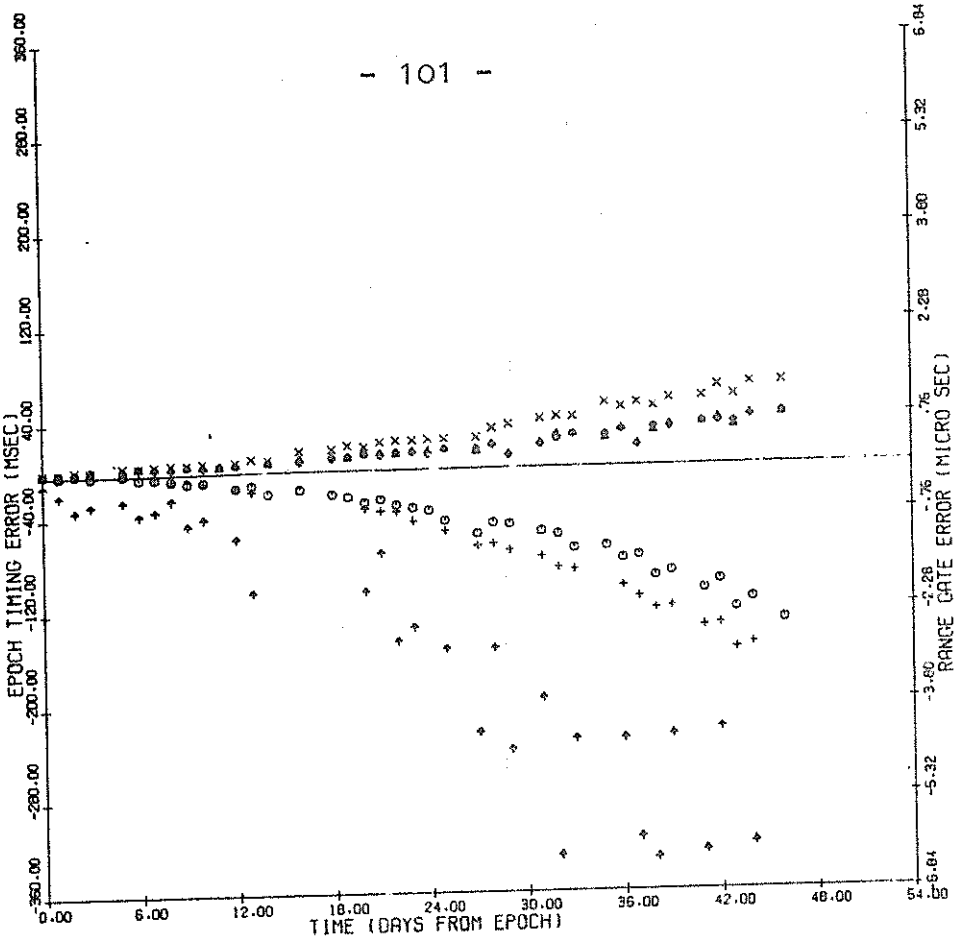

Actual data vs.:

⧫ = old GRIPE (no solar) ṅ = .5E-8	X = new GRIPE (solar) 7 station orbit (18 days) ṅ = -.5E-9
+ = new GRIPE (solar) 1 station orbit (9 days) ṅ = .7E-8	⧋ = new GRIPE (solar) 7 station orbit (9 days) fixed rates ṅ = .43E-9
⧫ = new GRIPE (solar) 7 station orbit (9 days) ṅ = .5E-8	◇ = new GRIPE (solar) 7 station orbit (18 days) fixed rates ṅ = .43E-9

Figure 2. Results of orbit quality tests. From bottom to top, series are:
a) current technique (no solar perturbation)
b) add solar, one station, 9 day arc
c) solar, 7 stations, 9 day arc
d) solar, 7 stations, 9 day arc, fix rates
e) solar, 7 stations, 18 day arc, fix rates
f) solar, 7 stations, 18 day arc

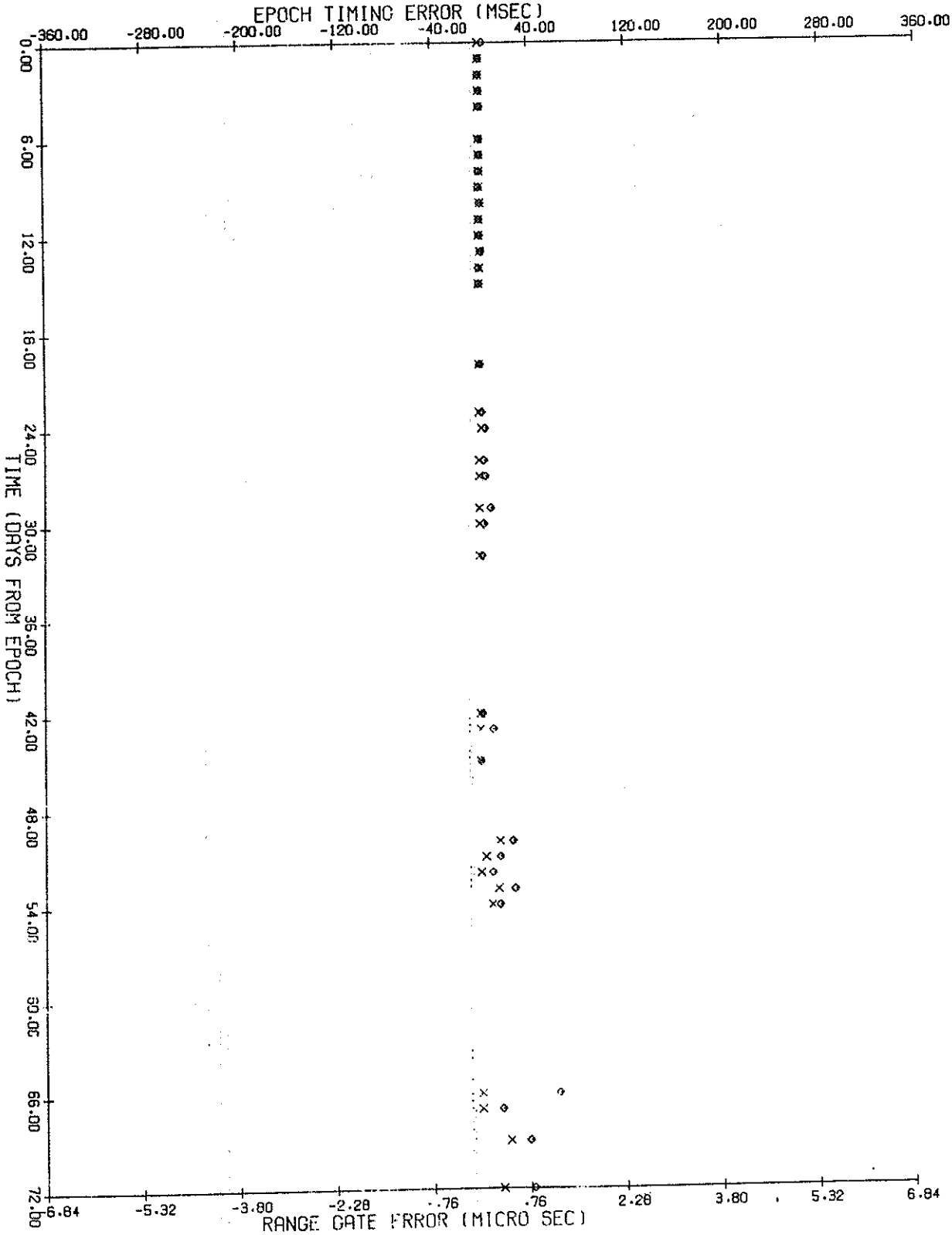

Figure 3.

Results of orbit quality tests for fall, 1980 period. Same technique as Figure 2e. In some cases, two estimates are available, X represents either second estimate or zero.

APPENDICES
LUNAR PERTURBATION OVERLAY

S. Vrtilek
May 1981

The lunar perturbation overlay uses the luni-solar perturbation theory developed by Y. Kozai as reported in Smithsonian Special Report 349. All source codes necessary for this overlay are on FLPPS Disk One.

THE SUBROUTINES USED IN THIS OVERLAY ARE:

RDZON--Loads registers with Zonal harmonics
INST--Calculates instantaneous elements at epoch of observation
GETSMA--Calculates Semi-major Axis
NFINC--Calculates Inclination function
HANSEN--Calculates Eccentricity function
FACCAL--Computes factorials
LUNARK--Calculates long period and short-period luni-solar perturbations
SETUP--Assigns variables for integration
KIND--Integrates terms for lunar and solar perturbations
SUNVECT--Calculates vector to Sun
LUNVECT--Calculates vector to Moon
PRECESS--Calculates terms due to precession
EVA--Computes sin and cos terms for eccentricity and mean anomaly

THE FUNCTIONS USED IN THIS OVERLAY ARE:

CONSOC--Stores the constants used in overlay
ERIQA--Solves Kepler's equation
LOAD--Takes lower order 4 bytes from a Real*8 and puts them into an Integer*4
PUT--Puts Integer*4 into bits 0-3 of a Real*8
ASIN--Finds arcsin
ATANG--Finds modified arctan

THE LIBRARIES USED IN THE OVERLAY ARE:

STDLUNLIB--Contains binary for all of
above
WFWLTUTIL--System utilities
WFWRUN--Fortran utilities
WFWSOS--System utilities

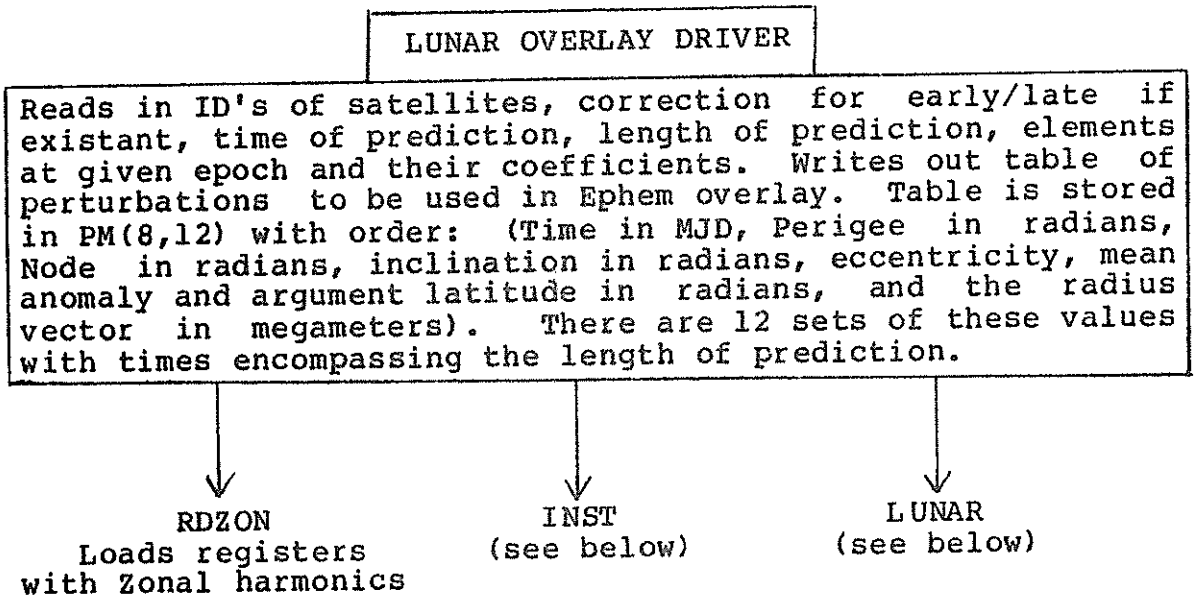
LUNAR OVERLAY DRIVER
Reads in ID's of satellites, correction for early/late if existant, time of prediction, length of prediction, elements at given epoch and their coefficients. Writes out table of perturbations to be used in Ephem overlay. Table is stored in PM(8,12) with order: (Time in MJD, Perigee in radians, Node in radians, inclination in radians, eccentricity, mean anomaly and argument latitude in radians, and the radius vector in megameters). There are 12 sets of these values with times encompassing the length of prediction.
RDZON
Loads registers with Zonal harmonics
INST
(see below)
LUNAR
(see below)

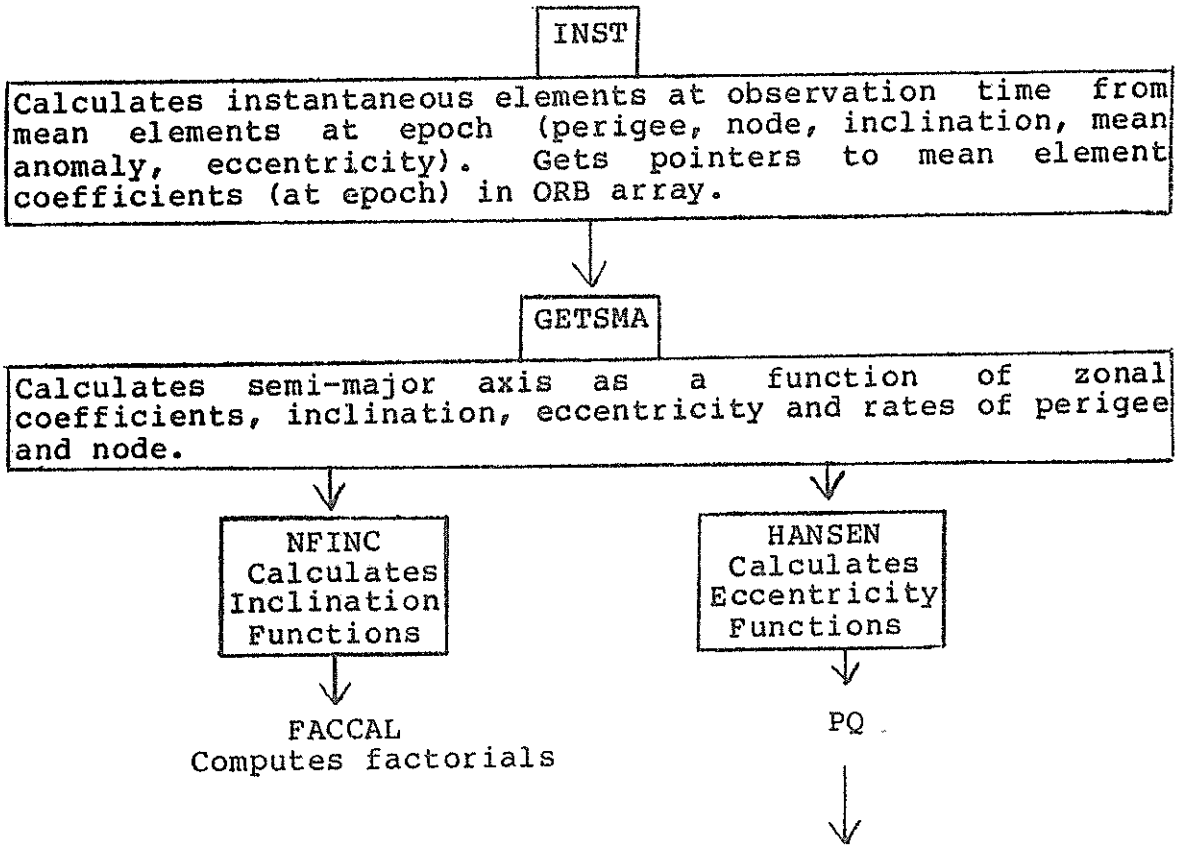
INST
Calculates instantaneous elements at observation time from mean elements at epoch (perigee, node, inclination, mean anomaly, eccentricity). Gets pointers to mean element coefficients (at epoch) in ORB array.
GETSMA
Calculates semi-major axis as a function of zonal coefficients, inclination, eccentricity and rates of perigee and node.
NFINC
Calculates Inclination Functions
HANSEN
Calculates Eccentricity Functions
FACCAL
Computes factorials
PQ

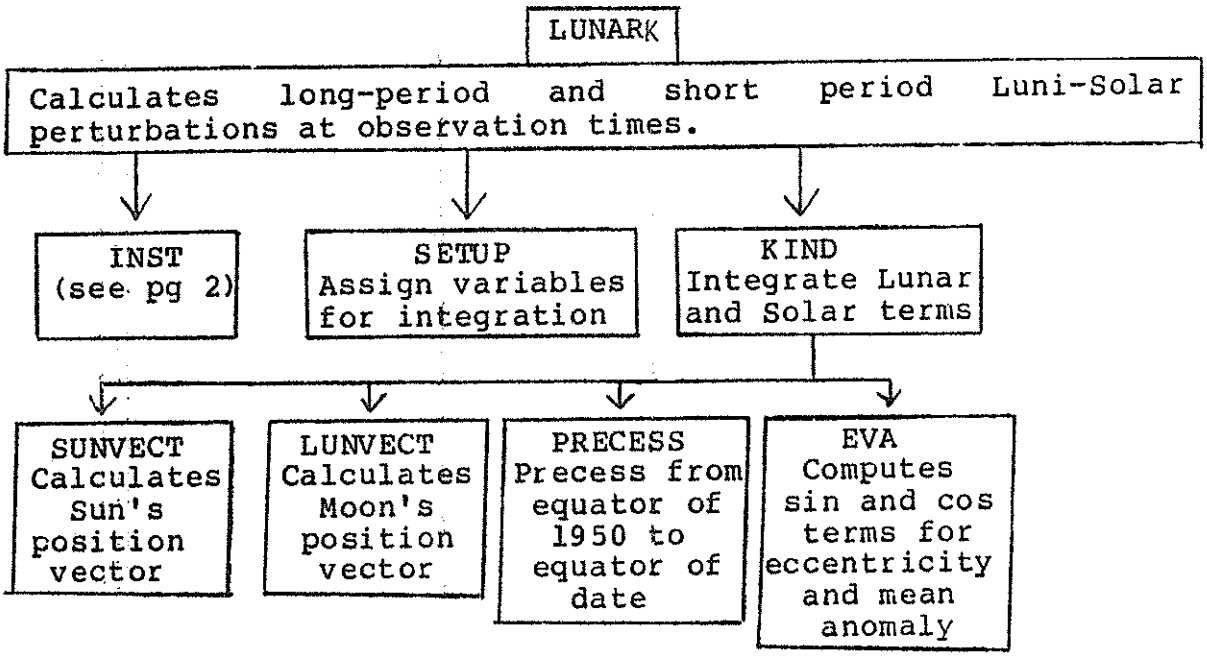
LUNARK
Calculates long-period and short period Luni-Solar perturbations at observation times.
INST
(see pg 2)
SETUP
Assign variables for integration
KIND
Integrate Lunar and Solar terms
SUNVECT
Calculates Sun's position vector
LUNVECT
Calculates Moon's position vector
PRECESS
Precess from equator of 1950 to equator of date
EVA
Computes sin and cos terms for eccentricity and mean anomaly

A REVIEW OF NETWORK DATA HANDLING PROCEDURES

J. H. LATIMER, J. M. THORP,
D. R. HANLON, G. E. GULLAHORN

SMITHSONIAN ASTROPHYSICAL OBSERVATORY

ABSTRACT

We review communications formats for ranging data, and data handling and techniques. Examples of code used for producing or reading various data types are machine-accessible.

DATA FLOW

Network Data handling today is concerned with a variety of data paths and data types. The so-called Quick-Look data cycle is in reality a complex of three information paths which help maintain orbits for a vital network.

The first path is the flow of acquisition ephemerides from central computing facilities to field sites. These data have evolved from centrally-computed pointing angle lists teletyped in lengthy messages to rather brief trajectory descriptions, either Keplerian elements, or IRVs (Inter-Range Vectors). This evolution was made possible by the advent of mini-computers which were placed at field sites.

The second path is the return of a sampling of observational data to the computing center for ephemeris maintenance and data quality monitoring. To be effective, the data must be timely and accurate, yet to be efficient, the data must be evenly sampled and the message format must be reasonably concise.

The third and final path is that used to feed back quality control information to site personnel. Particularly some of the systematic errors can be very subtle and difficult to spot with the information normally available at a remote site. Range biases or epoch timing biases are naturally noticed more readily at a central computing facility. Speed of detection and rectification of such problems is important in order to avoid contamination of large quantities of data.

Final Data

Having organized a Quick-Look data processing cycle to maintain tracking orbits, we must take care to process the complete and final data set for dissemination to the scientific community in as careful a manner as possible. Our problem will tend not to be speed so much as the large quantity of data with which we must contend. The data processing can go much smoother if reasonable data representation is adopted, and of course, submission of data to a data bank such as the National Space Science Data Center run by NASA/Goddard for archiving and distribution requires well understood standard formats.

DATA FORMATS FOR LASER RANGING

The purpose of this section is to document the common data formats in use currently, and to provide code for the creation or transformation of these formats.

Quick-Look

Two well-known Quick-Look formats, the SAO and NASA, are defined in the appendices, and code from the Data General Nova 1200 at SAO field sites which produces 333 data is appended The companion package, a set of routines that are used at SAO's central facility which read 333 data, is listed. These routines also read the NASA Quick-Look format.

Intermediate

At SAO we have two forms of intermediate data representation, for two very different reasons. Because of the large investment in the GRIPE orbital program its coded observation format (known as the DOI format) is retained for use by this program. One advantage of retaining this format was the capability of representing very old data so that long time-span analyses could be undertaken without the

problems of data transformation or program code modification.

Two years ago we adapted to a new computer and in the process of conversion we introduced a machine-specific binary format closely related to the DOI format, but more efficient for data processing (sorting, selection, performing I/O). We treat as utilities those packages which transform from coded representation to binary and vice versa.

Both internal formats are defined in the appendix, and Fortran code is provided for the SAO & NASA Quick-Look to binary transformation and for the SAO final log data to binary transformation. Code is also provided for binary to SEASAT coded, and to DOI coded transformation.

Final

There are two formats in use for representing final data for archiving and distribution. These are the binary and coded formats used by the National Space Sciences Data Center at NASA/GSFC. The coded format is known as the SEASAT format and is broken down in the appendix, and an example of code to produce this format is provided separately. A problem that users of NASA binary data can have is the use of this data on byte-oriented machines such as the DEC VAX. In the code portion of this paper we provide NASABIN which is a utility to transform NASA binary data to SAO internal binary format.

DATA REVIEW PROCEDURES

The most powerful information that a central facility can provide to a remote site is just that information unavailable at the remote site, that is, how well data fits when combined with a global data set in an orbit determination. At SAO we have designed a procedure which does this in a systematic way. Our implementation relies on a post-processor run subsequently to orbit determinations. This post processor reads a file of intermediate information left by the orbit program, and thus has essential information as it existed after the final iterative orbit estimation. In particular, range residuals are available, and partial derivatives to aid in the following simple computation.

The procedure considers each pass from a station individually, and makes a least squares solution for two parameters: a systematic range bias for the pass and a systematic epoch timing bias. This simple procedure builds upon the complicated orbital information already contained in the range residuals from the final orbit estimation process, and we can obtain very reliable noise estimates when there are no large biases present or oscillations in residuals caused by poor orbital modelling. In addition, the estimates of range and time biases can be interpreted. When they are small, there is no problem, as they reflect only the residual long wavelength uncertainties in the orbit modelling process. When they are large, it is indicative of either some defect in the model, such as station coordinates, or error in processing of the data, or real data problems or equipment malfunction.

At SAO all data are reviewed each week and cooperating sites are supplied with comments and interpretation of the post-processor printout. The appendix contains a few examples of these runs showing the summary listings and the individual scatter plots and histograms.

ACKNOWLEDGEMENT

This work was supported by Grant NGR 09-015-002 from the National Aeronautics and Space Administration

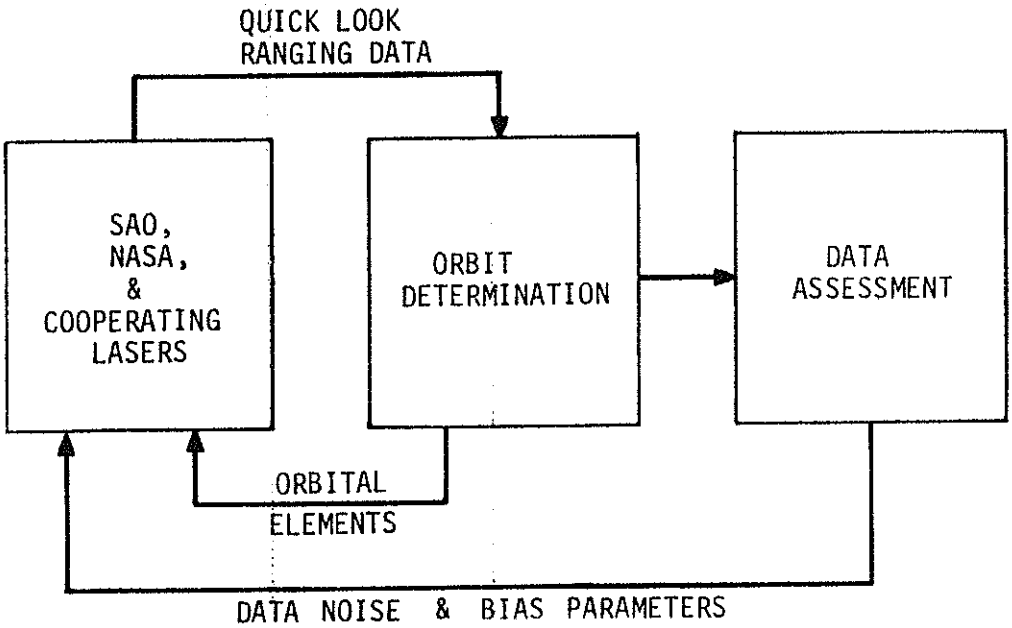

Figure 1.
Network data flow chart.

APPENDICES

SAO QUICK LOOK FORMAT

The SAO laser QL data format is shown below The format consists of five parts:

1. The seven characters "..LASER"
2. Station header line (words 1 through 3)
3. Pass header line (words 4 through 9)
4. Data lines (words 10 through 14 in each line)
5. The three characters "END".

Each word (1 through 14) has five decimal characters. Words are separated by one space. An explanation of each word follows:

WORD	CHARACTER	EXPLANATION
1	1 through 5	Always 33333
2	1 through 4	Station no.
2	5 and	
3	1	Year of century
3	2,3	Month of year
3	4,5	Day of month
4	1 through 5 and	
5	1,2	COSPAR Satellite ID
5	3	Sky/Shadow code for first point of pass: 0 => night, satellite illuminated; 1 => night, satellite in shadow; 2 => day
5	4,5	Relative humidity in percent
6	1	Sign of temperature. 0 => positive, 1 => negative
6	2 through 4	Temperature in units of 0.1 degree Celsius
6	5	Unused, always zero
7	1 through 4	Barometric pressure in millibars
7	5 and	
8	1 through 5	Pre-pass calibration average in units of 0.1 nanosec
9	1 through 5	Post-pass calibration average with ten thousand nanosec digit implied equal to that of Pre-pass
10	1,2	Epoch of pulse transmission hours (UT)
10	3,4	Minutes
10	5 and	

11	1	Seconds
11	2 through 5 and	
12	1,2	Microseconds
12	3,4	Check word
12	5	Confidence: 0 => probably good; 1 => probably bad
13	1 through 5 and	
14	1 through 5	Two-way range in 0.1 nanoseconds

The seven characters "..LASER" appear once at the beginning of each data transmission. The station header line is repeated for each different day of data within the transmission message. A pass header line begins each pass. Each data transmission ends with the three characters "END".

Sample 333 Quick Look laser data message

..LASER

Word 1	2	3			
33333	79438	01013			
Word 4	**5**	**6**	**7**	**8**	**9**
76039	01099	10500	09141	28659	28661
Word 10	**11**	**12**	**13**	**14**	
14311	49407	96610	05422	23382	

END

NASA Quicklook Format

Character	Description
1	"CR"
2	"CR"
3	"LF"
4	"1"
5	"B"
6	"B"
7-10	SIC (Spacecraft Identification Code)
11-12	VID
13-14	STATION ID (from STDN 724)
15-16	MOVE NUMBER - Sequence from birth
17	MOUNT TYPE "0" = AZ/EL "1" = X/Y
18	LASER/LAST FRAME INDICATOR "0" = Prime Laser/Not Last Frame "1" = Backup Laser/Not Last Frame "4" = Prime Laser/Last Frame "5" = Backup Laser/Last Frame
19	MODE "0" = Program Track "1" = AUTOTRACK (not currently available).
20	"SPACE"
21-25	WAVELENGTH in nm
26	"SPACE"
27-28	YEAR (mod 100)
29-31	DAY OF YEAR
32-36	SECONDS OF DAY
37-42	MICROSECONDS OF SECONDS
43	"SPACE"
44-49	ANGLE 1 (X or AZ) in 001 For X angle: If plus, then lead character will be a zero; if minus, then lead character will be minus sign. For AZ angle: Lead character will be 0, 1, 2, or 3.
50	"SPACE"
51-56	ANGLE 2 (Y or EL) in .001 In plus, then lead character will be a zero. Otherwise there will be a minus sign.

Character	Description
57	"SPACE"
58-69	RANGE (roundtrip time) in .01 nsec.
70-72	"SPACES"
73	"4"
74	"F"
75	"F"

NOTE: All values in quotes are constants and should be replaced by either their ASCII or BAUDOT representations (depending on whether it is 8 or 5 level).

DOI Data Card Format

This document describes the observation card format as read by GRIPE.

Field	Cols.	Description
1	1-7	Cospar Satellite Identification
2	8-12	Sequence Number
3	13-17	Station Number
4	18-23	Date of Observation
	18-19	year
	20-21	month
	22-23	day
5	24-33	Time designation
	24-25	hour
	26-27	minute
	28-29	second
	30-36	fraction of seconds to .1 microsec
6	37-46	observed range in meters, to .01 meters (xxxxxxxx.xx) or 2-way range in nano-seconds, to .1 nanosec. (xxxxxxxxx.xx)
7	49-52	refraction correction, to .01 meters (xx.xx) to be subtracted from range. This value, if present, may or may not have already been applied to the range (see columns 57&58)
8	53-58	Index Codes

Field	Cols.	Description
9	53	Time-precise index Code — Standard error in timing σ_t 0 — no estimates 1 — $\sigma_t \leq .003$sec 2 — $.003 < \sigma_t \leq .002$ 3 — $.002 < \sigma_t \leq .005$ 4 — $.005 < \sigma_t \leq .02$ 5 — $.02 < \sigma_t \leq .05$ 6 — $.05 < \sigma_t \leq .2$ 7 — $.2 < \sigma_t \leq .5$ 8 — $.5 < \sigma_t \leq 2.0$ 9 — $2.0 < \sigma_t$
	54-55	Standard Deviation a) either in meters and tenths of meters (or n.s and .1 n.s) (if col 54-55 < 25) or b) x, where x = 25 (log + 3) and = weight in meters (if col 54-55 > 25)
	56	Observation type index: always 8 for laser range
	57	Epoch System/Corrections Applied Index If col 56 = 8 (range obs.), then column 57, in conjunction with column 58, determines the time of the data taken and the corrections (refraction and center of mass) that have been applied and/or given

57	laser type	epoch	ref. corr	center of mass	weather info
0	A	trans	none	none	given
1	B	rcvd	given	none	given
2	new B	rcvd	given	given	given
3	old D	at sat.	applied	none	optional
4	new D	trans	see 58	see 58	given
5	E	trans	see 58	see 58	given

Field	Cols.	Description
	58	For col 56 = 8 (range in meters or nanosec) it gives obs. units and correction applied information. Values 1-7 refer to new laser D and E only. Values 8 & 9 refer to laser A, B and old D.

58	Explanation
1	one way range, in meters, not corrected for atmospheric refraction or spacecraft center of mass
2	one way range, in meters, corrected for atmospheric refraction and spacecraft center of mass
3	two way range, in nanoseconds, not corrected for atmospheric refraction or spacecraft center of mass
4	two way range, in nanoseconds, atmospheric refraction and spacecraft center of mass given, neither applied
5	two way range, in nanoseconds, atmospheric refraction and spacecraft center of mass corrections given, and applied
7	one way range, in meters, refraction correction and spacecraft center of mass corrections given, neither applied
8	one way range, in meters, see column 57 for atmospheric refraction and spacecraft center of mass correction information

Field	Cols.	Description
9	59-62	Calibration Stability
	59-61	Difference between pre and post calibration (absolute value) in nanoseconds included when code in column 62 is 2; no estimate otherwise
	59	tens
	60	units
	61	tenths
	62	Calibration index

Code no.	Explanation
2	Pulse processer system-pre & post
3	Pulse processer system-only one calibration
4	Pulse processer system-no pre or post calibration

10	63-66	Spacecraft center of mass correction
	63	Blank
	64-66	Spacecraft corr. to .01 meters to be added to range. This value, if present, may or may not have already been applied to the range, depending on cols. 57 and 58.
11	67-76	Weather Data
	67-70	Pressure (millibars)
	71-72	humidity (percent)
	73-76	temperature (Celsius to tenths)
12	77-81	Elevation angle to .001 degree
13	82-94	Predicted range
	82	blank
	83-92	2-way range to .1 n.s.
	93-94	blank

Field	Cols.	Description
14	95-100	Azimuth Angle to .001 degree
15	101-103	Speed of Light Code
	101	blank
	102-103	= 00 if c = 2.997925E10 cm/sec was used in reduction = 01 if c = 2.99792458E10 cm/sec was used in reduction
16	104-105	Range noise - given as 25 (log y + 3) where y = range noise in meters
17	106-107	Estimated Range Error - given as 25 (log z + 3) where z = estimated range bias in meters

SAO INTERNAL BINARY FORMAT FOR LASER OBSERVATIONS

ITEM 1 Satellite Identification (I*4)
ITEM 2 Observation Sequence no. and REJECTION FLAG (I*4)
This number, when negative, indicates that the observation has been rejected.
ITEM 3 Station no. (I*2)
ITEM 4 Modified Julian Date of Observation (I*4)
ITEM 5 Fractional part of Day of Observation (R*8)
ITEM 6 Type of Observation:
0 = end of pass
8 = laser observation
18 = laser observation; processed by GRIPE
ITEM 7 Observed Range (R*8) (Units depend on items 11, 12 - see GRIPE Manual)
ITEM 8 Refraction Correction in meters (R*4)
ITEM 9 Time precision (Standard Error) in seconds (R*4)
ITEM 10 Range Precision (Standard Error) in meters (R*4)
ITEM 11 Epoch System/Corrections Applied Index (identically same meaning as col. 57 of DOI format in GRIPE manual) (I*2)
ITEM 12 Observation Units/Corrections Applied Index (identically same as col. 58 of DOI format in GRIPE manual) (I*2)
ITEM 13 Calibration Stability (Pre-calibration minus Post-calibration in nanoseconds when Calibration Index = 2, Null otherwise) (r*4)
ITEM 14 Calibration Index(Same as col. 62 of DOI format) (I*2)
ITEM 15 Center of Mass correction in meters (r*4)
ITEM 16 Atmospheric pressure in millibars (R*4)
ITEM 17 Percent Relative Humidity (R*4)
ITEM 18 Atmospheric temperature in degrees Celsius (R*4)
ITEM 19 Predicted Elevation Angle in degrees (R*4)
ITEM 20 Predicted Range (Two-way) in nanoseconds (R*8)
ITEM 21 Predicted Azimuth Angle in degrees (R*4)
ITEM 22 Speed of Light Index (same as col. 102-103 of DOI format) (I*2)
ITEM 23 Estimated Range Noise in meters (R*4)
ITEM 24 Estimated Range Bias in meters (R*4)
ITEM 25 Year of Observation minus 1900 (I*2)
ITEM 26 Month of Observation (I*2)
ITEM 27 Day of Observation (I*2)
ITEM 28 Hour of day of Observation (I*2)
ITEM 29 Minute of hour of Observation (I*2)
ITEM 30 Seconds of minute of Observation (R*8)
ITEM 31 Pass Sequence Number (Negative for Quick Look, Positive for Final) (I*2)
ITEM 32 Twelve bytes of zeroes reserved for future expansion

TOTAL OBSERVATION RECORD LENGTH = 128 (8-bit) bytes

SAO INTERNAL BINARY FORMAT FOR LASER OBSERVATIONS

INDEXING SCHEME

ITEM NUMBER	VAX MNEMONIC	FIRST BYTE	LAST BYTE (= 8 bits)
1	I*4	1	4
2	I*4	5	8
3	I*2	9	10
4	I*4	11	14
5	R*8	15	22
6	I*2	23	24
7	R*8	25	32
8	R*4	33	36
9	R*4	37	40
10	r*4	41	44
11	I*2	45	46
12	I*2	47	48
13	R*4	49	52
14	I*2	53	54
15	R*4	55	58
16	R*4	59	62
17	R*4	63	66
18	R*4	67	70
19	R*4	71	74
20	R*8	75	82
21	R*4	83	86
22	I*2	87	88
23	R*4	89	92
24	R*4	93	96
25	I*2	97	98
26	I*2	99	100
27	I*2	101	102
28	I*2	103	104
29	I*2	105	106
30	R*8	107	114
31	I*2	115	116
32	12 Bytes	117	128

Sample implementation of reading the new internal SAO laser observation record:

Having declared:
INTEGER*4 SATELLITE, OBSNO, MJD
INTEGER*2 STATION, TYPE, DUMMY(52)
DOUBLE PRECISION FRACTION
we can then read any type of data, laser or otherwise:

```
READ (filespec) SATELLITE, OBSNO, STATION, MJD, FRACTION, TYPE, DUMMY
                  (INT)    (INT)   (INT)   (INT)   (DP)     (INT) (INT)
```

Then, if TYPE = 8 (indicating a laser observation) the following equivalences will apply:

LASER OBS WORD	DUMMY
7	1
8	5
9	7
10	9
11	11
12	12
13	13
14	15
15	16
16	18
17	20
18	22
19	24

LASER OBS WORD	DUMMY
20	26
21	30
22	32
23	33
24	35
25	37
26	38
27	39
28	40
29	41
30	42
31	46

where LASER OBS WORDS 7, 20, and 30 are DOUBLE PRECISION, and LASER OBS WORDS 11, 12, 14, 22, 25, 26, 27, 28 and 31 are short integers (I*2), and the remaining LASER OBS WORDS are (R*4) single precision floating point numbers.

NASA BINARY FORMAT

The FORTRAN variable types used in this format description are:

I*2 - Half-word integer
I - Single word Integer
R - Single word Floating Point
DP - Double word Floating Point

Description of Bytes 1-28 for all measurement types.

Bytes	FORTRAN Variable Type	Description
1-4	I	Satellite ID
5-6	I*2	Measurement Type 20 = Laser 64-69 = X-Y Angles (North-South) 68 = Laser 70-79 = Azimuth and Elevation Angles 70 = Laser
7-8	I*2	Time System Indicator (nm) n value description 1 Satellite Transponder/(reflector) Transmitter Time m value description 3 UTC
9-12	I	Station Number
13-16	I	Preprocessing Indicators/Report The preprocessing indicators are bit switches packed into a single 32 bit word. The rightmost bit (bit 31) is of lowest order and the leftmost bit (bit 0) is of highest order.

Bytes	FORTRAN Variable Type	Description

The preprocessing bits are configured as follows:

Bits	Value	Description
0		This bit should always be zero filled
3		Beacon Activity Indicator (types 10-14)
	0	Beacon Inactive or No Beacon
	1 or	Beacon Active Center of Mass Offset Correction Indicator (range, range rate, altimeter)
	0	Data corrected for offset
	1	Data uncorrected for offset
		Unused Equator Designation (types 10-14)
5-6		Date of Equator and Equinox (types 10-14)
		Speed of Light Indicator, (Range, Range Rate, and Altimeter)
	0	2.997925 x 10 meters/sec
	1	2.997925 x 10 meters/sec
	2	2.997925 x 10 meters/sec
	3	2.99792458 x 10 meters/sec

Bytes	FORTRAN Variable Type	Description		
		10-12		Tropospheric Refraction (all but Types 10-14)
			0	Data has been corrected and meteorological data not present
			1	Data has not been corrected
			2	Data has been corrected using the correction formulas for international laser data. Correction value is for zero zenith
			3	Data has not been corrected. Correction Value is for zero zenith.
			4	Data has been corrected and meteorological data is present.
			5	Data has not been corrected and meteorological data is present.
		13		Ionospheric Refraction (all but Types 10-14)
			0	Data has been corrected
			1	Data has not been corrected
		15		Antenna Axis Displacement (Types 20-29)
			0	Data has been corrected (or no correction required)
			1	Data has not been corrected (correction is required)
		16-17		Receiever Mount Type (all but Types 10-14, and Types 38-59)
			1	X-Y (North-South)
			2	Azimuth-Elevation

Bytes	FORTRAN Variable Type	Description
		18-19 Transmitter Mount Type (all but Types 10-14, and Types 38-59)
		1 X-Y (North-South)
		2 Azimuth-Elevation
17-20	I	Modified Julian Date (MJD) of observation. JD = MJD + 2400000.5
21-28	DP	Fraction of Day Past Midnight (GMT)
29-36	DP	Observation Value in Radians for Right Ascension, or Hour Angle, or Azimuth, or X-Angle
37-44	DP	Observation Value in Radians for Declination, or Elevation, or Y-Angle
Bytes 29-68 for Range and Range Rate Measurements (Types 20-39)		
29-36	DP	Observation Value in Meters for Range (Types 20-29) and Meters/Second for Range Rates (Types 30-39)
49-52	I	Average Range Rate Data (Types 30, 33, 34, and 38: Counting Interval in Microseconds.
		Laser Data: Tropospheric Refraction Correction in Same Units as Observation.
53-56	R	Meteorological Data
57-60	R	Ionospheric Refraction Correction in Same Units as Observation
65-68	R	Other than Laser Data: Transmitter Antenna Axis Displacement in Meters.
		Laser Data; Correction to Spacecraft Center of Mass.

SEASAT FORMAT FOR LASER RANGING OBSERVATIONS
A 90 character card image representation.

Column	Subset	Description
1-7		Satellite ID
8-9		Always 20 for laser ranging data
10-11		Time System Indicator
	10	0 => Ground Received Time
		1 => Satellite Transponder/Transmitter Time
		2 => Satellite Receiver Time
	11	0 => UT-0
		1 => UT-1
		2 => UT-2
		3 => UT-C
		4 => A.1
		5 => A.3 (AT BIH)
		6 => AS (SAO)
12-16		Station ID
17-32		GMT of Observation
	17-18	Year of century
	19-21	Day of year
	22-26	Time of day (Seconds from midnight GMT)
	27-32	Fractional part of seconds in units of microsec.
33-35		Preprocessing Indicators
	33	0 => Data has been corrected for tropospheric refraction.
		1 => Data has not been corrected for tropospheric refraction.
		2 => Data has been corrected for tropospheric refraction, using the correction formulae for international laser data (see cols. 76-80).
		3 => Data not corrected for tropospheric refraction. Cols. 76-80 contain coefficient for use with international laser formulae.
		4 or 5 => Cols. 57-66 will contain meteorological data.
	35	Data (0 => has; 1 => has not) been corrected for transponder delay effects.
36-54		Observation data
	36-45	Range in km units
	46-54	Fraction of km Range in units of micrometers
55-56		Preprocessing Indicators
	55	Preprocessing report (Spare, always 0)
	56	Transponder type
		1 => coherent; 2 => non-coherent
57-66		Meteorological data if col. 34 contains a 4 or 5.
	57-60	Surface pressure in millibars
	61-63	Surface temperature in degrees Kelvin
	64-66	Relative humidity in percent

69-73	Measurement standard deviation in millimeters
74-75	Not used for laser data
76-80	Tropospheric refraction correction in millimeters or Coefficient of tropospheric refraction international lasers in millimeters (see col. 34)
81	Speed of light indicator 0 => 299792.5 km/s 1 => 299792.458 km/s
82	Center of mass correction application indicator 0 => applied 1 => not applied
83-88	Center of mass correction in millimeters
89-90	Log10 of the standard deviation of the time of observation in microseconds.

SAMPLE DATA REVIEW OUTPUT

7090 YARRAGADEE														
7603901	39	39	39	40	2	38	40	40	40	40	39	40		
7110 MONUMNT PK														
7603901	40	40	2	40	39	37	39	40	1	40	1			
7120 MAUI														
7603901	39	49	44	35	43	39	40	10						
7102 G F S C														
7603901	8													
7112 PLATTEVILL														
7603901	39	39	3	6	39	14	3	11						
7105 GODDARD														
7603901	42	40	32	40	40									
7210 HALEAKALA														
7603901	39	39	38	37	30	39	38	40						
7831 HELWAN														
7603901	10	24	12	13	28									
7833 KOOTWIJK														
7603901	6													
7834 WETTZELL														
7603901	14	22	16	15	18									
7805 METSAHOVI														
7603901	25	16	27											
7943 ORRORAL V														
7603901	39	30	39	23	10									
7907 AREQUIPA														
7603901	38	37	37	1	38	39	36	39	3	33	37	39	34	31
7929 NATAL														
7603901	25	27	27	34	10	38								

pass	site	satellite	mod julian dy	sigma	timebias(msec)		rangebias(M)		good-bad		day	yr	mon	dy	time
1	7090	7603901	44849.074121	0.16	0.049	0.022	-0.021	0.039	39	1	WED	81	SEP	2	146
2	7090	7603901	44849.216864	0.21	-0.339	0.032	-0.691	0.034	39	1	WED	81	SEP	2	512
3	7090	7603901	44849.736898	0.09	-0.267	0.035	0.108	0.054	39	1	WED	81	SEP	2	1741
4	7090	7603901	44854.598912	0.19	-0.029	0.033	-0.536	0.042	40	0	MON	81	SEP	7	1422
5	7090	7603901	44856.630510	0.00	0.000	0.000	0.000	0.000	2	0	WED	81	SEP	9	15 7
6	7090	7603901	44856.656088	0.12	0.571	0.107	-2.004	0.252	38	0	WED	81	SEP	9	1544
7	7090	7603901	44856.782234	0.12	-0.042	0.017	-0.257	0.019	40	0	WED	81	SEP	9	1846
8	7090	7603901	44857.060591	0.22	0.201	0.027	0.270	0.045	40	0	THU	81	SEP	10	127
9	7090	7603901	44857.577604	0.24	-0.167	0.043	-0.091	0.038	40	0	THU	81	SEP	10	1351
10	7090	7603901	44857.721760	0.12	-0.353	0.011	0.114	0.019	40	0	THU	81	SEP	10	1719
11	7090	7603901	44858.005058	0.16	-0.268	0.025	0.315	0.027	39	1	FRI	81	SEP	11	0 7
12	7090	7603901	44858.145116	0.28	-0.108	0.030	-0.060	0.046	40	0	FRI	81	SEP	11	328
13	7110	7603901	44849.157801	1.14	2.336	0.151	12.522	0.187	40	0	WED	81	SEP	2	347
14	7110	7603901	44849.303345	0.86	3.792	0.097	5.350	0.157	40	0	WED	81	SEP	2	716
15	7110	7603901	44849.827674	0.00	0.000	0.000	0.000	0.000	2	38	WED	81	SEP	2	1951
16	7110	7603901	44850.249179	1.17	2.397	0.136	9.109	0.237	40	0	THU	81	SEP	3	558
17	7110	7603901	44856.195510	1.88	2.785	0.180	5.741	0.301	39	1	WED	81	SEP	9	441
18	7110	7603901	44856.349584	0.20	4.045	0.040	-0.849	0.042	37	3	WED	81	SEP	9	823
19	7110	7603901	44857.155058	0.25	0.475	0.079	15.122	0.119	39	1	THU	81	SEP	10	343
20	7110	7603901	44857.283334	1.02	4.223	0.095	4.670	0.162	40	0	THU	81	SEP	10	648
21	7110	7603901	44857.960417	0.00	0.000	0.000	0.000	0.000	1	16	THU	81	SEP	10	23 3
22	7110	7603901	44858.232361	1.19	2.651	0.122	8.392	0.199	40	0	FRI	81	SEP	11	534
23	7110	7603901	44858.759560	0.00	0.000	0.000	0.000	0.000	1	15	FRI	81	SEP	11	1813
24	7120	7603901	44849.301713	0.17	0.624	0.019	-0.027	0.027	39	1	WED	81	SEP	2	714
25	7120	7603901	44849.456100	0.09	-0.183	0.030	0.668	0.053	49	2	WED	81	SEP	2	1056
26	7120	7603901	44851.331760	0.15	-0.319	0.014	-0.331	0.023	44	1	FRI	81	SEP	4	757
27	7120	7603901	44852.280533	0.09	0.647	0.182	-0.146	0.339	35	1	SAT	81	SEP	5	643
28	7120	7603901	44852.428241	0.23	0.170	0.027	-0.063	0.037	43	0	SAT	81	SEP	5	1016
29	7120	7603901	44857.291482	0.12	0.603	0.016	-0.030	0.019	39	1	THU	81	SEP	10	659
30	7120	7603901	44857.432176	0.25	0.314	0.026	-0.358	0.039	40	0	THU	81	SEP	10	1022
31	7120	7603901	44858.247338	0.16	-0.030	0.132	-1.019	0.066	10	3	FRI	81	SEP	11	556
32	7102	7603901	44858.083617	3.99	0.626	1.404	-2.384	2.162	8	32	FRI	81	SEP	11	2 0
33	7112	7603901	44849.164294	0.86	1.229	0.128	12.353	0.199	39	0	WED	81	SEP	2	356
34	7112	7603901	44849.306794	0.32	3.840	0.067	4.626	0.053	39	1	WED	81	SEP	2	721
35	7112	7603901	44851.854028	0.00	0.000	0.000	0.000	0.000	3	3	FRI	81	SEP	4	2029
36	7112	7603901	44855.776922	19.83	-28.168	33.402	-16.530	21.475	6	12	TUE	81	SEP	8	1838
37	7112	7603901	44856.209595	0.33	0.739	0.092	13.685	0.143	39	1	WED	81	SEP	9	5 1
38	7112	7603901	44858.751262	9.11	-2.499	4.695	6.775	3.699	14	16	FRI	81	SEP	11	18 1
39	7112	7603901	44858.769433	0.00	0.000	0.000	0.000	0.000	3	7	FRI	81	SEP	11	1827
40	7112	7603901	44858.904306	17.03	-7.244	11.142	10.616	18.741	11	21	FRI	81	SEP	11	2142
41	7105	7603901	44856.191379	0.26	0.160	0.037	0.288	0.046	42	0	WED	81	SEP	9	435
42	7105	7603901	44857.132664	0.18	1.112	0.019	-0.575	0.039	40	0	THU	81	SEP	10	311
43	7105	7603901	44857.658023	0.06	-0.334	0.025	-1.823	0.011	32	1	THU	81	SEP	10	1547
44	7105	7603901	44858.079921	0.05	0.396	0.006	-1.097	0.009	40	0	FRI	81	SEP	11	155
45	7105	7603901	44858.230037	0.08	0.527	0.018	1.304	0.013	40	0	FRI	81	SEP	11	531
46	7210	7603901	44849.303091	0.55	-0.016	0.093	1.176	0.110	39	1	WED	81	SEP	2	716
47	7210	7603901	44849.447396	0.48	0.324	0.057	-0.421	0.077	39	1	WED	81	SEP	2	1044
48	7210	7603901	44851.335429	0.74	-0.715	0.095	0.008	0.138	38	2	FRI	81	SEP	4	8 3

49	7210	7603901	44851.485463	0.51	0.063	0.115	0.847	0.091	37	3	FRI	81	SEP	4	1139
50	7210	7603901	44852.433091	0.48	0.390	0.076	-0.764	0.114	30	10	SAT	81	SEP	5	1023
51	7210	7603901	44856.342836	0.71	-0.615	0.081	0.147	0.136	39	1	WED	81	SEP	9	813
52	7210	7603901	44857.290220	0.23	0.243	0.044	1.194	0.045	38	1	THU	81	SEP	10	657
53	7210	7603901	44857.434838	0.40	0.136	0.053	-0.650	0.064	40	0	THU	81	SEP	10	1026
54	7831	7603901	44852.759723	0.23	1.968	0.096	-8.885	0.073	10	0	SAT	81	SEP	5	1814
55	7831	7603901	44852.902315	0.62	1.136	0.280	1.049	0.378	24	4	SAT	81	SEP	5	2139
56	7831	7603901	44853.843403	0.25	1.890	0.218	4.079	0.424	12	0	SUN	81	SEP	6	2014
57	7831	7603901	44854.790463	0.23	1.603	0.053	-1.371	0.064	13	1	MON	81	SEP	7	1858
58	7831	7603901	44855.878264	1.05	2.506	0.351	7.328	0.533	28	0	TUE	81	SEP	8	21 4
59	7833	7603901	44850.887640	0.42	0.182	0.342	1.475	0.177	6	0	THU	81	SEP	3	2118
60	7834	7603901	44851.819096	0.24	-0.130	0.140	-0.483	0.259	14	2	FRI	81	SEP	4	1939
61	7834	7603901	44851.970002	0.22	0.672	0.273	1.805	0.401	22	1	FRI	81	SEP	4	2316
62	7834	7603901	44854.807093	0.24	-0.265	0.193	0.196	0.112	16	0	MON	81	SEP	7	1922
63	7834	7603901	44854.948875	0.27	-1.570	0.667	-1.909	0.786	15	0	MON	81	SEP	7	2246
64	7834	7603901	44857.921731	0.26	0.230	0.249	0.149	0.366	18	0	THU	81	SEP	10	22 7
65	7805	7603901	44851.819786	1.95	-0.060	0.263	12.470	0.393	25	0	FRI	81	SEP	4	1940
66	7805	7603901	44853.854685	3.12	-0.606	0.548	12.779	0.811	16	0	SUN	81	SEP	6	2030
67	7805	7603901	44854.796003	2.73	0.183	0.310	9.234	0.526	27	0	MON	81	SEP	7	19 6
68	7943	7603901	44854.592446	0.37	0.251	0.043	0.248	0.071	39	1	MON	81	SEP	7	1413
69	7943	7603901	44854.752865	0.52	-0.974	0.314	0.957	0.515	30	0	MON	81	SEP	7	18 4
70	7943	7603901	44855.535329	0.47	0.942	0.046	0.387	0.077	39	1	TUE	81	SEP	8	1250
71	7943	7603901	44855.690365	0.37	0.271	0.105	0.207	0.080	23	0	TUE	81	SEP	8	1634
72	7943	7603901	44857.564755	0.92	0.146	0.315	0.090	0.586	10	0	THU	81	SEP	10	1333
73	7907	7603901	44852.098522	0.31	-0.083	0.033	-0.123	0.050	38	2	SAT	81	SEP	5	221
74	7907	7603901	44852.246438	0.41	-0.047	0.048	0.546	0.090	37	3	SAT	81	SEP	5	554
75	7907	7603901	44853.205641	0.72	-0.490	0.167	-0.165	0.386	37	2	SUN	81	SEP	6	456
76	7907	7603901	44853.634807	0.00	0.000	0.000	0.000	0.000	1	0	SUN	81	SEP	6	1514
77	7907	7603901	44854.138886	0.38	-0.240	0.056	-0.022	0.071	38	2	MON	81	SEP	7	319
78	7907	7603901	44854.290712	0.53	-0.448	0.121	0.712	0.170	39	1	MON	81	SEP	7	658
79	7907	7603901	44855.077605	0.48	-0.040	0.079	0.342	0.102	36	4	TUE	81	SEP	8	151
80	7907	7603901	44855.221960	0.40	0.070	0.049	0.196	0.084	39	1	TUE	81	SEP	8	519
81	7907	7603901	44856.167188	0.00	0.000	0.000	0.000	0.000	3	0	WED	81	SEP	9	4 0
82	7907	7603901	44856.181591	0.33	-0.495	0.056	0.113	0.129	33	4	WED	81	SEP	9	421
83	7907	7603901	44856.321353	0.67	-0.982	0.171	0.930	0.149	37	2	WED	81	SEP	9	742
84	7907	7603901	44857.108158	0.45	0.095	0.047	0.154	0.083	39	2	THU	81	SEP	10	235
85	7907	7603901	44858.057550	0.54	-0.687	0.105	0.286	0.100	34	6	FRI	81	SEP	11	122
86	7907	7603901	44858.195137	0.60	-0.402	0.064	0.397	0.167	31	9	FRI	81	SEP	11	440
87	7929	7603901	44850.067101	0.51	-0.381	0.066	-0.032	0.104	25	15	THU	81	SEP	3	136
88	7929	7603901	44852.104602	0.37	-0.121	0.116	-0.307	0.094	27	13	SAT	81	SEP	5	230
89	7929	7603901	44853.991580	0.36	-0.012	0.101	0.967	0.070	27	2	SUN	81	SEP	6	2347
90	7929	7603901	44854.138802	0.65	-0.262	0.120	-0.356	0.111	34	6	MON	81	SEP	7	319
91	7929	7603901	44855.077864	0.56	-0.325	0.425	-1.102	0.864	10	0	TUE	81	SEP	8	152
92	7929	7603901	44856.022828	0.39	-0.151	0.074	0.635	0.066	38	2	WED	81	SEP	9	032

92 PASSES 2700 "GOOD" OBS 286 "BAD" OBS

```
* * * *
station 7831   weight  1.   satellite 7603901  from   81   9   5   44852.9023152   to      44852.9143985  POLE SOLUTION   HELWAN
ITERATIONS  2 3-TIMES A PRIORI SIGMA  0.2E-04 A PRIORI SCALE  0.000E+00 OBS REJECT FLAG 0-AUTO,1-MANUAL 0  DELTA GM/2GM  0.000E+00
SOLUTION VECTOR (DAYS,MEGAMETERS)    0.4586E-08 -0.1533E-06      ITERATION  1
SIGMA IS   1.519     1.457 RMS(M)
SOLUTION VECTOR (DAYS,MEGAMETERS)    0.8557E-08  0.1203E-05      ITERATION  2
 21 39 20.036       -0.178    1.  41.   -1.19     1
 21 39 32.036       -0.706    1.  41.   -1.69     2
 21 39 56.036        1.028    1.  42.    0.09     3
 21 40  8.036        1.420    1.  43.    0.51     4
 21 40 12.036       -0.826    1.  43.   -1.72     5
 21 40 36.036        0.141    1.  44.   -0.70     6
 21 40 52.036        0.018    1.  44.   -0.79     7
 21 41 36.036        0.019    1.  46.   -0.68     8
 21 41 44.036       -1.554    1.  46.   -2.24     9
 21 41 52.036        0.016    1.  46.   -0.65    10
 21 41 56.036       -0.246    1.  46.   -0.90    11
 21 42 12.036       -0.027    1.  47.   -0.64    12
 21 42 44.036       -0.003    1.  48.   -0.54    13
 21 44  4.036        0.782    1.  50.    0.45    14
 21 44 16.036        0.036    1.  51.   -0.26    15
 21 44 20.036       -0.559    1.  51.   -0.84    16
 21 44 36.036       -0.068    1.  51.   -0.31    17
 21 45  8.036        0.263    1.  52.    0.11    18
 21 45 52.036        0.467    1.  53.    0.44    19
 21 46 36.036       -0.010    1.  54.    0.09    20
 21 47 16.036        0.595    1.  55.    0.81    21
 21 47 32.036       -7.027    0.  56.   -6.77    22
 21 48 12.036       -0.039    1.  56.    0.34    23
 21 49 56.037       -0.289    1.  58.    0.40    24
 21 50 28.037       -0.278    1.  58.    0.51    25
 21 52 32.037      -46.825    0.  58.  -45.65    26-
 21 54  0.038      -66.657    0.  58.  -65.22    27-
 21 56 44.027      -96.862    0.  55.  -94.94    28-
*     7831         7603901
*    81  9  5     21 39 20.036
*    28 POINTS    24 ACCEPTED     4 REJECTED
*  RANGE  NOISE =    0.622 RMS =    0.596
*  TIME  OFFSET =       1.136 +OR-    0.280 MSEC
*  RANGE OFFSET =       1.049 +OR-    0.378 METER
                                     SIGMA
```

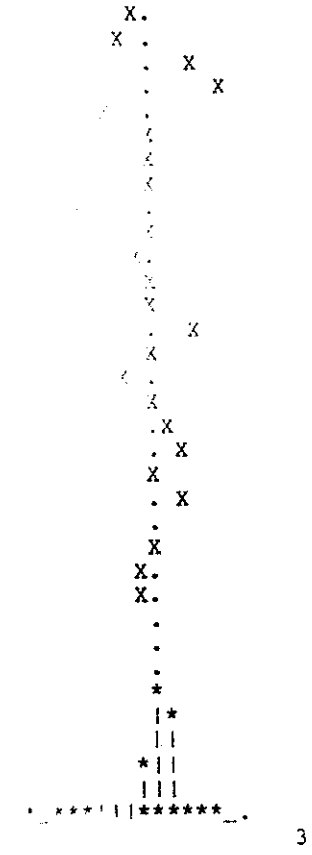

```
* * * *
station 7834   weight  1.   satellite 7603901  from    81   9   7   44854.8070929   to      44854.8115229  POLE SOLUTION   WETTZELL
ITERATIONS  2 3-TIMES A PRIORI SIGMA  0.2E-04 A PRIORI SCALE  0.000E+00 OBS REJECT FLAG 0-AUTO,1-MANUAL 0  DELTA GM/2GM  0.000E+00
SOLUTION VECTOR (DAYS,MEGAMETERS)  -0.3067E-08  0.1963E-06      ITERATION  1
SIGMA IS   0.235     0.220 RMS(M)
SOLUTION VECTOR (DAYS,MEGAMETERS)  -0.3463E-19 -0.1933E-16      ITERATION  2
 19 22 12.828      -0.380   1.  67.  -0.16    1
 19 22 36.079       0.137   1.  67.   0.34    2
 19 23 38.827       0.432   1.  67.   0.58    3
 19 23 49.577       0.019   1.  67.   0.16    4
 19 24  6.827      -0.115   1.  66.   0.01    5
 19 25  2.826       0.275   1.  65.   0.35    6
 19 25 13.076      -0.052   1.  65.   0.02    7
 19 25 28.078       0.149   1.  65.   0.21    8
 19 25 35.826      -0.208   1.  65.  -0.16    9
 19 25 54.326      -0.047   1.  64.  -0.01   10
 19 26  7.576      -0.152   1.  64.  -0.12   11
 19 26 38.326      -0.185   1.  63.  -0.18   12
 19 26 44.576      -0.140   1.  63.  -0.14   13
 19 27  0.325      -0.122   1.  63.  -0.14   14
 19 27 13.325       0.414   1.  62.   0.39   15
 19 28 35.575      -0.025   1.  59.  -0.11   16
*     7834        7603901
*    81  9  7    19 22 12.828
*    16 POINTS   16 ACCEPTED     0 REJECTED
*   RANGE  NOISE =    0.235 RMS =    0.220
*   TIME  OFFSET =     -0.265 +OR-    0.193 MSEC
*   RANGE OFFSET =      0.196 +OR-    0.112 METER
                                     SIGMA
```

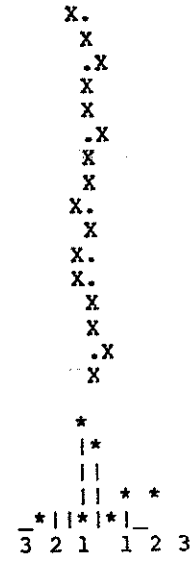

Ideas on feedback in satellite ranging systems

David W. Morrison
Drews Systems, Inc.
599 North Mathilda Avenue
Suite 245
Sunnyvale, California 94086
U.S.A.

1.0 Introduction

Because laser ranging systems differ so significantly in funding and objectives, it is probably most useful here to discuss some general guidelines for specifying the operator feedback in such systems. To make the presentation more concrete, some examples from the system in Wettzell, Bundesrepublik Deutschland, are presented. They demonstrate one approach that has been reasonably effective in solving the problems of feedback.

2.0 Include the feedback in the initial design

The desired feedback should be at least as carefully thought out in the early design phases as is the hardware. Feedback needs and content should be determined with enough detail that (1) the proper computer and peripherals can be considered, (2) the hardware designers can plan to provide the feedback data in convenient form, (3) a reasonably accurate cost estimate can be made, and (4) the ultimate

success of the feedback can be assured.

3.0 Include a software designer

Nearly, if not as, important as adequate early feedback design is the need to involve a software professional in the project design team at the earliest possible date. The inclusion of an experienced programmer will work toward assuring (1) reasonable hardware-software tradeoffs, (2) balanced, achievable requirements for both the feedback and the system as a whole, and (3) a flexible software base for future expansion.

The Wettzell system is a case in point. The original request for proposal specified support for future expansion but made no stipulations about the language or operating system which would form the base of the tracking software itself. Because of existing in-house experience the first inclination of the system builder was to write the tracking software in PDP-11 assembly language and use a small, home-grown, real-time executive as the controlling software entity. The "future expansion" would be covered by providing as separate items a standard DEC operating system and a Fortran compiler.

The software engineer, however, argued for a more integrated system-wide approach using a DEC real-time operating system and the newly-available Fortran-IV-Plus compiler that generated in-line, fast machine code. That approach was viewed with skepticism by some of the project planners but was ultimately accepted. In the end, however, it was generally agreed that the fully integrated approach had been correct because the Wettzell system

proved quite adaptable to even unforeseen system requirements. At the same time a second, somewhat similar system being developed in parallel under the "in-house" approach was relatively rigid and unreceptive to change.

The important point of this history is the impact which the early use of the programmer's normal professional experience had on the ultimate success of the system. Similar rewards are to be expected on any ranging system that uses a significant amount of software.

A short, final note on picking a programmer:

- he must be a listener;
- he must be flexible enough to consider various software solutions for the very real hardware problems involved in a laser system;
- he must know that software is only one of several important means in such an undertaking;
- he must have the trust of the hardware people;
- he must be consulted regularly and often;
- he needs up-to-date knowledge so that his responses can be timely and effective.

Without this close cooperation, a haphazard software system will probably result, a system that satisfies no-one, which cannot attract and hold good programmers, and which never ceases to cost the project money.

4.0 Other factors

Beyond the overriding importance of including the software designer in the earliest design phases, several other factors will mold the feedback and its effectiveness in a ranging system.

4.1 What are the main system objectives?

Is the tracking data the only objective? Will someone want to detect dynamic events at the satellite (e.g., Wobble)? Will monitoring of laser performance be part of the computer's responsibility? Will the system be used to train inexperienced operators or students? Will the computer system perform complicated data analysis? Will graphs, maps, or charts be created? Is this a system which anticipates another system (that is, a feasibility study)?

In other words, potential aims as well as the possibly more restricted current ones should be considered. In feedback terms this may mean, for instance, designing a flexible system for handling CRT displays, plots or graphs. Such generalized packages need not be elaborate. They can be either purchased from vendors (though speed is often a problem with vendor software) or created by project personnel. In any case the rewards are fast in materializing as the ideas for feedback often change early in the project development.

As an example, in the Wettzell system standardized display and command entry formats were adopted from the earliest stages of the project. A software package to create and use these forms was written as the first major programming effort. The entire package was no more than fifty small subroutines. Yet use of that standard interface provided a valuable overall coherence and control to the entire system.
One example: when it was decided to add a standard control character on a system-wide basis, only one subroutine was changed.

4.2 Identify the users

Will experienced astronomers operate the system? If so, succinct phrases, jargon, or symbols might suffice on CRT or listing formats as opposed to more word-oriented approaches.
Technicians? An emphasis on numbers with accompanying graphs where appropriate might be more effective.
Undergraduates? Textual headers, graphs, generally more informative output is probably required.

The more technical, jargon-rich approaches limit system usage to more highly trained operators. On the other hand the wordy, self-explanatory solutions often become burdensome to anyone who gains familiarity with the system. These restrictions can become obviously confining only after the system is in operation.

The method which has proven effective in the Wettzell system for reducing "chatter" yet maintaining an atmosphere of operator assistance is "coded menus". The operator is shown on the CRT a list of the valid choices for the particular portion of the program in execution. Each choice is presented as a short descriptive title (about 35 characters) and a code (2 characters). A menu item is selected by typing the code. This approach provides enough prompting to allow the manual to remain on the shelf yet imposes a minimum amount of typing for those already knowledgable in the system's operation.

4.3 What kind of information is familiar to the users?

Do they think easily in symbols? Graphs? Numbers? Charts? Sentences? Abbreviations? Will the long range

users of the system think this way? Frequent users can usually remember the form and meaning of many abbreviated entries and readouts. Infrequent users will be regularly driven to the manual (and the wall) by excessive shortenings.

4.4 Identify the computer resources

Does the computer have great speed? Large memory? Fast mathematical calculations? An operating sytem? Disk storage? Does the operating system support parallel taksing? Overlays? Inter-task communication? Powerful languages? Do the languages generate in-line code? Are multiple computers available? Are pre-coded packages for plotting and CRT display creation available?

All these factors influence speed, flexibility, and availability of programmer time to create various forms of feedback. For example, a system which has a relatively primitive operating system may require much programmer time (i.e., budget) to satisfy basic tasking and control needs leaving little opportunity for anything beyond bare-bones feedback features. Indeed, it is generally the case that expenditure of funds on flexible, expandable, vendor-supported computers, peripherals, and programming tools more than repays itself in improved productivity of the programmers.

Consider this example from Wettzell: the initial system was developed on a machine with only one small disk, a magnetic tape unit, and a primitive utility program for copying between tape and disk. This forced the software to reside on tape since only small subsets of the entire system could be stored on disk at one time. This, in turn, forced

programmers to spend a significant part of their expensive time (often as much as one hour per day) waiting for tape-disk transfers to occur. The "economy" of only one disk drive was in fact a major project expense.

4.5 Identify the operating environment

Is the facility dedicated to laser ranging? If so, extra computer time can be devoted to maintaining informative, dynamic displays or graphs. If not, the limited computer availability dictates stripped down, data-rich displays which give maximum information in the shortest possible computer execution time. Also in this case, on-line operator aids (e.g., a "help" command) might be desirable to allow the observer to make maximum, efficient use of the time available to him.

Is the facility noisy? Quiet? Bright? Dark? These factors influence the visual or auditory impact that the feedback must have to gain the operator's attention.

Are other computers available in a network? If so, non-time-critical processing can be assigned to them to provide extra feedback beyond the capability of the tracking computer.

4.6 Determine the required data

What must the operator see before him to detect success? At least as important, what does he require to be able to correct failure? Essential information certainly includes mount position, expected position, elapsed time of the mission, operator-entered system pertubations (such as AZ/EL offsets, a time delta), and an indicator of satellite

acquisition (perhaps a display showing the range delta).

4.7 Determine the presentation format

The way the data is presented to the operator usually represents a difficult tradeoff between (1) desirable or elegant presentations with visual impact, (2) the computer time and peripheral equipment requirements to provide such feedback, (3) cost - both equipment and programmer, and (4) the operator's ability to understand and retain the data presented to him.

For example, CRT displays of dynamic graphs showing azimuth and elevation positioning relative to predicted values are impressive visually and provide rapid operator understanding. However, they are also very costly in CPU utilization and programming time. Plots on paper provide excellent hardcopy records of the mission. But they are slow relative to CRT displays and, therefore, may not be adequate for providing real-time tracking feedback. A display of number registers allows a good deal of information to be shown on a single, relatively inexpensive, alphanumeric CRT screen. Such displays generally lack visual impact (a major aid to understanding and recognition) and require a great deal more operator concentration to detect trends. (For example, a gauge or dynamic graph will quickly show the azimuth reading and the direction of movement; a number register only shows the former. The operator must mentally integrate several successive register values to detect direction).

4.8 Make the computer do the work

Computer projects of all kinds are usually under budge-

tary pressure. Shortcutting the operator feedback system often appears to be a good way to save money. The programmers can work on the "important parts of the system".

What budgets really are, however, are disguised opportunities. They offer the chance to design and build the best feedback system in the most compact form at the best price without all the extras that no-one really needs anyway?

Shortcuts, on the other hand, are rigid. Unyielding beasts that lunge out at any programmer who dares enter their domain. They are entrenched shortsightedness. They deny the inevitable need for adaptability in something as complex, as evolving, as a laser ranging system.

But most importantly, shortcuts show a lack of concern for the people who must use the system. The computer is a tireless doer of drudgery. The human is not. The best systems incorporate these truisms. The results are pleasant to use, allow operators to solve their problems rather than the computer's, and open the system to a wide audience of users and onlookers (it helps to have a system that management can visually understand!).

In short, spend time for the humans. You have nothing to lose but complaints.

LAGEOS EPHEMERIS PREDICTIONS

B. E. Schutz, B. D. Tapley, R. J. Eanes and B. Cuthbertson

Department of Aerospace Engineering and Engineering Mechanics
The University of Texas at Austin
Austin, Texas 78712
512/471-1356

Abstract

The operational procedures used at the University of Texas to generate Lageos ephemeris predictions for the TLRS and MLRS are described. The procedures which have been adopted for Lageos use two months of quick-look range data to estimate the satellite orbit elements and a "drag" parameter at a specified epoch. These parameters are used to predict the ephemeris for four to six months beyond the two months used in the estimation process. The accuracy of this predicted ephemeris has been evaluated with specific cases. These cases show the ephemeris error to be less than 100 m after four months past the estimation interval. The operation and software design considerations used in the development of the TLRS and MLRS software for reconstructing the predicted ephemeris are described also. The ephemeris reconstruction software has been designed to use a simplified model of the satellite dynamics to enable its operation in a mini- or microcomputer environment, as well as to reconstruct the predicted ephemeris to meter-level accuracy. By adjusting the initial conditions, model mismatches between the prediction software and the reconstruction software can be accommodated. The performance and characteristics of this software is described.

Introduction

The successful operation of satellite laser ranging (SLR) systems is dependent, in part, on the ability to point the laser/telescope in the approximate direction of the satellite. The allowable pointing error is essentially determined by the laser beam divergence and the signal-to-noise ratio. This error stems from the following sources:

- errors in the predicted satellite ephemeris,
- errors in the predicted earth orientation,
- errors in the a priori knowledge of the SLR location,
- errors in pointing the instrument to a commanded position, and
- errors in the SLR clock.

If the site is permanent or has been previously occupied by an SLR system, the third source should contribute only a small error. However, sites which have not been occupied previously may require the approximate specification of coordinates from a topographic map, thus introducing errors of tens or hundreds of meters. Range acquisition can be seriously degraded if any of these error sources, singly or in combination, exceed the beam width at the satellite's altitude. Although all sources are important, the latter two are hardware-dependent and will not be treated in this paper.

The error in the predicted satellite ephemeris arises from two distinct sources. First, the ephemeris is obtained by estimating the satellite state from observations taken over some interval of

time. This estimation procedure is performed using an adopted model for the forces and kinematics used to describe the satellite motion. With the estimated state and the adopted model, the satellite equations of motion are solved and the predicted satellite states beyond the estimation interval are obtained. This predicted ephemeris will inevitably be in error because of 1) inaccurate state estimates, 2) inaccurate or incomplete models for the satellite dynamics/kinematics and 3) the approximation technique used to solve the satellite equations of motion. In general, however, the dominant characteristic of the ephemeris prediction error is in the satellite's "along-track direction," i.e., direction of motion. In the subsequent discussion, the predicted ephemeris will refer to the ephemeris generated in the manner described above, usually at a site with access to data from many sites and to significant computer facilities which may be required to analyze the available data.

The second error may be introduced at a laser site which uses the predicted ephemeris to generate on-site pointing predictions. This error is distinctly different from the ephemeris prediction error since it will result from the use of an approximation technique which is compatible with the limited computer resources available within the SLR system. Consequently, the SLR may not reproduce the predicted ephemeris exactly due to the inherent differences in the models or approximation methods used at the central site compared to those used in the SLR station. The ephemeris generated on-site within the SLR will be referred to as the reconstructed ephemeris. The selection of

a technique to generate the reconstructed ephemeris within the SLR will be based on the following factors:

- the amount of data which must be transmitted to the SLR,
- the frequency with which the data must be transmitted,
- the computer resources required by the SLR to provide a usable ephemeris from the transmitted data.

For example, a one-day ephemeris provided to the SLR at one-minute intervals would require 1440 time points with three components of satellite positon at each time. To reduce the amount of data, only the data points from the predicted ephemeris which pertain to the satellite passes for a particular SLR should be provided; however, this procedure places severe sort/merge problems on the central site due to different observing schedules at each station. Furthermore, in this example, the SLR computer resources must still be used to interpolate between the available points for the instrument pointing. The disadvantage of providing a large number of points to the SLR becomes even greater when considering highly mobile laser ranging systems.

Highly mobile laser ranging systems which operate in remote areas may have limited access to high-speed communication resources, thus requiring the frequent transmittal of data via disk or cassette storage media. As a consequence, a highly mobile laser station must assume a significant degree of autonomy, especially for operation in undeveloped areas where access to even ordinary telephone communication may be difficult. In these circumstances, the station should be able to operate for long periods without external communica-

tion during which the on-site resources should be fully utilized for the following objectives:

- generate laser/telescope pointing predictions,
- update the predictions using previously acquired data,
- evaluate the quality of the laser pulse returns.

The first two objectives are necessary to acquire successful laser pulse returns, while the last objective is neccessary to enable on-site evaluation and assessment of system performance. In addition, the computer implementation of the algorithms necessary to achieve the foregoing objectives within the computer capability of the station has further requirements, namely:

- The prediction software and procedures should not introduce abrupt changes in the predicted ephemeris except at infrequent and specified times when the ephemeris is updated from external sources.
- The prediction quality should gracefully degrade.
- The prediction software and hardware should be capable of computing considerably faster than real-time.
- The prediction software should not use overlayed and virtual memory but should occupy the directly addressable memory of typical minicomputers to enhance the transferral of software between distinctly different machines.
- Maximum ephemeris information should be compressed into a small number of parameters.
- To enhance the system performance, especially the signal detection, it is desirable that the maximum allowable prediction error be less than 100 m at all times for Lageos.

The design and analysis of algorithms and procedures to accomplish the previously stated objectives require further considera-

tion of the available computer resources within the station. Compact systems will have limited computer power, as represented by the central processor performance capabilities and the main memory storage capacity. These limitations are imposed by the following:

- available hardware technology and available space within the cabinetry,
- power requirements and available power supply,
- heat dissipation and available cooling system.

These three limitations are interrelated and, because of the speed at which technology is changing, are difficult to fully evaluate in the algorithm and procedure design process. Consequently, the design has been directed toward the hardware available in the Transportable Laser Ranging System-1 (TLRS-1) and the McDonald Laser Ranging Station (MLRS) developed for NASA by the University of Texas at Austin [Silverberg, 1981].

The following sections describe the procedures which have been adopted and which have evolved for the generation of the predicted ephemeris and the reconstructed ephemeris, particularly for Lageos. The accuracy of these predictions and the models used in their generation are described. The considerations for the TLRS prediction software development are discussed, and the software performance in generating the reconstructed ephemeris is summarized also.

The Predicted Ephemeris

The ability to predict the state (position and velocity) of a satellite is dependent on several factors, namely, 1) the accuracy of the satellite state at some epoch, 2) the accuracy of the models used to describe the forces acting on the satellite, 3) the accuracy of the models used to describe the kinematic contributions in the various coordinate transformations, 4) the accuracy of predictions which influence the representation of forces and kinematics, and 5) the accuracy of the method used to solve the differential equations of satellite motion. These factors, which are not completely independent of each other, are discussed in the following paragraphs.

Applying the principles of Newtonian mechanics, the motion of a satellite is described by a system of second-order ordinary differential equations which relate the inertial acceleraton of the satellite's center of mass to the forces which act on it. This description is an initial value problem, hence, the position and velocity of the satellite, $\bar{r}_o$ and $\bar{v}_o$, are required at some time t_o. The solution of the initial value problem yields the position and velocity at other times, t. However, the initial values are typically not known to an adequate accuracy to achieve the required accuracy in prediction. As a consequence, observations must be used to determine the state at a selected epoch. The determination of the orbit, however, requires consideration of all of the other factors listed above. In general, the model characteristics and the techniques utilized in

the state estimation will be identical or nearly identical to those used to perform the state prediction.

In support of TLRS and MLRS, the determination of the orbit utilizes quick-look laser range data reported from the NASA systems, the Smithsonian Astrophysical Observatory (SAO) systems and participating European systems. These data are transmitted to the University of Texas at Austin through the NASA Communications Network (NASCOM), usually within a few hours of acquisition. The precision of the quick-look laser range data is system-dependent and varies from a few centimeters to several decimeters.

The models used for the estimation of the epoch state ($\bar{r}_o$ and $\bar{v}_o$) have evolved from analysis of over five years of Lageos data. These analyses have included several refinements in the force model based on "long-arc" solutions spanning the entire data set. However, because some small forces observed in these long arcs are not fully understood and cannot be accurately predicted, they have been partially ignored in the models adopted for the orbit determination aspect in support of the predicted ephemeris generation. The models adopted for the state estimation and prediction process are summarized in Table 1. To accommodate the unknown and variable forces, a constant along-track force is estimated simultaneously with the satellite state. In addition, the differential equations of motion are solved by a fourteenth-order multi-step numerical integration method described by Lundberg [1981]. The software used in the estimation

process is UTOPIA [Schutz and Tapley, 1980].

The interval of time used for the Lageos orbit determination portion of the prediction process will be referred to as the estimation interval, usually an interval of approximately two months. The state and parameters obtained from the estimation process, combined with the adopted models, are used to generate the predicted ephemeris for a period at least as long as the estimation interval. The interval of time beyond the estimation interval is referred to as the prediction interval. The estimation and prediction intervals of two recent predicted ephemerides are summarized in Table 2.

In order to evaluate the accuracy of the ephemerides summarized in Table 2, the available quick-look data for August and September, 1981, were used in a separate state estimation. The resulting estimated ephemeris has an accuracy of about one meter over the estimation interval and will be referred to as the "truth ephemeris." By comparing the truth ephemeris with the predicted ephemerides, the differences can be resolved into the radial, transverse (along-track) and normal (cross-track) differences. These differences are shown in Figures 1 to 3. In addition, for comparison, ephemerides generated at the NASA Goddard Space Flight Center (GSFC) are also shown. These ephemerides, referred to as GSFC Inter-Range Vectors (IRV), provide pointing predictions for the NASA network of laser stations.

It is of particular interest to note from Fig. 2 that the error in the predicted ephemeris LAG0013 has grown to about 80 m at

the end of a four-month prediction interval. In addition, the radial and normal components of the error are less than 10 m. The GSFC IRV's, however, exhibit significantly larger errors in this time period. While these large errors may not totally prohibit acquisition, they are likely to be a contributing factor to poor daytime tracking of Lageos and the signal-to-noise ratio of the return. The manner in which the errors illustrated in Figs. 1 to 3 are "seen" at a particular SLR site will be dependent on the viewing geometry of the satellite with respect to the SLR.

The Reconstructed Ephemeris

The ideal procedure for reconstruction of the predicted ephemeris at the SLR is to use the same dynamic and kinematic models used for the generation of the ephemerides. In such an ideal case, only the estimated position and velocity at a chosen epoch would be required for the SLR to completely reconstruct the predicted ephemeris. Consequently, only one set of six quantities would be required for a several-month prediction interval.

Because of the complexity of models used in the creation of the predicted ephemeris, it is not feasible with current technological and budgetary constraints to achieve the ideal case. Consequently, the SLR software, which reconstructs the predicted ephemeris, must operate within the available computer resources. Various procedures are feasible, for example:

- The predicted ephemeris fit with simple approximating functions, e.g., spline or Chebychev polynomials. In these cases, the parameters associated with the approximating function would be provided to the SLR;

- Analytical orbit theory, requiring mean orbit elements consistent with the theory;

- Simplified versions of the models and techniques used to generate the predicted ephemeris.

Although numerous factors were considered in the evaluation process, the overriding factors were maximal use of existing software and techniques, as well as the transmission of a small number of parameters for the reconstruction process. Consequently, the last procedure listed above was adopted for the TLRS operation.

In general, the use of a simplified model for the ephemeris reconstruction will cause a degradation at a rate which is dependent on the degree of simplification, assuming that initial conditions from the predicted ephemeris are directly used. An alternate procedure, however, is to provide the reconstruction software with initial conditions which have been adjusted with respect to the predicted ephemeris in order to reduce the reconstruction error. This "tuning" of the initial conditions is transparent in the use of the reconstruction software; the burden for generating the tuned initial conditions rests with the facility which generates the predicted ephemeris. The

procedure is illustrated in Fig. 4. It is important to note that the purpose of the tuning is to essentially eliminate prediction errors which can be introduced by the reconstruction software. With a chosen reconstruction interval, i.e., the time interval for which the initial conditions have been tuned, the software reconstructs the predicted ephemerides as illustrated in Fig. 5. Although discontinuities will exist between adjacent tuned intervals, the proper combination of simplified model and tuning interval will ensure small discontinuities.

The degree of simplification in the reconstruction software is dependent on the acceptable error magnitude and the reconstruction interval. After considering various intervals for providing the predicted ephemeris (in the form of adjusted initial conditions), the interval of one day was chosen as the nominal goal for TLRS. With this selection, only one set of satellite position and velocity per day need to be provided to the reconstruction software, thereby allowing even verbal transfer of several days of data to the SLR if it is required.

With the selection of a nominal one-day predicted ephemeris interval, consideration of various models for the reconstruction software was necessary. By faithfully reconstructing the predicted ephemeris, the satellite ephemeris available at the SLR will reflect only errors in the predicted ephemeris, instead of the errors from both the prediction and the reconstruction. With this consideration, the design criteria was adopted that the reconstruction error be less

than five meters RMS over the reconstruction interval.

Using UTOPIA, the software used for the generation of the predicted ephemeris, various experiments were performed to evaluate various simplified models for Lageos. These experiments utilized an ephemeris comparison mode in which points on an ephemeris can be used as "observations" for a least-squares adjustment of epoch state or other parameters. The nonlinear estimation process requires iteration; however, the initial iteration always began with the state directly available from the predicted ephemeris. To assist in the interpretation of results, the differences between the "observed (predicted) ephemeris" and the "computed ephemeris" are resolved into components in the radial (R), transverse (T) and normal (N) directions. These differences are expressed in terms of their Root Mean Square (RMS) for each iteration. Furthermore, only the epoch state was adjusted in the results which are described in the following paragraphs.

Because of the Lageos orbital characteristics, degree seven, order six spherical harmonic coefficients produce a 2.66-day long-period effect. Consequently, experiments have shown the necessity for inclusion of these terms in the reconstruction process, especially when the software will predict the state for one day from a single position and velocity. The influence of these coefficients is summarized in Tables 3 and 4.

Similarly, the moon produces an effect on the Lageos orbit which is characterized by 14- and 28-day periods, while the effect of the sun has annual and semi-annual periods. While the effect may be small within one day, the day-to-day effects can be expected to change, as exhibited in Tables 5 and 6. As shown in these tables, the use of points on the predicted ephemeris as the initial conditions for the reconstruction process without inclusion of the sun and moon yields errors of as much as 150 m. This violates the stated criteria that the ephemeris reconstruction be accurate to less than five meters. Even after tuning the initial conditions for this model deficiency, the error still exceeds the 10 m level. Inclusion of the sun and moon shows that the specified criteria can be met, even without tuning the initial conditions. This conclusion, however, assumes that the reconstruction process uses a model of the sun and moon coordinates, which is identical to that used in the generation of the predicted ephemeris, which requires a large supporting data base (DE-96).

Based on the preceding results, the reconstruction software was developed by Cuthbertson [1981] using the characteristics shown in Table 7. Particular characteristics include the use of Pines [1974] nonsingular formulation for the gravitational spherical harmonics, modified to directly use normalized coefficients. In addition, the software utilizes an analytical theory of the moon and sun to avoid the necessity of a large supporting data base. Evaluation of the accuracy of this approach compared to the use of DE-96 in the

reconstruction software is in progress. It is to be noted, however, that by appropriate tuning of the initial conditions most of the differences in the models can be eliminated.

The reconstruction software is coded in Fortran and has been operated on a PDP 11/60 minicomputer using the RSX11M operating system, as well as on a Data General Nova computer. The software uses less than 32000 16-bit words of memory for execution. With the system's hardware floating point processor, predictions for a full day require less than five minutes of computer time, typically about two minutes.

The reconstruction software has been evaluated through the use of points from the predicted ephemeris as well as with quick-look data. In the former case, a set of initial conditions from the predicted ephemeris were used for a one-day prediction and points generated by the reconstruction software were directly compared with points from the predicted ephemeris. The latter case used quick-look range data from Yarragadee, Australia, on October 10, 1981. Using the initial conditions from the predicted ephemeris, LAGO014, and without tuning, a range residual RMS of 5.1 m was computed, approximately equivalent to 34 ns in two-way propagation time. It is important to note that the last data used in the creation of this predicted ephemeris was 3 September 1981.

Conclusions

The results have demonstrated that the errors from a several-month prediction of the Lageos ephemeris are less than 100 m. With expected further improvements in the force models used for the state estimation and ephemeris prediction, simultaneous improvements in prediction accuracy will result also.

The ephemeris reconstruction accuracy is dependent on 1) the model used and 2) the interval of time for which the reconstruction is applied. The model requirements can be relaxed by adjusting initial conditions used in the reconstruction software to accommodate the model differences. This tuning of the information provided to the reconstruction software can produce meter-level accuracy in reconstructing the predicted ephemeris.

Acknowledgements

The contributions of John Ries in providing the ephemeris-tuning capability in UTOPIA is gratefully acknowledged. This research has been supported by NASA Contract No. NAS5-25991 and NASA Contract No. NAS5-25948.

REFERENCES

Cuthbertson, B., "User's Guide to Ephemeris Reconstruction Software," University of Texas at Austin, in preparation, 1981.

Eanes, R. J., B. E. Schutz and B. E. Tapley, "Earth and Ocean Tide Effects on Lageos and Starlette," Proc. of Ninth International Symposium on Earth Tides, New York, To Appear, 1981.

Lieske, J. H., T. Lederle, W. Fricke and B. Morando, "Expressions for the Precession Quantitives Based Upon the IAU (1976) System of Astronomical Constants," Astron. Astrophys. 58, 1-16, 1977.

Lerch, F. J., S. M. Klosko, R. E. Laubscher and C. A. Wagner, "Gravity Model Improvement Using Geos 3 (GEM 9 and 10)," JGR 84 (B8), 3897-3916, 1979.

Lundberg, J. B., "Multistep Integration Formulas for the Numerical Integration of the Satellite Problem," Inst. for Advanced Study in Orbital Mechanics, The University of Texas at Austin, TR81-1, 1981.

Pines, S., "Uniform Representation of the Gravitational Potential and its Derivatives," AIAA J. 11 (11), 1508-1511, 1973.

Schutz, B. E. and B. D. Tapley, "UTOPIA: University of Texas Orbit Processor," Inst. for Advanced Study in Orbital Mechanics, The University of Texas at Austin, TR80-1, 1980.

Schwiderski, E. W., "On Charting Global Ocean Tides," Rev. of Geophys. and Space Physics 18 (1), 243-268, 1980.

Silverberg, E. C., "The TLRS and the Change in Mobile Station Design Since 1978," Proceedings of the Laser Ranging Workshop, Austin, Texas, 1981.

Standish, E. M., M. Keesey and X. Newhall, "JPL Development Ephemeris Number 96," JPL TR 32-1063, Jet Propulsion Laboratory, Pasadena, California, 1976.

Tapley, B. D., B. E. Schutz and R. J. Eanes, "Global Station Coordinate Solution from Lageos Laser Ranging," presented at Fall AGU Meeting, San Francisco, California, December 1980.

Wahr, J. M., "Body Tides on an Elliptical, Rotating, Elastic and Oceanless Earth," Geophys. J. R. Astr. Soc. 64, 677-703, 1981a.

Wahr, J. M., "The Forced Nutations of an Elliptical, Rotating, Elastic and Oceanless Earth," Geophys. J. R. Astr. Soc. 64, 705-727, 1981b.

Table 1

MODELS USED FOR LAGEOS ESTIMATION/PREDICTION (LAG0014)

Force Models:

Gravitational

GEM 10 (Lerch, et al., 1979); complete to degree and order 13 plus selected resonance coefficients

Sun and Moon; coordinates from JPL DE-96 [Standish, et al., 1976]

Solid Earth Tides*; Wahr (1981a) model using 1066A earth model

Ocean Tides*; Schwiderski (1980) nine-constituent model

Nongravitational

Solar Radiation Pressure; assumed constant

Drag-like Force; estimated parameter, assumed constant (LAG0014 value, -2.60×10^{-12} m s^{-2})

Equations of Motion:

Mean equator and equinox of 1950.0 nonrotating reference system

Earth Orientation:

1976 IAU Precession [Lieske, et al., 1977]

Wahr Nutation (1981b)

Pole Position and UT1 from BIH Circular D; for prediction, values adopted from extrapolation of BIH Circular D

Laser Station Coordinates, LSC 80.11 [Tapley, et al., 1980]

Numerical Methods:

Fourteenth-order multi-step [Lundberg, 1981]

Software:

UTOPIA [Schutz and Tapley, 1980]

* Implementation and results are given by Eanes, et al. [1981].

Table 2

RECENT PREDICTED EPHEMERIDES FOR LAGEOS

Ephemeris Identification	Estimation Interval*	Prediction Interval
LAG0013	18 March 1981 to 10 May 1981 (54 days)	11 May 1981 to 19 September 1981 (131 days)
LAG0014	16 July 1981 3 September 1981 (49 days)	3 September 1981 to 1 February 1982 (151 days)

* Interval during which quick-look laser range data are used to estimate the epoch orbit elements and drag parameter.

Table 3

ONE-DAY EPHEMERIS RECONSTRUCTION: 4 x 4 GRAVITY
EPHEMERIS DIFFERENCES (m)

Day	R	T	N	RMS Overall	RMS Tuned Overall
1	3.4	44.3	4.5	25.8	3.0
2	3.6	30.9	3.9	18.1	2.9
3	3.3	32.5	5.4	19.1	2.9
4	4.5	13.1	4.5	8.4	3.2
5	4.0	19.5	2.6	11.5	3.1

Table 4

ONE-DAY EPHEMERIS RECONSTRUCTION: 7 x 7 GRAVITY

Day	R	T	N	RMS Overall	RMS Tuned Overall
1	0.8	5.2	0.3	3.0	0.6
2	0.3	4.8	0.5	2.8	0.6
3	0.8	3.7	0.4	2.2	0.5
4	1.1	2.6	0.3	1.7	0.6
5	0.8	2.7	0.3	1.7	0.6

Table 5

ONE-DAY EPHEMERIS RECONSTRUCTION: NO SUN/MOON EPHEMERIS DIFFERENCES (m)

Day	R	T	N	RMS Overall	RMS Tuned Overall
1	8.9	523.3	73.8	152.4	21.9
2	5.2	52.2	127.7	79.7	19.6
3	4.9	27.7	109.2	65.1	16.3
4	4.8	16.2	90.0	52.9	13.5
5	5.7	14.2	79.5	46.8	12.9

Table 6

ONE-DAY EPHEMERIS RECONSTRUCTION: SUN/MOON EPHEMERIS DIFFERENCES (m)

Day	R	T	N	RMS Overall	RMS Tuned Overall
1	0.7	6.7	0.6	3.9	0.5
2	0.3	4.1	1.2	2.5	0.7
3	1.0	4.2	1.7	2.7	0.6
4	1.0	2.4	1.1	1.6	0.6
5	1.0	3.1	0.8	1.9	0.7

Table 7

MODELS USED FOR LAGEOS EPHEMERIS RECONSTRUCTION SOFTWARE

Force Models:

Gravitational

GEM 10, complete to degree and order 7

Sun and Moon; coordinates from analytical theory

Nongravitational

None

Equations of Motion:

True-of-date nonrotating reference system defined by initial epoch

Numerical Methods:

Fourteenth-order multi-step integrator [Lundberg, 1981]

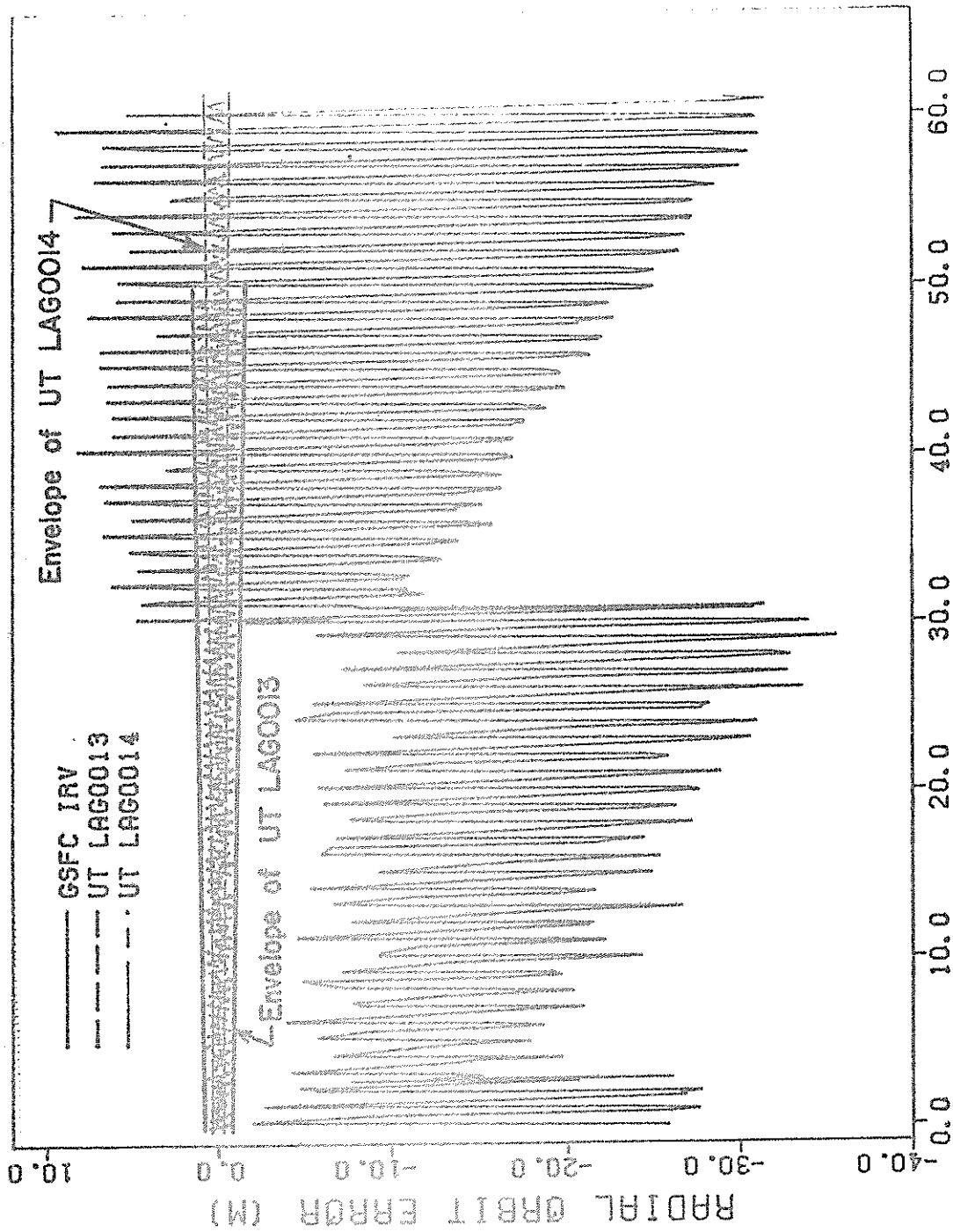

FIG. I RADIAL PREDICTION ERROR

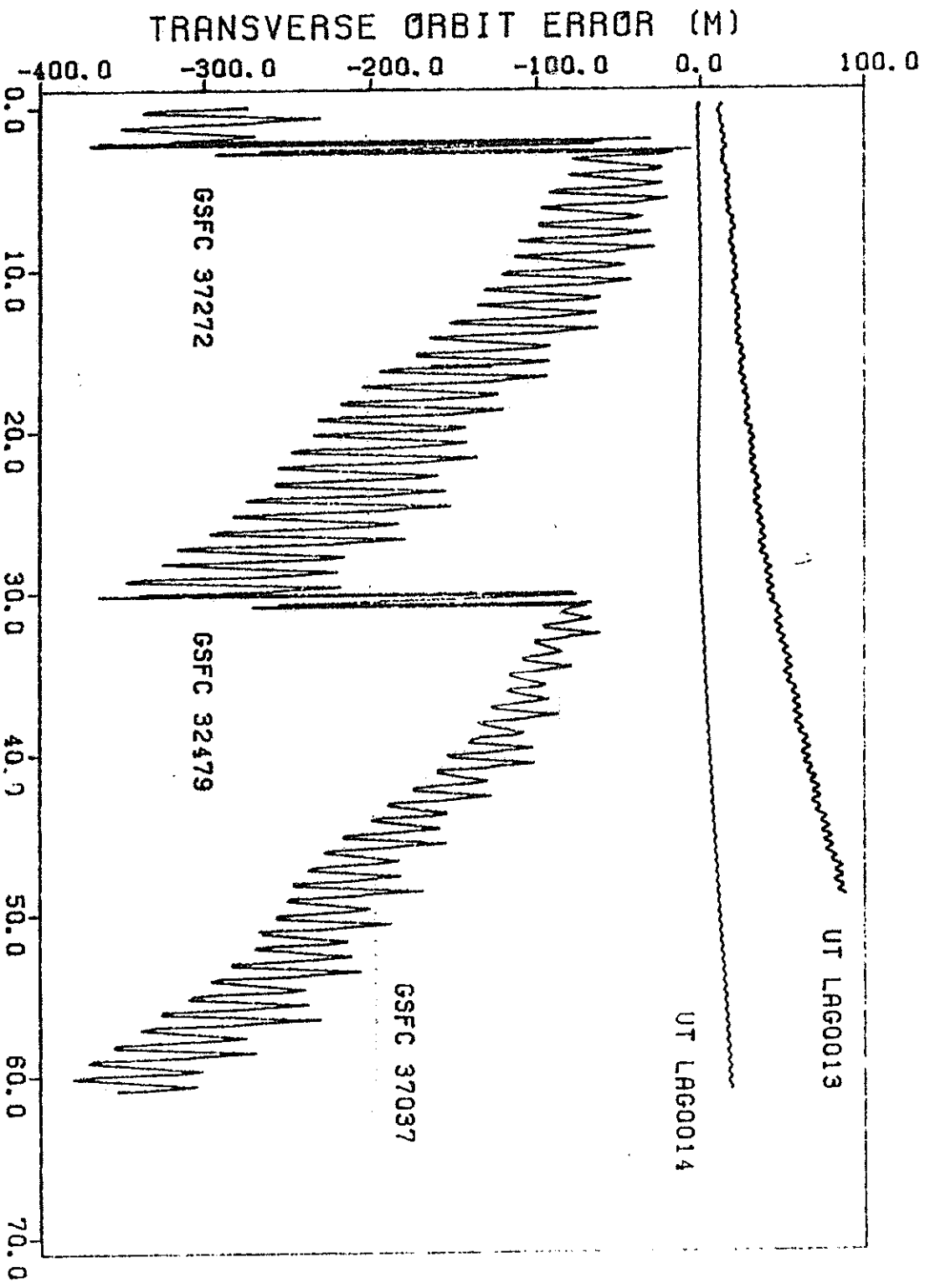

FIG. 2 TRANSVERSE PREDICTION ERROR

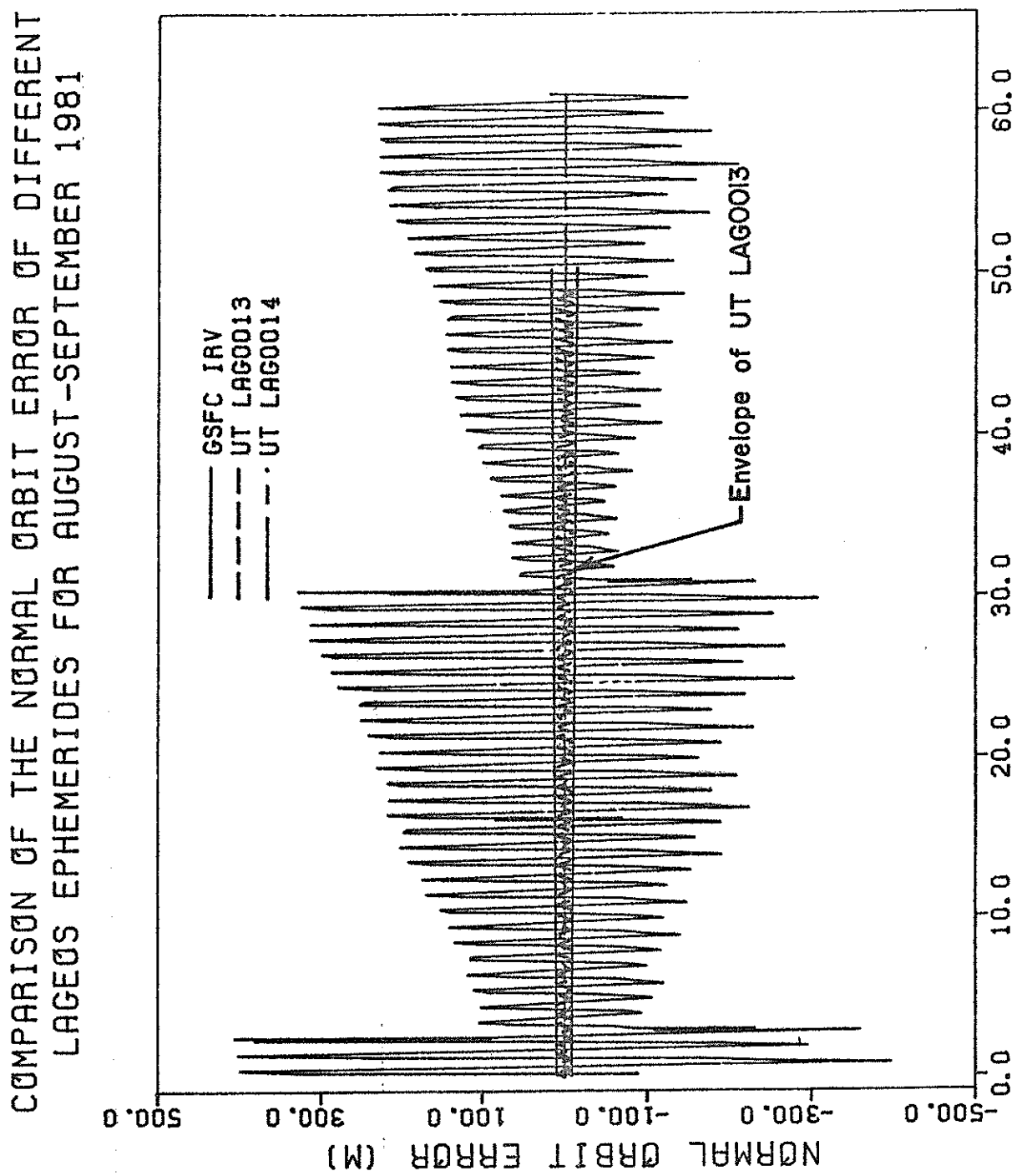

FIG. 3 NORMAL PREDICTION ERROR

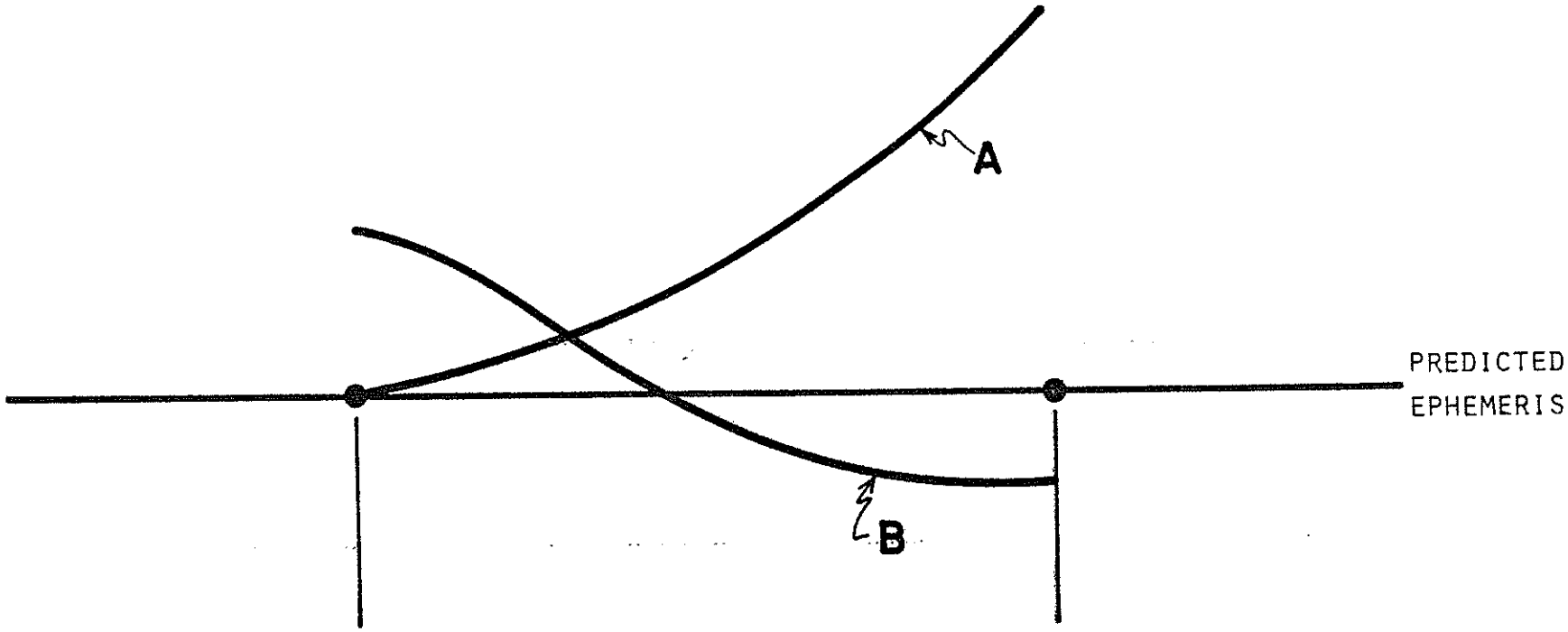

A: RECONSTRUCTED EPHEMERIS USING PREDICTED EPHEMERIS FOR INITIAL STATE

B: RECONSTRUCTED EPHEMERIS USING INITIAL STATE TUNED TO BEST FIT SLR MODEL TO PREDICTED EPHEMERIS

FIG. 4 TUNED INITIAL CONDITIONS

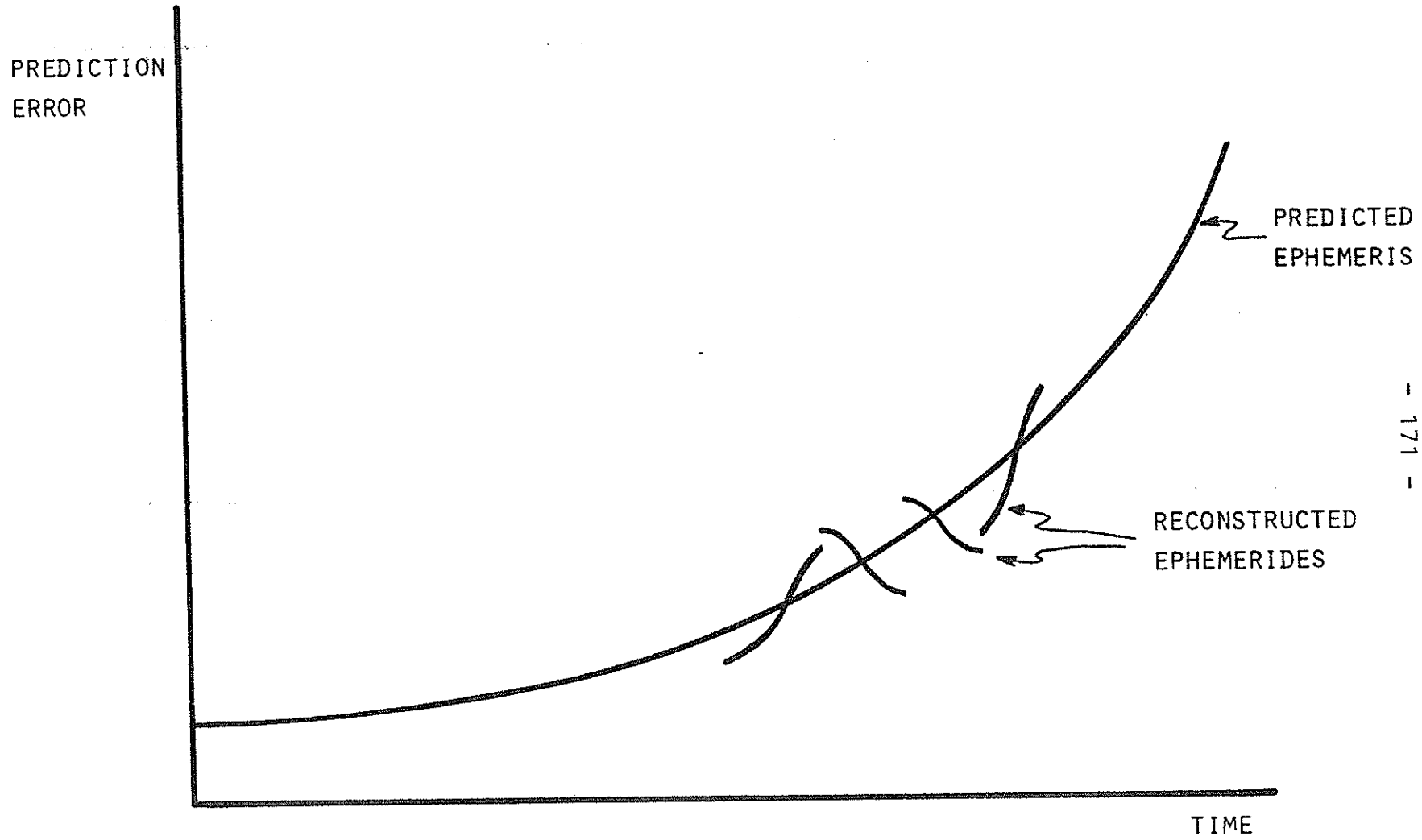

FIG. 5 PROCEDURE

PRACTICAL ASPECTS OF ON-SITE PREDICTION

E. Vermaat

Working Group for Satellite Geodesy, Kootwijk,
Delft University of Technology, Delft, The Netherlands.

Abstract:

The amount of success of satellite laser ranging, apart from efforts in instrumental design, largely depends on the production of accurate satellite orbits by a prediction center.

This paper reviews some of the aspects of the interaction between a prediction center and mobile laser ranging systems.

Practical techniques for real-time prediction optimisation are reviewed. The feasibility of on-site estimation of orbital parameters is discussed.

1. Introduction

Satellite laser ranging systems should be provided with orbital parameter messages, which are sufficiently compact

for ease of data-communication and which allow for efficient on-site computation of look-angles. Section 2 reviews techniques for this.

The frequency with which satellite orbits should be upgraded, from the reduction of recent quick-look data largely depends on orbital characteristics. Low flying satellites, especially those affected significantly by air drag, cannot be predicted accurately for more than 2 or 3 weeks ahead [Dunn,1979].

The required prediction accuracy obviously depends on equipment characteristics. An important overall quality is the maximum beam divergence allowing for a reasonable probability of satellite return detection. In daylight, at high background noise levels, this value will be most critical.

If the a-priori quality of the look-angle predictions does not allow for "hands-off" tracking due to e.g. poor orbital information or, in case of mobile ranging, inaccuracies in site coordinates, mount orientation or timing, real-time facilities as described in section 3 could help optimising acquisition rates significantly.

In case of interrupted data communication with the prediction center, possibly happening to remotely operating mobile stations, a great deal of continuity of operation can be obtained from on-site orbital parameter estimation techniques. These are discussed in section 4.

2. Reproduction of the orbit on-site

Obviously it will be highly impractical to transmit sets of look-angles from a prediction center to the individual laser ranging stations. The prediction center

should define a set of parameters which describe the predicted orbit accurately and which allow for an efficient process of computing look-angles using on-site computing facilities. Thus one requires a parameterisation of the orbit to a sufficient degree of accuracy with a limited set of data involved on one hand, and reasonable simplicity in the reconstruction and in the subsequent computation of look-angles on the other hand.

A well known example of this approach is the SAO mean element message comprising Keplerian mean elements at an epoch and terms describing secular and long-periodic perturbations [Thorp,1978]. The reconstruction of the orbit requires an analytical theory for updating the orbit to any epoch t(i) and the addition of significant short-periodic perturbations. The famous SAO-Aimlaser programme does just that.

An alternative approach is the use of osculating elements (a state vector) which describe the actual satellite state at an epoch in a well-defined coordinate system, e.g. NASA IRV messages. The reconstruction of the orbit can be accomplished by numerical integration of the equations of motion derived from a dynamical model. Pertinent to this model a choice out of three cases could be made.

a. The formally only correct way is to use the original dynamical model for the equations of motion as being used for the quick-look data analysis at the prediction center. This would precisely reconstruct the orbit as it has been predicted from the data analysis, at the unrealistic price however of heavily burdening the on-site computing facilities.
b. Alternatively one could derive the equations of motion from a simplified model. The permissible degree of simplification depends basically on the satellite orbit

characteristics and the arc length required. The reconstructed orbit being tangential at the initial epoch will gradually diverge from the originally predicted orbit. In table 1 the committed error is summarized using a given state vector for STARLETTE and LAGEOS. Results are given at various arc lengths and using two very simple dynamical models, accounting for the influence of earth gravity up to the J2 term or up to degree and order 4 respectively, neglecting all other forces.

These results suggest the use of one state vector for each observable pass of STARLETTE (about 5 or 6 per day), where the J2-field is already sufficient and one state vector for every one-day arc of LAGEOS, utilising up to C,S(4,4). Thus the computational effort required on-site as well as the number of state vectors involved is quite limited.

c. A third possibility is that the prediction center fits an arc of certain length to the predicted orbit in an adjustment process using a simplified dynamical model, yielding a new estimate for the initial state vector. Utilising this "mean" state vector, the fitted arc can be reproduced on-site by numerical integration applying the same simplified model. Again the permissible arc length and the degree of simplification are related and depend on the orbit. But the absence of the divergence occurring in the former case, as a result of the technique of approximation applied here, will allow for a considerably greater arc length to be derived sufficiently accurately from a single state vector. Fig 1 depicts the deviation from the original orbit for a 7-day STARLETTE arc, utilising a tailored dynamical model comprising 23 selected coefficients of the earth

STARLETTE	20 min	1 hour	1 day
J 2,0	77 m/ 16 "	205 m/ 43 "	-
J 4,4	15 m/ 3 "	63 m/ 13 "	-
LAGEOS	**20 min**	**1 hour**	**1 day**
J 2,0	-	71 m/ 2.4"	-
J 4,4	-	12 m/ 0.4"	229 m/ 7.9"

Table 1. Errors in satellite position due to truncation of the earth gravity model up to the J_2-term and up to degree and order 4 respectively, at various arc lengths.

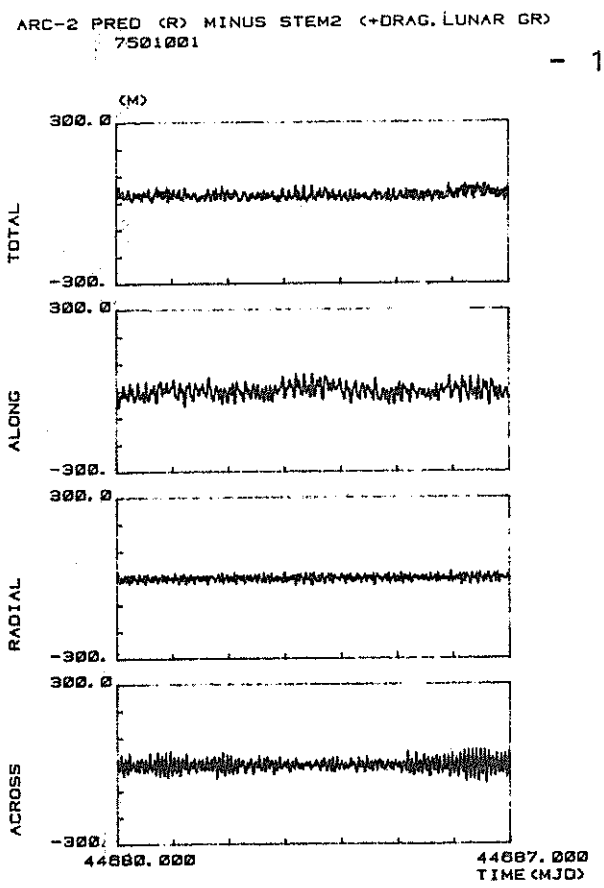

Figure 1.

Deviation of the approximated arc from a reference orbit. The taylored model comprises earth gravity terms up to degree and order 6 together with the sectorial terms of degree 13 and 14, as well as models for lunar gravity and air drag.

Figure 2.

A similar graph for LAGEOS. The taylored model comprises earth gravity terms up to degree and order 4, as well as models for solar and lunar gravity.

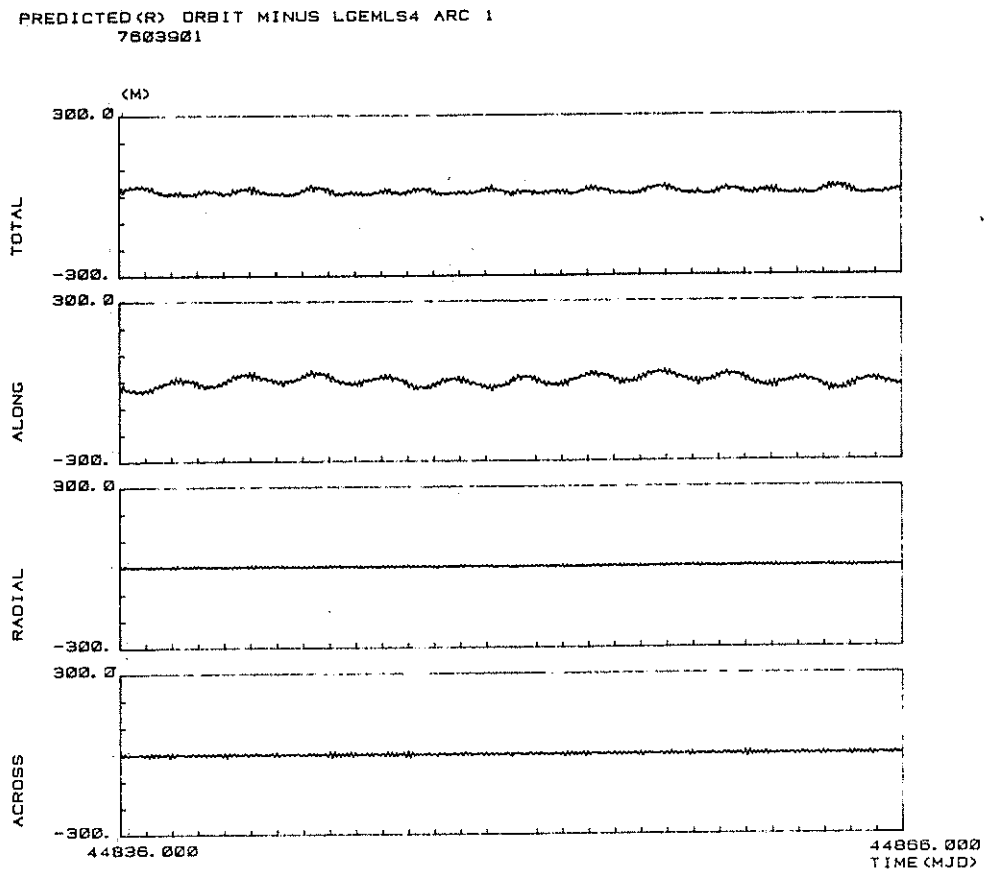

gravity field basically to degree and order 6, as well as models for air drag and lunar gravity. Fig. 2 gives similar results for a 30-day arc of LAGEOS derived from an earth gravity field up to degree and order 4, and models for lunar and solar gravity.

In both cases the maximum error is less than 50 m in the along-track, radial and across-track components. More details on this approach are given in [Vermaat,1981].

From these various approaches it can be concluded that ways exist to optimize both the amount of input data demanded from a prediction center and the simplicity of the on-site software producing the look-angle information required for tracking.

3. Real-time techniques for prediction optimisation

Basically three goals should be accomplished while tracking the satellite, in order to optimise the data acquisition:

a. obtaining the satellite within the laser beam and obtaining the occurrence of its return signal within the time window,
b. discriminating satellite returns from noise,
c. deciding on corrections to the look-angles, delay and size of the time window to enhance the signal to noise ratio.

If a. is not accomplished automatically when tracking has commenced, eventually at the maximum permissible beam width and time window, there is little else to do then to engage some search-and-find process, primarily adjusting

the along-track component.

The second goal should obviously also be aimed at immediately, in order to be able to judge the amount of success in actually hitting the satellite. This discrimination could be facilitated by graphically displaying the occurred events e.g. in terms of observed - predicted values or by constructing histograms counting events in a number of classes defined in the travel time domain. This graphical data will require operator intervention to conclude about the actual offset in predicted range. Simple numerical techniques for processing range residual data could be imagined to arrive automatically at the range offset.

An increased acquisition rate resulting from the deployment of a multi-event timer, especially at high noise levels, could significantly speed up this process of locating the satellite.

Angular information could be derived from data sampling with a quadrant detection system, such as anticipated in the Delft mobile system [Visser,1981]. This data, sampled with four independent PMT's, could likewise be processed either graphically or numerically, to decide on the angular displacement of the satellite with respect to the optical center of the detection system.

Once the satellite has been located with some degree of reliability, the corrections to be applied to the predicted delay or, in case of quadrant detection to the look-angles, can be decided upon easily by the operator or eventually from dedicated software. An example of a curve fitting technique rapidly concluding accurately on improved range prediction is given in fig. 3. As soon as a curve is fitted to 7 to 20 early range observations in the pass, utilising a second degree polynomial and a Keplerian model with three free parameters resp., the remaining range predictions in

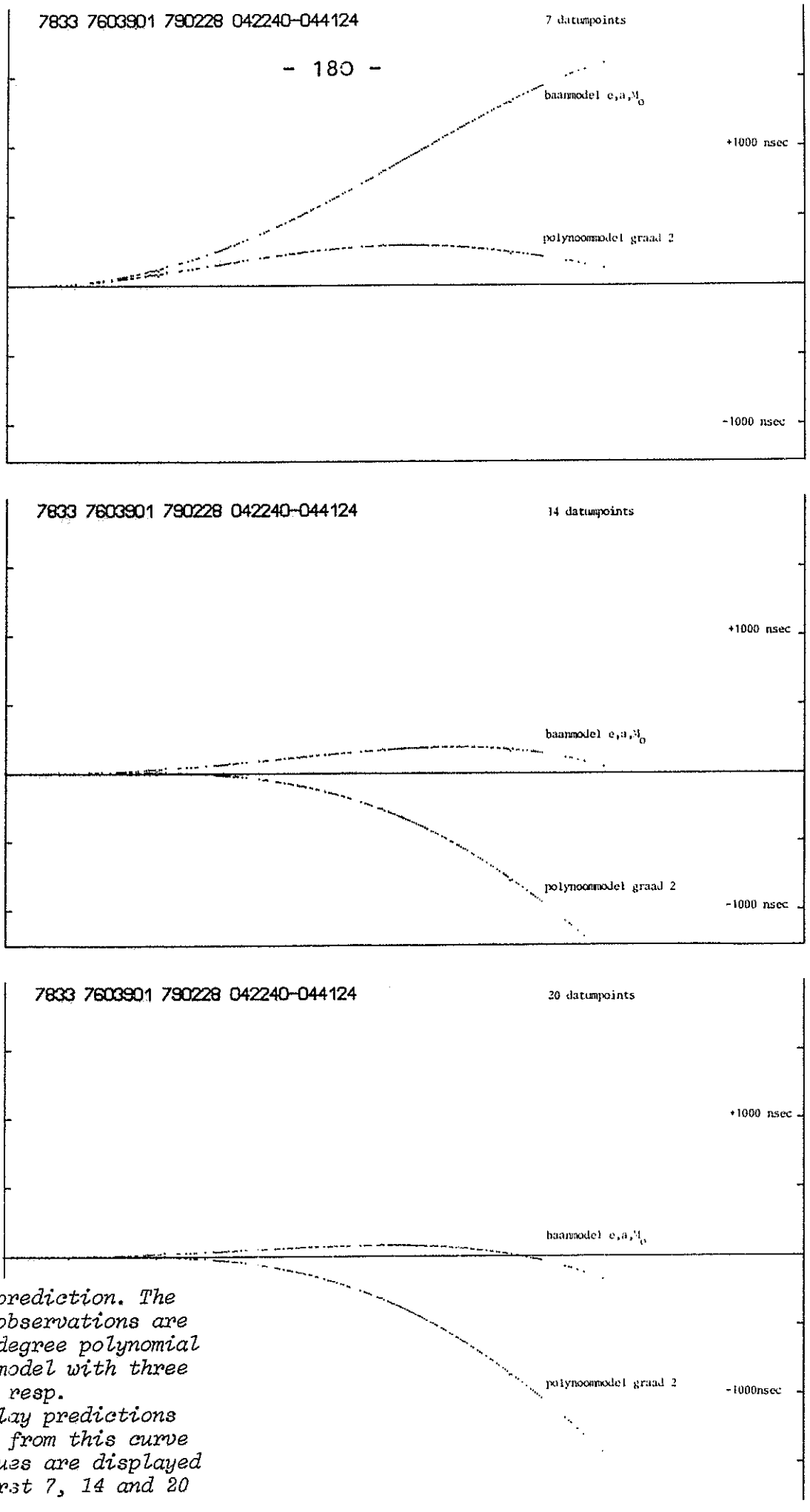

Figure 3.

Real-time delay prediction. The first few range observations are fitted to a 2nd degree polynomial and a Keplerian model with three free parameters, resp. The remaining delay predictions are extrapolated from this curve fit. The O-C values are displayed utilising the first 7, 14 and 20 datapoints resp.

the pass are extrapolated from the curve. The graphs display the residuals with respect to the actual observations. It is concluded that already after processing the first 14 range observations, the improved range predictions obtained from the Keplerian model result in range predictions accurate to at least 200 ns for the remainder of the pass.

Thus, with the techniques described, improved satellite predictions can be produced, allowing for the decrease of both the time window produced by the range gate generator and the width of the laser beam, which in turn yields improved signal to background noise levels. It is expected that these detection hardware facilities in concert with simple but cleverly designed software, will considerably improve the amount of data acquisition in case of initially marginal observability conditions like daylight ranging at low signal levels of poor a-priori information on either the satellite's orbit or on mount position and orientation, or in case of the occurrence of unknown clock offsets.

4. Orbital parameter estimation from on-site analysis

The quality of orbital predictions for low orbit satellites (say less than 1500 km), especially those with unfavourable area to mass ratio, tends to deteriorate quite rapidly in a few weeks time. Regular re-estimation based on recent tracking data is therefore important, requiring a prediction center collecting quick-look data from different tracking stations and transmitting newly derived orbital parameters regularly. If remotely operating mobile laser ranging systems encounter problems in data communication with the outside world, successful ranging on these satellites might become increasingly difficult. Some de-

gree of independence for these mobile systems in terms of on-site prediction capability therefore might add to the success of laser ranging campaigns.

Major drawbacks in this on-site data reduction and estimation process will be the poor geometry of the solution as a consequence of the use of one-station range data only and the severe simplifications in the dynamical model from which the equations of motion will be derived, dictated by the limited on-site computer capacity. The feasibility of this approach however has been indicated by several authors (e.g. [Schutz,1978],[Wakker,1981]).

The geometry problem will have to be solved by reducing data from a sufficient number of different passes, thus increasing the estimability of the orbital plane orientation parameters. But even in clearly non-singular solutions, systematic errors which might easily go undetected, could corrupt the significance of the estimated orbital parameters. Therefore this type of analysis always will have to be done with care.

The limited computer capacity will be most severe in real-time, because high priority programs will be in execution e.g. for monitoring the tracking and data formatting, etc. The necessity for orbital parameter estimation in real-time could be questioned however. Some of the more appropriate candidates for efficiently improving tracking parameters in real-time were outlined in the previous section. The corrections to the look-angles derived in this way, usually have limited validity for future passes however. Therefore, once serious offsets in the look-angles or delays due to poor orbital prediction quality have been encountered, programmes for data reduction and parameter estimation should be executed off-line in the periods between pass observations, thus exploiting the otherwise

idle computer capacity to the full.

The feasibility of the sequential KALMAN filter approach for this analysis has been clearly demonstrated in [Wakker,1981]. In this reference the application of the extended KALMAN filter technique to the problem of orbital estimation utilising one-station range data, is outlined. Of specific interest is the solution to the filter divergence problem due to non-linearity of the dynamical equations. The cautious application of a correlation correction factor slighthly affecting the state covariance matrix prior to each observation-update step, effectively eliminates this instability. The notorious filter divergence problem occurs also in presence of undetected gross errors in the range data. [Vermeer,1981] describes a theoretically derived technique based on the "limited gain" philosophy, bounding the influence of gross errors. Without the use of this kind of techniques, the effect of gross errors, especially when occurring at the beginning of a new pass, is generally fatal to the filter stability. From these studies it can be concluded that with carefully designed software and cautious analysis, the KALMAN filter method proves to be a powerful tool to solve the problem of upgrading orbital parameters from on-site range data analysis.

For those who insist, this sequential technique could be applied in real-time, feasible for satellite ranging stations equipped with sufficient computer capacity.

Obviously batch type approaches could also be employed, exclusively in the off-line case. Reducing batches of data principally has the advantage of better control of the influence of gross errors in the data, than sequential techniques, although as indicated above, the quite poor geo-

metry due to the exclusive use of range data only from one station, might in many cases largely neutralise this quality, especially when a small number of passes has been observed. A candidate for a simplified dynamical model describing the satellite's orbital motion could be the model outlined in section 2, used for the approximation of an arc, estimating a "mean" state vector. This new initial state vector defines the arc with sufficient accuracy, deploying dynamical equations derived from the tailored force model. If this model would have been installed already for the computation of look-angles, it would require relatively little extra coding to allow for the reduction of range data, re-estimating the initial state in the same dynamical system. Promising results were obtained from a preliminary investigation upgrading a 7-day STARLETTE arc utilising the tailored model described in section 2. Fig. 4 illustrates the effect of the reduction of 9 passes of range data. In this simulation study, the initial state was corrupted causing a considerable divergence between the "real" and the corrupted arc, illustrated in the top figure. The graph at the bottom shows the deviation of the updated arc from the "real" arc after processing 9 passes of range data, taken within 48 hours from the beginning of the arc. It should be noted that the original initial state vector was derived from a 7-day arc. The latter 7 days depicted in this figure shows the results of sheer extrapolation, suggesting the feasibility of continuing this on-site analysis with recent data, thus obtaining a good deal of independence from external orbital information. Considerable interrupts in the data acquisition due to e.g. weather or site change would easily corrupt this process of "bootstrapping", compelling re-initialisation from external information.

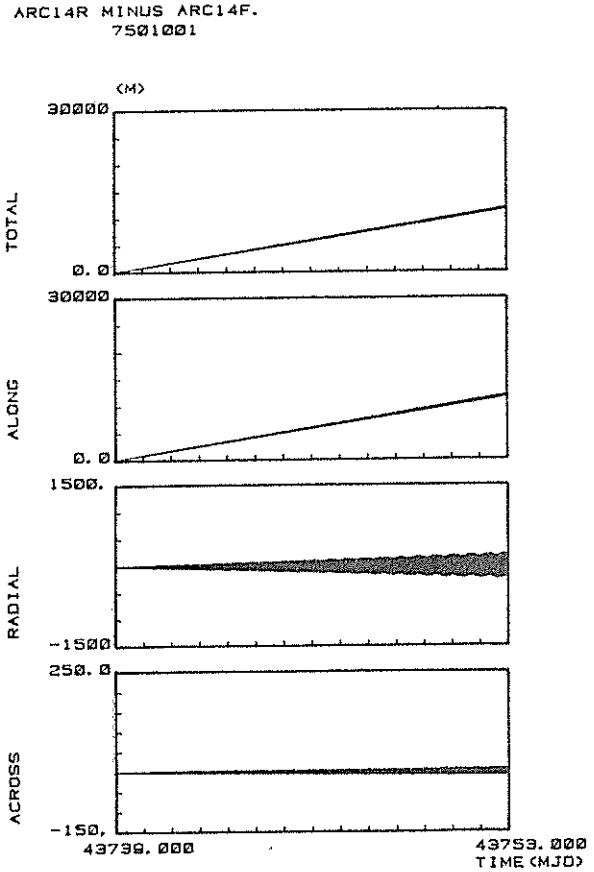

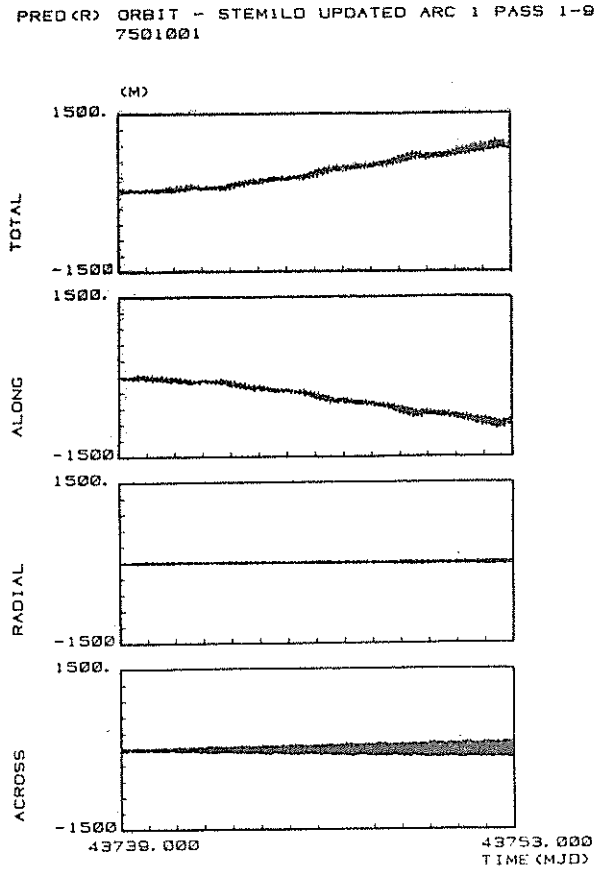

Figure 4.

Satellite orbit improvement from on-site analysis. A poorly predicted arc of STARLETTE is upgraded from the reduction of one-station range data taken in 9 passes during the first 48 hours of the arc. The deviations from the reference orbit are displayed for the predicted arc (top) and the improved arc (bottom).

5. Concluding remarks

A dedicated prediction center communicating regularly updated orbital parameters for the low satellites to SLR stations, could eliminate all serious on-site prediction problems. Nevertheless a great deal of flexibility and reliability can be obtained from clever hardware/software features at the stations for real-time prediction optimisation. Some degree of independence from data communication with the prediction center by means of on-site facilities for orbital parameter estimation, is advisable and feasible.

References

Dunn, P. and S. Lewis, Laser System Prediction Capability, EG&G Washington Analytical Services Center, Inc. Riverdale, January 1979.

Schutz, B.E. Laser Pointing Predictions from on-site Analysis. Proceedings of the Third International Workshop on Laser Ranging Instrumentation. Lagonissi, May 1978.

Thorp, J.M. et al. SAO Ranging Software and Data Preprocessing, ibid.

Vermaat, E. On-site Numerical Integration of the STARLETTE Orbit in a Tailored Force Field. Presented at the Fourth International Workshop on Laser Ranging Instrumentation. Austin, October 1981.

Veermeer, M. Kalman Filter Orbit Determination for Geodetic Satellite Laser Ranging; a Theoretical Inquiry. Reports of the Department of Geodesy, Section Mathematical and Physical Geodesy, Nr. 81.2, Delft University of Technology, Delft, May 1981 (in press).

Visser, H. and F.W. Zeeman. Detection Package for the German/Dutch Mobile System. Presented at the Fourth International Workshop on Laser Ranging Instrumentation. Austin, October 1981.

Wakker, K.F. and B.A.C. Ambrosius. Kalman Filter Satellite Orbit Improvement Using Laser Ranging Measurements from a Single Tracking Station, In: Advances in Theory and Applications of Non-linear Filters and Kalman Filters. NATO AGARD, 1981 (in press).

Latest Trends in Optics and Mount Development

Yoshihide Kozai

Tokyo Astronomical Observatory
Mitaka, Tokyo, Japan 181

In early days of the space age most of the artificial satellites were tracked by radio interferometry, optical and radio doppler methods. Since the accuracy of their predictions was usually very poor because of the lack of knowledge of the upper atmosphere density and its temporal variations and of rather large values of the area-to-mass ratios of the artificial satellites, wide-angle cameras of Schmidt type, for an example, had to be used for the optical tracking purpose. Also as any computor-controlled device to drive the telescopes was not available at that time, a third axis, so-called tracking axis, was introduced so that by rotating the telescope around this axis only satellites could be tracked. However, since any satellite does not move along a great circle in the sky it was not possible to track them accurately along a long arc with one tracking axis only. Therefore,some tracking telescopes such as AFU-75 have fourth axes for the precise trackings.

Now only a few laser ranging telescopes have tracking axes. Most of them are on alt-azimuth mounts and the telescopes follow the motions of artificial satellites by rotating them around the two axes simultaneously. This can be done very easily by using small computors which compute predicted directions of the satellites as functions of time and drive the telescopes by comparing their directions in the sky with the predicted ones. Some of the telescopes are on X-Y mounts to avoid the dead angle near the zenith by introducing another horizontal axis instead of the vertical axis for the alt-azimuth mount.

In early days just after satellite laser ranging instruments had become available laser oscillators were usually very compact and short. Therefore, they could be put on the same mount as the telescopes. Now in order to reduce the laser pulse length to the order of a few hundred pico-seconds, to change the original laser frequency for some cases and to amplify the laser power many devices besides the oscillators are necessary. Therefore, the laser oscillator systems are very large and heavy and cannot be, usually, put on the same

mount as the telescopes. Instead they are put on fixed platforms. In order to fire the laser beam towards the satellite it should be introduced to the transmitting telescope through its coude focus. Then it is necessary to take alignments among optical axes of the transmitting and receiving telescopes and also laser beam axis very carefully. It is a very time-consuming job. Now some very ingenious devices for the alignments have been developed and introduced in most of the existing systems.

Major modifications of the satellite laser ranging systems were made after Lageos satellite was launched. We can compute predicted positions of the satellite very accurately, namely with two arc second errors. Therefore, it is possible now to range the satellite with very narrow beam divergence if the system can follow the satellite motions with the same accuracy. If so, a moderate size telescope can be used for Lageos satellite ranging and as not so high energy laser is necessary the pulse length can be made very short. For such systems requirements for the optical system and mounts are more severe. The mount should be designed so that the telescopes can be pointed to the predicted positions very precisely with and without guiding and the optical system must be designed so that the alignments can be taken very accurately, easily and quickly.

Now at several institutes mobile(or transportable) laser ranging systems have been developed and in operation. In fact most of recently developed systems are mobile or transportable in some senses. The requirements for such systems are the most severe, however, they have been achieved for most of the systems.

In the session of latest trends in optics and mount developments the report on mount and telescope for the German/Dutch mobile system is presented by H. Visser and F.W.Zeeman and the satellite ranging mount system of Contraves Coerz Corporation is explained by G. Economou and S. Snyder. Moreover, the 1.5 meter telescope realized by INAG for the CERGA lunar laser ranging system is described by M. Bourdet and C. Dumoulin. The three papers appear in the proceedings. The other two papers which are presented in the session cannot be published here unfortunately because they have not come in written form by the deadline. They are the paper on TLRS II(Tansportable Lunar Ranging System) by T. Johnson and that on MLRS(Mobile Lunar Ranging System) by B. Greene. It is expected that you can have informations on these two systems in the tables of the proceedings and by contacting the authors.

DESCRIPTION OF THE 1.5 M TELESCOPE REALIZED BY INAG FOR THE CERGA LUNAR LASER RANGING SYSTEM

. BOURDET
.N.A.G. - Avenue Denfert Rochereau - PARIS - FRANCE

. DUMOULIN
ERGA - ROQUEVIGNON - GRASSE - FRANCE

INTRODUCTION

In 1973, the National Institute of Astronomy and Geophysics (I.N.A.G.) was entrusted with the design of a Lunar Laser Ranging System. The scientific objective is the measurement of the Lunar distance with an accuracy of several cm., by means of the round trip travel time of a Ruby laser pulse. The measure must be obtained within about 10 mn. interval during the firing sequence. The first shots insure the result, the following ones improve the precision.

Our first duty, was to work out the specification for this special experiment. The acquired knowledge from the Mc Donald Observatory and the results of the tests made in France at Pic du Midi Observatory allowed us to choose the important parameters. After approximating the characteristics of the laser, the receptor and the backscattered beam, we were able to define the features of the optical instrument. The most important were the tracking and guiding accuracy, the high collimation between the emission, reception and guiding paths and the telescope size. A preliminary theorical study has shown, that the telescope would have at least 1.4 m in diameter in order to satisfy the scientific objectives.

BACKGROUND INFORMATION

The telescope is located near Grasse on a Plateau, at an altitude of 1 250 m. Its construction began in 1974. The first stars were observed in August of 1978 with a simplified tracking program.

The basic layout of the facility is shown in fig. 1. A 44 m² room where the operators stand, shelters the computers, electronics and laser. The laser stands on a concrete block with an independant foundation and is isolated by a wooden wall. At one end of this room is a circular attachment of which the wall sustains the dome. In the middle of this room is a concrete pier on which rests the telescope. This pier is constructed of six

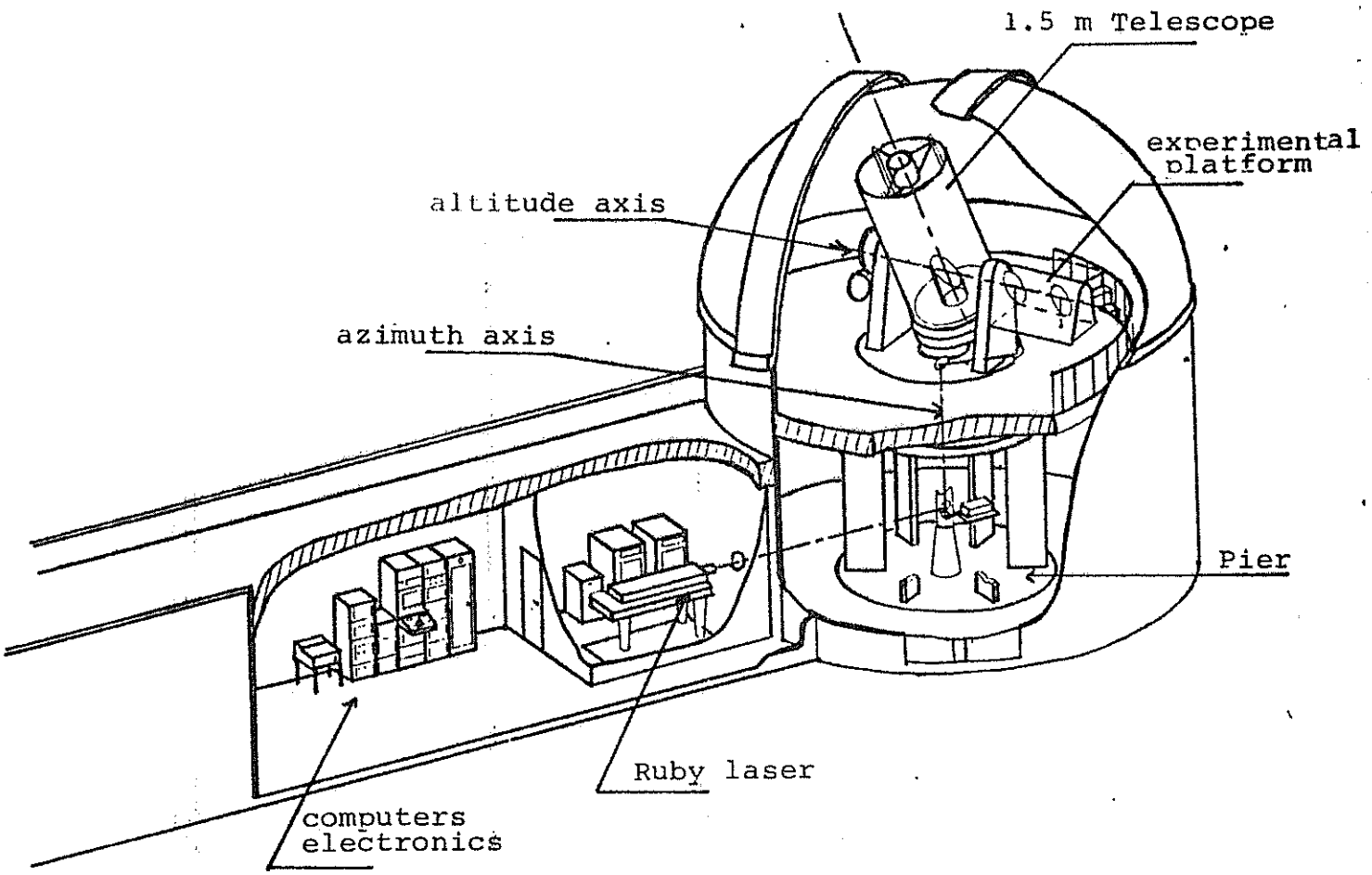

Fig. 1 : THE LOCATION OF THE LASER RANGING EQUIPMENT

radial walls which are tied at the top by a concrete ring and below by an independant bulky foundation. A floor, situated at 4.50 m from the ground, allows the observer to reach the experimental equipment attached to a platform which is fixed to the telescope. The dome of 9.5 m diameter is turned by hydraulic motors. It is slaved whith the rotation of the telescope. A thermal insulation covers the interior of the dome.

MAIN OPTICS OF THE SYSTEM

The optical system consists firstly of the telescope proper with a Nasmyth-Cassegrain focus and secondly of the auxiliary optics which separates the beam into emission, reception and guiding paths. This solution with a telescope used as transmitter, receiver and guider facilitates an alignment of the three paths better than one arc second. The diagram of the major optical components is drawn in fig. 2.

The telescope is composed of a main concave, a convex and a Nasmyth mirror. A diameter of 1.5. m was chosen for the primary mirror. With adequate light efficiency, this receptor surface appeared to offer a sufficient margin of security. Besides when used as a transmitter the divergence of the laser beam might be less than one arc second. The focal ratio of the primary is f/3. The secondary gives an effective single telescope focal ratio of approximately F/20 which corresponds to a 31 m focal length. The Ritchey-Chretien optical system allows the attainment of an utilizable 30 minutes field for the tracking (aberration less than 0.5 arc sec. on the curved focal surface).

There are various guiding methods. At the time of the design, a sure way to point the telescope to the site of a lunar retro-reflector array seemed to be by off-setting from a small reference crater with the electronic reticle of a T.V. camera. Hence, there is a moving guiding camera which is controlled by a computer. To calculate its position, the computer needs the focal length accurately (with a relative precision of 10^{-4}). The chosen solution allows the holding of the focal length during several months by avoiding the variation of the mirrors curvature

and of the critical primary-secondary separation. The mirrors are made of zerodur ceramic glass with a low expansion coefficient. The primary and the secondary are linked with three Invar rods. The secondary is connected to the three bars by only a three brace spider. This solution equally allows the maintenance of the focusing which eliminates a constant adjustment on the secondary, thus rendering its position very stable.

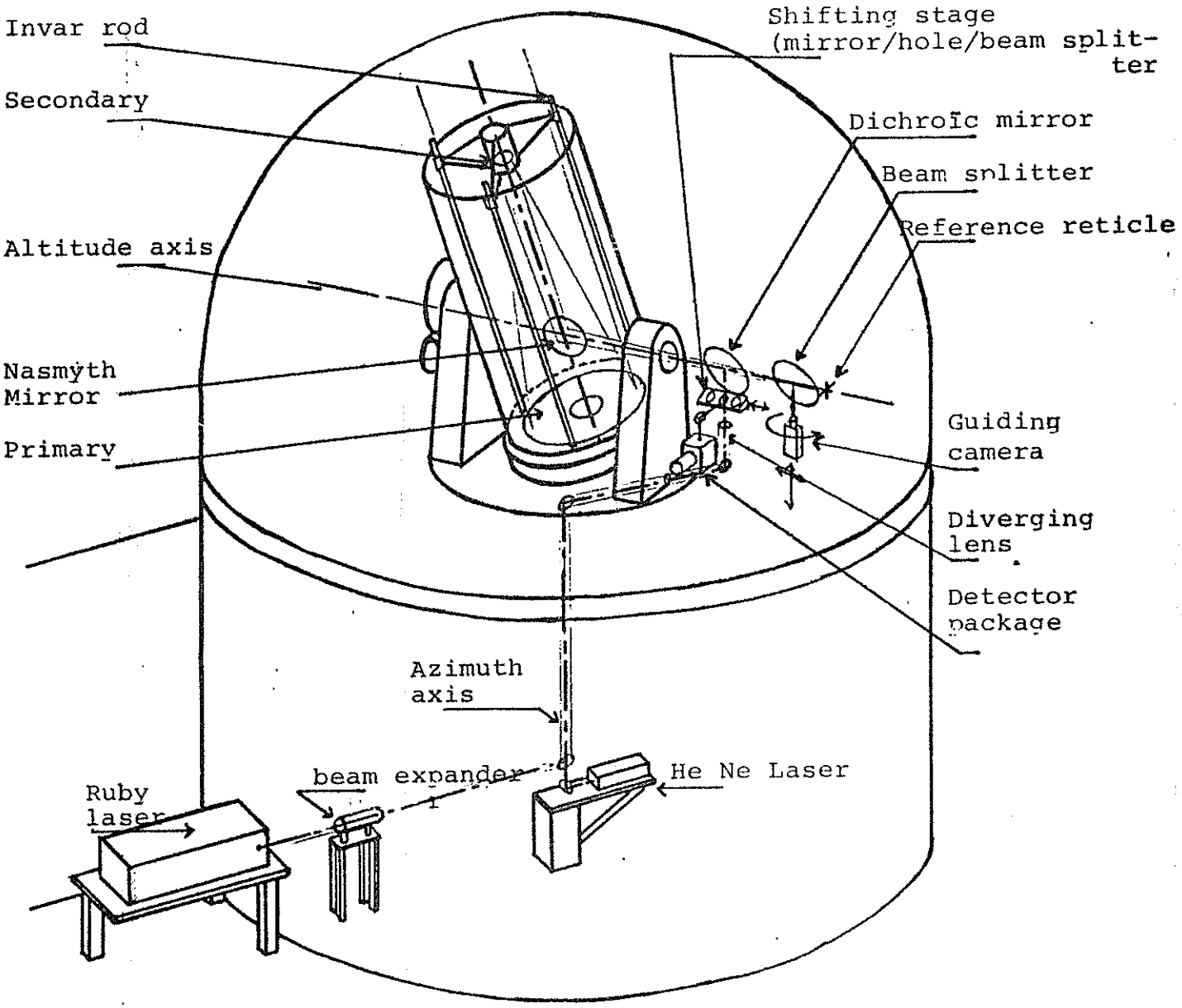

Fig. 2 : DIAGRAM OF THE MAJOR COMPONENTS

To improve the light efficiency, the secondary and flat mirrors are overcoated with silver (R≃98 %). For the same reason, the Cassegrain's location was determined by minimizing the central obstruction (taking into account the protecting light-baffles, a loss of only 11 % is obtained) . Furthermore, by frequently recoating and cleaning the mirrors the light efficiency obtained is greater than 0.8.

AUXILIARY OPTICS

The separation of the emission, reception and guiding paths is facilitated by the accessibility of the focus, due to the alta-zimuth mount Fig. 2 and 3 shows the principle.

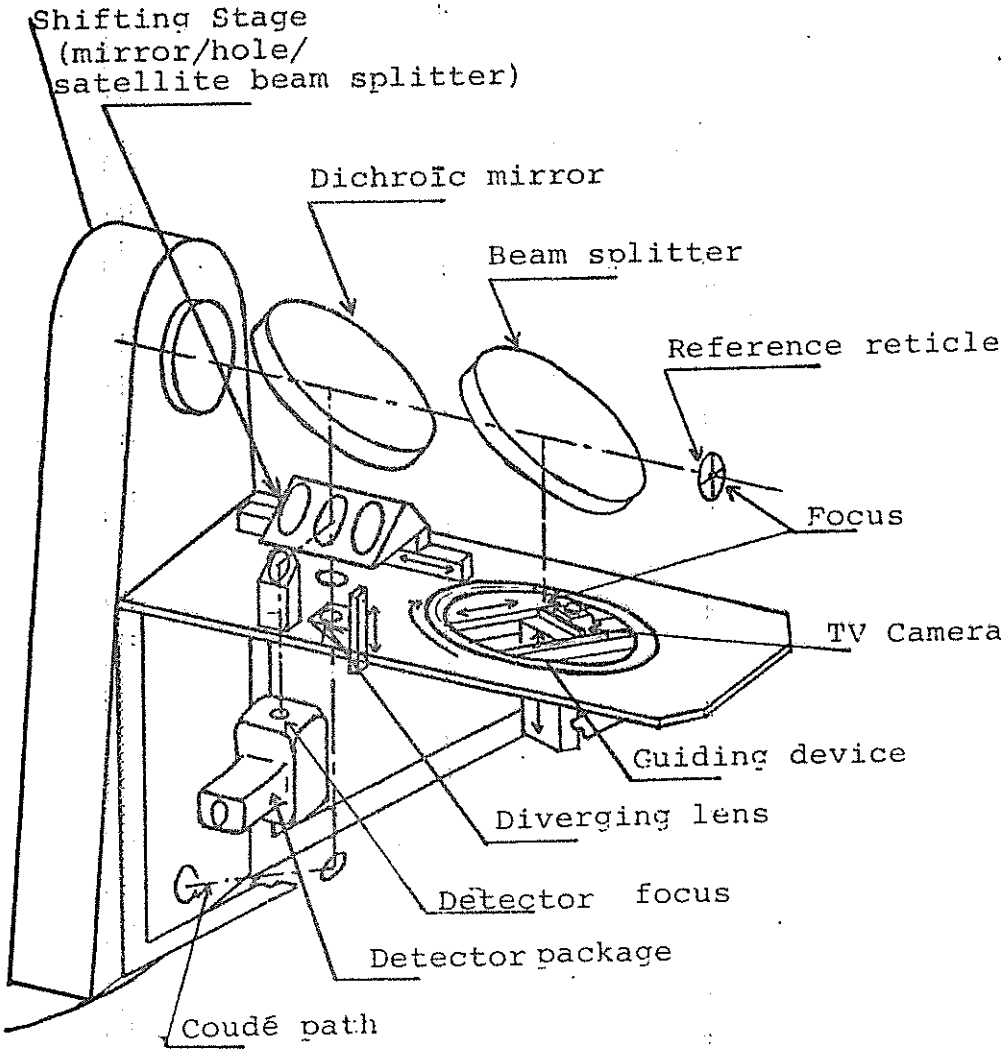

Fig. 3 : SEPARATION OF THE EMISSION, RECEPTION AND GUIDING PATHS

After emission, the laser beam is expanded to 30.5 m diameter and begins to follow the coudé trajectory. After the dichroïc mirror, the beam appears to issue from the focus of the telescope. On the return trip after the dichroïc, a shifting mirror reflects the light onto the detector package which contains a photomultiplier, spatial and spectral filters. In the case of shots at satellites or earth targets, a beam splitter is substituted which permits simultaneous emission and reception. All of these optical components have a multilayer dielectric coating. Due to special precautions against dust, the light efficiency is excellent.

The dichroïc, which reflects 99 % of the ruby wave-length, is transparent to the bulk of the visible spectrum used for guiding. A beam splitter reflects 75 % of this light while giving a horizontal guiding field. The searching of the focal surface is accomplished with the aid of a moving T.V. camera. Used without auxiliary optics, it receives a field of about 5 arc minutes in which the definition is sufficient. The camera is carried by a motorized micropositioning device controlled by a computer. This device consists of a rotary stage, which easily compensates for the rotation of the field, and two translatory stages, one for off-set field observation and the other for focusing. Due to the horizontal focal surface, the system operates in favorable mechanical conditions. Nevertheless, the original adjustment is important to hold the precision. Both the electronic reticle of the camera and the focus of the telescope must fall accurately on the rotation axis, when the camera stays in the center of the field. To make these adjustments, the focus is materialized by a projected reticle (this process is explained in the following paragraph). By rotating the device, the camera image of this focus describes a circle with a center on the axis of rotation. It now suffices to merge the projected and electronic reticles on this center.

The light transmitted by the beam splitter gives an available auxiliary focus. This one, in particular, is used as the reference focus of the telescope for aligning the three parths. A reticle define its position on the horizontal rotation

axis (or more exactly its image through the two beam-splitters). To put the reticle in place, a spherical mirror is attached to the horizontal bearing and turns with the tube. Its center of curvature was chosen to be in telescope's focal plane ; hence, the reticle and its image can be merged by tilting the mirror. The adjustment is achieved when the image superimposes with the reticle ands stays fixed with the turning of the tube. Both the reticle and the center of curvature are on the horizontal rotation axis. With the lighting of the reticle, the spherical mirror projects its image on the detector package and the guiding camera, thusly defining the focus of the telescope.

For the alignment of the ruby laser beam, a He-Ne laser situated under the telescope is used. Firstly, its beam is sent out parallel to the rotation axis by auto-collimation on a flat mirror attached to the telescope. This mirror is made perpendicular to the axis by rendering fixed the reflect beam with an azimuth rotation. Afterwards by translation, the beam is centered on the axis. Then the passage of the beams rests fixed with respect to the telescope when it turns. To adjust the emission direction, the diverging lens must be regulated so that the laser beam seems to issue from the telescope's focus. The spherical mirror, used once again, gives an image of the laser beam at the auxiliary focus. By shifting the diverging lens, this image is centered on the reference reticle. Furthermore, a beam comes back to the ruby laser and is later used to adjust it. Thus, a translation of this lens parallel to the optical axis gives the wanted divergence of the emission beam which may be chosen between 1 and 15 arc seconds. It remains to merge the ruby laser beam with the He-Ne one.

This method gives an alignment of the paths better than 1 arc second and permits an easy checking of the adjustment without looking at the sky. With this mount, gravity always works in the same way, so the reliability is high.

THE MECHANICAL STRUCTURE

To obtain a good pointing and tracking quality, the alt-azimuth mount was recognized for its many advantages. Its compact

and symmetrical structure which operates in favorable conditions is better adapted to the computation of distorsion. This permits mastery of design and results in excellent unit rigidity. The axles always operate in the same conditions. Their positions, with regard to the optics, simplify the use of oil bearings. This insures a greater stability and allows a sensitive driving due to negligible frictions even at quasinull speeds. The telescope erection is easy. The control of rotation optical axis adjustment is facilitated, resulting in improved accuracy for setting and tracking. In addition, residual adjustment, defects, bending, gear faults, etc..., give an analytical expression which is easily inserted in the control program.

The mounting and the mechanical structure have been designed and drawn at the INAG Technical Division and manufactured in France. The principle elements are shown in Fig. 4. At the lower part of the telescope is a bulky platform of 2.75 m diameter. Below, a bright ring is attached and rests on 6 flats oil pads while 3 spherical ones hinder horizontal translatory movements of the axle. Above the platform, two tines support the altitude bearings.

The pads glide on spherical surfaces and their centers, which are unaffected by errors of adjustment and elastic deformations, define a steady position of the rotation axis. One of the bearings is fixed, while the other is free to move parallel to the axis with thermic dilation. The tube, formed of a 6 mm coiled sheet iron, is strengthened at the axle and holds up the primary mirror cell with its lever-weights at one hand and the secondary support at the other. The observing platform and the drive are attached to different fork-tines. The driving gear, identical on the two axes, is a worm and wheel system, with a 360 gear ratio. The torque motor, tachogenerator encoder and safety inertia wheel are directly mounted on the screw to benefit from the rigidity of the driving system. To improve the gear efficiency, contact is made with only one flank of the gear-tooth. To prevent blacklash, the worm-wheel is preloaded with a torque produced by an inert weight.

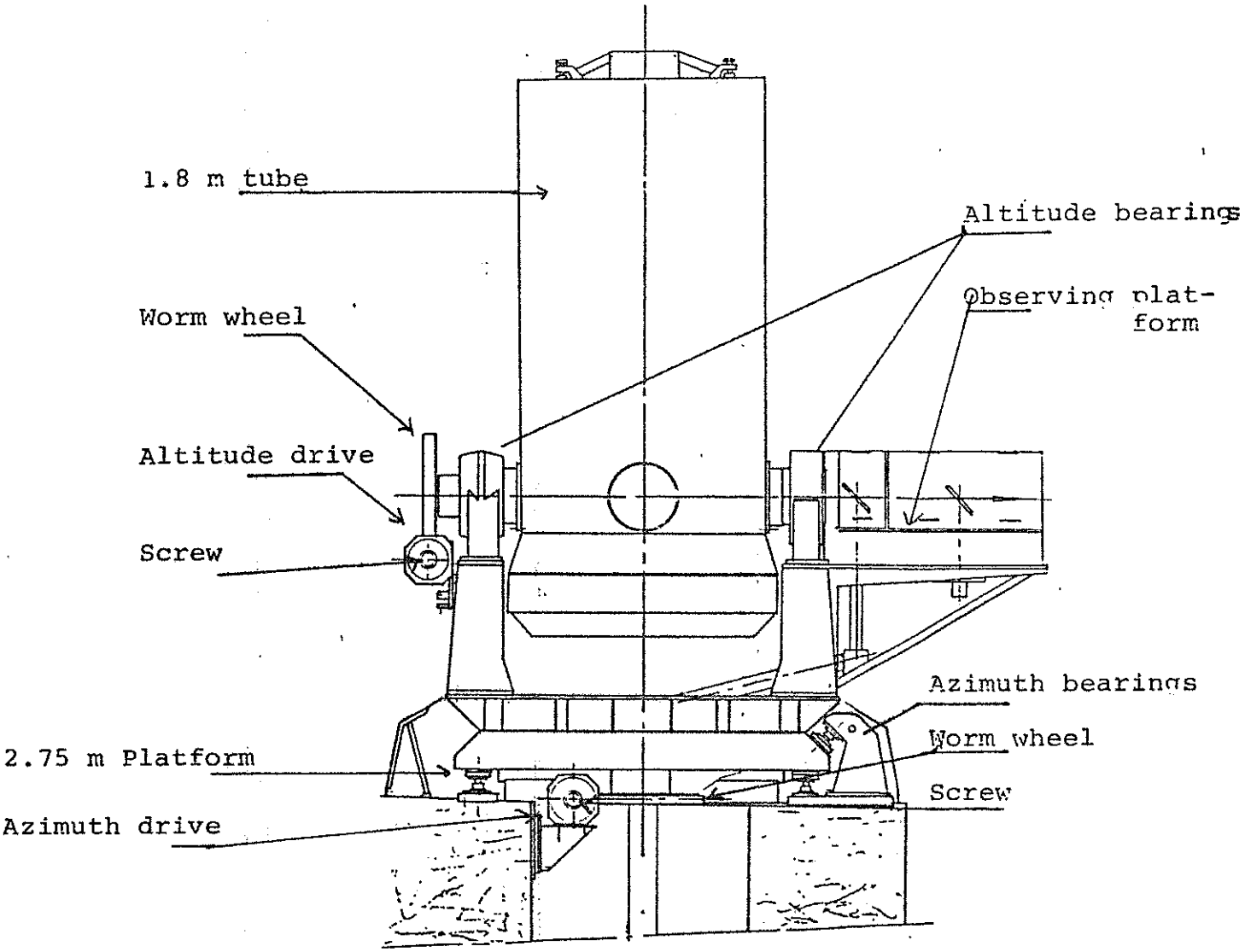

Fig. 4 : SCHEMATIC DRAWING OF THE STRUCTURE

CONTROL DRIVE SYSTEM

The control drive system is affected by the altazimuth mounting which causes the tracking speed to vary on the two axles. This produces the need of a servodrive with an important range of speeds controlled by a computer. At the conception of the telescope, the servodrive system was not evident. The technological progress permitted the finding of this satisfactory solution. Afterwards, it was noted that the recent large telescopes utilize nearly the same type of system.

The control drive system, which consists of a servo-mechanism directed by a computer runs succintly as described below. The computer calculates the trajectory of the telescope from the given data. To follow a star, a transformation of co-ordinates is sufficient. For the moon or a satellite, an inter-polating formula is added. Moreover, the program takes into consideration the atmospheric refraction and corrects the sys-tematic errors linked to the telescope. Over a steady interval, it gives the servosystem the necessary angle variation that the telescope must cover at constant speed. The tracking speed varies so slowly that it is nearly the same from one second to another, making a period of one second adequate.

To control the pointing, the computer needs the position of the telescope which is supplied from the encoder device. The incremental encoders, mounted on the worm screw, have a zero track which allows the position of the telescope to be known. This is achieved by relating the sum of the number of pulses to the angle turned through from a given starting point. This device produces an unambigous read-out encoder with a resolution of 0.1 arc-second on the sky, and gives the position of the sighting direction of the telescope with an average precision subordinated to the knowledge of the mechanical faults. For the tracking, the computer is outside the servoloop and does note use the encoder position.

The servosystem is identical on the two axes. It works out the speed command from the computer instructions, encoder position and possibly from manual corrections introduced by the guiding observer. Each axis is composed of an analog speed servoloop including the tachometer generator and a numeric position servoloop including the encoder. With respect to the restrictions of speed and acceleration, the numeric component generates the law of movement in terms of time, the average speed and the position error signal to control and adjust the speed of the analog component.

The obtaining of high performance with an important speed range characterizes the system. The maximum speed of the teles-cope is 1 revolution per 10 minutes on the two axes. On the ele-

vating axis, the maximum tracking speed only attains 11"/s ; but, it becomes 0"/s at the meridian. In this region the working is equivalent to that of a stepper system. On the azimuth axis, as the star goes through the zenith, the tracking speed approaches infinity. However, at one degree, it becomes only a quarter of the available speed and on the moon trajectory, it never exceeds 45"/s. For a speed slightly larger than this, the sighting error during tracking is less than 0.3 arc second on the encoder. On the azimuth axis, this error is greater than the sky sighting one, because the encoder read out is the projection of the sky error. Furthermore, the encoder error stays less than 2 arc seconds for a tracking speed of 600"/s which corresponds to the maximum satellite speed that this telescope can track.

CONCLUSION

Since August 1978, this telescope has been functioning regularly. The first shots at satellites took place in June 1980 and from June 1981 the measurement of Lunar ranging began. These successes confirm the tracking quality and the alignment accuracy of the emission, reception and guiding paths. As for the pointing quality, the root mean square actually obtained is about 4 arc second, with a rough correction of mechanical faults. Using a large number of star observations, the correcting factors can be hoped to be significantly improved. If this is the case, this could open new prospects of range measurement during the new moon period where the optical guiding seems quite impossible.

REFERENCES

E. SILVERBERG and D. CURRIE - A description of the lunar ranging station at Mc Donald Observatory (Space Research XII - Akademic Verlag, Berlin 1972),

E. SILVERBERG - Operation and performance of a lunar ranging station (applied optics, 1974, vol. 13 n° 3),

A. ORSZAG - Mesure par laser de la distance Terre-Lune (thèse de l'Université de Paris Sud - 1972),

E.S.O. Conferences - Large telescope design (1971 - ESO Garching b München - Germany).

SATELLITE RANGING MOUNT SYSTEM
(HALF METER APERTURE)

AUTHORS, G. ECONOMOU AND S. SNYDER

CONTRAVES COERZ CORPORATION

PITTSBURGH, PENNSYLVANIA

1.0 INTRODUCTION

The latest satellite tracker designed, fabricated, tested, and delivered by Contraves Goerz Corporation is the system being installed at the Royal Greenwich Observatory. A second system has been delivered and installed at the Technical University, Graz, Austria (Figures 1, 2, and 3).

Like most alt-azimuth or elevation over azimuth trackers, this system utilizes a laser transmit path with Coudé mirrors and a beam expander. The satellite redirected energy is collected with a receiving optic. The system provides a customer specified detector interface. (The customer is designing and fabricating their own detector assembly.)

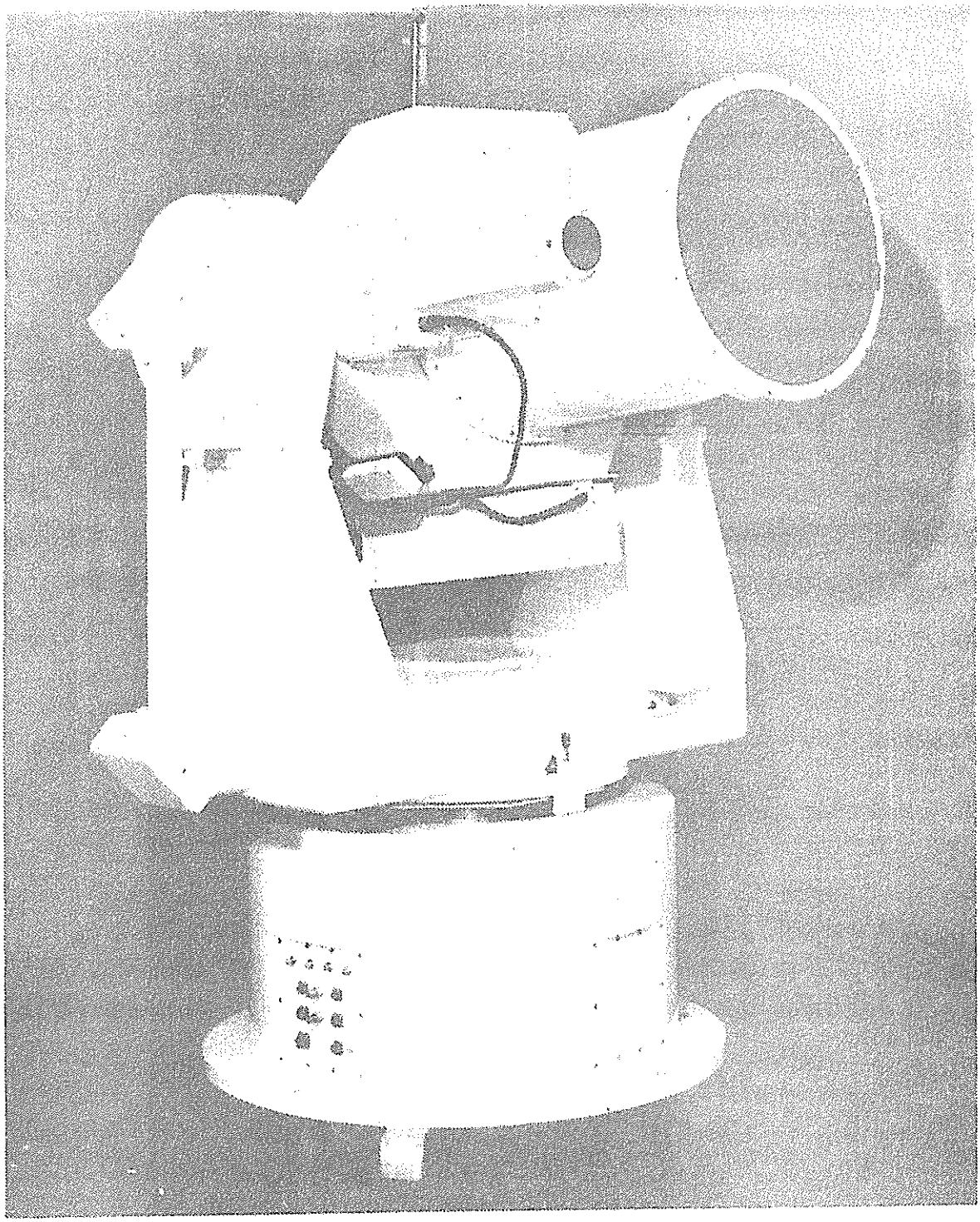

Figure 1. Graz Mount

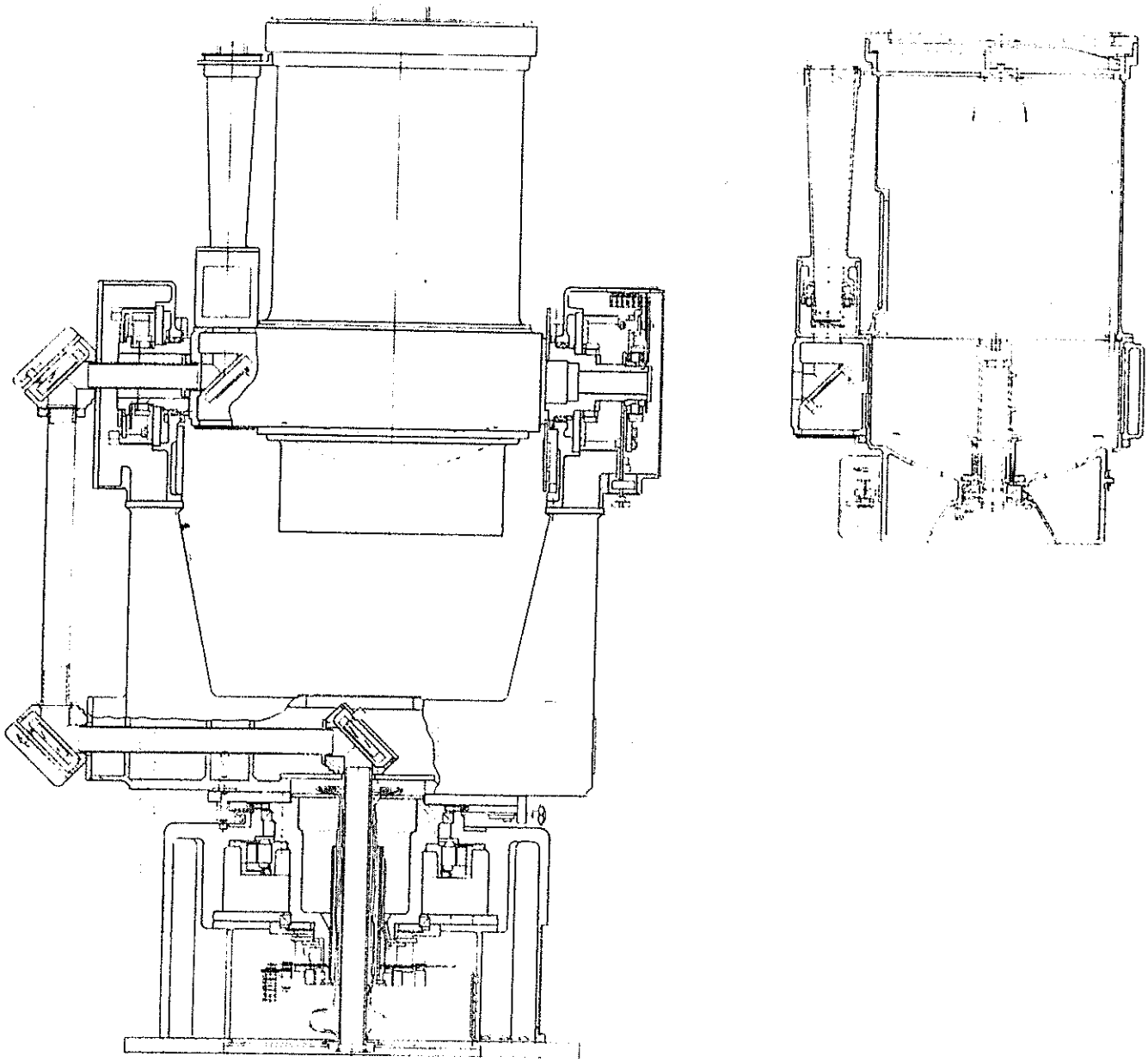

Figure 2. Gras Mount

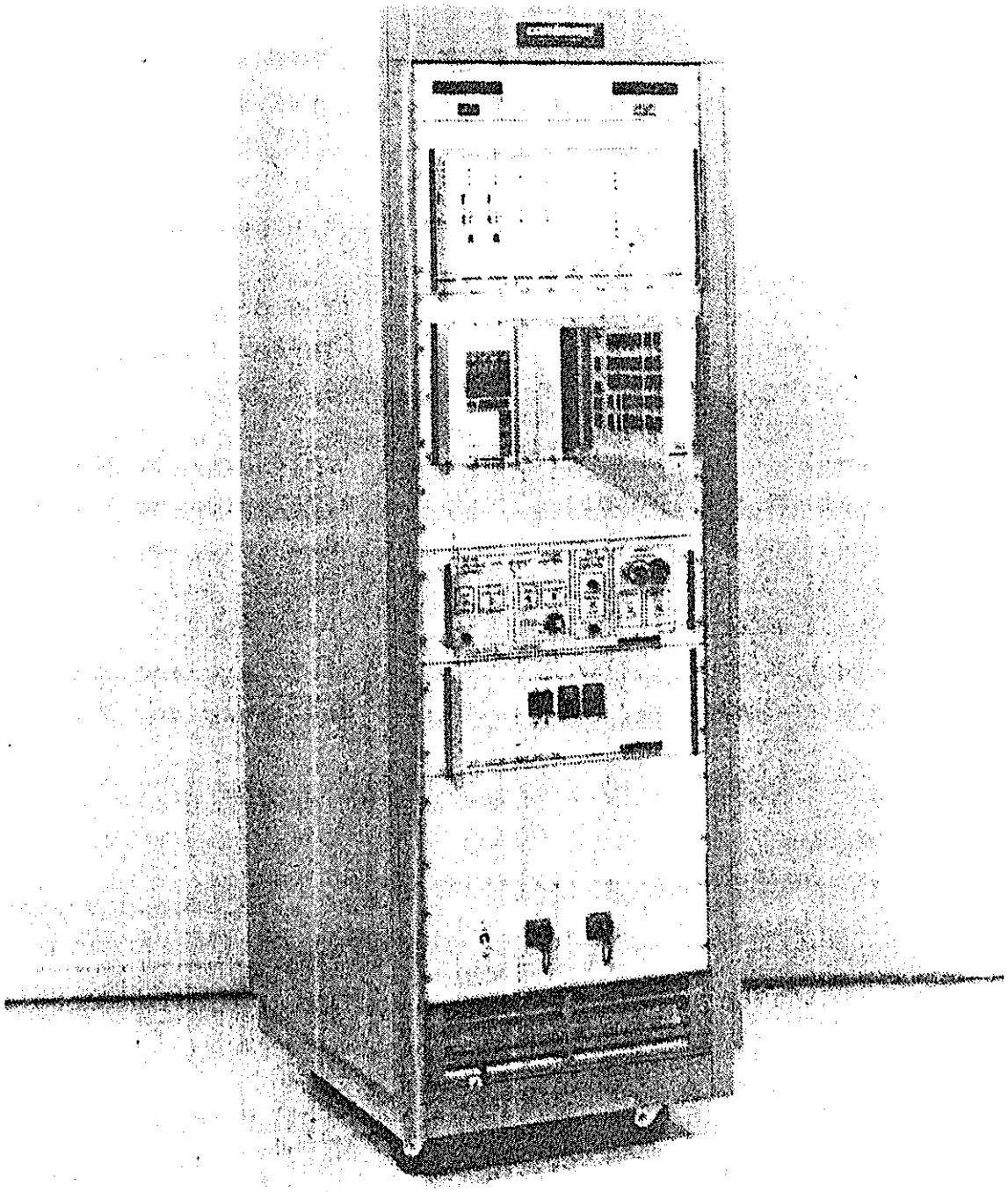

Figure 3. Mount control console

1.1 SPECIFICATIONS

1.1.1 PHYSICAL CHARACTERISTICS

Weight	2000 pounds
Height, Floor to Elevation Axis	67"
Elevation Swing Radius	36"
Azimuth Swing Radius	36"
Payload Capability	110 pounds
Rotational Freedom	
Azimuth	±350 deg
Elevation	-10 to 190 deg
Static Precision	
Azimuth Axis Wobble	0.316 arc sec RMS
Elevation Axis Wobble	0.762 arc sec RMS
Orthogonality	±0.15 arc sec
Optical Tube Sag (calculated)	0.3 arc sec
Optical Axes Parallelism	2 arc sec
Azimuth Encoder	0.533 arc sec RMS
Elevation Encoder	0.421 arc sec RMS

1.1.2 OPTICS

Receive Optics	
Clear Aperture	20 inches f/11 telescope system f/2 primary mirror
Transmission Losses (without window)	<15% (to detector)
Obscuration Losses	<7%
Mirror Materials	Fused Silica
Performance	80% energy from a point source is imaged in a 3-arc second blur circle.
Video	
Camera	RCA TC1040/H Camera ISIT Tube
Field of View	10 arc minutes
Tube Protection	Sun Shutter

Transmit Optics	Four independently adjustable Coudé mirrors allowing a 2-inch clear aperture laser beam transmission through the mount to the beam expander

Mirror Parameters

Flatness	$\lambda/10$ at 653 nm
Energy Handling Capability	10^{12} watts per square meter in a pulse of 3 ns duration at a repetition rate of 20 Hz
Reflective Coating	95% reflectivity at laser wavelength 70% at visual wavelengths
Beam Expander	2-inch clear aperture input 4-inch clear aperture output Variable beam divergence of 5 to 200 arc seconds

1.1.3 SERVO WITH PAYLOAD

Acceleration

Azimuth	47 deg/sec^2
Elevation	18 deg/sec^2

Velocity

Azimuth	0.008 to 23 deg/sec
Elevation	0.008 to 21 deg/sec

Encoding System and Control

Range	0.00 to 359.9999 deg
Velocity Error	1 arc sec/rad/sec
Acceleration Error	2 arc sec/rad/sec

Transducer	720-pole, 1 arc sec Inductosyn
Resolution	0.0001 deg, 0.36 arc sec
Accuracy	±1 arc sec
Repeatability	0.1 arc sec

Precision Range Command (Tracking Mode)

Rate Range	0.0001 to 199.9999 deg/sec
Resolution	0.0001 deg/sec
Accuracy (long term)	0.001% + 0.001% per year
Position Step Size (Rate modes of operation)	0.0001 deg

2.0 SYSTEM HARDWARE

The mount and telescope assemblies are aluminum castings and weldments, ground to a smooth exterior finish and painted for high solar reflectivity with a titanium base white point. Light paths are painted with a flat black and other elements are alodined or anodized for corrosion resistance.

The measured resonant frequency of the system is 73 Hz.

2.1 AZIMUTH AXIS

The stationary base consists of a cylindrical casting with a bolted plate flange. The angular contact bearing pair supports the azimuth shaft with the torque motor directly coupled to the shaft between the bearings. The bearing spread provides a very stable axis.

Below the lower bearings is the Inductosyn plates (encoding transducer), tachometer, and the gear driven synchros and electrical limit switches. Passing inside the azimuth shaft is the stationary laser transmist tube, with the rotary seal being at the tube-yoke mirror housing interface.

An azimuth torquer between 75 and 300 foot pounds can be accomodated without alteration of the manufacturing drawings. Further, the present design accomodates a vertical incoming laser beam, but a Coudé housing can be added inside the base allowing a horizontal beam. This is accomplished by simply adding to the cylindrical portion of the base.

Cables and wiring to the elevation axis and payload are distributed and wrap about the beam transmit base. The azimuth rotation, as stated in Section 1.1.1, is approximately ±350 degrees.

The yoke, a part of the azimuth assembly, supports the elevation pillow blocks and thus the elevation axis, telescopes, and payload. It also supports the outboard Coudé mirrors and provides a conduit for wiring. The yoke is a weldment. Wiring to the payload is via a table drape across the elevation axis, the connector panel being on the yoke tine inner wall.

2.2 ELEVATION AXIS

The pillow blocks are standard. The casting pattern was generated in 1973 and used through these instruments. We have had 1000 pounds on the gimbal ring without deteriorating the wobbles or orthogonality.

Our standard configuration is an identical torquer in each pillow block. Then, the Inductosyn plates are mounted on the one side, usually with the Coudé path interface. The opposite pillow block houses the limit switches, synchros, and tachometer.

Like the azimuth axis, there are mechanical snubbers for end stops, a stow lock pin, and manual slow motion/lock assembly.

An integral part of the elevation axis is the gimbal ring. The ring is designed to accomodate a 24-inch clear aperture receiver assembly. This mount has the previously mentioned 20-inch receiver telescope.

2.3 OPTICS

The optics are normally part of the payload. However, the payload cited in Section 1.1.1 is the detector assembly that mounts aft of the receiver telescope.

2.3.1 TRANSMIT

The terminus of the Coudé path is the 2X transmit beam expander. The remote driven beam expander consists of a fixed front lens element and rear air spaced doublet. The second element of the doublet is driven to cause the divergence to range from 5 arc seconds to 200 arc seconds, a milliradian.

This movement is also sufficient to provide collimation for laser wavelengths between 0.5 μ and 1.1 μ. The Coudé mirrors are coated for 0.532 μ wavelength energy and different coatings are necessary to optimize the other wavelengths.

Four individual Coudé mirrors, manually adjusted, direct the beam through the azimuth and elevation axes and into the beam expander. The allowable transmit beam is two inches.

2.3.2 RECEIVER

The receiver telescope is a Cassegrain with a fused silica primary and secondary. Invar spacer rods are used between the primary and secondary, with the tube structure being cast aluminum.

The receiver has a field lens and a collimating doublet that is motorized and used for focus. The outgoing beam, approximately 1.25 inches in diameter, passes through a beam splitter, the 0.532 μ wavelength passing through to the detector and all other energy reflected to the TV cameras. As stated previously, the detector responsibility was retained by the customer. However, subsequently, the customer requested an iris to be integrated with the field lens. This was accomplished using an iris that cut the field of view (FOV) in half to approximately 5 arc minutes.

2.3.3 RETROREFLECTOR

As part of the optical package, a retroreflector (simulated corner cube) was built to place the transmit beam in the receiver. The retro assembly makes the beam to the receiver parallel to the transmit output. This device allows the mount to be exercised full range across both axes and to observe beam movement with the TV.

The specification was axis parallelism of 2 arc seconds and differential fixture of 3 arc seconds. With this technique, separating the two error sources is nearly impossible and observations of movement of less than 5 arc seconds on the TV screen becomes very subjective. Nonetheless, all observers felt the movement was less than 5 arc seconds.

2.4 CONTROL SYSTEM

The control system consists of the MPACS (Modular Precision Angular Control System) control chassis, dual power amplifier, display module, and joystick box, which can be housed in a 19-inch console. The control chassis contains the controls for focus, beam diverger, reticle intensity, and mount limit functions. MPACS is the heart of the control system and contains the digital and analog servo circuitry that implements all the different modes of operation and provides position readout. The dual power amplifier drives the azimuth and elevation DC torque motors in response to outputs from MPACS. The joystick box provides MPACS with a rate command proportional to the stick deflection.

2.4.1 MPACS

The MPACS chassis is a modular precision absolute control system. It is an integrated control module, the CGC MPACS form of control system which features minimum distraction placed on the customer's control computer during operation. This is significant in two ways.

1. The position control servo loop is controlled within the MPACS system, with only the position command being generated by the customer's computer.

2. The MPACS system accepts a digital rate command input from the customer's computer which commands the system to rotate at a very precise rate, such that the predictability of position versus time velocity is better

than 1 part per million. As a result, during a normal satellite pass, the customer's computer has to output rate only when a rate change is necessary in order to keep the mount pointed on a correct line of sight to the satellite. For the extreme case of a 200 km orbit which approaches 4° from zenith, rate update of once per second will ensure that the deviation, as the mount pointing angle from the desired line of sight, will be less than 2 arc seconds.

2.4.1.1 CONTROL MODES

Keyboard Control Mode (Manual)

Control via hand-held (25-meter extender cable) or front panel mounted Keyboard Control module.

Access to all Position/Rate Readout/Self-Test modes.

Computer Control (Remote)

Multiplexed, bidirectional, general purpose computer interface (16-bit parallel or GPIB module) providing Position, Rate, Readout, and Self-Test mode control from remote computer.

Manual Rate Mode

The servo system provides closed-loop rate control. The loop is closed via the Servo module using the tachometer input provided from the joystick in the remote pendant control box. This provides the operator with the option of moving the azimuth or elevation axis while in Computer mode.

2.4.2 CONTROL CHASSIS

The control chassis contains the control circuitry for the FOCUS, BEAM DIVERGER, SHELTER PROTECT, and MOUNT STATUS indicators. The beam expander control consists of two switches. The SPEED switch allows the selection of either HIGH or LOW speed when the DIAMETER switch is activated. The DIAMETER switch increases or decreases the size of the beam that exits the beam diverger.

The focus is controlled by the SPEED and DIRECTION switches. The above switches are active when the LOCAL/REMOTE switch is in the LOCAL position. The REMOTE switch position allows the above functions to be controlled by the customer.

A SUN SHUTTER control switch allows the selection of AUTOMATIC operation or REMOTE operation of the sun shutter. An indicator lamp tells when the shutter is closed.

A SHELTER PROTECT switch is provided which will indicate, via a closure, if the elevation axis has reached 20 degrees above horizontal.

The MOUNT DUMP switch, when on, allows the elevation axis to travel through its normal 95-degree limit until it reaches 180 degrees. If at any time a limit condition occurs, an alarm will sound until that condition is clear. The alarm can be disabled.

EXPANDER LENS COVER and MAIN LENS COVER indicators tell when the covers are in place.

2.4.3 DUAL POWER AMPLIFIER

The dual power amplifier contains two 60-CG-500 linear amplifiers. The chassis also contains the 60 VDC power supply for the power amplifier as well as the on/off control logic for the output contactor.

MOUNT AND TELESCOPE FOR THE GERMAN/DUTCH MOBILE SYSTEM

H. Visser
Institute of Applied Physics TNO-TH, Delft, The Netherlands

F.W. Zeeman
Delft University of Technology, Delft, The Netherlands

1. Introduction

In close co-operation with the Working Group for Satellite Geodesy in Kootwijk (a part of the Delft University of Technology) the Institute of Applied Physics is manufacturing two mobile laser ranging stations. One system will be delivered to the "Institut für Angewandte Geodäsie" (IFAG) in Frankfurt, Germany and the other system will be used by the group in Kootwijk.
The co-operation can roughly be characterized by stating that the mechanical and optical aspects of the system are handled at the Institute of Applied Physics while the electronical hardware and software is developed by the Working Group in Kootwijk.

2. Station configuration

In figure 1a the mobile ranging station is shown in its road transportable configuration. The telescope mount, detection package and pulse laser are built into a small cart of about 2,1 x 1,8 x 1,9 m^3 (l x d x h) inside the off-loadable truck cabin. In the operational configuration (figure 1b) the cart is rolled out of the truck cabin over rails of more than 10 m length to the selected location of the telescope mount. When the cart is positioned at its location the wheels of the cart are lifted and the cart will stand with four feet on the ground. The mount itself is supported independently of the cart with three feet directly on the ground.

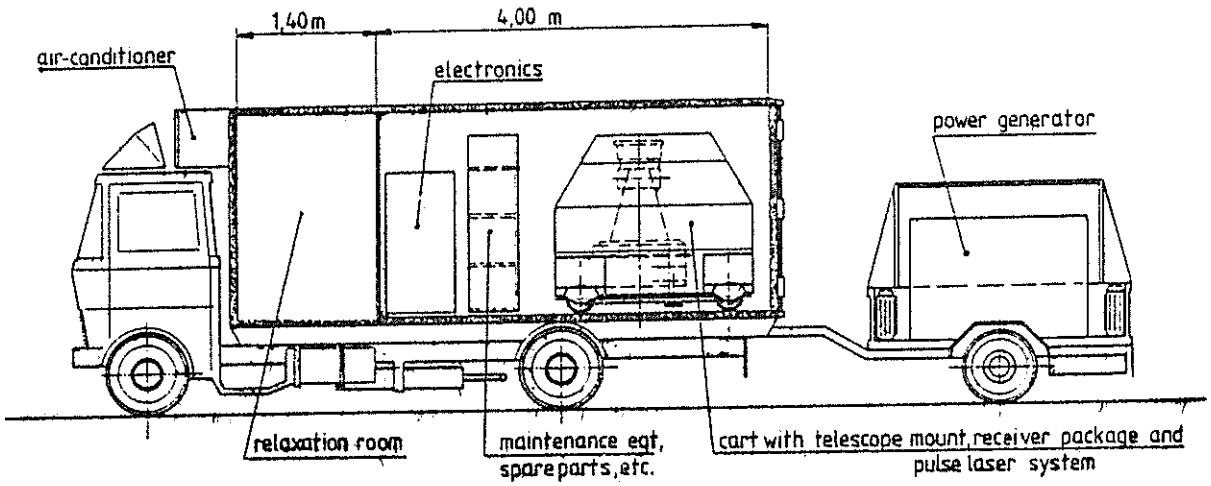

Figure 1a Road transportable configuration

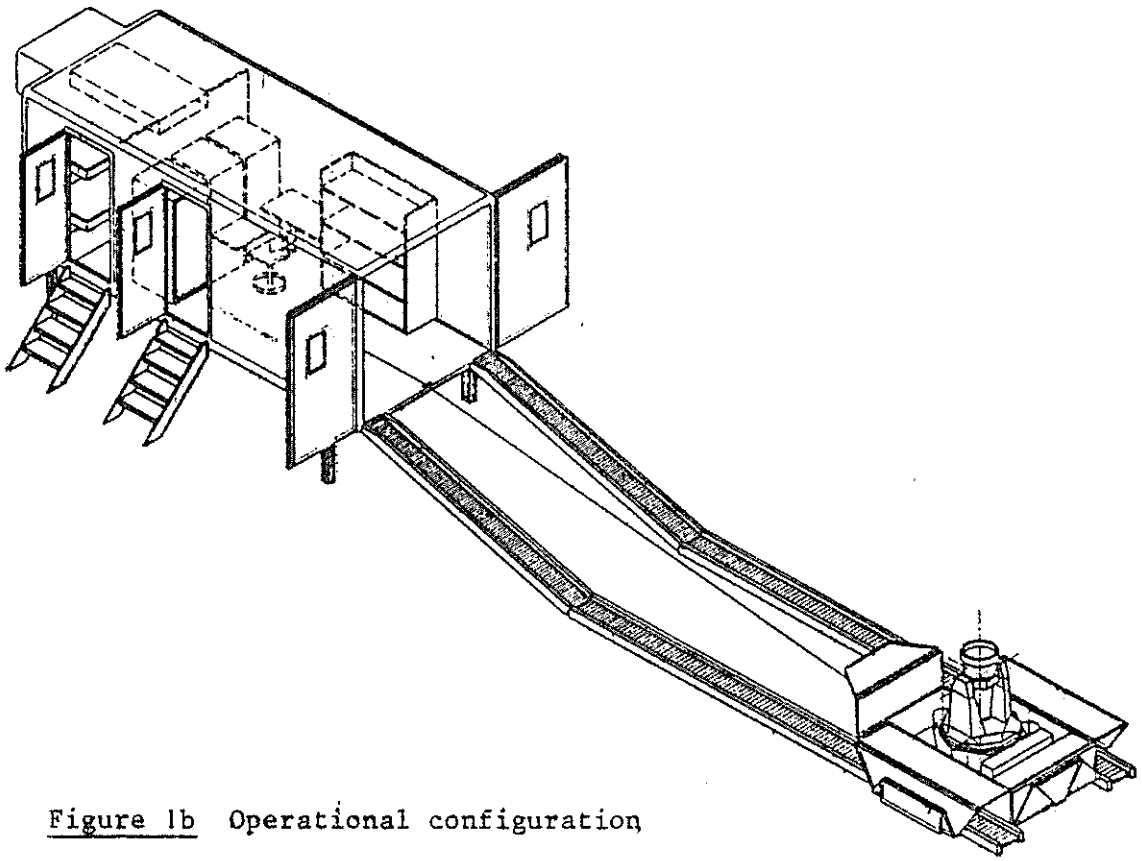

Figure 1b Operational configuration

The truck can be driven from underneath its ground supported cabin to maintain the contact between the ranging station and the outside world.
The thermally insulated, air-conditioned cabin has a relatively large observation room of about 4,0 x 2,1 x 2,1 m^3 interior and a small relaxation room.

Transformation from the road transportable configuration to a fully operational status inclusive precise orientation and a functional calibration can be achieved within a single 24 hours time period, given good weather conditions.

The actual ranging system can also be transported by regular air transportation. The cart with the telescope mount, pulse laser and detection package, together with the entire electronics-racks, can just be stowed on one standard air freight pallet of 3,1 x 2,1 m^2 maximum loading area.

3. Telescope mount

3.1 Mechanical aspects

In figure 2 a schematic outline of the altazimuth telescope mount is presented. Except for the aluminum telescope tube all the major mount structures will be made of welded steel. The total weight of the telescope mount will be no more than about 500 kg.
The axial and radial bearing of the azimuth axis are separated. Three conical wheels carry the weight of the rotating part of the mount and provide for the axial bearing of the azimuth axis.
A preloaded set of ball bearings near the main gear-wheel defines the position of this gear-wheel with the respect to the rest of the drive system. D.C. servo motors drive both axes through a combination of high grade spur and spiroïd gears. All backlash in the gearboxes will be removed.
Angular read-out is by incremental encoders coupled to axes in the gearing system that are 36 times faster than azimuth and elevation axis. The incremental encoders give 50.000 pulses per revolution of the encoder axis which corresponds to 0,0002 degree (0,72 arcsec) of the azimuth or elevation axis.
The encoders are provided with zero indexers that give one pulse per revolution of the encoder axis (10,000 degrees of the azimuth or elevation axis). The zero pulses reset the counters that give the angular position of the telescope to the nearest exact tens of degrees. In this way lost or incorrectly added counts are corrected every ten degrees of rotation of the azimuth or elevation axis.
In table I the most important design specifications of the mount are presented.

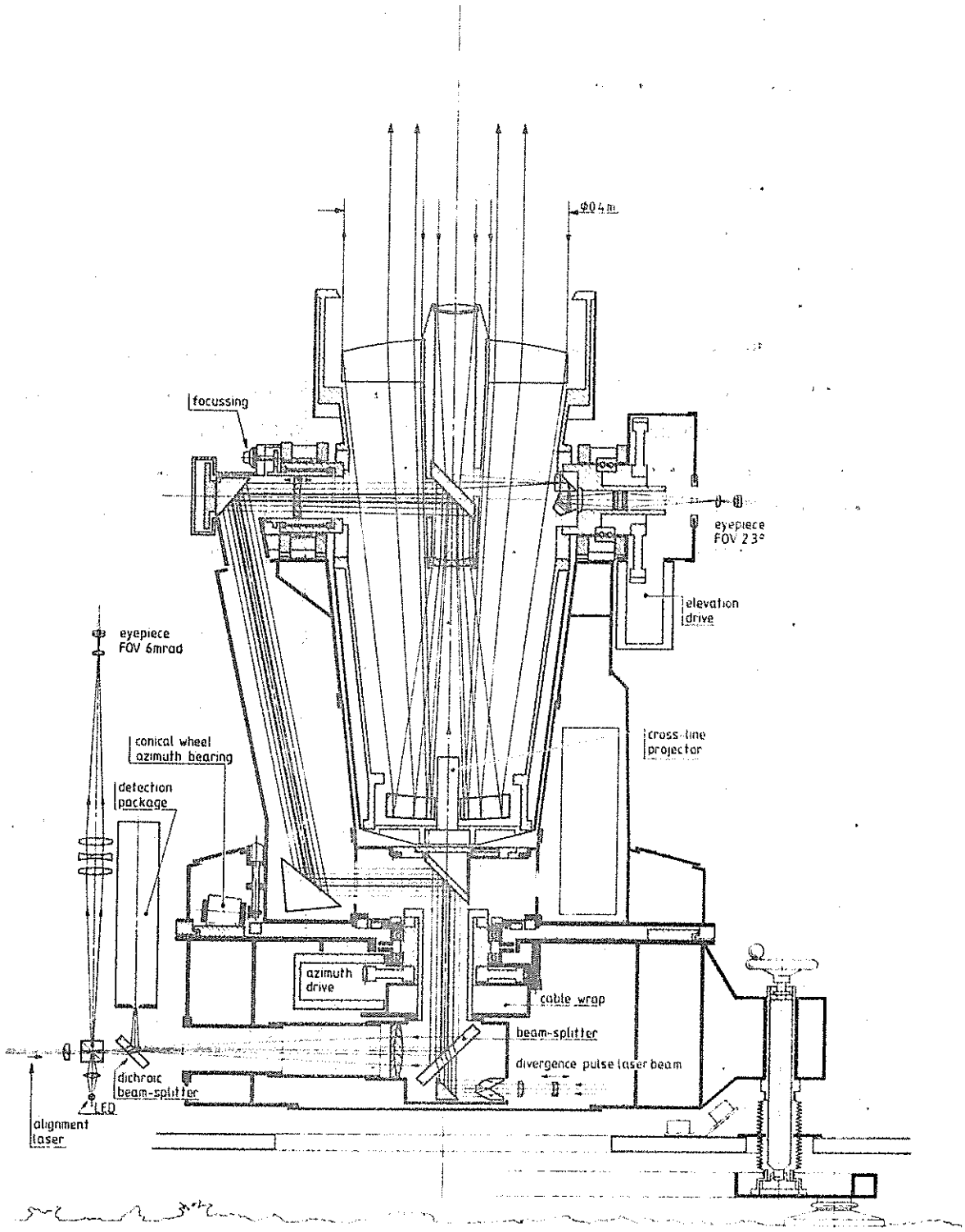

Figure 2 Schematic outline of the telescope mount

Table I Design specifications of the mount.

- max. angular velocity: in azimuth > 10 ^{o}/sec
  in elevation > 4 ^{o}/sec
- max. angular acceleration: in azimuth > 5 ^{o}/sec^{2}
  in elevation > 2 ^{o}/sec^{2}
- total angular travel: in azimuth 720^{o}
  in elevation 200^{o}
- tracking of all present co-operative satellites
- static pointing possibility
- maximum pointing error due to flexure, wobble, non-orthogonality of the axes, gear and encoder errors: less than 10 arcsec without computer correction
- maximum angular jitter: less than 2 arcsec r.m.s.
- operational environment: temperature -20 ^{o}C to +50 ^{o}C
  humidity 0 % to 95 %
  altitude 0 km to 4 km.

3.2 Mount guidance

A hard wired digital servo system will handle the signals from the optical encoders and will supply a control voltage to the (speed-) servo amplifiers.

The digital servo unit will display:

- the actual position of both axes;
- the difference between desired and actual position of both axes;
- the speed of both axes during tracking.

The digital servo unit accepts desired positions and/or rate commands from a micro-processor based fixed program controller (Motorola 6809). This controller translates the desired positions at given times (with e.g. 1 second intervals) into commands for the digital servo unit, using adequate interpolation techniques.

3.3 Optical aspects

As shown in figure 2 there is one common catadioptric coudé telescope system with an aperture of 0,4 m diameter for both transmitting and receiving.
The freqüency doubled Neodymium pulse laser system is not shown in figure 2 but this laser is mechanically connected to the base of the telescope mount in such a way that the direction of the pulse laser beam is defined by the telescope mount without loading the mount with the full weight of the laser system.
The laser beam is directed into the base of the telescope mount where first the divergence of the beam is adjusted to the desired value. By the indicated movement of the negative lens the divergence of the beam that leaves the telescope mount can continuously be adjusted from less than 0,05 mrad (10 arcsec) to over 1,0 mrad (200 arcsec).
After the divergence adjustment lens system the laser beam is split into two halves by two plane plates of glass at the brewster angle so that the central obscuration of the main telescope will not introduce a "hole" in the beam in the "far field".
The pulse laser beam is coupled into the coudé optical train by means of a beamsplitter. This beamsplitter is used as a mirror for the received beam while two semi-circular holes in the mirror coating transmit the laser beam. The reduction of the effective receiver aperture that is introduced by the two holes in the mirror coating will be less than 20%. The rest of the transmitting optics consists of the coudé mirrors and the main telescope.
The overall optical efficiency of the entire transmit optical train of figure 2 will be over 80%.

The received light is collected by the common main telescope and is also directed through the coudé optical train. At the beamsplitter most of the received light is reflected and is then focussed by an achromatic doublet.

The unvignetted field of view of the telescope system as receiver is limited by the aperture of the coudé optical train to about 2,0 mrad.
At the dichroic beamsplitter a wavelength band around the laser wavelength (green) is reflected into the entrance diaphragm of the detection package. This detection package will be described in another paper to be presented during the Workshop. The rest of the visual spectrum is transmitted through the dichroic beamsplitter. This light is focussed on a beamsplitter cube that reflects the entire useful field of view of the telescope system (about 6 mrad diameter) to an eyepiece, except for a small pinhole in the reflective coating of the cube.
The position of this pinhole corresponds to the middle of the entrance aperture of the detection package. Through the pinhole a He-Ne alignment laser beam can be transmitted into the coudé optical train. A LED indicates the middle of the entrance aperture of the detection package in the eyepiece.
Visual viewing through the telescope system will be possible and eye-safe also when the pulse laser is firing. The eyepiece has a fixed and convenient position for an observer. With an eyepiece magnification of 8 times the magnification of the entire telescope system as seen through the eyepiece will be about 120 times.

In the central hole in the main telescope mirror a cross-line reticle projecting system is indicated in figure 2.
This cross-line can be seen in the eyepiece and is used as an alignment aid and for the determination of the station position from a geodetic star program.

In the central hole of the 0,4 m diameter front lens of the main telescope the objective of an auxiliary sighting telescope with a 78 mm clear aperture is located. The light of this small telescope is directed through the motor side of the elevation axis to an eyepiece.

With an eyepiece magnification of 8 times the auxiliary sighting telescope has a magnification of about 20 times and a field of view of over 2 degrees.

4. Brief description of the rest of the ranging system

The third generation ranging system will be capable of day and night time ranging to all present co-operative satellites (Lageos, Starlette, etc.).

The pulse laser will be an actively mode-locked, frequency doubled Nd-YAP or Nd-YAG system (539 nm or 532 nm respectively), that has been ordered at Kristalloptik in Germany (near Munich). Besides the oscillator the laser will have one double pass amplifier. The laser system has the following general specifications:

- pulse width: 0,2 ns
- pulse energy: 10 mJ of green light
- repetition rate: 10 pps
- operational environment: as for the telescope mount.

The detection system will be described in another paper to be presented during the Workshop.

The ranging station will be equipped with several micro-computers. A large micro-computer system (HP 1000 Model 5) will perform all activities that are not directly related to hardware. This "central computer" is, for instance, used for predictions, data recording, data screening, diagnostics, etc. A smaller micro-processor (Motorola 6809) with a fixed program will take care of detector control, laser firing control and data formatting. Another small micro-processor (Motorola 6809) with a fixed program controls the mount servo system and the range gate generator. Operation of the ranging system during a satellite pass will be through an "operator control panel" with switches and displays. This control panel is connected to the central computer. The central computer controls the two micro-processors.

SESSION 4 : LASERS

Chairmen: K. Hamal, Czech Technical University, Prague, Czechoslovakia
D.R. Hall, Applied Physics Dept., Hull University, Hull, England

INTRODUCTION

While it is clearly self evident that high precision long range optical distance measurements are only made possible with the aid of wide bandwidth laser transmitters, it is also apparently true that lasers, at the heart of satellite and lunar ranging systems have been, historically, a likely source of ulcers and high blood pressure for those charged with the responsibility for producing high quality ranging data on a regular basis from operational stations. Over the years there have been problems, not only with laser reliability, resulting in station 'down' time but also with data interpretation because of range uncertainties due to temporal fluctuations in the laser output pulse as well as variations in the spatial distribution of transmitted energy.

Following this Session of the Workshop there was a distinctly more optimistic air both from the standpoint of the understanding and control of fluctuations in laser output and also in view of improvements in demonstrated performance reliability.

The Session was organised in two parts, the first - a collection of five papers from the U.S., England, Czechoslovakia and Germany, followed, after a short break, by a panel discussion addressing the topic of "Lasers for Ranging - Present Problems and Future Prospects".

In the first paper in the Session, John Degnan described some important work in which a range of laser types, Q-switched, cavity dumped, passively mode-locked and actively mode-locked were assessed in a ranging system operating over a fixed terrestrial range for the contribution to rang uncertainty due specifically to laser fluctuations. The results clearly indicate that mode-locked lasers offer superior performance not only because they offer shorter pulses, but also because of the absence of spatial effects due to variation in the transverse mode structure of the laser output.

S.R. Bowman presented the next paper on the design and early development stages of a laser intended for lunar ranging. It is designed to produce an output of 1 Joule in 100 psec pulses at up to 10 Hz in the green, and utilise a face-pumped slab of YAG as the final amplifier. D.R. Hall described the design and performance characteristics of a passively mode-locked, oscillator-amplifier, doubled YAG system developed for use in the U.K. SLR system to be sited at

Herstmonceux. This was followed by a presentation from the Czech Technical University on Laser Activity in the Interkosmos Network. In particular, Helena Jelinkova discussed the technique of constant gain Q-switching and presented results on its application in both Nd:YAG and ruby lasers. Finally, H. Puell described the outline design of the planned actively mode-locked laser for use in the German/Dutch Mobile SLR systems (described elsewhere).

After a short break at the end of the formal presentations, the Session recommenced with a Panel Discussion. A somewhat hastily assembled Panel of J. Degnan, T. Johnson (NASA), D. Burns (Sylvania) J. Wohn (Smithsonian), H. Puell (Kristalloptik) chaired by D. Hall (Hull University) discussed a number of issues relating to lasers in and for ranging systems, with considerable "audience" participation. Topics discussed included difference in laser requirements for satellite and lunar ranging systems, laser reliability, servicing frequency, ultra-small lasers for mobile systems and the commercial realities relating to the small size of the extra terrestrial ranging systems market and the impact this has on the developments in which companies are prepared to invest resources to produce well-engineered lasers for field us. Finally, some time was spent airing the inevitable dichotomy between system/laser users who want regular data now and hardware specialists who are inclined towards continual hardware improvement and refinement.

Fourth International Workshop
on Laser Ranging Instrumentation
Austin, Texas October, 1981

THE NEW UNIVERSITY OF MARYLAND RANGING LASER †

S. R. Bowman, W. L. Cao, J. J. Degnan*,
C. O. Alley, M. Z. Zhang, C. Steggerda

University of Maryland
College Park, Maryland

* Now at Goddard Space Flight Center

ABSTRACT

For the last year and a half, a new laser for laser ranging and time transfer has been taking shape at the University of Maryland. This paper describes our objectives and design considerations, as well as the progress made on the construction of the laser.

† Work supported by U.S. Naval Observatory and Office of Naval Research.

OBJECTIVES

The new ranging laser is being built in two stages. When completed near the end of this year, the major portion of the new laser will replace the existing laser in the University of Maryland ranging station at the Optical Site of the Goddard Space Flight Center[1]. The resulting system will be used as a ground-based relay station in the LASSO (Laser Synchronization from Stationary Orbit) experiment[2]. This experiment is designed to demonstrate the feasibility of achieving time synchronization between remote atomic clocks with an accuracy of one nanosecond or better. The Maryland station will serve as the connection between the atomic clocks at the Naval Observatory in Washington, D.C. and the clock on a SIRIO-2 geostationary satellite. Similar laser ground-based stations in Europe will complete the link.

To complete the round-trip link with the SIRIO-2 satellite, the new laser must provide at least 200 millijoules at 530 nanometers. This must be delivered in a single pulse with a duration of less than a nanosecond. The designed performance is several times these minimum requirements.

The second stage in the construction of the new laser is the addition of a final amplifier. This will allow the Maryland ranging system to do lunar ranging. Our objective is to prove the feasibility of high accuracy lunar ranging using modest size telescopes. To accomplish this, we need a sub-nanosecond, high average power laser with good beam quality. Our goal is to obtain one joule of green light in a 100 picosecond pulse at ten shots per second while maintaining less than ten times the diffraction limit at the laser.

LASSO LASER DESIGN

Meeting the above requirements for laser energy, pulse duration, and beam quality do not present a serious technological problem. The problem lies with the requirement on the repetition rate. To avoid damage from high power densities, the laser rod cross-section must be large. This, in turn, increases the thermal decay time. Thermally induced lensing and birefringence then limit the repetition rate, if the beam quality is to be preserved.

In order to minimize thermal problems, the laser rod diameters are kept as small as possible. Damage from high peak power densities is avoided by keeping the laser environment clean, the spatial profile of the beam smooth, and minimizing the number of optical components exposed to high intensities.

Three different laser materials were seriously considered for use in the new laser. Their most important characteristics are compared in Table 1. Athermal Neodymium doped glasses are available with the required physical dimensions and have relatively low nonlinear indices. However, their combination of low absorbtion cross-section and low thermal conductivity make high repetition rates difficult.

Neodymium doped yttrium aluminum garnet (Nd:YAG) has been a standard laser material for many years. It has a higher thermal conductivity and absorption cross-section than glass, but limited crystal diameters have excluded YAG as a candidate for high energy, short pulsed systems until very recently[3].

Neodymium doped yttrium lithium fluoride (Nd:YLF_4) is a very promising laser material which has recently become commercially available. It is similar to YAG but with the advantage of low nonlinear index and large diameter crystals. Also, YLF_4 is naturally birefringent, so beam depolarization from thermal birefringence should not be a problem.

The initial stage of the laser is being built with YAG rods. Replacement YLF_4 rods have been obtained for research purposes. Present plans are to build the final amplifier out of YAG because of the delay and expense of obtaining larger YLF_4 rods.

To operate an amplifier chain efficiently without damage, a stable input pulse is needed. This is achieved by using both an acousto-optic modulator and a saturable dye to modelock the oscillator (Figure 1.). Proper adjustment of the dye concentration and cavity length have produced 30 picosecond, TEMoo mode pulse-trains with less than ten percent fluctuations in the shot-to-shot energy. Improved stability is expected after current modifications to the dye circulation system. Pulse durations can be lengthened using intracavity etalons.

The growth of the laser pulse in the oscillator is monitored by a bulk semiconductor detector with a risetime of 30 picoseconds[4]. (Figure 2). This detector triggers a voltage level discriminator whose output in synchronized with the 50 MHz signal from the acousto-optic modulator. A single three volts pulse with one nanosecond rise is produced. This signal triggers a planar-triode amplifier to launch a travelling, high voltage pulse to the Pockels cells. Risetime of the high voltage is 1.8 nanosecond and the internal jitter of the amplifier is only 30 picoseconds. (In addition, the amplifier's lifetime is effectively not a function of the repetition rate.) When the half-wave voltage reaches the Pockels cell in the oscillator, the laser energy is reflected out by a thin-film polarizer. Single pulse energies of 1.5 millijoules have been obtained.

After the oscillator lies a double-pass, 1/4-inch diameter amplifier. This is followed by a single-pass, 3/8-inch amplifier. Two Pockels cells and several thin-film polarizers isolate the amplifiers and oscillator until the cavity dump occurs. This reduces amplified spontaneous emission and amplified leakage from the oscillator.

Each amplifier is followed by a vacuum spatial filter. Spatial filters serve several functions:

1.) Reduce optical damage by smoothing out the spatial profile of the beam.

2.) Restrict the growth of nonfocusable energy.

3.) Correct for thermal lensing and diffraction ripples by imaging amplifier output to amplifier input.

4.) Expand beam to fill amplifier.

Following the second spatial filter is a KD*P, type II, doubling crystal. Conversion efficiencies of 60 to 70 percent are expected. Table 2 summarizes the expected output parameters of the LASSO laser.

FINAL AMPLIFIER

To accomplish our lunar ranging objectives, more energy per shot must be obtained than the above laser can deliver. Unfortunately, adding a larger laser rod amplifier would reduce the repetition rate below an acceptable level. For this reason, we intend to build the final amplifier in a face-pumped. slab geometry (Figure 3). In this geometry, the thermal gradients are linear so thermal birefringence problems are avoided. The slab will consist of a rectangular YAG crystal with dimensions of 1.0 x 5.0 x 9.0 centimeters and will be mounted similar to the glass slabs developed by Professor R. Byers and his group at Stanford. Unlike the glass slabs, it will not use multiple internal reflections. When finished, it will replace the second amplifier in the LASSO laser (Figure 4). A cylindrical optics beam expander will fill most of the slab's end face with an eliptical beam. The same optics will then convert the beam back to a circular cross-section after a double-pass through the slab. The expected output parameters of the modified laser are listed in Table 3.

CONCLUSION

The initial stage of the new laser should be ready for interfacing to the telescope by the first of 1982. Construction of the final amplifier will probably take six months longer. When completed, we hope this laser will be successful enough to serve as a prototype for future systems.

Table 1: LASER MATERIALS PROPERTIES

PROPERTY		Nd:YAG	Nd:YLF_4	Q-98
Index of Refraction	η_0	1.82	$(1.45)_o(1.47)_e$	1.55
Laser Wavelength	λ	1.064μ	$(1.047\mu)_\pi(1.053\mu)_\sigma$	1.053
Emission Cross Section	σ	$4.6 \times 10^{-19}cm^2$	$(6.2 \times 10^{-19}cm^2)_\pi(1.8 \times 10^{-19}cm^2)_\sigma$	$4.5 \times 10^{-20}cm$
Density	ρ	$4.55\ gr/cm^3$	$3.99\ gr/cm^3$	$2.5\ gr/cm^3$
Thermal Conductivity	K	$0.13\ ^{W}/cm\text{-}°K$	$0.06\ ^{W}/cm\text{-}°K$	$0.01\ ^{W}/cm\text{-}°K$
Specific Heat	c	$0.59\ ^{J}/gr\text{-}°K$	$0.79\ ^{J}/gr\text{-}°K$	$1.2\ ^{J}/gr\text{-}°K$
Diffusity	k	$0.048\ ^{cm^2}/s$	$0.019\ ^{cm^2}/s$	$0.003\ ^{cm^2}/s$
Thermal Expansion	α	$6.9 \times 10^{-6}°K^{-1}$	$(13 \times 10^{-6}°K^{-1})_A(8 \times 10^{-6}°K^{-1})_c$	$8.2 \times 10^{-6}°K^{-1}$
$\frac{dn}{dT}$ (1.06μ)	$\frac{dn}{dT}$	$7.3 \times 10^{-6}°K^{-1}$	$(-2.0 \times 10^{-6}°K^{-1})_A(-4.3 \times 10^{-6}°K^{-1})_c$	
Nonlinear Index	η_2	$4.09 \times 10^{-13}esu$	$0.59 \times 10^{-13}esu$	$1.2 \times 10^{-13}esu$
Fluorescence Lifetime	τ	(1%) $2 \times 10^{-4}s$	(1.5%) $4.8 \times 10^{-4}s$	(6%) $2.7 \times 10^{-4}s$
Fluorescence Linewidth	$\Delta\nu$	$6\ cm^{-1}$	$12.5cm^{-1}$	$216cm^{-1}$
Damage Theshold	D	$10.1\ ^{GW}/cm^2$	$18.9\ ^{GW}/cm^2$	$8\ ^{GW}/cm^2$
Livermore Figure of Merit ($\frac{\sigma\eta_0}{\eta_2}$)	F	2.05×10^{-6}	15.2×10^{-6}	0.58×10^{-6}

Table 2: EXPECTED OUTPUT PARAMETERS OF MARYLAND LASER STAGE ONE

Pulse Duration (picoseconds)	Energy @ 530nm (millijoules)
100	180
250	285
500	400
1000	570

Repetition Rate	3 - 6 Hz
Beam Divergence	$\leq$ 0.5 milliradians
Doubling Efficiency	60%

Table 3: EXPECTED OUPUT PARAMETERS OF MARYLAND LASER STAGE TWO

Pulse Duration (picoseconds)	Energy @ 530nm (millijoules)
100	760
250	1200
400	1520

Repetition Rate	3 - 6 Hz
Beam Divergence	$\leq$ 0.5 milliradians
Doubling Efficiency	60%

FIGURE 1 : Optical Layout for New Nd:YLF Ranging Laser

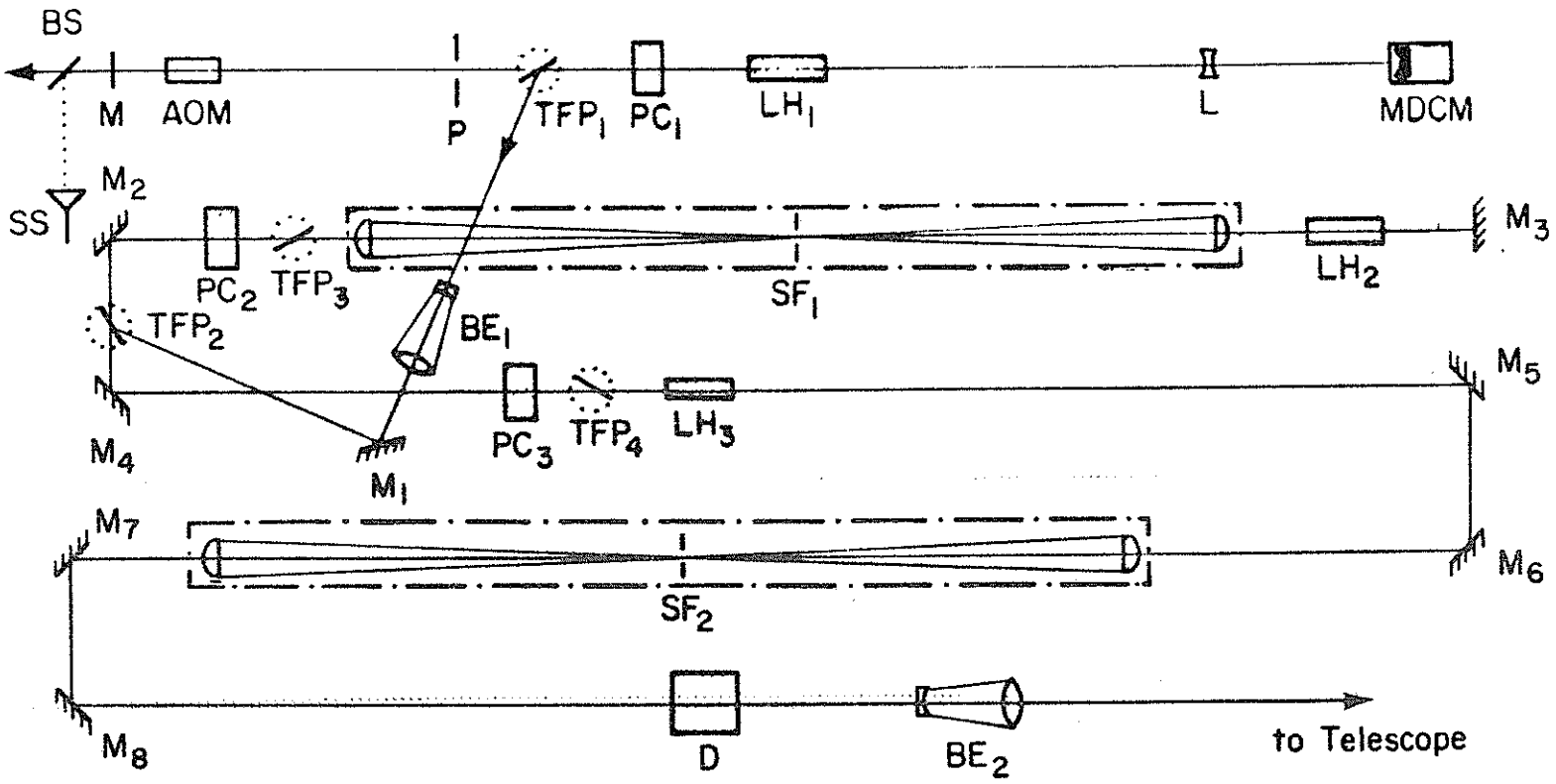

MDCM — Modelocking Dye Cell and Mirror (r=3/4 m, R=100 %)
L — Lens (f=-33 cm)
LH_1 — Laser $Head_1$ (3.0 x 65 mm)
LH_2 — Laser $Head_2$ (7.0 x 100 mm)
LH_3 — Laser $Head_3$ (9.5 x 100 mm)
PC — λ/2 Pockel Cell (KD^*P)
TFP — Thin Film Polarizer
SF — Spatial Filter
BE — Beam Expander

P — Pinhole (φ = 2 mm)
AOM — Acousto-Optic Modulator
M — Flat Mirror (R=65 %)
BS — Beam Splitter (R=8 %)
SS — Semiconductor Switch (GaAs)
M_i — Mirror (R=100 %)
D — Doubling Crystal (KD^*P)

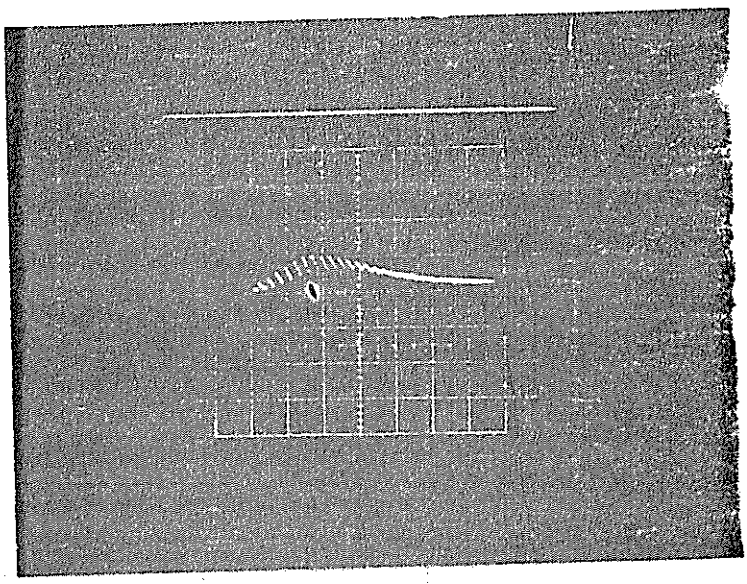

Fig. 2a. Bulk Semiconductor Detection Output
(100 ns/cm, 1 volt/cm)

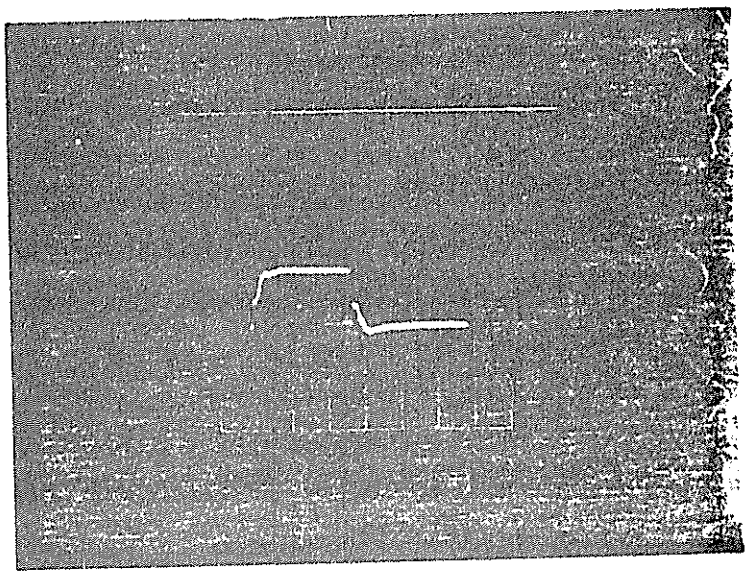

Fig. 2b. Voltage Level Discriminator Output
(100 ns/cm, 1 volt/cm)

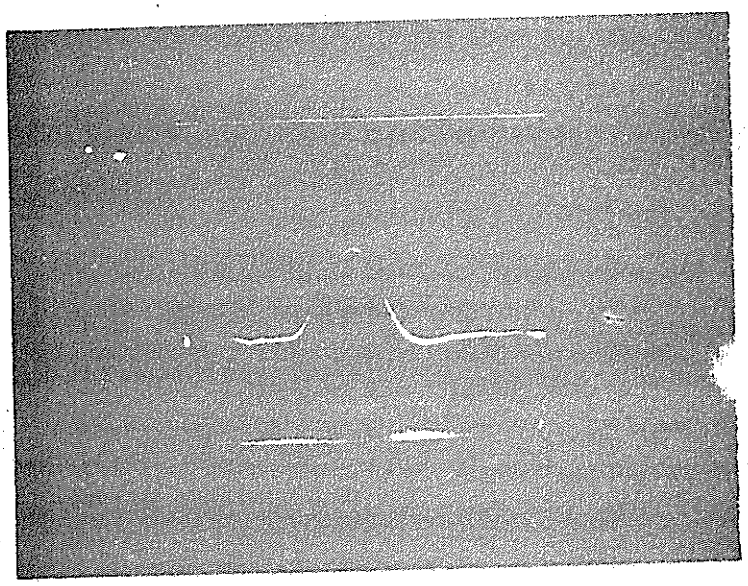

Fig. 2c Planar-Triode Amplifier Output
(0.4 volts/cm, 50 db, 2 ns/cm)

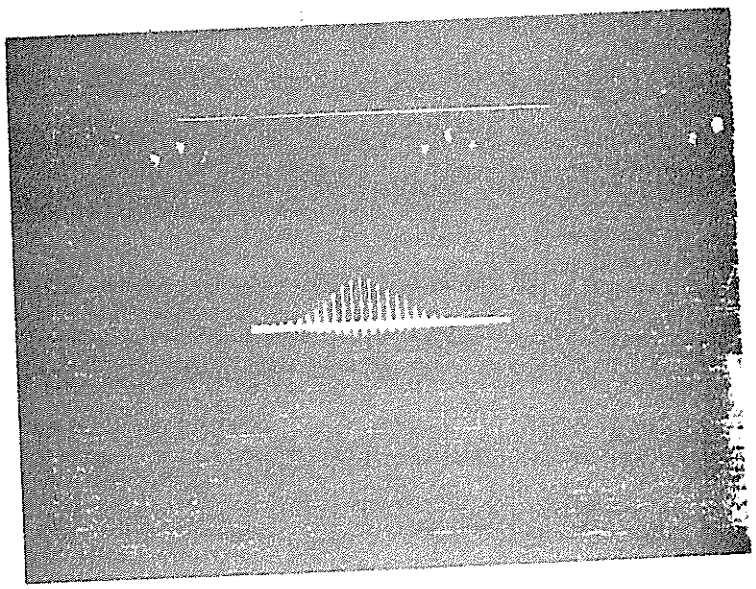

Fig. 2d Laser Pulse Train, No Cavity Dump
(40 ns/cm)

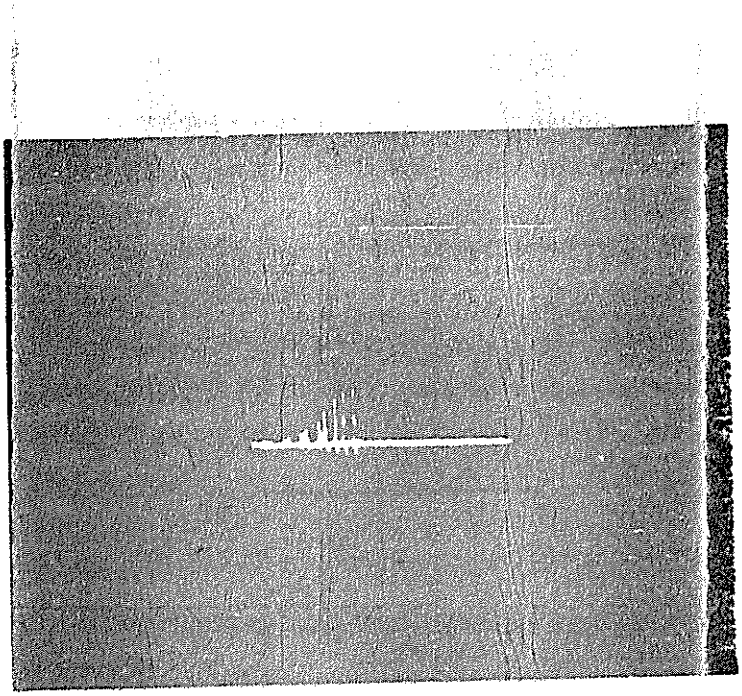

Fig. 2e. Laser Pulse Train with Cavity Dump (40 ns/cm)

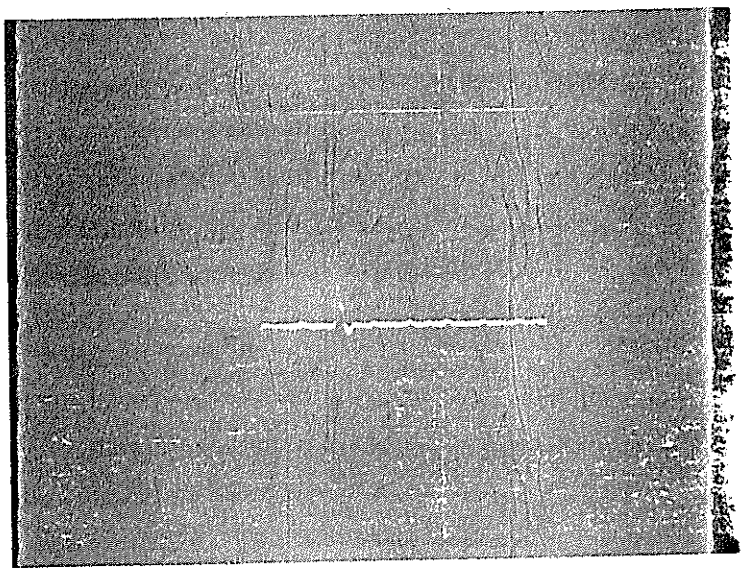

Fig. 2f. Single Laser Pulse from Cavity Dump

YAG SLAB CONCEPT

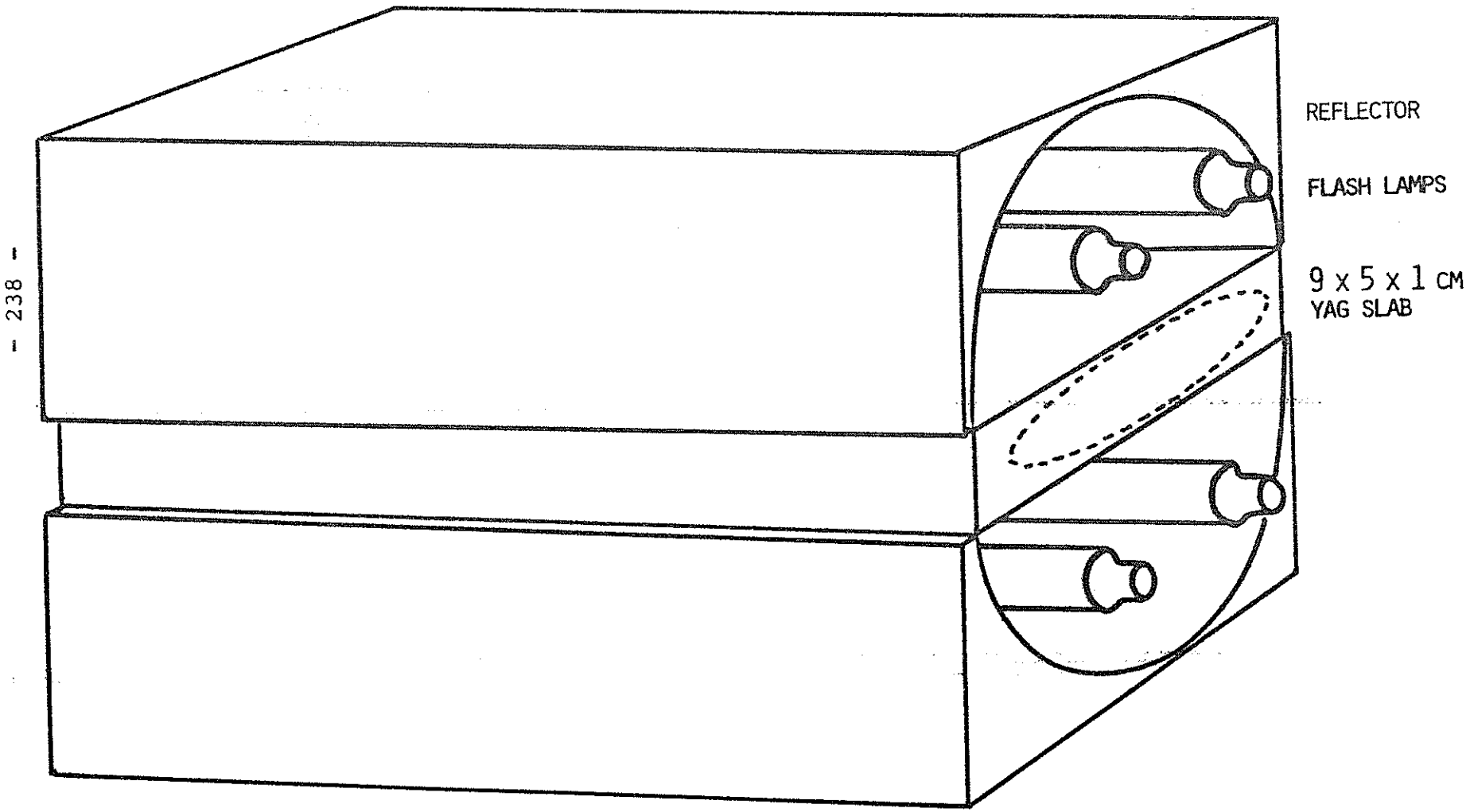

FIGURE 3

FIGURE 4 : Optical Layout for New Nd:YAG Ranging Laser

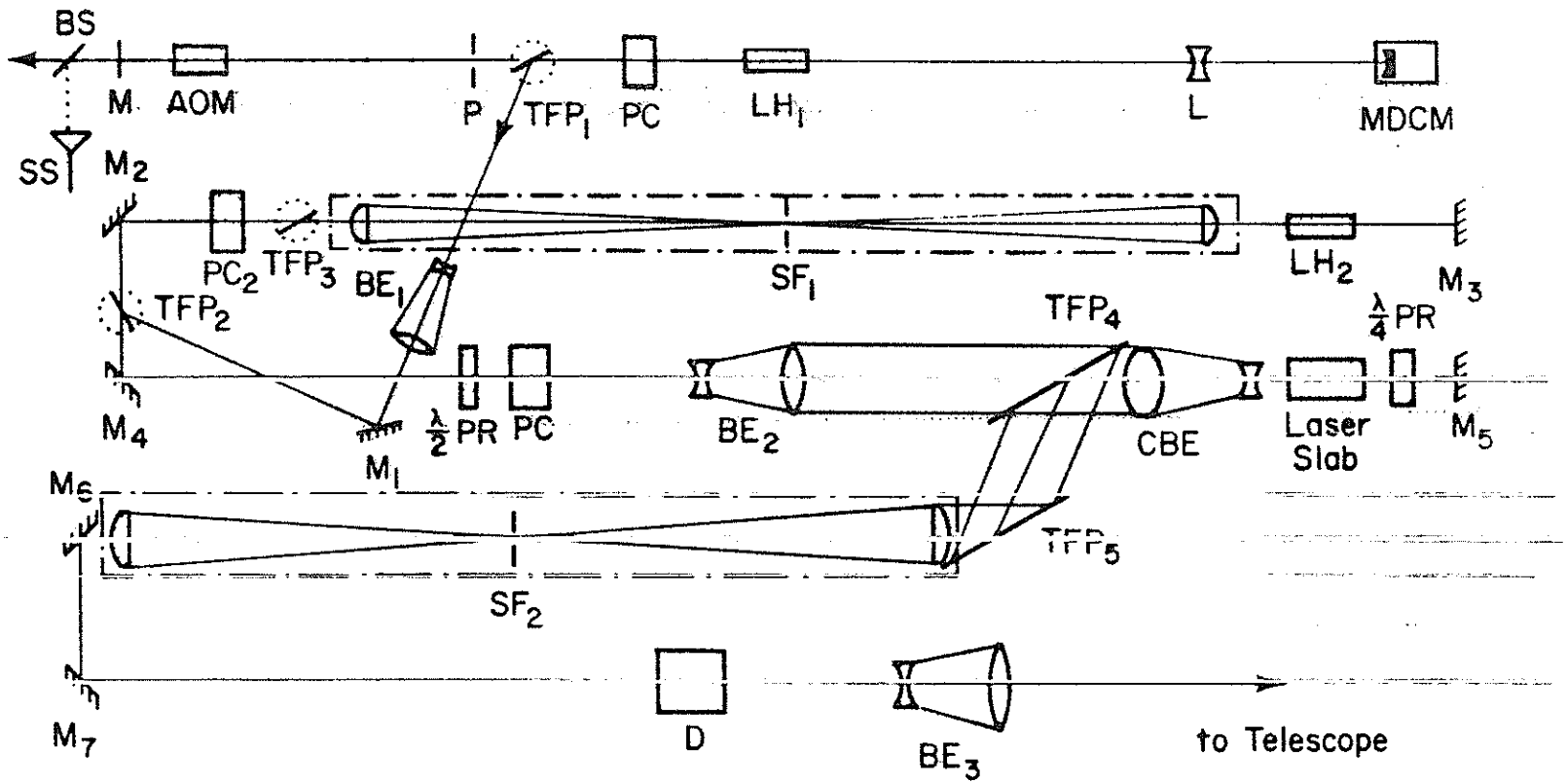

MDCM — Modelocking Dye Cell and Mirror (r = 3/4 m, R=100%)
LH — Laser Head (3.0 x 100 mm, 9.5 x 100 mm)
PC — λ/2 Pockel Cell (KD*P)
L — Lens (f = -33 cm)
TFP — Thin Film Polarizer
SF — Spatial Filter
BE — Beam Expander
CBE — Cylindrical Beam Expander
D — Doubling Crystal (KD*P)
P — Pinhole (φ=2 mm)
AOM — Acousto-Optic Modulator
M — Flat Mirror (R=65%)
BS — Beam Spliter (R=8%)
SS — Semiconductor Switch (GaAs)
M_i — Mirror (R=100%)
PR — Polarization Rotator

REFERENCES

1. C. O. Alley, J. D. Rayner, R. F. Chang, R. A. Reisse, J. Degnan, C. L. Steggerda, L. Small, and J. Mullendore: Experimental Range Measurements at the Single Photo-Electron Level to the Geos-A and BE-C Satellites, a paper from the Third International Workshop on Laser Ranging at Lagonisi, Greece, May, 1978.

2. B. E. H. Serene, Progress of the LASSO Experiment, Proceedings of the Twelve Annual Precise Time and Time Internal: Applications and Planning Meeting, NASA Conference Publication 2175, December, 1980.

3. John Degnan, University of Maryland Ph.D. thesis, 1979: Physical Processes Affecting the Performance of High Power, Frequency-Doubled, Short Pulse Laser Systems: Analysis, Simulation and Experiment.

4. Chi Hi Lee, A. Antonetti, and G. Mourou: Measurements on the Photoconductive Lifetime of Carriers in GaAs by Optoelectronic Gating Technique, Optics Communications, Vol. 21, April, 1977.

A COMPARATIVE STUDY OF SEVERAL TRANSMITTER TYPES FOR PRECISE LASER RANGING

CONTACT: JOHN J. DEGNAN
THOMAS W. ZAGWODZKI
CODE 723
NASA/GODDARD SPACE FLIGHT CENTER
GREENBELT, MARYLAND 20771 USA

1.0 Introduction

During the past three years, a total of ten laser transmitters have been submitted to a fairly standardized laboratory test program in order to determine their expected contribution to the range biases and RMS noise in a satellite laser ranging system. Among the transmitter types tested were four Q-switched configurations varying in pulsewidth from four to eight nanoseconds (FWHM), three PTM Q-switched (cavity dumped) configurations varying in pulsewidth from 1.5 to 4.0 nanoseconds (FWHM), and three mode-locked transmitters with FWHM pulsewidths in the range 60 to 225 picoseconds. The lasers tested are summarized in Table 1.

In order to isolate the errors contributed by the transmitter, it was necessary to construct, test, and calibrate a range receiver whose time walk and time jitter contributions were at the subcentimeter level for the laser pulsewidths being tested. Furthermore, during the ranging experiments, special care was taken to keep the average signal level well within the low time-walk regime of the constant fraction discriminator. Details of the receiver hardware and the calibration techniques employed are described elsewhere[1].

In this paper, we will provide some detailed data for one laser in each of the three categories, i.e. (1) simple Q-switched; (2) PTM Q-switched (cavity dumped); and (3) modelocked. A detailed discussion of some of the Q-switched and cavity-dumped tests is given in an earlier report[1]. The modelocked results have not been published previously.

2.0 Experiment Description

Two basic tests were performed on each laser. The first is a ranging repeatability or "stability" test which attempts to identify time dependent biases in the range data to a fixed retroreflector. The second is a "range map" which is designed to identify biases associated with the location of the target in the transmitter far field pattern resulting from the presence of higher order transverse modes in the laser output.

In the ranging repeatability test, the mean of 100 successive range data points is calculated, plotted against time of day, and repeated over a time frame comparable to or longer than a typical LAGEOS pass (> 45 minutes). The target retroreflector, located on a water tower located approximately 0.455 Km from the ranging laboratory, is placed in the approximate center of the transmitter beam and signal levels are adjusted via attenuators so that the start and stop input voltages to the discriminator lie in the low time walk regime. The following procedure was used to generate the angular range map:

1. Center the target in the transmitter beam and average the on-axis results of 100 pre-calibration range measurements.
2. Change the transmitter beam direction by a 25 to 30 arcsecond step in one axis using a calibrated pointing mirror.
3. Adjust the amplitude of the received signal, via a neutral density attenuator wheel, so that the average signal level is in the center of the low time walk regime of the receiver.
4. Take two sets of range measurements of 100 data points. Compute the local mean range and standard deviation for each set.
5. Subtract the on-axis pre-calibration mean range from the two local means and print the results adjacent to the corresponding azimuth/elevation coordinates on the map along with the corresponding standard deviation. The deviation of the local mean and the standard deviation (one sigma) are expressed in centimeters.

6. Repeat sets 2 through 5 until the map is completed.
7. Center the target on the transmitter beam and average the on-axis results of 100 post-calibration range measurements. Compare with the pre-calibration results.

3.0 Representative Test Results

Figures 1 through 3 show representative results of the ranging repeatability test and the range map for three different transmitter types. Figure 1 presents the results for a modified Q-switched General Photonics laser. The laser is identical to that originally installed in the Mobile Laser Ranging Stations[2] except for a somewhat shorter oscillator. This reduced the pulsewidth to about 4 nsec (FWHM) compared to 7 nsec in the original design. When operated at a 1 pps rate, system bias would drift at rates up to 0.6 cm per minute of operation. At 5 pps, the on-axis drift rate was often considerable with the system bias changing by about 25 cm during a 40 minute period as in Figure 1. The range map in the same figure shows a peak-to-peak variation in the mean range of 18.2 cm. At 5 pps, the peak-to-peak variation was as much as 75 cm. Interestingly enough, the RMS standard deviations for a given 100 point data set were always in the 2 to 6 cm (one sigma) range as in the map of Figure 1.

Figure 2 summarizes the results for a PTM Q-switched (Q-switched and cavity dumped) laser built by General Photonics and modified by NASA. The original cavity-dumped electro-optic switch was too slow and was replaced by an inhouse NASA design[3] which provided subnanosecond switching and a steep leading edge on the output pulse. The mean range was typically stable to better than ± 1.5 cm during two hours of continuous operation as in Figure 2. The peak-to-peak variation in the mean range over the angular map was always less than 4 cm (± 2 cm). The RMS standard deviation of all 100 point data sets was stable at the 2 to 3 cm level (one sigma).

Figure 3 gives the corresponding results for a prototype compact subnanosecond laser built for NASA by International Laser Systems. The system consists of an electro-optically modelocked, PTM Q-switched Nd:YAG laser oscillator, followed by a double-pass amplifier and a KD*P Type II doubling crystal. The oscillator is folded four times yielding a fairly compact system which is described in more detail elsewhere[4,5]. The laser is currently serving as the test transmitter in the TLRS-2 system[2]. As one can see from the figure, the peak-to-peak variation in the mean range for the repeatability test is only ± 0.5 cm while the peak-to-peak variation in the angular map was always less than ± 1 cm. The one sigma RMS standard deviation for all 100 point sets was in the range of 1 to 3 cms.

4.0 Summary

Table 1 summarizes the overall ranging performance of ten different laser configurations. Each laser has been assigned two ratings (poor, fair, good, very good, or excellent) summarizing its performance in each of the two tests, ranging repeatability and angular range map. The ratings are based on the peak-to-peak variations in the mean range as computed from 100 point data sets in the two tests according to the criteria outlined in Table 1.

Q-switched lasers, in general, were rated "poor" to "fair" in both categories. This is most likely due to several factors. The pulses are temporally longer and have slower risetime. Multiple transverse modes build up randomly and at different rates within the laser oscillator and are allowed to leak out of the cavity at arbitrary times by the partially reflecting output mirror. Because of their different antenna patterns, the individual temporal profiles of the modes do not sum uniformly in the far field. As a result, the stop waveform returning from the retroreflector may vary significantly from the start waveform leading to angularly dependent range biases and this has been observed. Finally, unstable temporal profiles were observed periodically in all of the Q-switched lasers except the Westinghouse military laser. The pulses would vary between smooth Q-switched waveforms

through partially modulated waveforms to full self-modelocked profiles. The Quanta-ray laser, which utilized an "unstable" resonator, was rated "very good" in stability but "poor" in the range map. This laser also exhibited self mode-locking effects at times.

In the cavity dump system, no radiation is permitted to leave the resonator until the dump electro-optic switch is fired. Thus, even though many transverse modes are present, they leave the resonator at the same time. Furthermore, the speed of the switch determines the risetime of the pulse as seen by the target, and a fast switch appears to reduce the bias errors in the far field map. The NASA-modified General Photonics laser had the best overall performance in this category.

Not surprisingly, subnanosecond modelocked lasers gave the best results with peak-to-peak variation in the mean of less than 2 cms in both tests. This was true not only of the prototype actively modelocked ILS laser discussed previously but also of two commercial passively mode-locked units built by Quantel. The YG40 is a low repetition rate (0.5 pps), low energy (3 mJ green) laser while the YG402 is a medium repetition rate (10 pps), medium energy (<100 mJ green) transmitter. The latter system is currently installed in a MOBLAS trailer for tests as part of NASA Laser Tracking System Upgrade program[2].

REFERENCES

1. J.J. Degnan and T.W. Zagwodzki, "Characterization of the Q-switched MOBLAS Laser Transmitter and its Ranging Performance Relative to a PTM Q-switched Systems," NASA Technical Memorandum 80336, October 1979.

2. J.J. Degnan and A. Adelman, "Upgrade and Integration of the NASA Laser Tracking Network," Proceedings of the Fourth International Workshop on Laser Ranging Instrumentation, this issue.

3. T.S. Johnson and J.G. Lessner, NASA Goddard Space Flight Center, Greenbelt, MD, USA, unpublished.

4. R.H. Williams, L.L. Harper, and J.J. Degnan, "Ultrashort Pulsed Solid State Transmitter Development," presented at Lasers' 78, Orlando, Florida, December 1978.

5. T.S. Johnson, J.J. Degnan, and T.E. McGunigal, "200 Picosecond Laser Development - A Status Report," Proceedings Third International Laser Ranging Workshop, Lagorrissi, Greece, May 1978.

TABLE I: LASERS TESTED BY GSFC

TYPE	MANUFACTURER	PULSEWIDTH (FWHM)	REPEATABILITY	RANGEMAP
Q-SWITCHED (S)	GENERAL PHOTONICS (MOBLAS)	7 NSEC	POOR	POOR
Q-SWITCHED (S)	MODIFIED GENERAL PHOTONICS	4 NSEC	FAIR (1PPS) POOR (5PPS)	FAIR (1PPS) POOR (5PPS)
Q-SWITCHED (S)	WESTINGHOUSE (MILITARY)	8 NSEC	POOR	POOR
Q-SWITCHED (U)	QUANTA-RAY	5 NSEC	VERY GOOD	POOR
PTM Q-SWITCHED	INTERNATIONAL LASER SYSTEMS (LL102)	4 NSEC	EXCELLENT	FAIR
PTM Q-SWITCHED	GENERAL PHOTONICS	3.6 NSEC	EXCELLENT	FAIR
PTM Q-SWITCHED	NASA-MODIFIED GP	1.5 NSEC	VERY GOOD	VERY GOOD
ACTIVE MODE-LOCK	INTERNATIONAL LASER SYSTEMS	225 PSEC	EXCELLENT	EXCELLENT
PASSIVE MODE-LOCK	QUANTEL INTERNATIONAL YG40 AND YG402	60 PSEC, 150 PSEC	EXCELLENT	EXCELLENT

CRITERIA FOR RANGING PERFORMANCE RATINGS

RATING	PEAK-TO-PEAK VARIATION IN 100 POINT MEAN
POOR	EXCEEDS 20 CM PEAK-TO-PEAK
FAIR	BETWEEN 10 AND 20 CM PEAK-TO-PEAK
GOOD	BETWEEN 6 AND 10 CM PEAK-TO-PEAK
VERY GOOD	BETWEEN 2 AND 6 CM PEAK-TO-PEAK
EXCELLENT	LESS THAN 2 CM PEAK-TO-PEAK

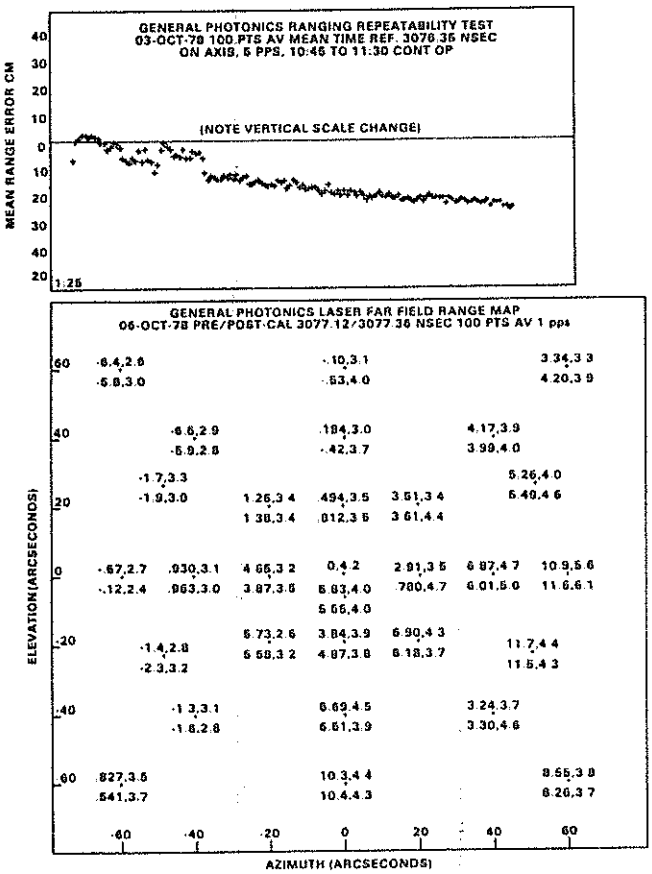

FIGURE 1: RANGING REPEATABILITY AND RANGE MAP TESTS OF FOUR NANOSECOND GENERAL PHOTONICS Q-SWITCHED TRANSMITTER

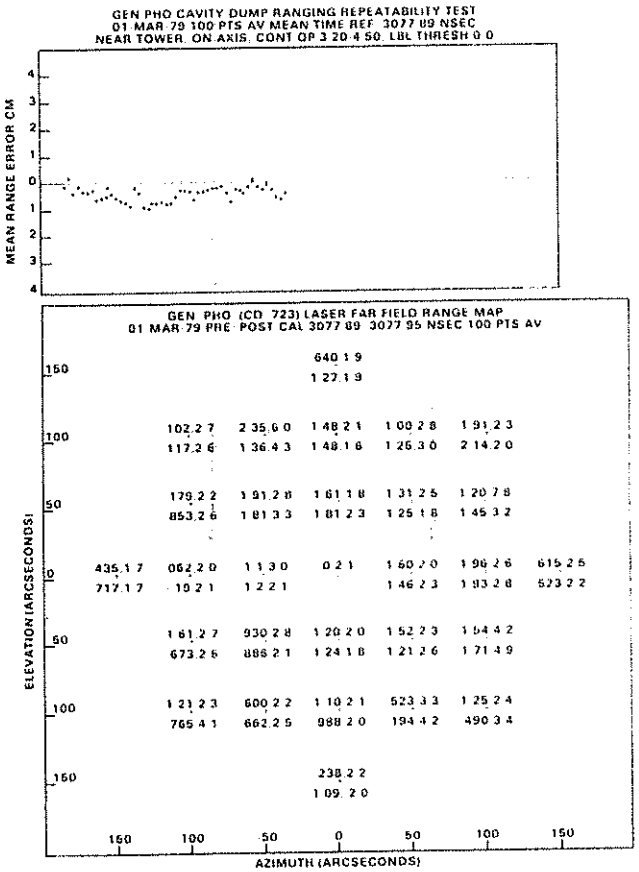

FIGURE 2: RANGING REPEATABILITY AND RANGE MAP TESTS OF NASA-MODIFIED GENERAL PHOTONICS CAVITY DUMP LASER

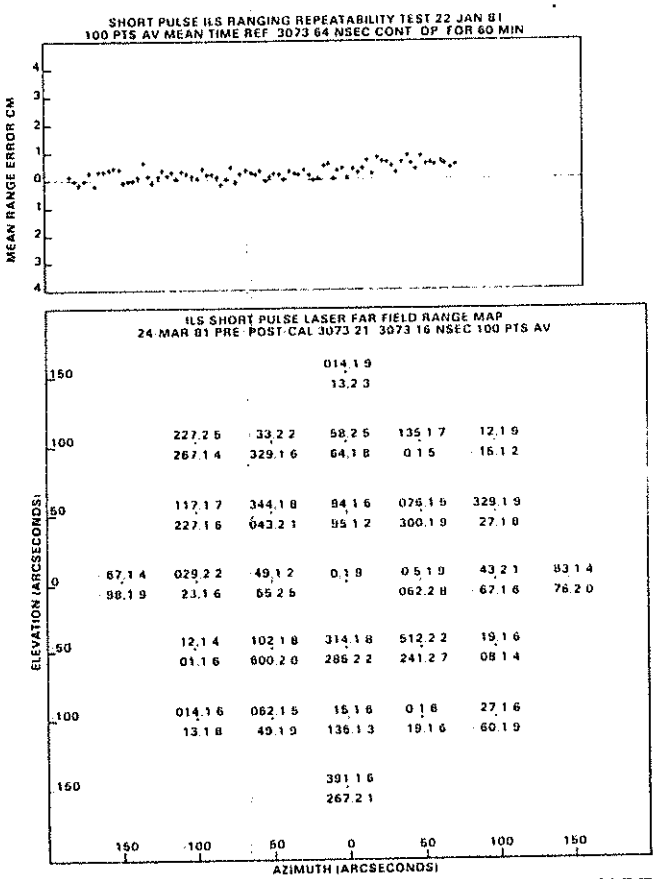

FIGURE 3: RANGING REPEATABILITY AND RANGE MAP TESTS OF ILS ACTIVELY-MODE LOCKED, PTM Q-SWITCHED LASER TRANSMITTER

SOME PROBLEMS OF SHORT PULSE, LOW ENERGY, HIGH REPETITION RATE LASERS APPLIED TO SATELLITE RANGING SYSTEMS *

R.L. Hyde and D.G. Whitehead,
University of Hull,
England

Introduction

It is generally accepted that to achieve a satisfactory photon return rate from satellite-borne reflectors, at an accuracy limited only by atmospheric uncertainties, sub-nanosecond, high peak power laser pulses are necessary. To provide adequate statistical data, a fast repetition rate is required, necessitating a high average power transmitter.

It is the purpose of this paper to outline the problems associated with such lasers and to suggest ways of overcoming them.

1. Laser Limitations

Solid state laser oscillators producing sub-nanosecond pulses are at present limited to around 20Hz repetition rate by thermal transients which disturb the fine balance within the optical resonator and high peak power non-linear effects which can lead to wavefront distortion and the irreversible breakdown of materials.

The effect of non-linear interaction with optical materials manifests itself as[1]

(a) non-linear lensing,

(b) small-scale self-focusing.

The physical process occuring is predominantly orbital electronic polarisation in the solid state.

---

* First presented to the 3rd Laser Workshop, Lagonissi, 1978 and revised in 1981.

The refractive index (n) of an optical material can be described thus:

$$n = n_o + \frac{\mu_o c}{n_o} \cdot n_2 I \qquad \ldots.(1)$$

where n_o is the linear refractive index and n_2 is a non-linear parameter, its term being dependent upon the beam intensity I. The intense part of the beam profile (usually the centre) traverses a marginally longer optical path, retarding the wavefront and causing the beam to converge. This is referred to as non-linear lensing, and may eventually result in very high intensities greater than the intrinsic dielectric breakdown strength of the material. We may define a critical power such that the natural diffraction is negated by this convergence. For a beam of Gaussian profile this is given by:

$$P_{critical} = \frac{1}{4\pi\mu_o c} \cdot \frac{\lambda^2}{n_2} \qquad \ldots.(2)$$

and is of the order of 600kw for Nd:YAG. The non-linear lensing focal length for a Gaussian beam is given by:

$$Z_f = \frac{2\pi}{\lambda} \cdot \omega^2 \cdot \left(\frac{P}{P_{critical}} - 1\right)^{-\frac{1}{2}} \qquad \ldots.(3)$$

where ω is the e^{-1} beam radius at the input. It is, of course, essential to ensure that Z_f is much greater than the extent of the laser optical system. As P varies within the pulse duration, Z_f will vary and limit a resonant cavity's stability.

When the power is much greater than the critical power the beam may break up into many parts. This is called small-scale self-focusing. The optical gain is a function of wavefront spatial frequency, and wavefront noise due to optical imperfection in the propagation path will be exaccerbated. This can be controlled in an amplifier chain by periodically filtering the wavefront noise before it is established, and in an oscillator will tend to be dispersed by diffraction. In either case it is a limiting factor.

In addition to these fundamental limitations to the use of very high power pulsed lasers, the laser sub-system itself will be the least reliable component in a satellite laser ranging system. This is because of the finite life-time of components such as flashlamps, dielectric coatings and crystal optics. Its development is still at an early state compared to, for example, tracking telescopes, and its reliability cannot compete with silicon-chip based technology.

It makes design sense therefore, to use a minimal laser and where possible to assign the residual requirements of the satellite laser ranger elsewhere.

2. The Minimal Transmitter

This is a laser oscillator only, consisting of a single traverse mode low loss resonator, a means of producing optical gain, a resonant modulator for longitudinal mode-locking and a resonator Q-switch to inhibit premature oscillation. Several designs are in existence and their categories may be described as CW, quasi-CW, or pulsed, each with a stable or an unstable resonator and modulated actively or passively. Such a device has an output of bandwidth-limited pulses at a very stable repetition frequency. Single pulse duration may be a few picoseconds and can be lengthened by auxiliary etalons.

CW systems require extensive amplification to be useful in satellite laser ranging applications, and we shall direct our comments to Nd:YAG pulsed and quasi-CW systems, having repetition rates of the order of 10Hz and an average power of the order of 30mW. The fundamental wavelength is 1.06μm and the pulse duration as short as 25 picoseconds.

It is prudent to consider such a minimum performance/maximum reliability specification and ask if, and how, it may be used in a satellite laser ranging system. We first ask whether the receiver can accept a repetitive burst of pulses (pulse burst mode) and whether they can be successfully analysed. Operation may involve several bursts in flight at any one time, each burst

consisting of a comb of precisely spaced pulses. Secondly, we consider what satellites are accessible to such a laser transmitter. Finally we question the necessity for second harmonic operation.

3. Pulse Burst Mode

The use of a pulse burst presents no great problem for the receiver and timing electronics if the spatial separation of each pulse is constant and greater than the time precision to which the satellite range is already known. Under these conditions the precise comb pulse, from which the return signal originated, can readily be identified. Unfortunately, at present, such precise satellite range predictions are not available. However, providing, that sufficient returns can be obtained from a sequence of shots, decoding of the comb can be carried out statistically. For example, it can be shown that[2] only some 15 returns are necessary to decode a comb to within 6 nanoseconds, the returning signals conserving the comb shape as they accumulate.

It should be noted that the transmission of a burst of accurately timed pulses creates the possibility, in favourable circumstances, of detecting photons for more than one pulse. However, multiple timers or some form of time store[3] must be used, as the computing period of the verniers, necessary to achieve picosecond resolution[4], is greater than the pulse separation. The probability of several returning photons being detected is small, but the difficulty of accurately locating the target would seem to indicate that there may be an advantage in being able to make use of two or more return signals following a successful target acquisition.

It is also desirable to be able to accept more than one signal when using single pulse ranging systems, thus preventing noise photons from invalidating a ranging shot. Subsequent analysis can then separate received noise photons (random epoch) from the true return.

4. Multiple Pulse Trains

The ability of the laser system to operate at relatively high repetition

rates, demands that the timing of pulse bursts be on an epoch basis, since several may be in flight at once. In practice, the number in flight will be limited by the necessity to shut down the laser when a return is expected, as the electrical noise generated by the laser would otherwise saturate a sensitive receiver. However, it is a relatively simple matter to control the firing of the laser, based on a prior knowledge of the target range.

5. Satellite Accessibility with a Minimal Transmitter

We define the Minimal Transmitter as a pulsed neodymium laser oscillator transmitting a comb of 3mJ at 10Hz (30mW).

It is necessary to determine the efficacy of such an emitter in ranging to, for example, LAGEOS.

1. The probability of a return ($\pi(R)$) must be greater than a n/p.t where n is the number of returns in a bin 'necessary for recognition' and p.t a specified number of shots;

$$\pi(R) > n(p.t)^{-1} \qquad \ldots.(4)$$

2. Assuming Poissonian statistics the probability of a return is given by;-

$$\pi(R) = \exp(-\bar{n}_B)\{1 - \exp(-\bar{n}_s)\} \qquad \ldots.(5)$$

where

$$\bar{n}_s = \left(\frac{E}{2\pi.\Omega_1.h\nu}\right)(A_3.\varepsilon_2.\eta)(S)^{-1} \qquad \ldots.(6)$$

and

$$\bar{n}_B = \left(\frac{N(\lambda)}{h\nu}\right)(A_3.\varepsilon_2.\eta.\Omega_2.\Delta\lambda)\, t_g \qquad \ldots.(7)$$

where the satellite-channel parameter

$$S(v,\alpha,\lambda) \equiv \frac{R^4}{a^2\sigma} \quad \text{and} \quad a^2 = \exp(-2\tau'_t.\sec(90-\alpha))$$

Figs. 1 and 2 shows how S varies with α for certain met. conditions and two wavelengths $\lambda = 1.06\mu m$ and $\lambda = 0.55\mu m$ for LAGEOS. Values of τ'_t are shown in Table 1.

Combining equation 4 and 5 and taking the zero background case for an example. i.e. when $\bar{n}_B \to$ zero. Then

$$p.\ \bar{n}_s \gtrsim n/t. \qquad \ldots(8)$$

for a given system

$$\bar{n}_s \eqsim \frac{K_s}{S.\Omega_1} \qquad \ldots(6a)$$

$$\therefore \quad p.\ \frac{K_s}{S.\Omega_1} \gtrsim \qquad \ldots(9)$$

Comparing the two cases of equation 9 for λ = 1.06μm and 0.53μm we have

$$r \equiv \frac{K_s.S^{-1}\ (\lambda = 1.06)}{K_s.S^{-1}\ (\lambda = 0.53)} \qquad \ldots(10)$$

$$r = \frac{8}{30} \cdot \left[\frac{S(.53)}{S(1.06)}\right].$$

i.e. the break-even point for $\frac{S(.53)}{S(1.06)}$ is $\simeq 4$.

This is plotted for LAGEOS in Fig. 3 where we see that the fundamental wavelength is preferable for low angles and visibilities. Returning to equation 9 and substituting some typical parameters

$$p = 10\text{Hz}$$
$$K_s = 1 \times 10^{11}. \quad (\lambda = 1.06\mu\text{m})$$

$$\frac{10^{12.}}{S\Omega_1} \gtrsim \frac{n}{t.} \simeq \frac{1}{10} \qquad \ldots(9a)$$

i.e. $S\Omega_1 < 10^{13}.$ $\qquad \ldots(11)$

now $S(5\text{km},\ 20^{\circ},\ 1.06,\ \text{LAGEOS}) \simeq 10^{22}\ m^2$

i.e. a 30 μ radians field of view is required, which is quite practical and realisable with current tracking telescopes.

6. Conclusions

This paper has identified some of the problems associated with the use of high power lasers for satellite ranging. It is pointed out that as the laser is inevitably the least reliable component in a ranging system, maximum system reliability can only be achieved by reducing the laser to its minimal configuration. The unique feature of the laser, the very high spectral radiance, and, in the case of mode-locked oscillators, a particular output format, should be utilised to the full. By transmitting a narrow beam in pulse burst mode at the fundamental wavelength, a greater degree of reliability is possible and techniques for accommodating such pulse trains can be readily applied to the detection and timing electronics.

7. Appendix I

n_o	Linear refractive index
n_2	Non-linear parameter
μ_o	Permeability of free space
c	Velocity of light
I	Intensity
λ	Wavelength
Z_f	Self-focusing distance
ω	$\frac{1}{e}$ Gaussian radius
P	Optical power
$\bar{n}_s$	Average signal return
$\bar{n}_B$	Average background return rate
$\eta(\lambda)$	Quantum counting efficiency
ε_2	Optical receiver efficiency
D	Telescope diameter ($A_3 = \frac{\pi}{4} D^2$)
E	Pulse energy
$h\nu$	Quantum energy
Ω_1	Full divergence solid angle
a	Atmospheric transmission
σ	Satellite cross-section
R	Satellite range
$N(\lambda)$	Background spectral radiance
Ω_2	Receiver field of view
$\Delta\lambda$	Receiver bandwidth
P	Repetition rate
t	Ranging period
t_g	Range gate
v	Meteorological range

8. References

1. 'Effect of Refractive Index Non-Linearity on the optical quality of High Power Laser Beams', B.R. Suydam, IEEE J. Quantum Electronics, Vol. QE-11, No. 6, June 1975.

2. Discussions with E.C. Silverberg, Lagonissi, May 1978

3. 'Multi-stop Timing Electronics for High Altitude Satellite Ranging', E.C. Silverberg, I.A. Malevich, Workshop on Laser Ranging Instrumentation, Lagonissi, 1978.

4. 'A Picosecond Timing System', M.J. Bowman, D.G. Whitehead, IEEE Trans. Inst. Meas., Vol. IM-26, No. 2, June, 1977.

5. Handbook of Geophysics and Space Environment, page 7-1, ed. S.L. Valley, (McGraw-Hill) 1965.

Table 1

	V	
λ (μm)	25km	5km
1.06	.14	.44
0.55	.36	.92

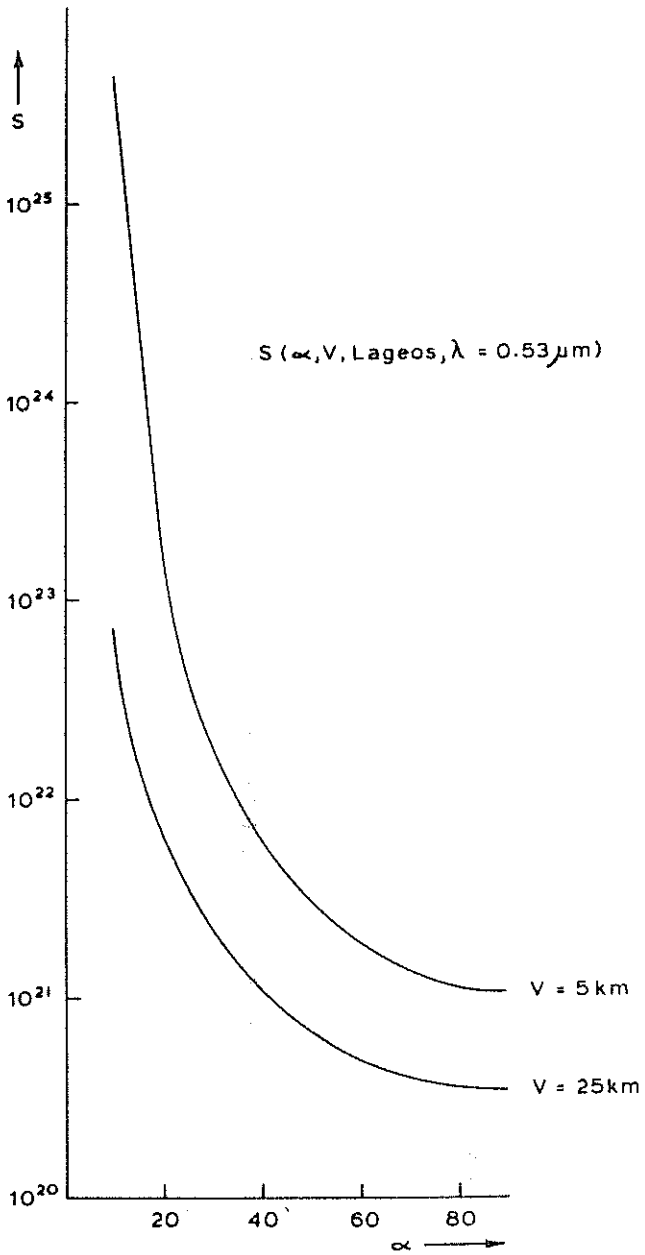

Fig. 1 Satellite - channel parameter S, versus angle of elevation α, with meteorological range as a parameter.

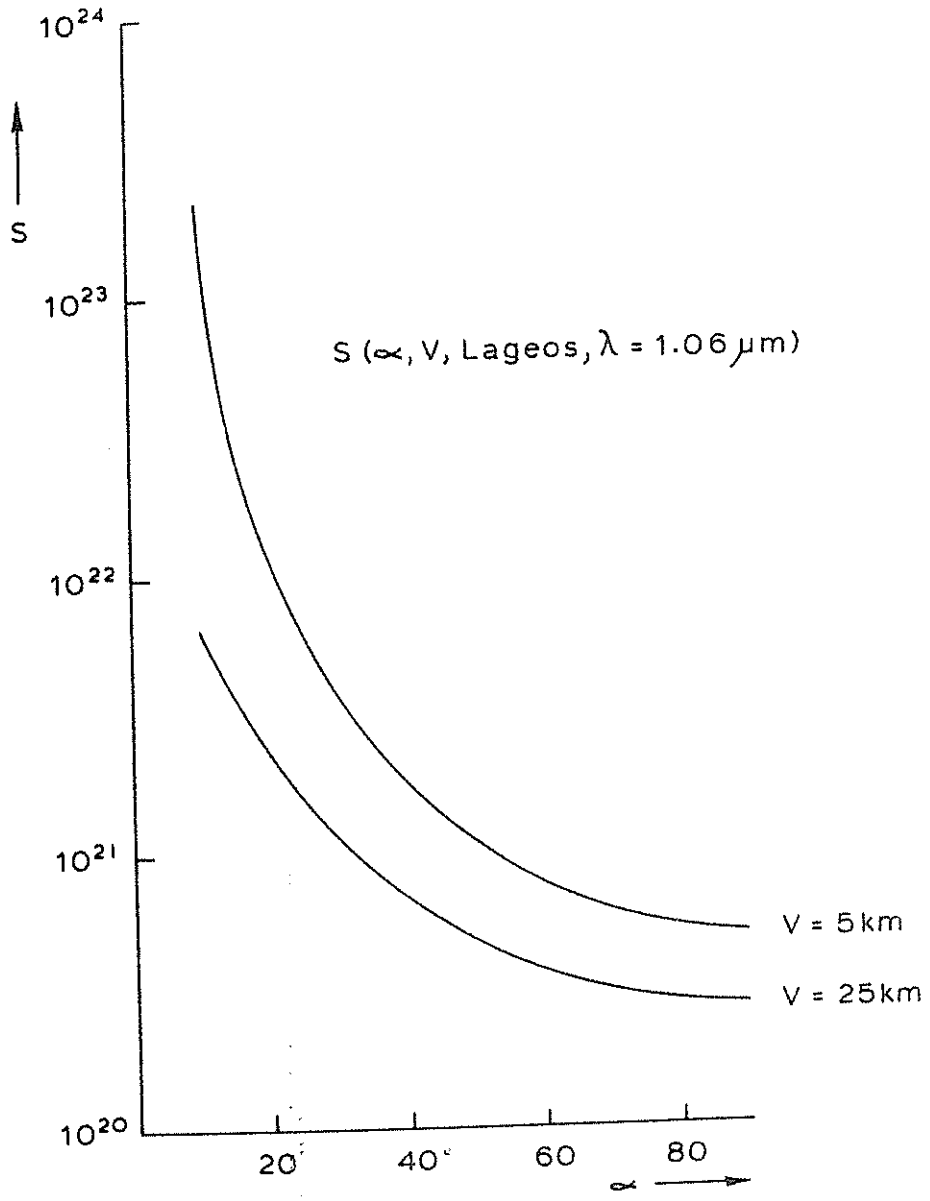

Fig. 2 Satellite - channel parameter S, versus angle of elevation α, with meteorological range as a parameter.

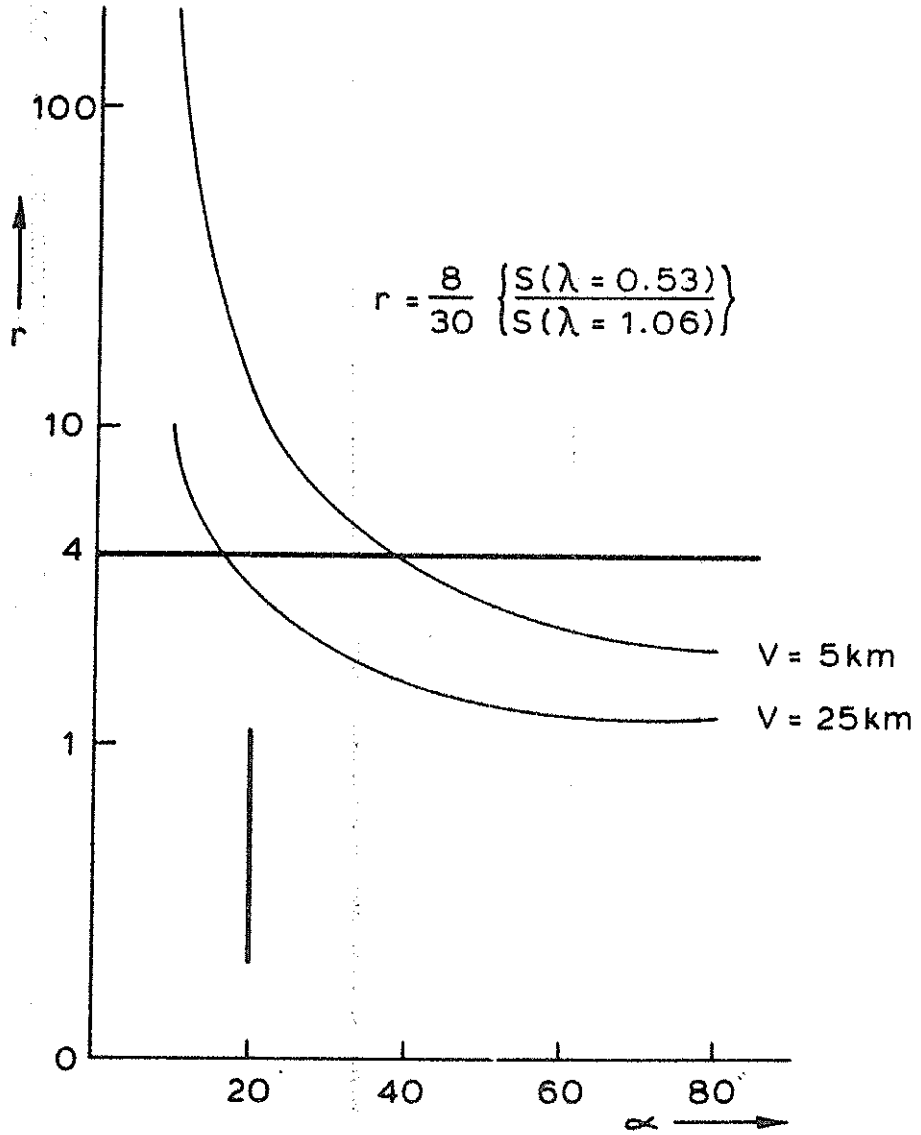

Fig. 3 The ratio of S for λ = 1.06 μm and λ = 0.53 μm against elevation angle with meterological range as a parameter.

MODE-LOCKED Nd-LASER FOR THE UK SATELLITE LASER RANGING SYSTEM

C.L.M. Ireland, J.K. Lasers Ltd., Rugby, England

D.R. Hall and R.L. Hyde, Applied Physics Dept.,
Hull University, Hull, England

INTRODUCTION

The major Satellite Laser Ranging activity in the United Kingdom is funded by the Science and Engineering Research Council and is centred around a collaborative programme between the Royal Greenwich Observatory (RGO) and the University of Hull. The present objective of this programme is to design and build an SLR system to be sited within the RGO at Herstmonceux Castle in Sussex.

The design goal for this system is to attain the necessary performance to range to Lageos at 20° elevation from the sea level RGO site, to have both day-time and night-time capability and to achieve range resolution of a few centimetres. Satellite ranging measurements are scheduled to begin during 1982 to Lageos, Starlette and Geos C, and the station is planned to be fully operational for, and to participate in the next phase of the MERIT campaign.

This paper describes the mode-locked Neodymium:YAG laser which has been developed to meet the system requirement. The receiver sub-system and the aircraft detection/laser lockout sub-system are described elsewhere in the proceedings.

OVERALL LASER SYSTEM

The system design calculations indicated that the laser performance should meet the outline specification indicated below.

Wavelength = 532 nm

Pulse Energy $\leq$ 30 mJ

Pulse Duration = 150 psec

PRF	$\leq$	10 Hz
Life	$\geq$	10^6 pulses free of service
Size, weight	-	minimal constraints for a static system

In addition, there are a number of extra features which it was felt necessary to incorporate into the design. These include built-in laser performance monitoring, eye safety precautions, beam processing optics and the provision of laser pulse timing signals. To achieve this performance a passively mode-locked Neodymium:YAG oscillator is used followed by two single pass amplifiers and a frequency doubler. A schematic diagram of the overall system is shown in Fig. 1. The laser optical system is mounted on a triple section optical rail two metres in length and 0.4 metres wide, and comprises, (a) a passively mode-locked and Q-switched Nd:YAG oscillator with a single pulse selector, (b) two optical single pass amplifiers, (c) a number of passive interstage optical components.

OSCILLATOR

The oscillator stage which occupies most of the right-hand side of the optical rail is shown schematically in Fig. 2. It comprises (A) a thin (0.25 mm) flowing dye cell contacted to a concave 100% reflecting rear cavity mirror, (B) a near field aperture, (C) a diamond pinhold, (D) an AR coated positive lens, (E) a ¼" diameter x 3" long Neodymium:YAG crystal with wedged anti-paralletl AR coated end faces in a single lamp pumping chamber fitted with optical corrector plates, (F) a temperature tuned output coupling etalon, (G) a single plate polariser in a vernier mount and (H) a single pulse selecting Pockels cell.

Since the peak output density can reach 2GWatt cm^{-2}, it is essential that the beam remain free of high spatial frequency noise as it propagates through the system. For this reason, the oscillator is designed to operate in the TEM_{oo} fundamental mode and produce a near Gaussian spatial intensity distribution, free of any high frequency modulation. This beam profile is achieved in the oscillator by the use of an intracavity spatial filter and a near field aperture adjacent to the mode-locking dye cell.

Another common problem with this type of laser relates to the incidence of optical damage to the window of the dye cell. The first indication of such damage is an acoustic "tick" from the dye cell. If the laser is operated beyond this point, very weak sparks can be seen in the cell after a further $\sim 10^4$ shots, and typically the mode-locking reliability drops to about 50% after another $\sim 3 \times 10^4$ shots. A large number of measurements have been made in monitoring and studying this problem and it is now clear that (a) there is a fairly sharp threshold value of energy density on the cell window above which damage is a near certainty after 50-100 thousand shots, (b) the effect is cumulative in that the energy density threshold is 2-3 orders of magnitude below the published single shot data for fused silica or BK7 glass. In this system, the dye cell damage problem has been addressed by careful attention to cavity optical design and dye cell geometry and flow, and the use of single pulse selector-cavity dump in the oscillator design. The latter is achieved by inserting the Pockels cell switch inside the cavity and configuring the single pulse selector unit such that it not only selects a single pulse for subsequent amplification and doubling but also cavity dumps the oscillator so terminating all subsequent laser action. The details of this scheme can be understood by reference to Fig. 2. The single pulse selector is triggered by an early pulse in the train. Subsequently, a voltage step is generated in the switchout unit and propagates along a single transmission line to the Pockels cell switch. When the amplitude of this step is equal to the quarter wave voltage of the Pockels cell, light making a double pass through the cell has its plane of polarisation changed by 90^o. Consequently, the pulse energy being fed back into the oscillator by the output etalon (F) is totally rejected at the intercavity polariser (G). The pulse energy being coupled out of the oscillator by the output etalon (F) makes a single pass through the Pockels cell and so is circularly polarised. At the subsequent polariser I, half the energy is transmitted and coupled into the rest of the system, and half is rejected. By this technique, the energy density incident on the damage sensitive mode-locking dye cell can be reduced by a factor of between 2 and 3.

AMPLIFIERS AND DOUBLER

The pulse produced by the oscillator passes through an in-line energy monitor which is coupled via suitable electronics to the computer, so that shot by shot monitoring of the oscillator performance can be logged. A pair of 45° mirrors are used to couple the beam into the other outer section of the rail and into a beam expanding telescope which preceds the first amplifier. Each amplifier contains a ¼" diameter x 4" long Nd:YAG crystal which has wedged anti-parallel AR coated end faces in a single lamp pumping chamber in which the lamp and rod are surrounded by a close-coupling diffuse ceramic reflector. The two amplifiers are separated by a Faraday isolator, comprising a 55mm x 12mm high concentration terbium oxide glass rod (Hoya FR5) in a pulsed magnetic field positioned between a pair of single plate dielectric polarisers, which are set at 45° with respect to each other to yield high forward transmission while blocking any retro-reflection and inhibiting any possible oscillation between the two amplifier stages.

To produce frequency doubled output, a type II KD*P crystal, mounted in a temperature controlled oven is used to obtain critical phase matching. The doubler is followed by a pair of dichroic mirrors which are arranged to reflect the 532nm green component into the centre section of the rail. The beam then passes through a second in-line energy monitor and another beam expanding telescope before exiting into the Coudé system of the main tracking telescope. The 1060 nm infrared beam is used to trigger a fast timing photodiode positioned as shown in Fig. 1.

EYE SAFETY PRECAUTIONS

Since the ranging site at RGO is close to London's Gatwich Airport, a system is required to detect aircraft near the beam and subsequently inhibit laser output. The X-band radar detection system, which is described elsewhere in the proceedings, will produce a signal in th event that an aircraft is detected in the danger zone and this signal is used to close an electro-mechanical shutter positioned in the optical train within the oscillator. It has a closing time of less than 10 milli-seconds. A second, two position, shutter is situated near the output of the laser system (Fig. 1).

Aside from the open (100% transmitting) position, there is a second position in which a neutral density filter is inserted in the beam. This is selected so that after subsequent beam expansion the beam emanating from the telescope is eye safe.

LASER PERFORMANCE

The laser system described here produces an output energy of 30mJ per pulse at 532 nm at pulse repetition frequencies up to 10Hz. The duration has been measured with a streak camera at 150 ± 20 psec, corresponding to a peak power of 200 MW and an average power of 300 MW. The precautions taken with the oscillator have resulted in the possibility of uninterrupted operation for well over 10^6 shots and with a mode-locking drop-out rate of about 1/3000 measured at a prf of 10Hz. A photograph of the complete system is shown in Fig. 3.

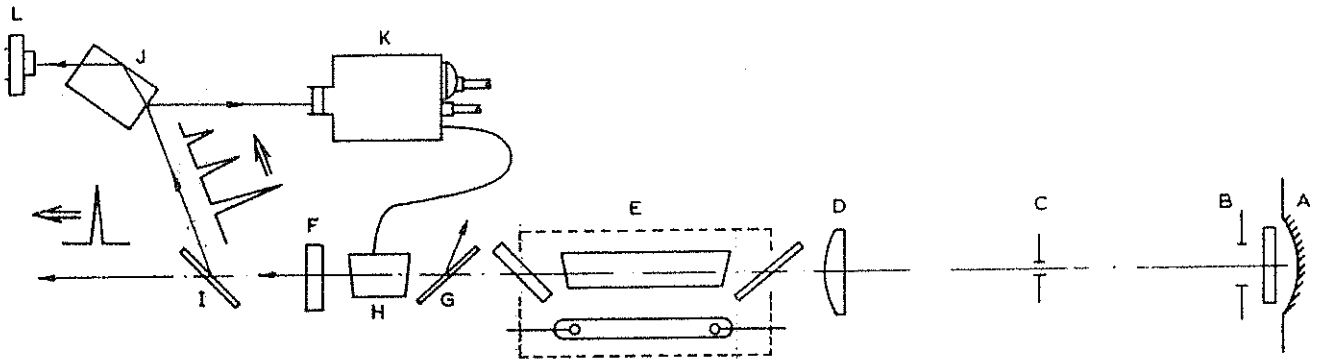

KEY

A. Contacted dye cell with flowing dye. Rear cavity 50cms radius, window 1/2° spectrosil wedge
B. Near field aperture
C. SF pinhole
D. Recollimating lens
E. Pumping chamber with 3" x 1/4" dia YAG rod and corrector plates
F. LaSF11 etalon
G. Dielectric polariser
H. Pockells cell with wedged windows and crystal
I. Dielectric polariser (crossed with G)
J. Beam steering glass block
K Photodiode triggered SPS unit generating quarter wave voltage step
L. Fast photodiode monitor

Schematic of mode-locked oscillator and SPS layout

Fig. 1 Oscillator Configuration

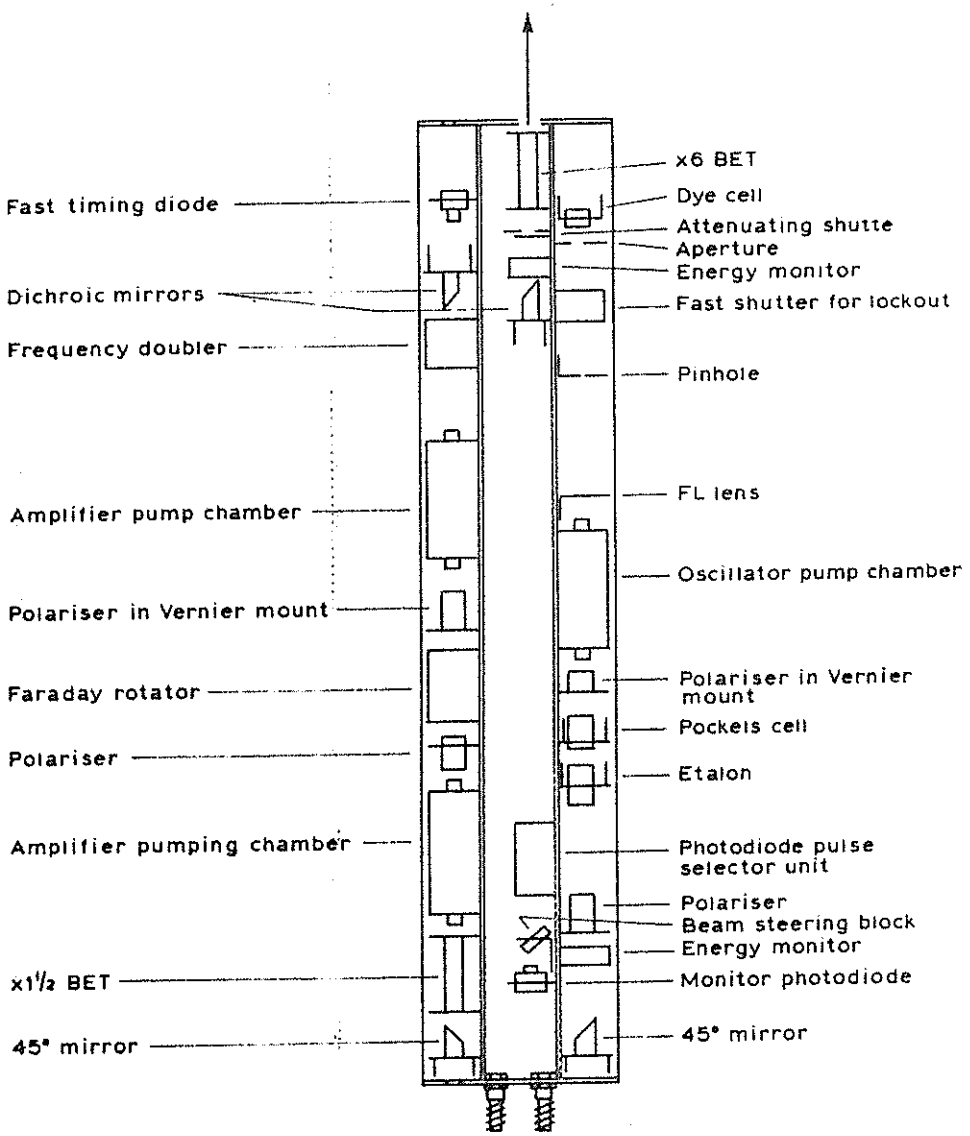

Fig. 2 Component Layout Schematic

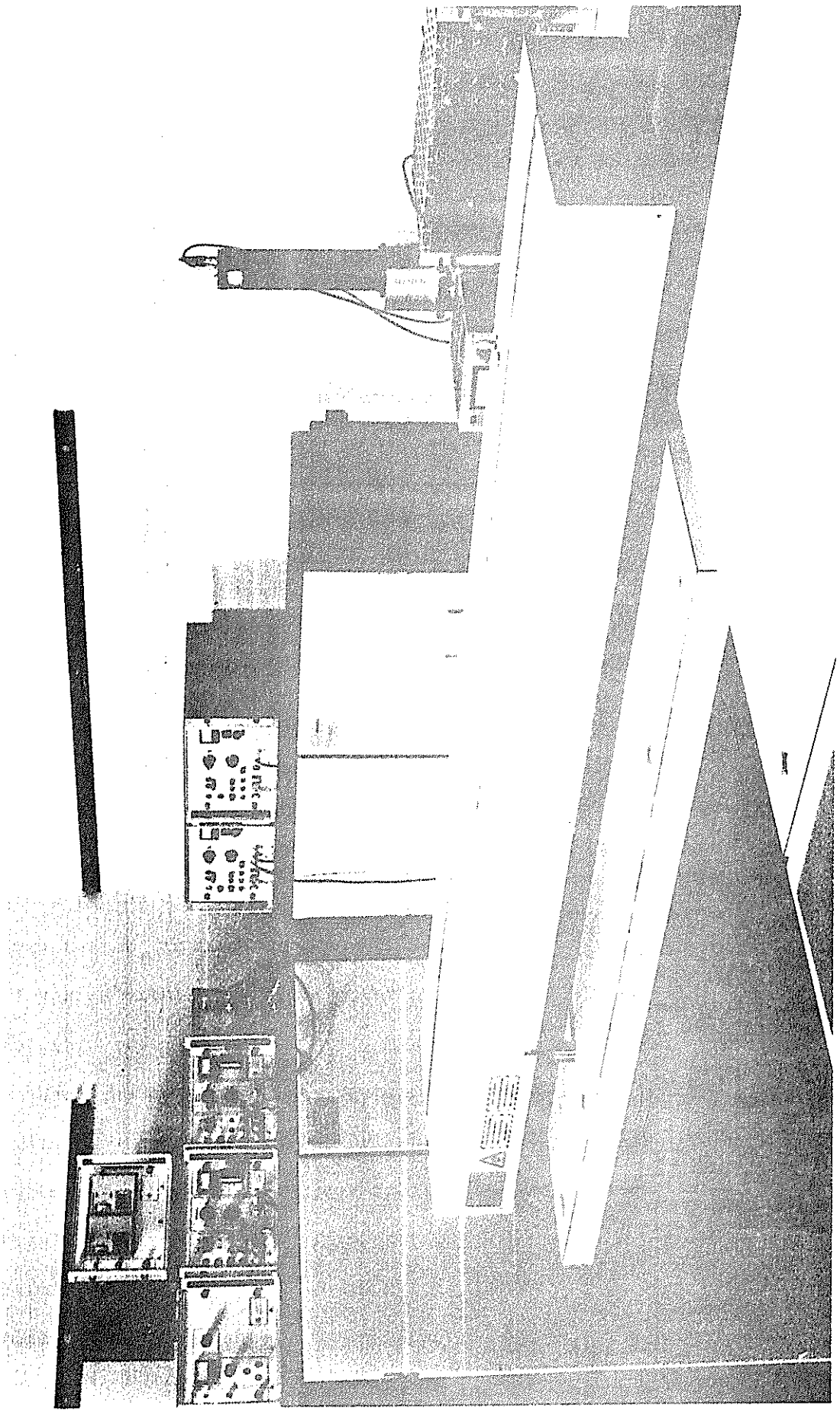

Fig. 3 Complete Laser System

CONSTANT GAIN PULSE FORMING LASER

H.Jelinkova

INTERKOSMOS

Faculty of Nuclear Science and Physical Engineering
Czech Technical University
Brehova 7, 11519 Prague 1
Czechoslovakia

There is a very strong interest to achieve a stable Q-switched output for any pulse laser application. For some of them, a pulse in nanosecond region, is desired. This report shows that both requirements are achievable using constant gain Q-switching plus pulse forming mode technique. The system has been applied for 2.generation laser radar.

CONSTANT GAIN REGIME

The long term instability (for example due to the lifetime of the flashlamp, cooling system dirty, blinding of pumping cavity surface, changing of coolant temperature, resonator distortion) results in a monotone change, usually, toward lower output energy and longer evolution time of the pulse. The short term instability (power supply voltage fluctuations, flashlamp output fluctuations due to the plasma formation instabilities, resonator distortion) results again in peak power and evolution time fluctuations from pulse to pulse.

To decrease the long and short term instabilities, instead of constant time, Q-switching at constant gain was implemented to Nd:YAG |1| and the ruby laser |2|,|3|. The peak power, evolution time and the length of the pulse are strongly dependent |3|,|4|,|5| on the starting gain, which is function of the total fluorescence emission from the lasing medium. Thus, monitoring this fluorescence (Fig.1) with a photodiode, we obtain a signal indicating the gain function. This signal is compared to a stable reference voltage and it is independent of the total flashlamp output. The laser is Q-switched when its gain has decayed to a fixed trigger level (Fig.2). The flashlamp variations are accommodated by variation of the Q-switch time. The laser output should be, in absence of optical resonator distortion, constant.

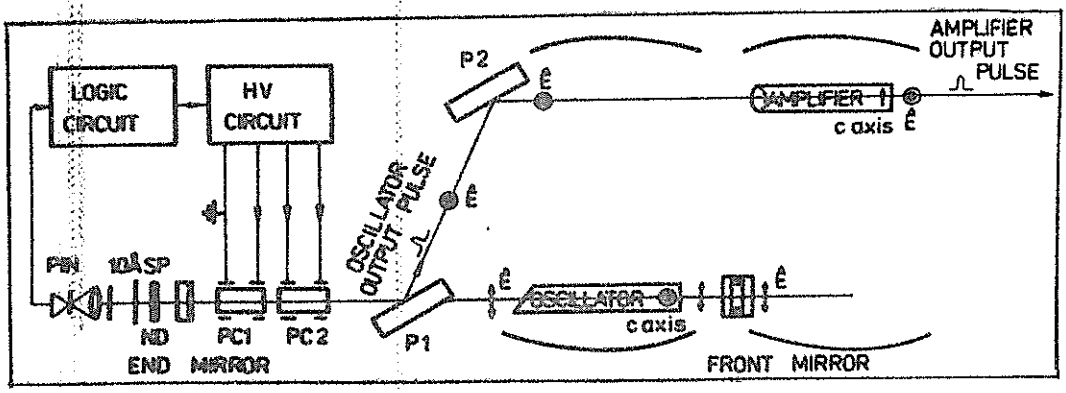

Fig.1 The principal scheme

To proof the stabilization when the laser is Q-switched at constant gain, we have set the desired gain via the reference voltage and we have changed the pumping energy from 1800 to 2400 J to simulate the instabilities. The stabilization of the output energy and the evolution time in dependence on input energy are shown on Fig.3 and Fig.4 resp. The stabilization, when the coolant temperature is changed, is shown on Fig.5.

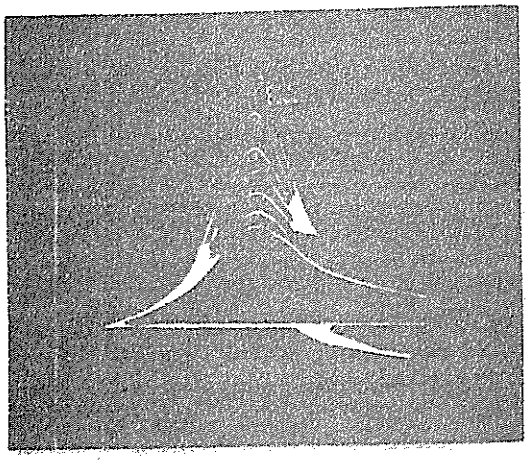

Fig.2 Ruby fluorescence versus time. The laser is pumped at different level and Q-switched at constant gain

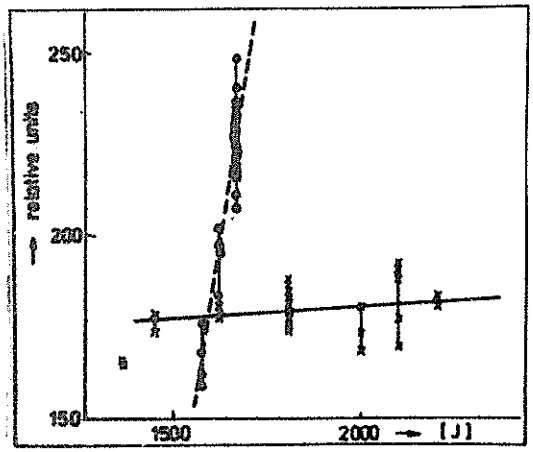

Fig.3 Output energy versus pumping. Dashed line ∿ constant time, solid line ∿ constant gain Q-switching resp.

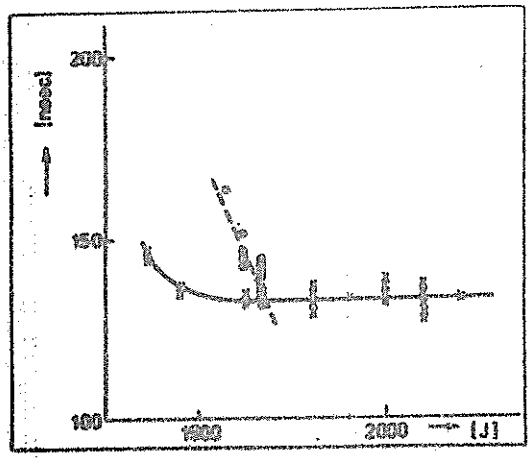

Fig.4 Evolution time of the pulse versus pumping. Dashed line ∿ constant time, solid line ∿ constant gain Q-switching resp.

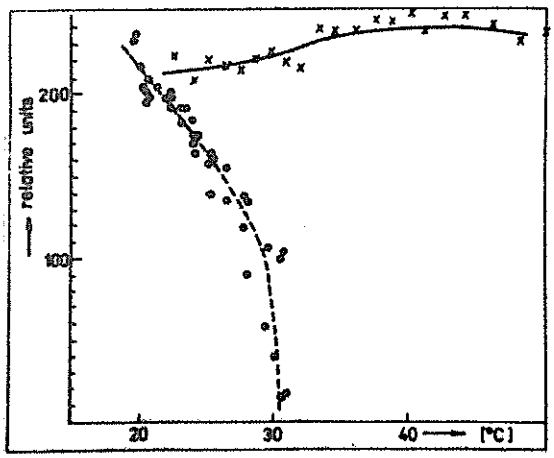

Fig.5 Output energy versus ruby coolant temperature. Dashed line ∿ constant time, solid line ∿ constant gain Q-switching resp.

THE PULSE FORMING MODE OR PTM MODE OF OPERATION

The implementation of constant gain Q-switching circuit into a ruby laser gave the possibility to use PTM mode |4| or the pulse forming mode (PFM) of operation with constant time delay. In our scheme (Fig.6), two krytrons are used for Q-switching and pulse forming of the laser pulse.

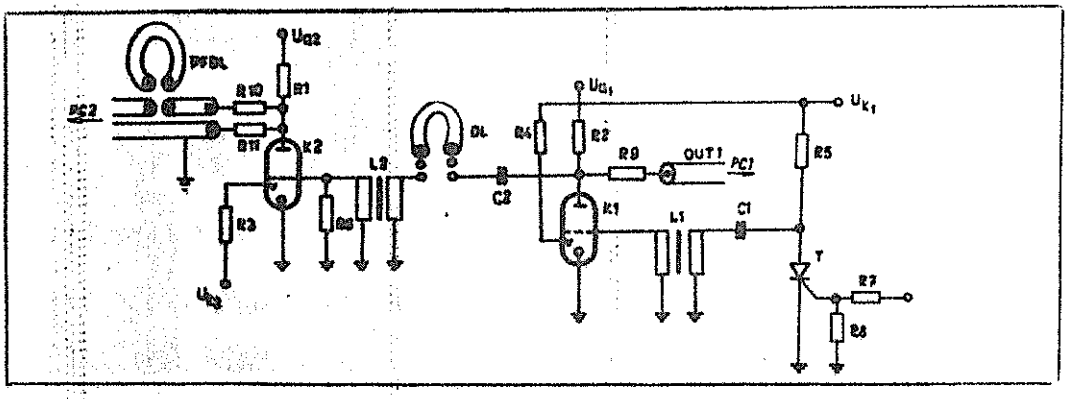

Fig.6 High voltage Q-switch and pulse forming circuit

The resonator is formed by the 90% plano dielectric mirror and the double plate crystaline quartz (or 80%) front mirror. As the active medium, 150x10 mm ruby rod cut perpendiculary and 1° resp., is used. Between the rear mirror and 1° ruby end the Q-switching plus pulse forming assembly, consisting of the thin film dielectric polarizer P1 and two Pockels cells PC1, PC2, is placed. 10% of light, going through the rear mirror, passing the neutral density filters ND, polarizer SP and 10 Å interference filter, is focused to the PIN photodiode. After the time delay (given by the cable DL) equal to the evolution time of the Q-switch pulse, the krytron K2 is switched. This voltage step pulse removes $\lambda/4$ voltage from one electrode of the Pockels cell PC2, thus re-introducing $\lambda/4$ relative phase shift to the passing light. It leads to rapid dumping of the opti-

cal energy from the cavity. After the time delay, from 1 to 5 nsec, given by the cable PFDL, zero voltage is on both electrodes of the Pockels cell PC2. The PFM pulse was generated. Using a longer cable than the laser cavity round trip, one obtains PTM operation. Records of resulted pulses are shown on Fig.7. Considering the rise time of our detection chain 1.8 nsec, the actual rise time of the output pulse is less than 2 nsec, the value typical for krytron KN 22B.

To amplify the output pulse, the polarizer P2 reflects the beam to the amplifier (Fig.1), the output energy is 0.1 - 0.2 J/nsec.

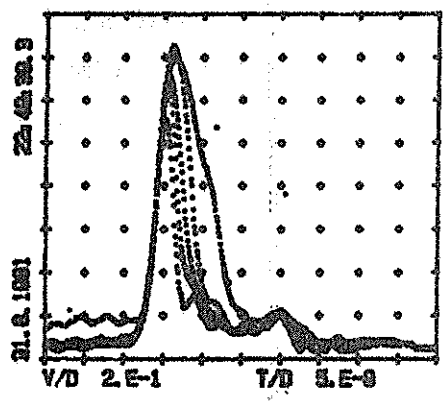

Fig.7 The output pulses

Consequently:

7 nsec	PTM regime
5 nsec	PFM regime
4 nsec	
3 nsec	
2 nsec	

CONCLUSION

The constant gain pulse forming technique gives the possibility to generate stable short nanosecond pulses. In principle, using a fast spark gap |6|,|7|, instead of krytron, this technique is one of the possibilities to obtain subnanosecond pulses.

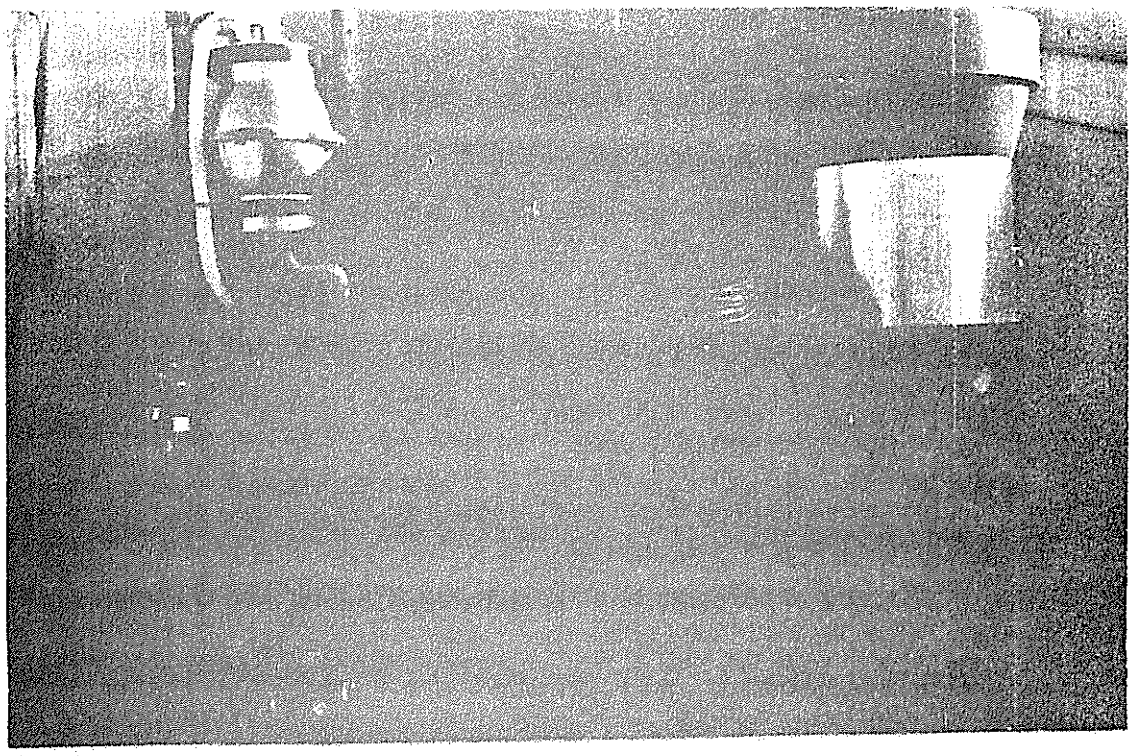

Fig.8 The photograph of the laser on the mount

REFERENCES

|1| Downs D.C., Murray J.E., Lowdermilk W.H., IEEE Journal of Quantum Electronics, vol.QE-14, No.8, August 1978, P.571-573

|2| Hamal K., Jelinkova H., Krajicek V., Novotný A., FJFI internal reports No.79/91, No.79/92, Prague 1979

|3| Jelinkova H., to be published

|4| Koechner W., Solid-State Laser Engineering, Springer-Verlag, New York 1976

|5| Jelinkova H., PhD theses, Prague 1975

|6| Jelinkova H., Hamal K., IEEE Journal of Quantum Electronics, vol.QE-14,No.10,October 1978, p.701

|7| Krajicek V., Hamal K., Kubecek V., Schmiedberger P., Proceedings of the 14th International Congress on High Speed Photography and Photonics, Moscow, USSR, October 1980, p.164

SUBNANOSECOND LASER SYSTEMS FOR SATELLITE RANGING

H. PUELL

KRISTALLOPTIK LASERBAU GMBH

AM SULZBOGEN 62

8080 FÜRSTENFELDBRUCK, GERMANY

INTRODUCTION

There is evidently great interest in pushing the accuracy for satellite ranging down to several centimetres or less. This implies the use of a new laser generation, operating in the subnanosecond domain. Pulse durations of this order may be achieved by two different methods:

i) mode-locking the laser oscillator, giving rise to a train of short light pulses equidistant in time, from which a single pulse may be selected and amplified further on. This method is readily employed with Nd:YAG lasers, generating light pulses as short as 30 psec.

ii) pulse-slicing the output of a conventional Q-switched laser oscillator by means of a fast electro-optical shutter. This method is usually employed in case of ruby lasers, which generally show a very unstable mode-locking operation. Typical pulse durations of the order of 1 nsec are achieved by this method.

In this paper we wish to present examples for each of these methods. First we will describe the actively mode-locked Nd:$YAlO_3$ laser system,

which will be part of the Dutch-German Mobile Laser Ranging System (MLRS) built by the Technisch Physische Dienst (TPD), The Netherlands. In the second part, the performance of a special pulse-sliced ruby laser system, which was built for the station at Wettzell, Germany, will be discussed.

ND:$YAlO_3$ LASER SYSTEM

The specifications of this laser system are shown in Tab.1. They result from the demands for high accuracy in ranging (pulse width), a large signal to noise ratio (output energy and repetition rate), and optimum adaption to the telescope and the detector (wavelength stability and bandwidth). Further boundary conditions concerning the power consumption, dimensions, and weight result from the mobility and the environment of the MLRS.

Wavelength	539	nm	Pulse width	200 - 300 psec
Stability	0.06	nm	Repetition rate	1, 2, 5, 10 Hz
Bandwidth	0.03	nm	Total weight	100 kp
Divergence	2	mrad	Dimensions	
Output energy	10	mJ	Power supply	100 x 35 x 60 cm
Stability	± 15	%	Optical bench	100 x 20 x 15 cm

Tab.1: Technical data of the frequency doubled Nd:$YAlO_3$ laser for MLRS

A schematic drawing of the proposed technical solution is shown in Fig.1. The laser system consists of a TEM_{00}-oscillator with a double pass amplifier, followed by a frequency doubling system. Nd:$YAlO_3$ crystals are used as the laser medium /1/. Their optical quality as well as their physical properties are comparable to those of Nd:YAG crystals. The main difference is the somewhat longer laser wavelength of the Nd:$YAlO_3$ crystals (1078 nm) and the optical biaxiality, which ensures polarized laser emission and less sensitivity to thermal birefringence.

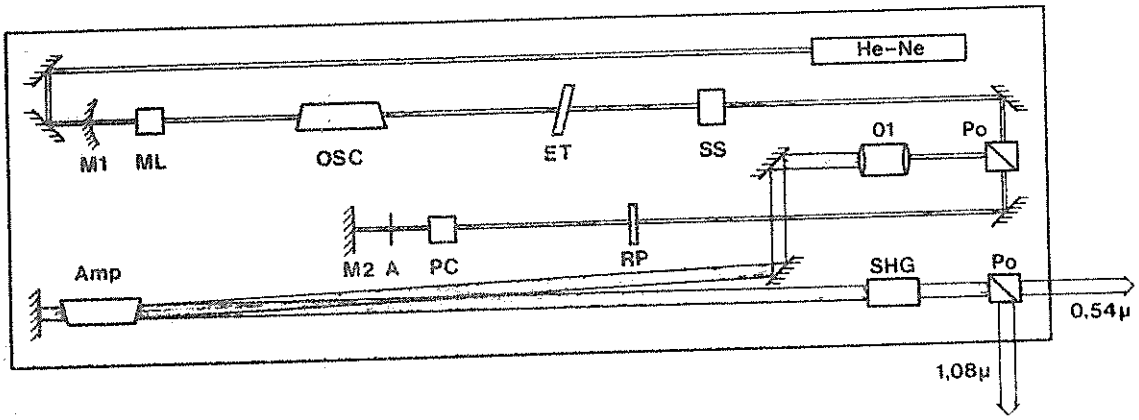

Fig.1 Schematic drawing of the Nd:$YAlO_3$ laser for MLRS.

The resonator of the oscillator is formed by two highly reflecting endmirrors (M1 and M2). Transverse mode selection is achieved by a 2 mm diameter aperture (A). The laser pulse is actively mode-locked by a KD*P electro-optical modulator (ML), its frequency being matched to the total resonator length of 150 cm. The pulse width is controlled by a bandwidth limiting quarz etalon (ET). Q-switching and single pulse selection is done by using the Pockels cell (PC) in the pulse-transmission mode. In order to get a stable mode-locking operation, the system is allowed to prelase for several µsec prior to Q-switching by a proper adjustment of the Q-switch voltage.

After switching out the mode-locked pulse from the resonator a telescope (01) expands the beam 2.5-times to fill the amplifier cross-section. The amplifier (Amp) is used in a double pass in order to reach the required energy level of 30 mJ/pulse. The amplified pulse is then frequency doubled in a temperature stabilized KD*P crystal, and the two wavelengths are seperated by the following polarizer (Po).

The electro-mechanical safety shutter (SS) prevents the system from accidental lasing. The same shutter serves also for switching the laser on and off, since the flashlamps are fired at a constant repetition rate of 10 Hz in order to establish well defined thermal conditions.

The active mode-locking concept has two mayor advantages: First, the buildup of the laser pulse can be easily controlled, synchronizing the Pockels cell with the frequency generator of the mode-locker. The time jitter for pulse emission is reduced down to less than 1 µsec, resulting in less data to be stored. Second, there are no volatile fluids involved as in case of passive mode-lockers, which could cause serious trouble outside the laboratory.

The MLRS will be operated under adverse environmental conditions. For this reason considerable attention is given to the mechanical and thermal stability of the laser system. The optical bench is a reinforced invar plate, integrated into the cooling system. It is covered by a heavy thermal isolation. All mayor alignements can be done without disturbing the thermal conditions with the aid of motor-driven differential micrometers integrated to the most important mirror mounts. Built-in photodiodes monitor the performance of the oscillator, the amplifier, and the harmonic generator.

First tests of the laser system will be under way beginning 1982, final tests will be held in the middle of 1982. The MLRS is scheduled to operate for the first time in 1983.

RUBY LASER SYSTEM

This ruby laser system was developed especially for satellite ranging and illumination applications. A first report on the system was given recently by W. Bäuml and K. Nottarp /2/. The specifications are shown in Tab.2. The special feature of the system is the twofold mode of operation:

i) as a high energy system, emitting 70 J within 300 µsec for illumination, and
ii) as a high power system, emitting more than 1 J within 700 psec for ranging.

Mode of operation	Illumination	Ranging
Output energy	70 J	1.4 J
Pulse width	300 µsec	700 psec
Output power	200 kW	2 GW
Divergence	2 mrad	2 mrad
Repetition rate	1 Hz	1 Hz

Tab.2: Technical data of the ruby laser system at Wettzell, Germany .

The system can be switched from one mode to the other by simple push-button operation. Both modes can be operated at a repetition rate of 1 Hz over an interval of 30 sec. In spite of the relatively large repetition rate, the rubies are kept constant in temperature within 1°C, and, hence, the output wavelength remains within the atmospheric window around 694.3 nm.

A schematic drawing of the laser system is shown in Fig.2. The resonator is formed by a concave highly reflecting endmirror (M1) and a sapphire resonant reflector (M2) for outcoupling. For Q-switch operation a Pockels cell (PC1) and a multiple glass-plate polarizer (Po) is included in the resonator.

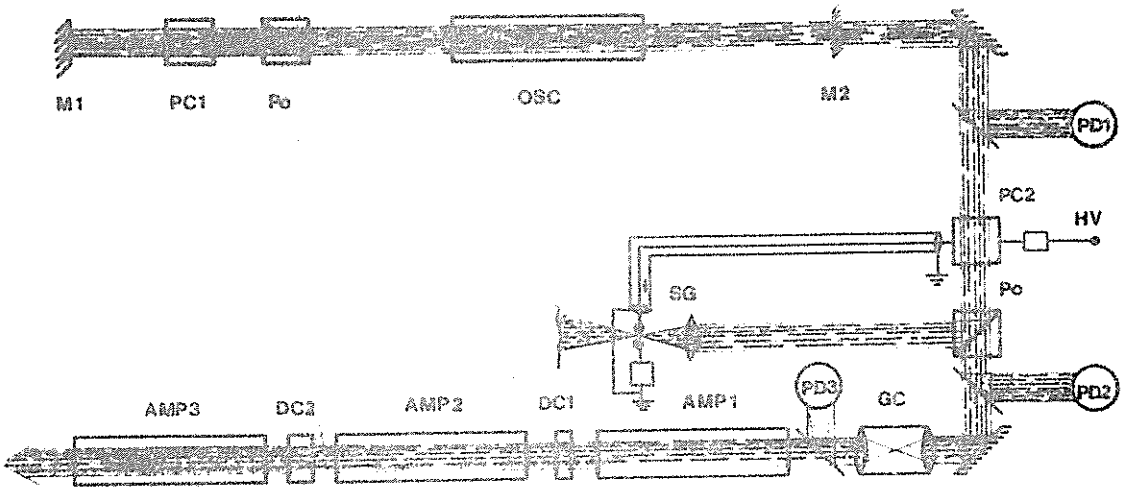

Fig.2: Schematic drawing of the ruby laser system at Wettzell.

Before entering the amplifier chain the oscillator pulse passes the pulse-forming system, which consists of a Pockels cell (PC2), a polarizer (Po), a laser triggered spark gap (SG), and a gas breakdown cell (GC). This system is activated when the laser is operated in the Q-switched mode for satellite ranging. The applied $\lambda/2$ voltage rotates the plane of polarization by 90° and the beam is deflected by the polarizer towards the laser triggered spark gap. By a proper selection of the trigger level one may switch the voltage of the Pockels cell down to 0 V right at the pulse maximum. The transmitted laser pulse has, hence, a very steep rising front. This pulse now enters the gas cell and induces a gas breakdown there. The buildup of the absorbing plasma is extremely fast /3/, transmitting only the very first beginning of the input pulse. The transmitted pulse has a typical pulse width of less than 1 nsec. This pulse is amplified by the following 3 amplifiers, which are optically decoupled by saturable dye cells /4/.

In case of normal mode operation, both Pockels cells are not activated. The laser pulse can pass all the polarizers without deflection. In this case the gas cell has no influence, since the input intensity is well below threshold for gas breakdown. The dye cells are moved out of the light path automatically in order to achieve maximum gain in the amplifier chain.

The performance of the pulse-shaping system is demonstrated in Fig.3. There the Q-switched laser pulse emitted by the oscillator (upper trace), the pulse transmitted by the polarizer (middle trace), and the pulse after passing the gas breakdown cell (lower trace) are shown. These signals were generated by the photodiodes PD1 - PD3, respectively. It is clearely seen how the pulse-shaper acts first on the leading edge and then on the trailing edge of the incoming pulse.

In Fig.4 the pulse shape of the amplified laser pulse is shown on an expanded 1 nsec/div time scale for a single event (upper trace) and for 10 pulses superimposed (lower trace). The reproducibility of the pulse shape is quite remarkable. The amplitude stability is $\pm$10 % in 90 % of the shots.

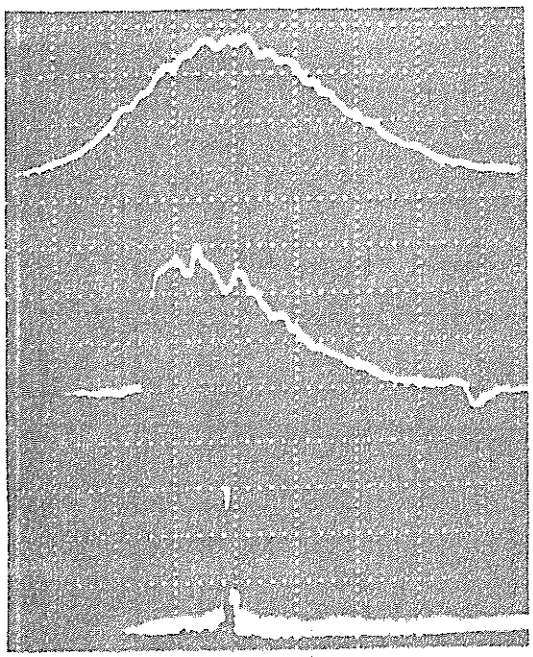

Fig.3 Laser pulse shapes recorded by the photodiodes PD1 (upper trace), PD2 (middle trace) and PD3 (lower trace), when activating the pulse-forming system. Time scale is 10 nsec/div.

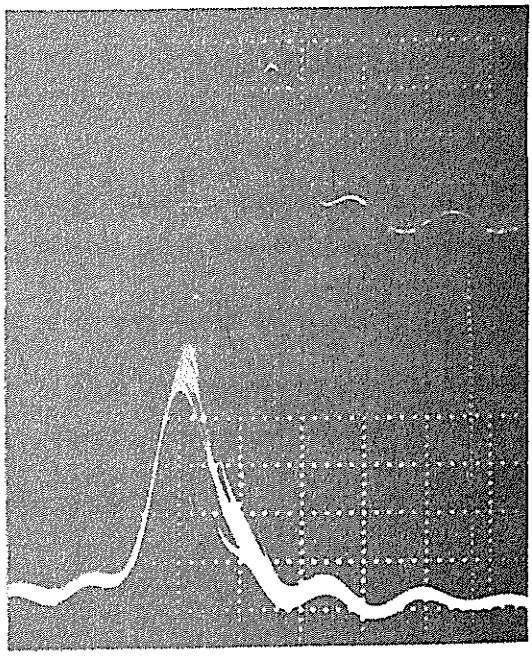

Fig.4 Laser pulses for ranging after leaving pulse-forming system and amplifier chain. Single event (upper trace) and 1 Hz operation superimposed (lower trace). Time scale is 1 nsec/div.

Finally, the subnanosecond pulse duration of the output pulse is demonstrated in Fig.5, where a recording taken by a Tektronix fast transient digitizer is shown. Taking into account the risetime of the photodetector (0.3 nsec) and the bandwidth of the oscilloscope's preamplifier (1000 MHz) a pulse duration (FWHM) of 700 psec results.

The above results show that the pulse duration of a conventional Q-switched ruby laser can be reduced from 25 nsec down to 700 psec with rather simple changes. However, it has to be pointed out that powerful amplifiers are necessary to regain the energy lost within the pulse-forming system (at the moment, the energy transmitted by the gas

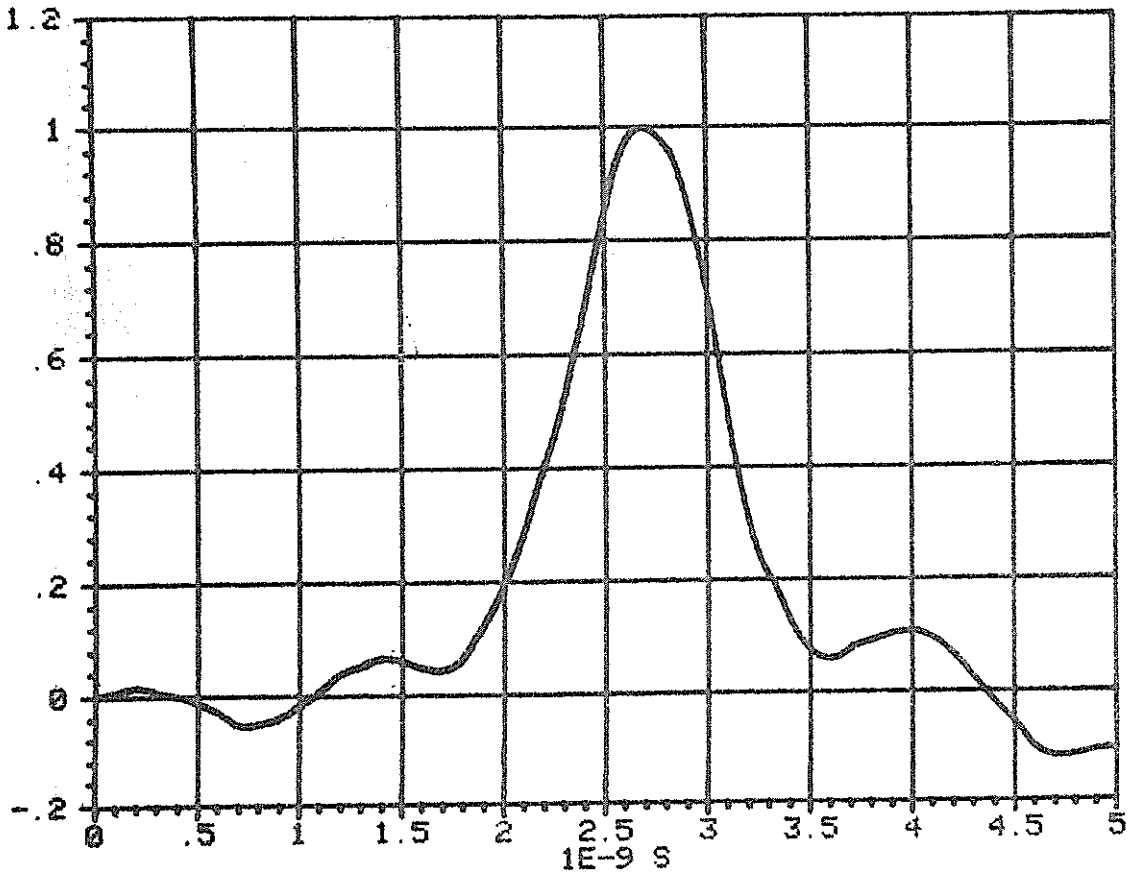

Fig.5 Pulse shape of the ruby laser in the ranging mode.

breakdown cell is of the order of 30 mJ). On the other hand our method certainly has the capability to achieve even shorter pulse durations in the range of 500 psec or less by optimizing the system parameters.

REFERENCES

/1/ Nd:$YAlO_3$ crystals are manufactured by Kristalloptik Laserbau GmbH

/2/ W. Bäuml and K. Nottarp, Die Arbeiten des SFB 78 Satellitengeodäsie der TU München im Jahre 1978, pp 40 - 43, Munich 1979

/3/ H. J. Neusser and H. Puell, Phys. Fluids 15, 1355 (1972)

/4/ H. Schüller and H. Puell, Opt. Commun. 3, 352 (1971)

LLR TARGET ACQUISITION

B.A. GREENE

Division of National Mapping

NATMAP

PO Box 31, BELCONNEN, ACT 2616
Australia

ABSTRACT

The problem of target acquisition in Lunar Laser Ranging (LLR) is discussed. The effectiveness of each guiding mode will be influenced by the response time and sensitivity of the real time analysis (RTA) used to indicate success. Without an absolute pointing capability of 3 arc seconds, the optimum guiding mode may vary with respect to moon phase, and for each mode suitable RTA must be provided.

The role of RTA in system ergonomics is emphasised, and an extremely sensitive method which is suited to all guiding modes and meets the requirements of human operators is confirmed.

1. Introduction

The application of single photoelectron detection (SPE) in satellite laser ranging (SLR) systems has recently reduced the number of problems unique to lunar laser ranging (LLR) systems. Those SLR systems operating with SPE generally employ full aperture transmission, narrow beam divergence, and precision tracking to reduce the laser power required for the ranging operation to a level which is not liable to cause eye damage. Thus there has been a convergence of LLR and SLR technologies in:

(a) detectors
(b) guiding and pointing
(c) data analysis
(d) system calibrations
(e) receiver filtering
(f) control systems technology

Concurrently, there has been a reduction in emphasis on aircraft detection and high power lasers in current SLR design - both of which continue to be of interest for LLR systems.

This paper will deal with the problem of target acquisition in LLR - a problem which remains identifiably different from SLR and which requires consideration of many aspects of system design ranging from laser and computer selection to system ergonomics.

2. Guiding Modes

There are several ways of tracking a target at the 3 arc second level for laser ranging. The most common methods are:

(a) Absolute Pointing and Tracking

If the target position at any time is known to better than 3 seconds of arc, and if the LLR telescope can point with equal precision, then the target can be acquired directly. The advantage of this method is that it is independent of target visibility (ie moon phase) and can be used for daylight ranging when even visible targets lose contrast and are difficult to track optically. No LLR currently operates in this mode.

(b) Relative Pointing

Systems which have no ability to point within 3 arc seconds absolute error may have a capability for very precise relative pointing over short angular distances. Thus if a well defined target (star or crater) which is angularly close to the laser target can be acquired, the telescope can be made to drive precisely to the target position.

(c) Imaging Devices

A telescope with only coarse pointing capabilities may make use of electronic imaging devices which 'recognize' the target area and provide drive input to maintain the telescope on target.

(d) Manual Acquisition

By viewing the target area from an optical system (eyepiece, TV) accurately boresighted with the telescope, an operator can control the tracking rates to keep the telescope on target if he is familiar with target area moonscapes.

The systems (a) - (e) may be associated with 'search' programs which scan the area around the commanded position in search of target returns. For all systems, criteria for successful ranging must be defined in terms of tests on the received data, so that the tracking

system can cease searching and lock onto the target.

3. Real Time Analysis

The laser ranging system should incorporate a real time analysis (RTA) facility to provide an indication that the ranging system is on target. The response time required for this analysis will be related to the occupation time of a point on the search grid and the response time of other units in the feedback path. Indeed each guiding mode should be designed as a closed loop servo system with full consideration of the bandwidths of each component.

The flagging of ranging success by a RTA unit has uses beyond locking onto the target. A continuous indication of ranging performance is satisfying and reassuring to the system operators, and minimises unnecessary and often derogatory manual adjustments to 'enhance' performance.

The RTA method used is constrained by almost every aspect of system design, and the requirement for RTA will have an influence in operating parameter selection. Clearly, the difficulty in detecting signal in real time will be related to the SNR in logged data. Using a dot display of residual vs time and a human operator as discriminator (1) is extremely sensitive and efficient. Extensive simulation (2) indicates that signal can readily be detected with this system for SNRs as low as 0.05.

Fully automated algorithms for defining 'on' and 'off' target are less sensitive than this when constrained to run in real time with large (100's of ns) uncertainties in range prediction. If background resident, which is most effective from a system operations viewpoint, the 'RTA' may increasingly lag the data acquisition. When an LLR is fully operational the uncertainty in the range should be much less than 100 ns, in which case an entirely machine resident RTA might be expected to manage easily. However, this is not so, since unobserved timing system (ephoch) errors, systematic error changes, atmospheric error fluctuations, and other variable biases make it undesireable to make rigid a priori range estimates. In fact it is occasionally the range residual (predicted minus observed range) which can indicate timing and other system errors.

Thus it is most desirable to have the most sensitive possible RTA, such that signal can be detected in very moisy environments as quickly as possible. Clearly the response time for RTA need not be less than other system time constants, however it is also clear that excessively slow or insensitive RTA will prolong search pattern execution.

4. SNR Selection

The SNR in data can be selected by the system designer. The parameters controlling this factor are shown in Figure 1.

The worst case design will be for full moon (maximum noise) ranging. The moon phase dependency of receiver noise can be approximated by a squared sinusoid, with noise proportional to $\sin^2$ (D/28), where D is the number of days since the start of the lunation.

The SNR can be made high by selecting (eg) a high laser pulse energy. However, maximum productivity for the system is associated (through another optimisation process) with maximum mean laser power, and the highest mean powers currently available are for 10 Hz (typically) pulse repetition frequencies. Thus, if tradeoff is to be avoided between guiding efficiency and productivity, the RTA should be made sensitive enough to detect signal at full moon using a maximum mean power laser.

Since the most sensitive RTA currently available will not give high confidence level success indication for SNR below 0.05 within 100 data points, the system designer is obliged to tailor the SNR to suit, or to sacrifice some observations. This is done by using established range equations and varying control parameters as indicated in Figure 1.

5. Effect of Atmosphere

For LLR, the transmit and receive optical axes should be within (about) 3 arc seconds of the target. The atmosphere plays an important role in the pointing process by adding random walk to both the transmit and receive optical axes. The large travel time (3 seconds) results in decorrelation of the transmit and receive axes by as much as the value of atmospheric seeing, which has 100 ms time constants. This can be modelled as a degradation of SNR by a factor of $(S/2)^2$, where S is the seeing in seconds of arc.

Similarly, for ruby lasers, the effect of precipitable water vapour can be approximated by an SNR degredation factor of $(W/3)^3$, where W is the precipitable water vapour in mm.

Thus if a system is to function satisfactorily in 6 arc seconds seeing with 6 mm of water in the atmosphere, the SNR for perfect conditions must be 32 times the treshold value.

The formulae for obtaining the factors are simple approximations, and based on observations of LLR data. The observations that no data at all has been observed in LLR for S greater than 8 or W greater than 9 is not incorporated into the models. More sophisticated models based on large data volumes will soon be possible as high productivity Nd:YAG systems become established.

6. Conclusion

The LLR system designer must clearly define the operating envelope for the system in terms of moon phase, atmospherics, and other considerations. He must then ensure that in operation, the SNR is within the limits imposed by available RTA, since if the guiding is not within specification, a potentially high productivity system will yield no results.

A high degree of awareness in the system operators of the influence of various parameters especially meteorological, on SNR is desirable to avoid false expectations which can corrupt the target acquisition process.

References

1. J. Rayner, Proc. Third International Laser Ranging Workshop, Lagonissi, Greece, May 1978.

2. R. Bryant, National Mapping unpublished report.

3. E.C. Silverberg, 'The Parameterisation of the Accuracy of a Lunar Laser Ranging System' University of Texas Res. Mem. 77-001, January 1977.

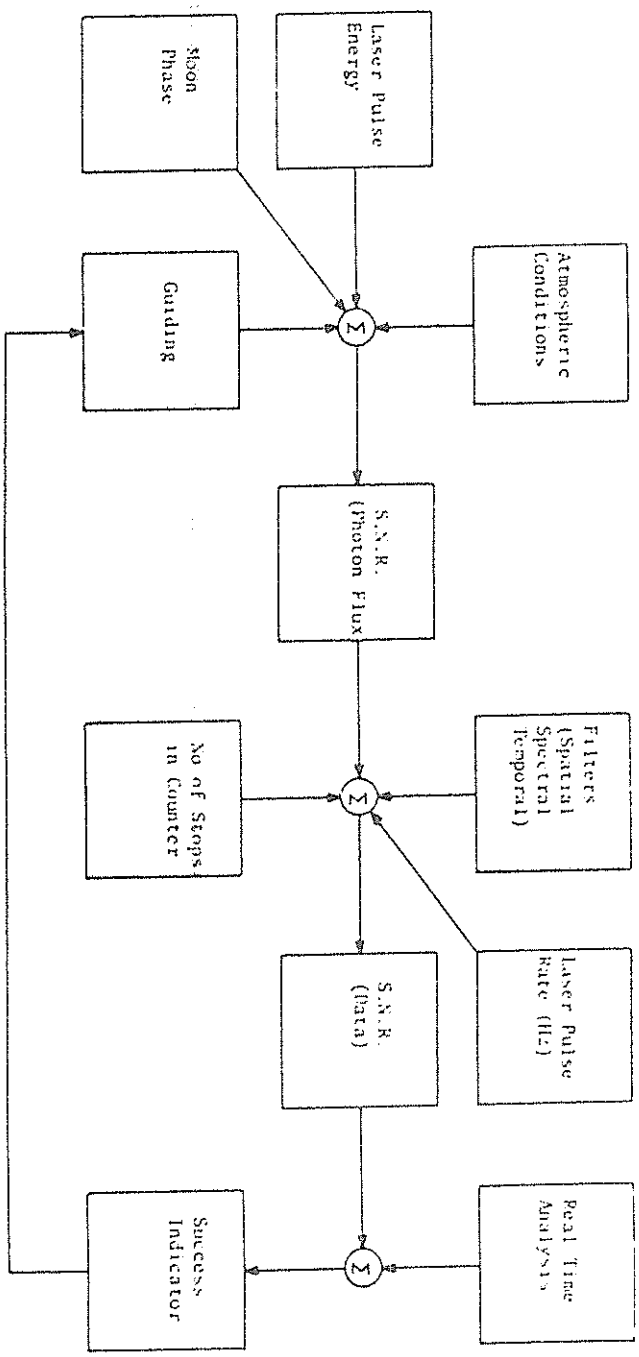

Fig 1 GUIDING CONTROL LOOP

DESCRIPTION AND FIRST RESULTS OF THE CERGA LUNAR-LASER STATION

by J.F. MANGIN, Ch. DUMOULIN, J.M. TORRE,
J.L. SAGNIER, J. KOVALEVSKY, D. FERAUDY
CERGA, Grasse, France

I - INTRODUCTION

A preliminary description of the CERGA lunar laser was given in the Lagonissi Laser Workshop (O. Calame and J. Gaignebet, Laser Workshop, Athenes, p. 139, 1980). The main features described three years ago have not changed. The aim of this presentation is to give some supplementary information on some sub-systems and to present the observing procedure that is adopted and had permitted to obtain the first returns.

The telescope (see M. Bourdet and Ch. Dumoulin in the present proceedings) is used for the three basic functions : emission, reception and tracking. The three corresponding optical paths are schematically described in figure 1.

II - EMISSION

Presently, the laser gives an impulse with a 3 ns width at half intensity. The mean energy is 2.5 Joules. The emission optical system includes three treated lenses, six mirrors and a dichroic mirror, three of which are treated for high energy impacts. The total loss in energy is estimated at 30 %, so that the outgoing energy is 1.75 Joule.

The natural divergence of the laser is $\pm$ 1".5. The accuracy of the focalization of the telescope - coupling lens system is also estimated $\pm$ 1".5. Presently, the observed defect of the secundary mirror (the glass was attacked during a treatment) is of the order of 4".

If we take 3" for the turbulence effects, we estimate to 5"5 the diameter of the beam on the Moon. A reduction to a little more than the spreading due to the turbulence is expected when the secundary mirror will be replaced.

III - RECEPTION

The return photons are reflected by the three mirrors of the telescope, the dichroic mirror, two other treated mirrors and then go through two lenses before reaching the photocathode. The gross effect of the transmission of the optics and of the quantic efficiency of the photomultiplier gives an overall transmission factor of 4.5 %. This was checked on stars, using a large (12") diaphragm. Smaller diaphragms (8", 5", 3", 2") are also available. Four successive events may be timed by the event-timer during the opening of the electronic gate.

IV - TRACKING

A beam splitter situated behind the dichroic mirror directs a part of the incoming beam for direct guiding using a reference reticle. Another part is sent in a TV camera. An offset device can drive the camera in a precomputed manner, so as to permit an offset guiding on a given crater, while the telescope is still pointing the retroreflectors.

At present, the offset guiding is not in service and the following procedure is used :

1. A given crater is tracked using reference ephemerides
2. The camera is centered on the crater and the offset in azimuth and elevation Δa, Δe are noted
3. The telescope is pointed blindly on the reflector using the ephemerides and the corrections Δa and Δe are applied. These corrections are essentially due to telescope flexures and other mechanical irregularities. Some of them have been empirically represented by trigonometric expressions, and the corresponding errors as well as a refraction model are included in the software control of the telescope.

The time necessary to execute these three steps is approximately 7 minutes. They are followed by a series of about 70-100 firings lasting another 7 to 10 minutes.

V - FIRST RETURNS OBTAINED BY THE STATION

A few series of returns were obtained during the summer of 1980 on GEOS 3 and STARLETTE. For instance, on the first of July, 49 events were obtained after 40 laser firings. Out of them 31 were retained as being returns with an internal consistency of $\pm$ 25 cm (fig. 2).

The first returns on the Moon were obtained on June 8th, 1981, when two series of 7 events were recognized as probable returns. The number of noise events received during the 7 minutes corresponding to the 80 laser shots were respectively 60 and 40 for a gate width of 10 microseconds.

Another result was obtained on July 7th, when from a first glance on 50 events, one could recognize 19 as probable returns (fig. 3). Three of them have residuals with respect to a linear function of time (due to UT1-UTC effect) of the order of 10 ns. This offset is now being studied, but has not yet been understood. The mean quadratic error of the remaining 16 returns is $\pm$ 1.5 ns (or $\pm$ 22 cm).

Presently only observations on Apollo 15 reflectors during lunar nights have been attempted. A significant improvement in the efficiency of the station is expected when a new secundary mirror and a narrower filter will be available.

The first returns have been confirmed by some other series in November 1981.

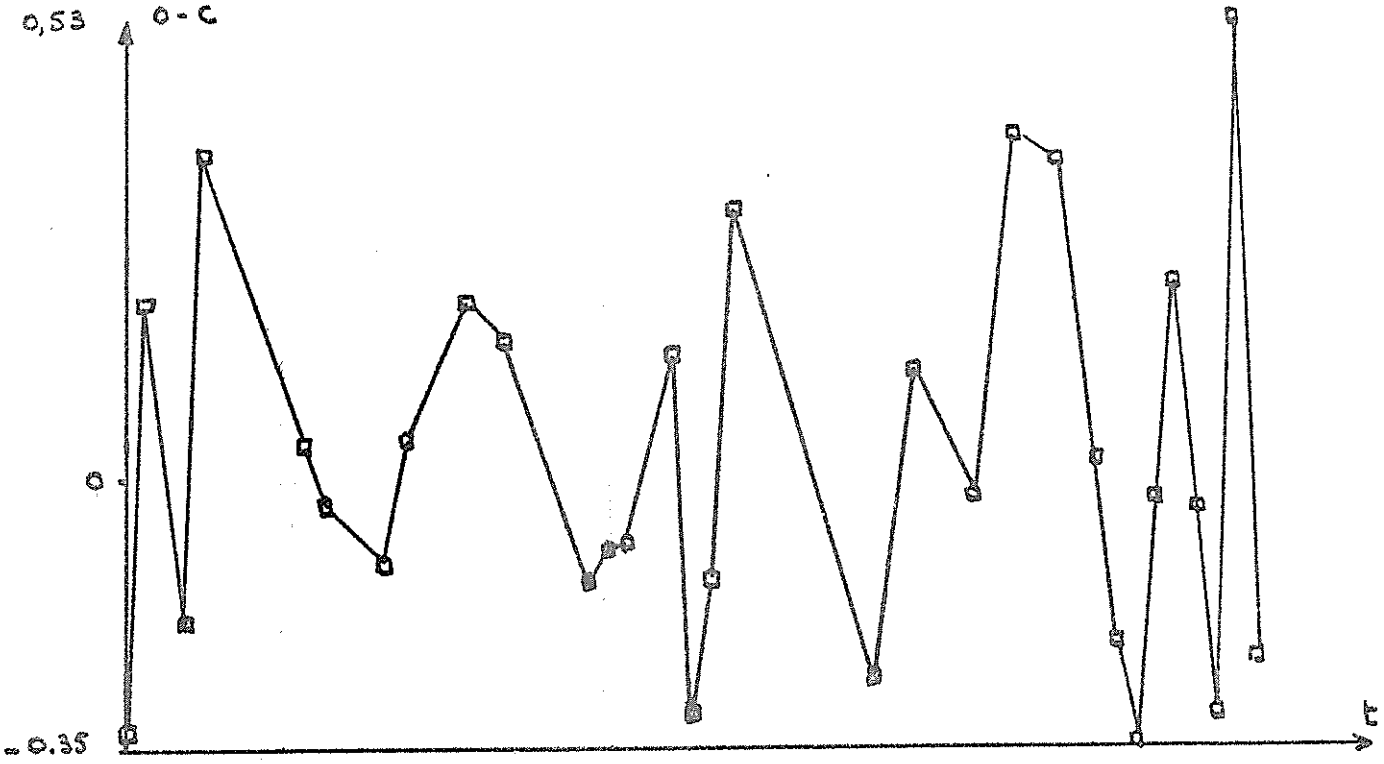

o - c of the 31 events obtained on GEOS 3 by the Cerga Luna Laser
July 1st 1980

Fig. 2

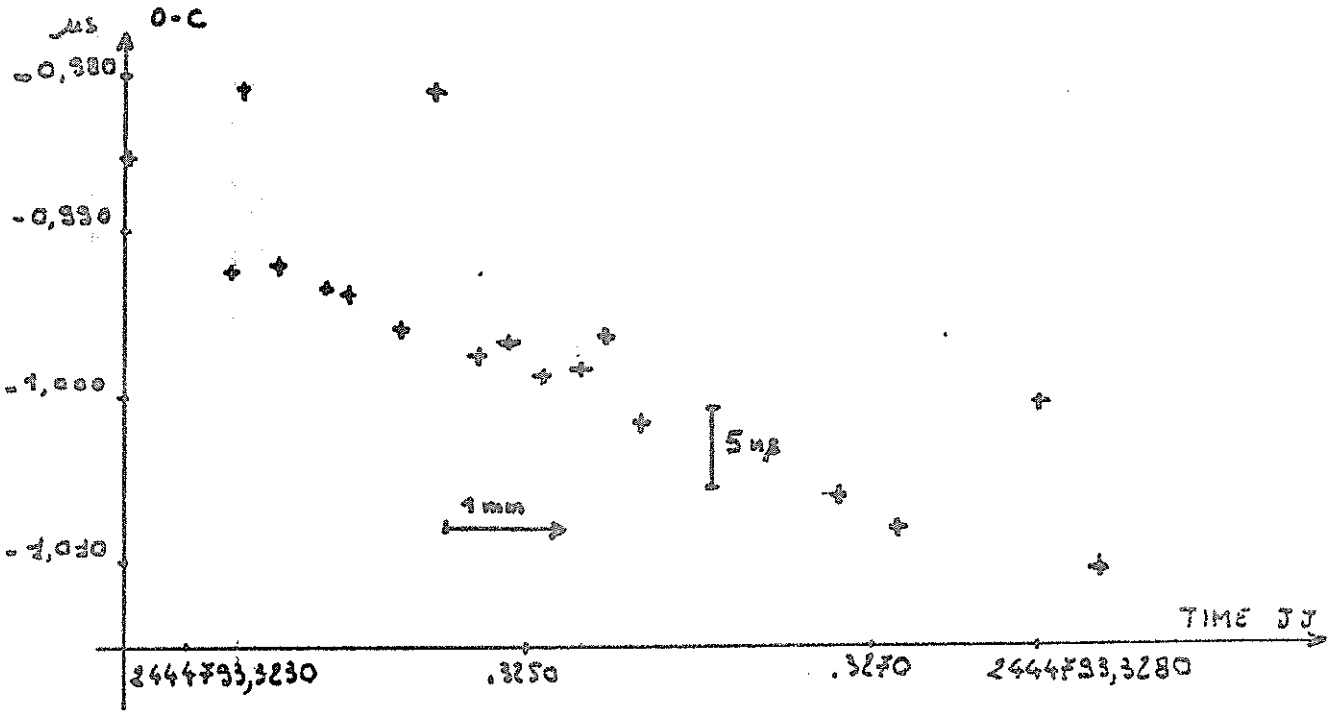

o - c of the 19 events obtained on the Moon by the Cerga Luna Laser
on July 7th 1981

Fig. 3

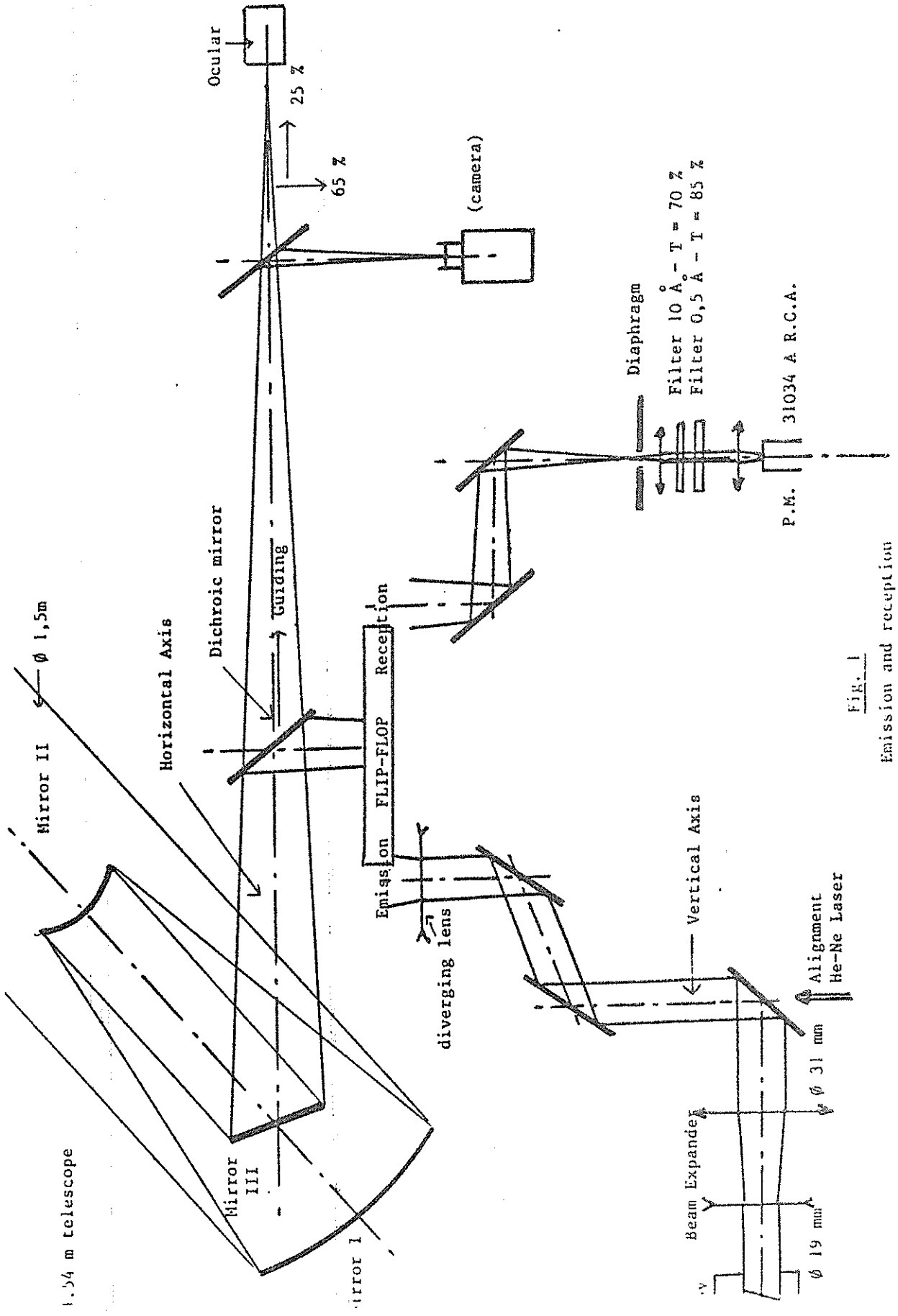

Fig. 1

Emission and reception configurations of the Cerga lunar laser.

McDONALD LASER RANGING OPERATIONS PAST, PRESENT, AND FUTURE

by

Peter J. Shelus and Eric C. Silverberg
Department of Astronomy and McDonald Observatory
University of Texas at Austin
Austin, Texas 78712 USA

ABSTRACT

The 2.7-meter lunar laser ranging system at McDonald Observatory in West Texas has been in regular operation since mid-1969. It has been the major source of LLR data since that time. We are now in the final stages of construction of a stand-alone, dual-purpose laser ranging station to replace it. Herewith is presented some of our accomplishments of the past and some of our expectations for the future.

1 INTRODUCTION

We are rapidly approaching the end of an era with lunar laser ranging as we begin the process of phasing out LLR operations on the 2.7 meter reflector at McDonald Observatory in west Texas. Over the past twelve years this station has been continuously and routinely operating to obtain the overwhelming percentage of the world's high accuracy lunar range data. This feat becomes even more remarkable when one considers the fact that this has been accomplished even though the experiment has been constructed around, and makes constant use of, a standard telescope which is scheduled 24 hours a day, 365 days per year for normal astronomical activity. The definitive document for the station continues to be that of Silverberg (1974).

The day-to-day operations, as well as most system problems, modifications and upgrades, have been chronicled in the station reports which were issued thrice per year under NASA Grant NGR 44-012-

165. With the demise of that grant and the transfer of McDonald Observatory laser ranging operations to NASA Contract NAS 5-25948, the reports on day-to-day activities continue to be made in the regular monthly submissions as well as in the documentation which accompanies the semi-annual data deposits into the National Space Science Data Center, i.e., Shelus (1981). All of these reports and documents have received wide distribution and should be readily available to all interested parties.

The operational philosophy of the McDonald LLR station has been a unique one. This philosophy is probably, in large part, responsible for the fine level of success which the station has experienced. Because of the fact that the station has always been considered to be an "operational" one (even initially) instead of one established primarily for research and developement, it has always been expected that data would be gathered under all but the most pressing of circumstances. Day-to-day problems have always received the primary attention of observatory staff members and all modifications and upgrades have been handled such that regular observing schedules are seldom compromised. Further, changes have been made in ways which do not force the immediate abandonment of older equipment and/or techniques; a change which proves to be problematical can be quickly rescinded and original operational procedures can be resumed while such changes are "debugged". The result of such an operational philosophy has been such that in the many years of 2.7 meter LLR activity at McDonald Observatory, only for a telescope drive spur gear change in September, 1972 has the station been continuously out of operation for more than a week.

Further, the aim of the McDonald LLR station has not been simply that of data gathering. A firm commitment has been made concerning the observational data obtained. If such data is not made available to the general scientific community in a timely manner, together with all clock, calibration, environmental and ancillary data, the scientific relevance of the experiment has been lost. To this end, the station has been molded to provide all relevant data to researchers with a minimum of delay and in a standard, well-defined machine-readable format. Success has been encountered here as well since all data is provided to the user, either through direct mailing, electronic data transmission or regular NSSDC deposits. Monthly distributions of filtered data and normal points are made within approximately six weeks of observation and semi-annual NSSDC deposits are made within approximately three months of oberrvation.

2 2.7 METER LLR SYSTEM

As has already been mentioned, most of the relevant material dealing with the 2.7 meter LLR operations at McDonald Observatory has been provided by Silverberg (1974). Figure 1 schematically depicts

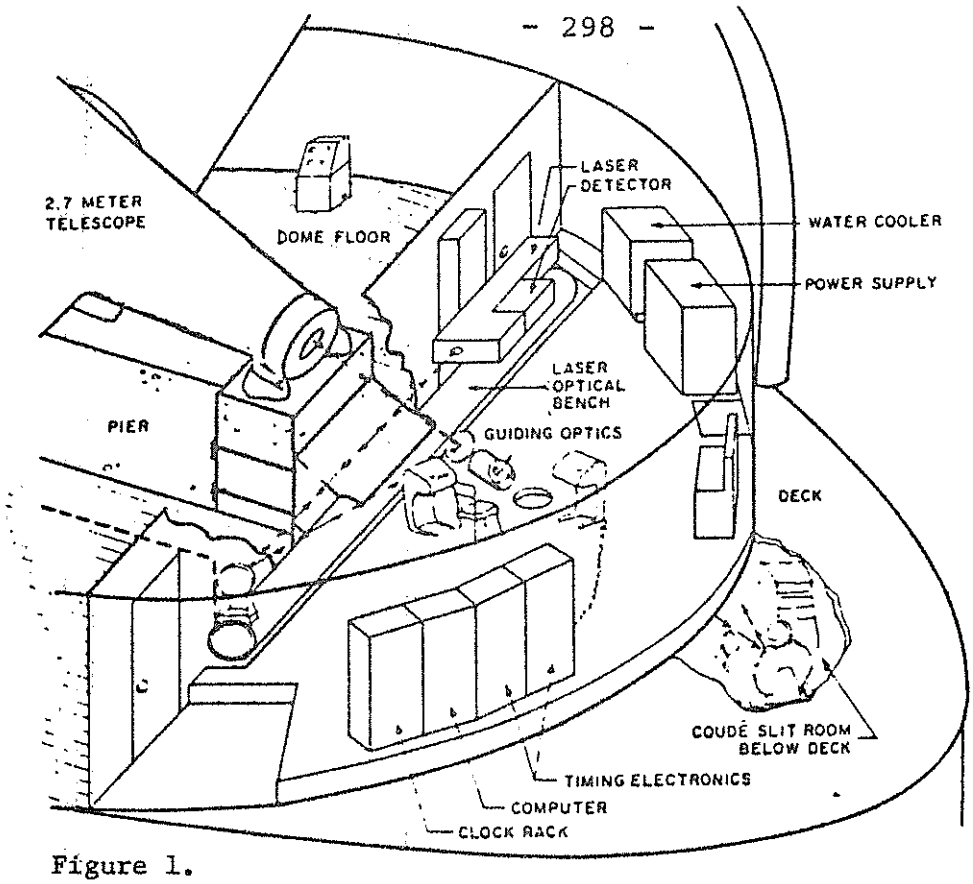

Figure 1.

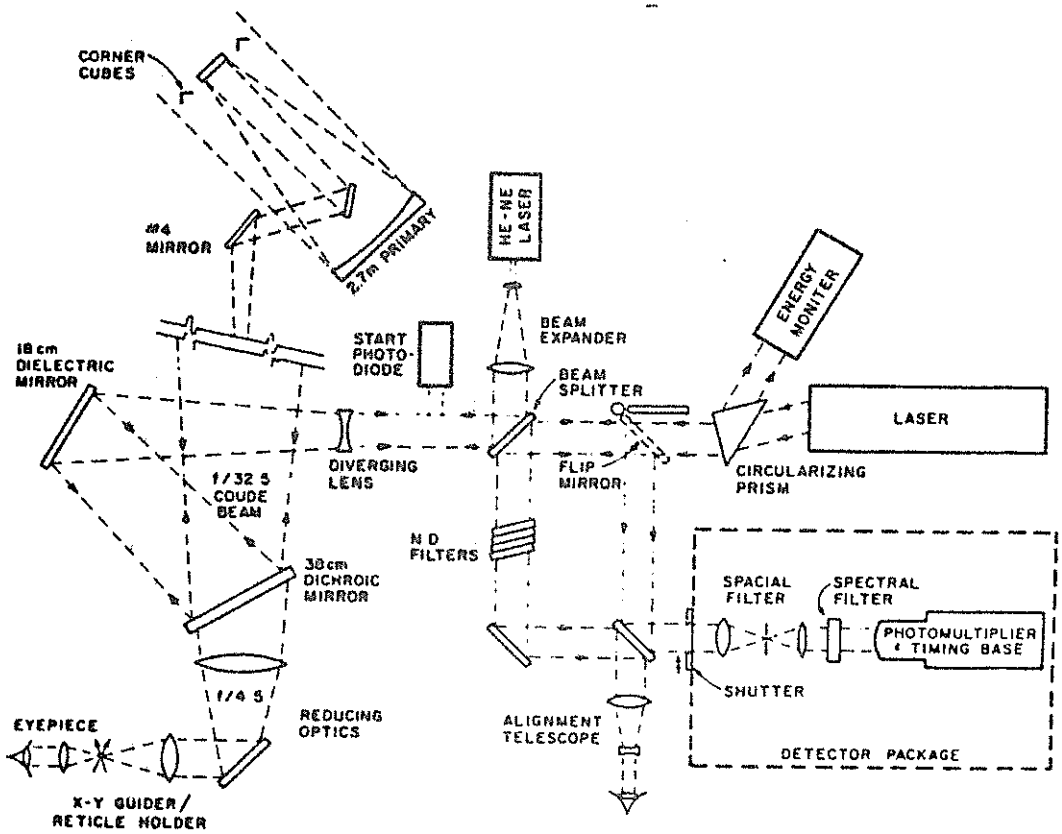

Figure 2.

the present configuration in the telescope dome. Figure 2 shows the major optical components which are used in conjunction with the 2.7 meter telescope. Table 1 gives the relevant McDonald LLR hardware specifications. Laser ranging operations are performed thrice daily on approximately 21 days per lunation. Forty-five minute observing sessions are held when the moon is approximately 3 hours east of, on, and 3 hours west of, the meridian. Each forty-five minute session is spent in obtaining ranges from one or more of the lunar surface retroreflectors (one at a time, of course). Calibration information is obtained in real-time as observations are being made; clock data is archived automatically through the month to allow the recovery of UTC from the station clock; environmental and ancillary data is recorded on the log.

Once a lunation (more often, under special conditions) a magnetic tape of all related LLR information is forwared to Austin for filtering, reformatting, compression, archiving and distribution. Table 2 summarizes observing statistics by year and by reflector; Figure 3 gives statistics on the data compression ratio; Figure 4 presents statistics of uncertainty estimates for the McDonald data set; Figure 5 summarizes normal point distribution with respect to the classical fundamental arguments of the lunar theory; Figure 6 gives information on the distribution of McDonald LLR data with respect to lunar local hour angle and declination.

3 McDONALD LASER RANGING SYSTEM - MLRS

At the present time we are in the process of establishing a new laser ranging station at McDonald Observatory. Unlike the present 2.7 meter system, the new station will be dedicated to laser ranging operations, and it will have the capability of ranging to lower (artificial) satellites as well as to the moon. Basic operating parameters of the MLRS can be found in Table 3. A line drawing which depicts its major components is found in Figure 7.

Although this station has been developed as a stand-alone replacement to the 2.7 meter LLR system, it has made extensive use of systems and procedures which were developed for the Transportable Laser Ranging Station. The TLRS is a very compact, mobile LAGEOS laser ranging station now in regular operation in the western United States under the NASA Crustal Dynamics Project. Timing electronics, photo-detector and calibration procedures are identical to those of the TLRS. The system software is also very similar to that of the TLRS with the major differnces concerning the lunar versus LAGEOS capabilities. The system contains a dual laser and lunar guiding is performed using a dichroic #3 mirror. Many of the hardware and software components of the TLRS/MLRS systems are being presented in various sessions of this Workshop. The interested reader should refer to the appropriate parts of the formal Workshop Proceedings for

TABLE 1

McD 2.7-m LLR Operating Parameters

APERTURE	2.7 m
MOUNT	EQUATORIAL
AV. POWER	0.4 w
DIVERGENCE	1.5 arcsec
WAVELENGTH	694.3 nm
PULSEWIDTH	3 nsec
REP RATE	1/3 Hz
SPATIAL FILTER	6 arcsec
SPECTRAL FILTER	0.7 Å

TABLE 2

Number of McD Normal Points

	YEARS	0	2	3	4
	1969	2	0	0	0
	1970	57	0	0	0
	1971	84	74	73	0
	1972	54	58	247	0
	1973	72	85	277	1
	1974	40	53	212	24
	1975	36	46	250	32
	1976	39	34	229	17
	1977	15	14	203	14
	1978	14	21	166	21
	1979	11	23	111	8
	1980	31	58	201	4
Jan-Jun	1981	14	18	82	5

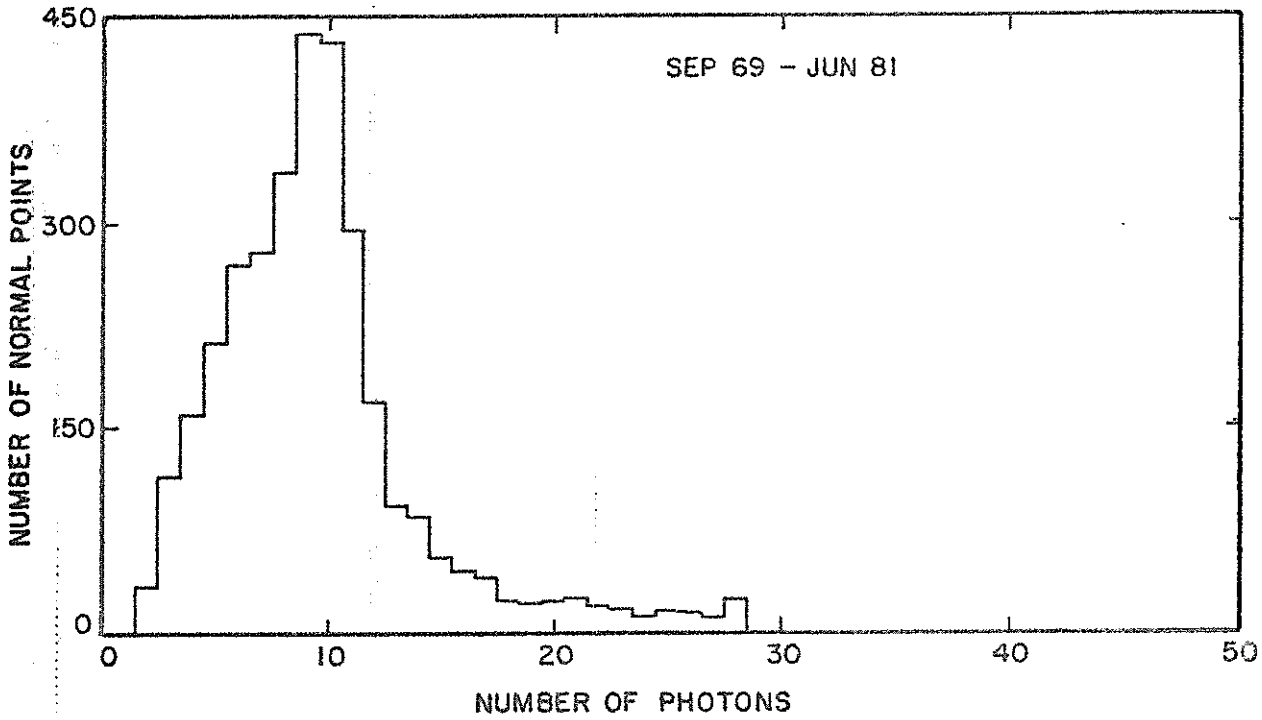

Figure 3.

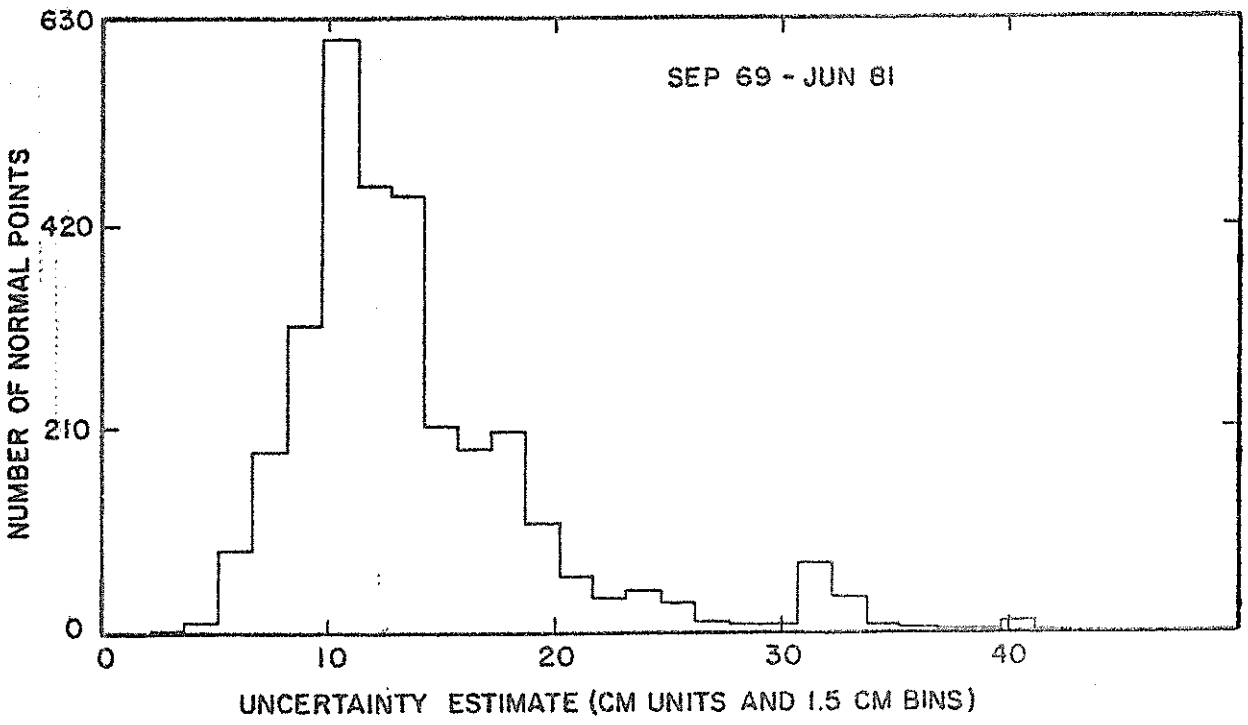

Figure 4.

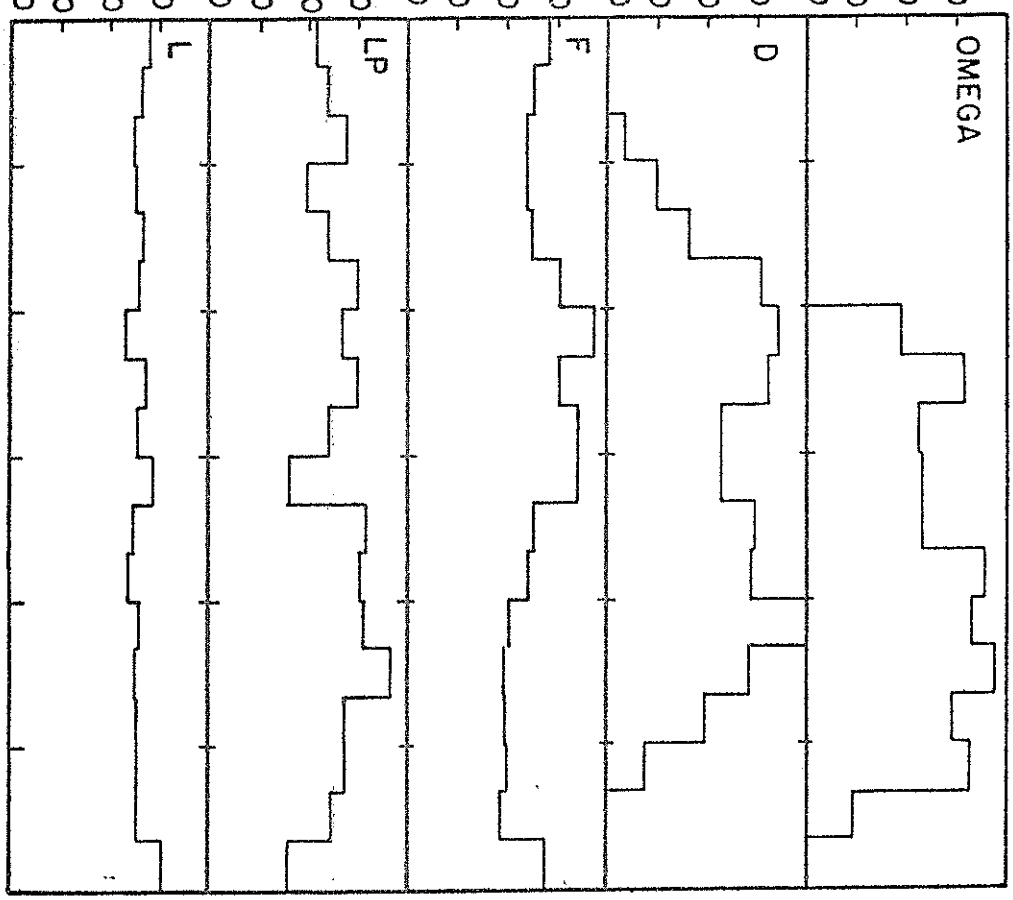

Figure 5.

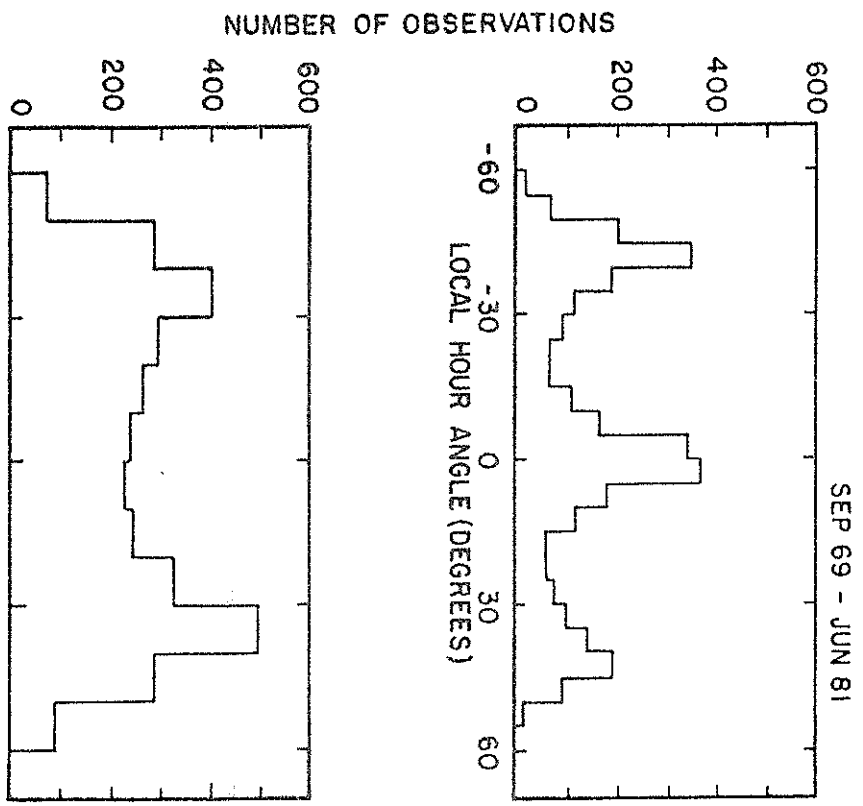

Figure 6.

TABLE 3

MLRS OPERATING PARAMETERS

	LAGEOS		MOON
APERTURE		0.76 m	
MOUNT		ALT-ALT	
AV. POWER	~10 mw		4-5 w
DIVERGENCE	~10 arcsec		~3 arcsec
WAVELENGTH		532 nm	
PULSEWIDTH	0.1 nsec		3 nsec
REP RATE		10 Hz	
SPACIAL FILTER	6-40 arcsec		6-12 arcsec
SPECTRAL FILTERS		0.8, 3, 10 Å	

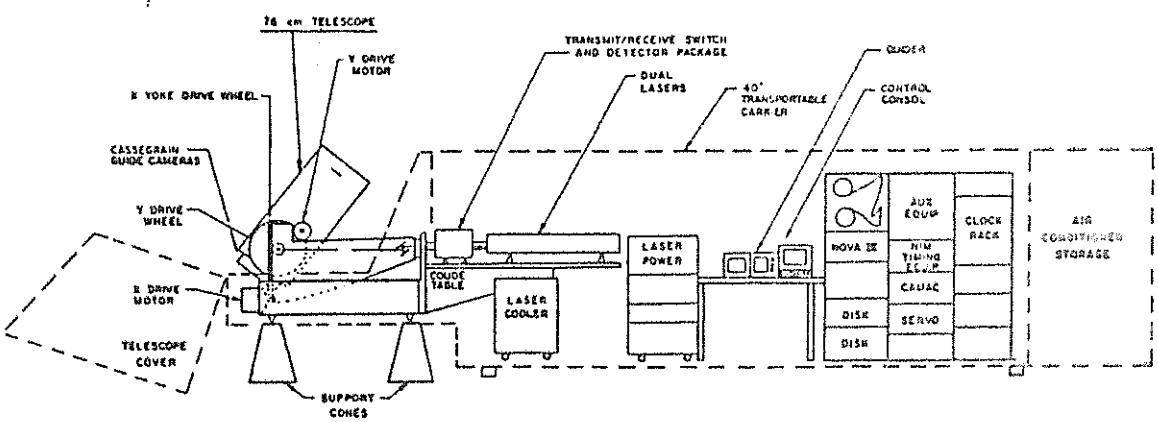

Figure 7.

further information concerning them.

As the system is presently envisioned the system is software intensive having been built around a sophisticated Data General Nova-based operating system. This operating system should be able to furnish computer support throughout all routine observing sessions from computing point angle and ranging predictions, pointing the telescope and firing the lasers, performing necessary calibration and clock maintenance; recording environmental data; and, finally, filtering, compressing and reformatting the data for data distribution.

4 CONCLUSIONS

A long and successful history surrounds LLR activity at McDonald Observatory. Many of the lessons which have been learned from the original 2.7 meter system and the TLRS mobile station are in the process of being incorporated into the new MLRS system. We feel that our basic philosophy of an "operational" station is important to successful operations). Many of the hardware aspects of the old and new stations have appeared in the Proceedings of earlier Laser Workshops as well as in those of the current Workshop. Many of our software algorithms are being presented during the Software sessions of the present Workshop here in Austin. We are looking forward to successful operations of the MLRS in the very near future.

5 ACKNOWLEDGEMENTS

The current McDonald Observatory lunar laser ranging operations are funded under NASA Contract NAS5-25948. The basic funding for the construction of MLRS comes from NASA Contract NASW-3296.

6 REFERENCES

Silverberg, E. C. 1974, "Operation and Performance of a Lunar Laser Ranging Station" Applied Optics, 13, 565.

Shelus, P. J. 1981, "Lunar Laser Ranging Data Deposited in the National Space Science Data Center - Normal Points, Filtered Observations, and Unfiltered Photon Detections for 1 January 1981 through 30 June 1981", UT Res. Memo. in Astronomy, Octiber, 1981.

GENERAL HARDWARE/SOFTWARE ORGANIZATION

by J.M. TORRE and J. KOVALEVSKY
CERGA, Grasse, France

I - GENERAL DESCRIPTION

The CERGA lunar-laser ranging system as described by J.F. Mangin et al. in these proceedings has been set up in such a way that the telescope control is strictly separated from the real time control of the ranging experiment. Consequently, two different computers are used in a completely independant modes. These are :

1) Data general "Eclipse 5200"

CPU with 64 K byte
Disk unit
Alphanumeric Tektronix display
Texas Instrument SILENT 700
TTY
16 bits interfaces (digital 1/0)
RS 232 C interfaces (asynchroneous line multiplexes)

Software support : Real time disk operation system
FORTRAN 4

2) Data General "Nova 1220"

CPU with 16 K byte
TTY
16 bits interfaces (digital 1/0)
RS 232 C interfaces (universal line multiplexes)

No software system. Machine language coding.

The various hardware subsystems that are linked with these two computers are schematically described in figure 1.

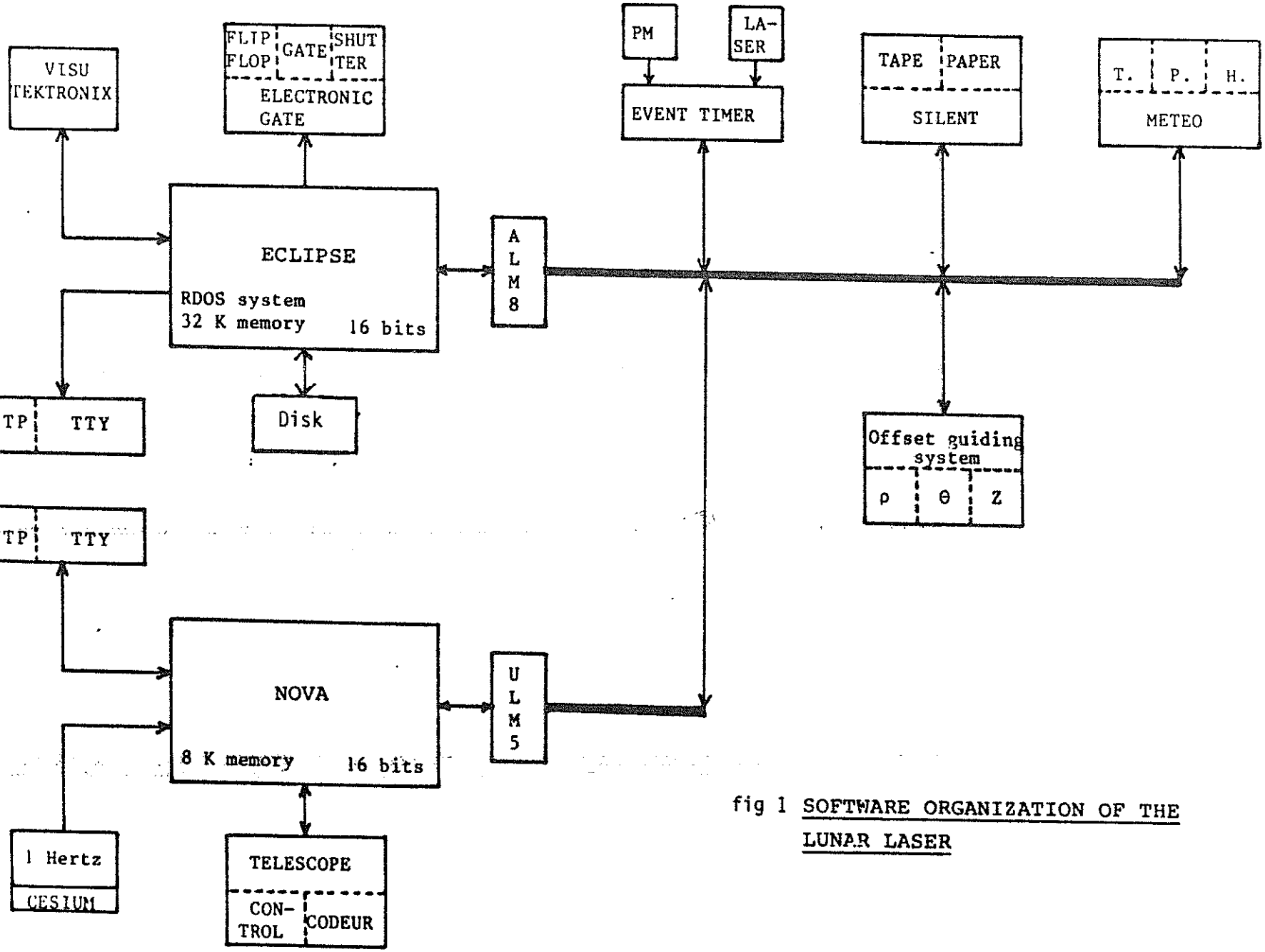

fig 1 SOFTWARE ORGANIZATION OF THE LUNAR LASER

II - COMPUTER ORGANIZATION

Four different functions are executed by these computers. Let us describe them.

1) Ephemeris treatment

The ephemerides of reflectors and reference craters are computed by O. Calame on the CNES CDC computers and transferred on cassette compatible with Texas Instrument Silent. These cassettes are read by the Eclipse computer and filed in the disk. Each cassette contains the ephemerides for about two weeks of observation.

Presently, before each observation, the ephemerides of the selected reference craters and of the reflectors are transcribed by the Eclipse on a paper tape, in a form that can be read by the Nova. In the future, it is contemplated to transfer these ephemerides directly from Eclipse to Nova through both RS 232 C connections.

2) Pointing and tracking

When the decision is taken by the observer to track a crater (or a reflector), the corresponding paper tape ephemerides are read by the Nova computer. It interpolates the apparent positions for every second. A 1 Hertz top provided by a cesium clock synchronizes the orders prepared by the computer and sent to the telescope. The link is made through a 16 bit input/output interface.

In the future, we intend to use an offset guiding so as to control the tracking by a crater observed with a TV camera, while the telescope is pointed at a reflector. It will be controlled by the Eclipse computer, linked to the offset guiding system by the RS 232 C interface (asynchronous line multiplexor ALM 8).

3) Real time control

The Eclipse computer linked to the event-timer through the ALM 8 records the time of the firing. Then, it computes and transmits to the electronic gate the expected time-delay between the instant of the firing and the return event.

Then, the Eclipse, reads on the event-timer the times of the events and compares them with the ephemerides. The residuals are computed and a histogram of the number of residuals in given time channels is displayed on the Tektronix screen.

4) Quick-look data evaluation

After the series of laser shots are over, it is possible to analyse all the delays obtained and construct histograms with various channel widths. The number of events for each 5 ns channel is printed on the teletype. The probable returns as shown on histograms are then treated by the Eclipse, and recorded on cassettes with other parameters (meteorology, noise, etc...) for scientific treatment. A mean quadratic error of the selected probable returns is computed and the corresponding observations and residuals are printed. This allows the observer to be aware of the quality of the observations a maximum of 5 minutes after the last laser shot.

LUNAR AND PLANETARY EPHEMERIDES: ACCURACY, INERTIAL FRAMES, AND ZERO POINTS

J. G. WILLIAMS

JET PROPULSION LABORATORY
CALIFORNIA INSTITUTE OF TECHNOLOGY
PASADENA, CALIFORNIA 91109

A new lunar and planetary ephemeris has recently been completed. I would like to briefly describe the accuracy of this ephemeris and to argue that such modern ephemerides are closely related to an inertial coordinate system. The ephemeris has a definable and repeatable zero point. It would be desirable to tie the VLBI frame together with the lunar and planetary celestial frame and to connect the terrestrial frames of the lunar and LAGEOS laser ranging systems.

The new JPL planetary/lunar ephemeris comes in two versions designated DE200/LE200 and DE119/LE63. The coordinates are on the equator and equinox of J2000 and B1950.0 respectively. Both are on a dynamical equinox and they differ from one another only by a rotation. The ephemerides result from joint integrations based on joint fits of the lunar laser and planetary data. The new IAU precession (Lieske et al., 1977; Lieske, 1979) and nutation (Seidelmann et al., 1982) expressions have been used. A compatible integration of the lunar physical librations has also been made.

It is clear that the parameters which describe the geocentric distance of the moon will be very well determined from range data and have high internal precision. Of more interest for coordinate frames are the uncertainties in the orientation angles and rates of rotation with respect to inertial or terrestrial systems. The uncertainty in the orientation of both the lunar orbit plane and the ecliptic plane with respect to the equator of the earth is less than 0.01" (at least during the decade spanned by the observations). High sensitivity to the orientation of the ecliptic results from the lunar range data because the lunar orbit plane effectively precesses along the ecliptic.

The 18.6 yr period of precession is longer than the existing span of lunar laser data so that these orientations are improving rapidly as the data span increases. In addition to the orientation of the equator and two orbit planes we wish to know the relative error in the geocentric ecliptic longitudes of the moon and sun. A reasonable uncertainty for the differential longitude (during the past decade) is 0.003", being somewhat worse at the ends than in the center of the data span (1975). The sensitivity to the differential longitudes comes through two very strong solar perturbations (amplitudes of 3000 kms and 4000 kms) in the lunar distance. Thus the relative positions of the moon and sun are well known as seen from the earth. Since planetary ranging data to Mercury, Venus, and Mars determines their orbits well relative to the earth's orbit, they are also well connected to the lunar orbit and the earth's equator.

It has been argued that the lunar orbit and the earth's orbit about the sun are highly consistent in angular orientation, but what about rate errors? The integration of the equations of motion assumes an inertial coordinate frame, but the accuracy with which the range measurements can be related to the frame depends on the uncertainty in the mean motion (there are no solution parameters corresponding to orbital rates about the other two axes). For the moon the mean motion uncertainty is about 0.0007"/yr at the center of the data span (middle 1975), but at five years on either side it degrades to about 0.001"/yr. This growth of uncertainty results from an uncertainty in the lunar tidal acceleration of about 0.00015"/yr^2. The errors in the lunar ecliptic longitude grow nonlinearly as one extrapolates the motion outside of the span of data. In terms of its value for future UT1 determinations, the error of the new ephemeris will propagate with components of about 0.05 ms/yr and 0.005 ms/yr^2 from the center of the data span. At the time of the MERIT campaign this error would look mostly like an offset in UT1, but this can be reduced considerably with ephemerides produced closer to the beginning of the campaign and can be effectively eliminated with post-campaign analysis. The uncertainty in the inertial mean motion of the earth about the sun is 0.0002"/yr, being tightly determined by the excellent Viking range data from earth to Mars. The lunar and planetary ephemerides are very good representations of the inertial motions of the earth and moon during the past decade. Relating the inertial frame to a terrestrial frame requires knowledge of the precession constant which has an uncertainty of 0.0015"/yr (Fricke, 1977), of which 0.0006"/yr can project into declination. The consequences of this larger error have been explored by Williams and Melbourne (1981). If the accuracy of the inertial frame is to be preserved for the terrestrial longitude and UT1 systems, then the equation for Greenwich Mean Sidereal Time would need to allow for future improvements in the precession constant.

The new ephemerides are on a dynamical equinox so that the mean equator and mean ecliptic cross (at the dates J2000 or B1950.0) at the zero point for right ascension and ecliptic longitude. It is intended that the FK5 star catalogue will have a zero point close to (within several hundreths arcsecond) the dynamical equinox. Since we can align the zero point of our ephemerides with the dynamical equinox

an order of magnitude more accurately than we can align with a star catalogue, we have done so. My colleague E. M. Standish has located the dynamical equinox with an accuracy of at least a few milliarcseconds, and perhaps as good as 0.001". The conceptual simplicity of the dynamical equinox can be contrasted with previous attempts to align JPL ephemerides with the catalogue equinox of the FK4, which has the zero point of the right ascension system shifted about 0.5" (at B1950.0) from the dynamical equinox (Fricke, 1981). The modeling for the optical positions included shifts of each observational star catalogue from the FK4, corrections for equinox drift and the precession constant, plus systematic phase corrections for each planet. The zero point would shift slightly with each addition of new optical data. For ephemerides to be used with range data adopting the dynamical equinox is a welcome way to stabilize the zero points of the celestial right ascension and terrestrial longitude systems, it matches the (IAU sanctioned) FK5 equinox within the optical errors, but it is not strictly an IAU convention.

When one realizes that the lunar and planetary ephemerides are both accurate and can be used to achieve a nearly inertial celestial frame, it then becomes desirable to link with the frame of the other accurate, nearly inertial technique, very long baseline interferometry (VLBI). My colleague X X Newhall is attempting to do this using differential VLBI data which was recorded when the Viking Mars Orbiters and a quasar were close together in the sky. Preliminary indications are that this link can be achieved to better than 0.01", so that the VLBI quasar coordinate frame can be put on the dynamical equinox in the near future. If this is done the terrestrial longitude systems will line up to comparable accuracy.

Achieving a similarly accurate link with the optical frame is harder, but there is a possibility that the Hipparcos astrometry satellite and the Space Telescope can be used to connect optical positions of quasars with their radio counterparts toward the end of this decade (Kovalevsky and Preston, 1981, private communication).

Artificial satellite ranging by itself achieves neither an accurate inertial celestial frame, nor absolute zero point information on terrestrial longitudes (relative longitudes are well determined). As several observatories will soon be ranging both LAGEOS and the moon, it will soon be possible to directly align the artificial satellite (terrestrial longitude) coordinate system with the lunar laser system by comparing the site coordinates. If the LAGEOS data reduction programs were to also use the long-term stable UT1 values available from lunar laser ranging and VLBI, then the satellite orbit frame would automatically be aligned with the inertial celestial frame.

In summary, lunar and planetary ephemerides have been generated which result from joint data fits and integrations. The lunar orbit and the earth's orbit are oriented with accuracies better than 0.01" about two axes, and several times better about the third (ecliptic pole) axis. The zero point in right ascension is adjusted to a dynamical equinox, and the motions of the earth and moon have uncertainties within 0.001"/yr of their true inertial values during the past decade. It should be possible to connect the celestial frames of VLBI and the ephemeris and to tie together the terrestrial frames of satellite and

lunar ranging, so that the three modern space techniques would be aligned within 0.01" of one another. If this unification were to be made in the near future it would cause the minimum inconvenience since a concurrent introduction of the new IAU constants and definitions would also introduce shifts in the coordinate systems.

ACKNOWLEDGMENTS

The planetary work which I have described is a product of the efforts of E. M. Standish. The lunar laser data analysis was a joint effort between J. O. Dickey and myself. This paper presents the results of one phase of research carried out at the Jet Propulsion Laboratory, California Institute of Technology, under contract No. NAS 7-100, sponsored by the National Aeronautics and Space Administration.

REFERENCES

Fricke, W., "Arguments in favor of a change in precession", Astron. Astrophys. 54, 363-366, 1977.

Fricke, W., Astron. Astrophys., in press, 1981.

Lieske, J. H., T. Lederle, W. Fricke, and W. Morando, "Expressions for the precession quantities based upon the IAU (1976) system of astronomical constants", Astron. Astrophys. 58, 1-16, 1977.

Lieske, J. H., "Precession matrix based on IAU (1976) system of astronomical constants", Astron. Astrophys. 73, 282-284, 1979.

Seidelmann, P. K., V. K. Abalakin, H. Kinoshita, J. Kovalevsky, C. A. Murray, M. L. Smith, R. O. Vicente, J. G. Williams, Ya. S. Yatskiv, "1980 IAU theory of nutation, the final report of the IAU working group on nutation", Celestial Mech., in press, 1982.

Williams, J. G. and W. M. Melbourne, "Comments of the effect of adopting new precession and equinox corrections", proceedings of IAU colloquium 63, High-Precision Earth Rotation and Earth-Moon Dynamics: Lunar Distances and Related Observations, ed. O. Calame, Grasse, France, in press, 1981.